Chapter 5

NUCLEAR RADIATION PHENOMENA

INTRODUCTION

As described in Chapter 1, one of the special features of a nuclear explosion is the fact that it is accompanied by the emission of nuclear radiations. These radiations consist of gamma rays, neutrons, beta particles, and a small proportion of alpha particles. Most of the neutrons and part of the gamma rays are emitted during the actual fission or fusion processes (see paragraphs 1-1 and 1-2, Chapter 1). The remainder of the gamma rays are produced in various secondary nuclear processes, including decay of the fission products. The beta particles are also emitted as the fission products decay. Some of the alpha particles result from the normal radioactive decay of the uranium or plutonium that does not fission in the weapon, and others are formed during the fusion reactions (paragraph 1-2).

As a result of the nature of the phenomena associated with a nuclear explosion, it is convenient to consider the nuclear radiations as being divided into two categories; initial and residual. The line of demarcation is somewhat arbitrary, but it is generally accepted to be about 1 minute after the explosion. The initial nuclear radiations consequently refer to the radiations emitted within 1 minute of the explosion. These radiations are discussed in Section I of this chapter. The residual radiations are further subdivided into neutron induced activity, which results from neutron activation of the earth below an air burst, and fallout, which is the deposition of radioactive residues following a surface or near-surface burst. These latter two forms of nuclear radiation are discussed in Sections II and III of this chapter, respectively.

The ranges of alpha and beta particles are short, and they can be neglected in the consideration of initial radiation. The beta particles, however, may be a hazard to personnel if fallout particles are in contact with the skin for protracted periods of time. The beta particles emitted by radioactive debris from high altitude explosions also may cause intense patches of ionization in the atmosphere that can interfere with, or disrupt, radio or radar communications as described in Chapter 8.

SECTION I
INITIAL NUCLEAR RADIATION

From the standpoint of total energy delivered, the principal sources of initial nuclear radiation (that delivered within 1 minute) are prompt neutrons (those emitted simultaneously with the fission or fusion events), gamma rays from the decay of fission products, and (in the case of an atmospheric burst) secondary gamma rays from neutron interactions with nuclei of the air and ground. Sources of lesser importance from the standpoint of energy delivered are delayed neutrons emitted by some fission products, secondary gamma rays from neutron interactions with the materials of the device, and gamma rays that are emitted simultaneously with fission. These latter components normally may be neglected in predicting total doses or exposures; however, the gamma components may be important for electronic components whose vulnerability is determined by dose rate rather than total dose.

5-1

89 3 02 044

NEUTRONS

5-1 Neutron Source

As mentioned previously, the neutrons of interest originate during the fission and fusion processes. The neutron source of interest is that which exists at the weapon case, i.e., the source of interest consists of those neutrons that escape from the exploding weapon. Both the number of neutrons and their spectrum are altered during transit through the weapon materials. Thus, the source of interest may be quite different from the source of origin (fission or fusion). The neutron source can be defined properly only by considering the actual design of a specific weapon. No average source can be defined that will represent most weapons with any degree of accuracy. It is beyond the scope of this manual to describe the output of a sufficient number of weapon types to present the user with adequate information concerning the neutron output for any possible specific situation. The examples that are presented in succeeding paragraphs are truly examples and should not be taken to be representative for pur-

poses of generalization. Further information concerning nuclear weapons as neutron sources may be obtained from "Status of Neutron and Gamma Output from Nuclear Weapons," DASA 2567 (see bibliography). On the other hand, the curves shown in Figures 5-9 through 5-13 that provide the total dose to personnel on or near the surface of the earth were calculated for eight specific sources. It is believed that, with the descriptions of the eight sources provided in Table 5-3, one of the eight sources may be selected that will represent a reasonable estimate of the total dose to personnel on or near the surface of the earth for most situations.

Table 5-1 shows the spectra for two weapons, one pure fission and one thermonuclear, for which calculations are available.[*] These spectra are also shown in Figure 5-1 and 5-2.

As mentioned before, the spectra shown in Table 5-1 should not be construed as

---

[*] These spectra are those that were used in the calculation of dose to personnel from weapon types II and VIII, respectively, as shown in Figures 5-9 through 5-13.

Table 5-1. Weapon Neutron Output Spectra

Neutron Energy (MeV)	Fission Weapon (neutrons/kt)	Thermonuclear Weapon (neutrons/kt)
12.2 −15.0		1.62×10^{22}
10.0 −12.2		8.53×10^{21}
8.18 −10.0	7.32×10^{20}	6.08×10^{21}
6.36 − 8.18	1.27×10^{21}	5.46×10^{21}
4.06 − 6.36	3.00×10^{21}	6.41×10^{21}
2.35 − 4.06	8.90×10^{21}	1.22×10^{22}
1.11 − 2.35	2.52×10^{22}	2.84×10^{22}
0.111 − 1.11	3.84×10^{22}	6.18×10^{22}
0.0033− 0.111	2.22×10^{22}	1.71×10^{23}
Total	9.97×10^{22}	3.16×10^{23}
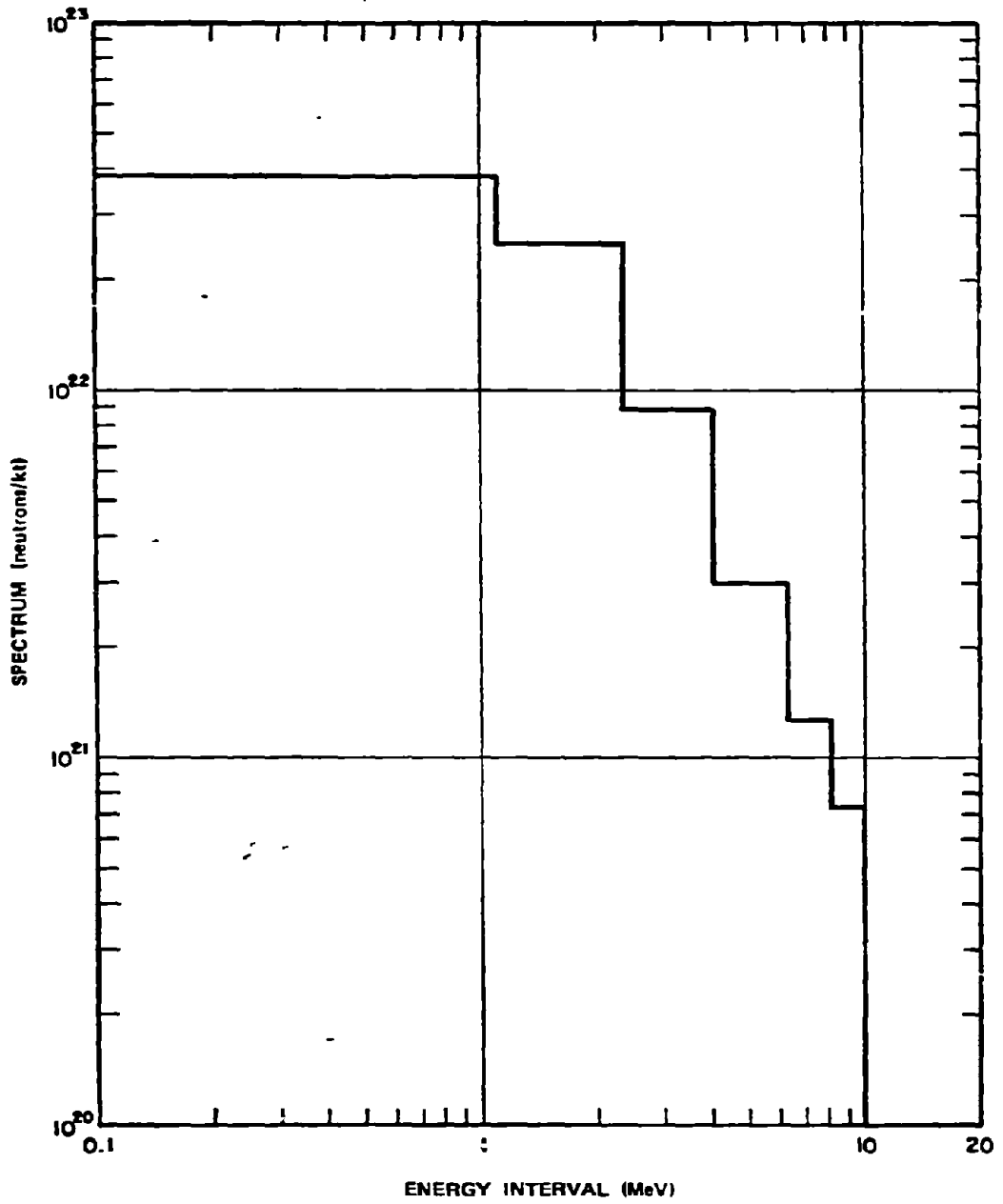
Figure 5-1. ███ Spectrum for a Fission Weapon (Normalized to 1 kt) ███

SPECTRUM (neutrons/kt)

ENERGY INTERVAL (MeV)
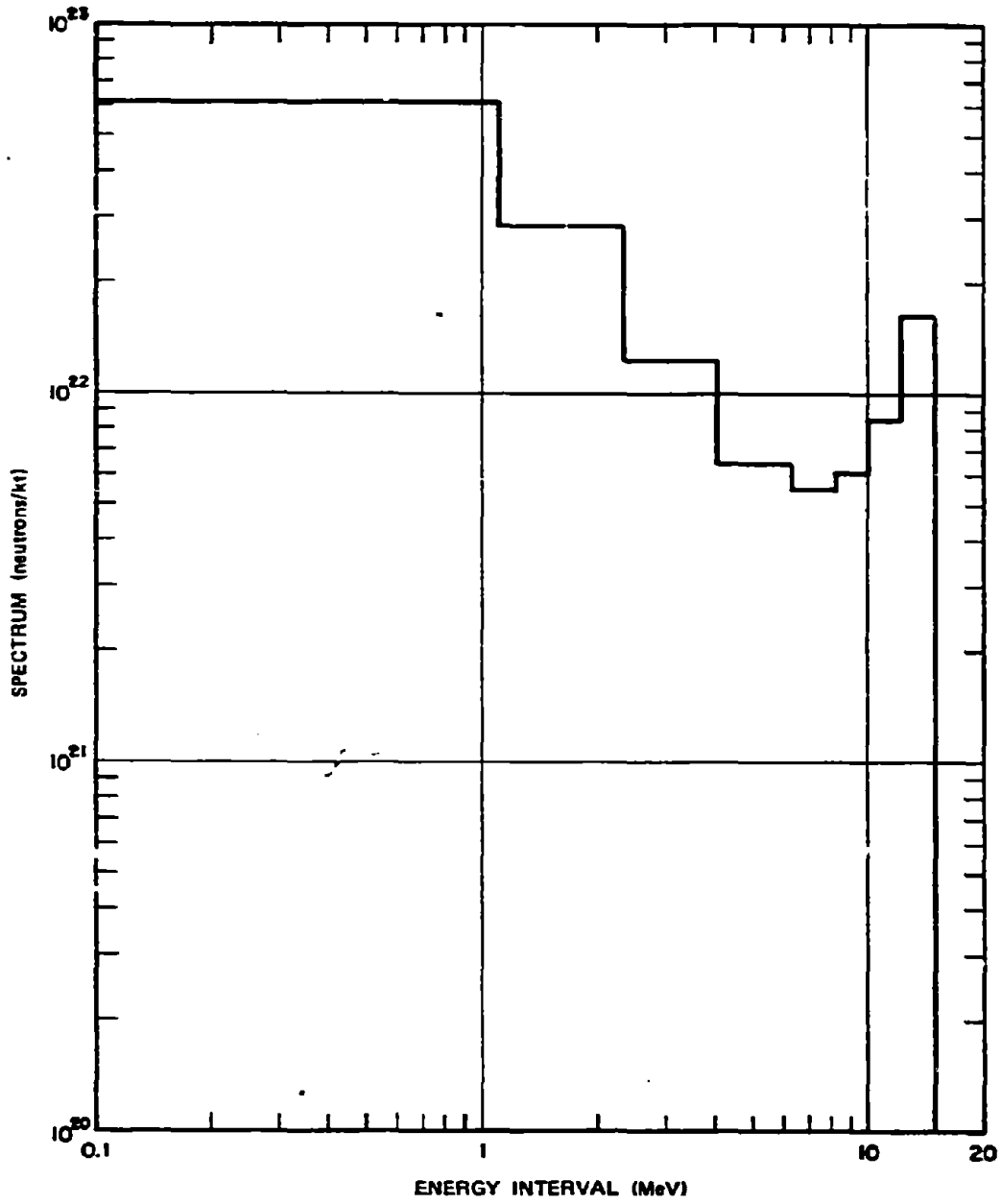
Figure 5-2. ▉ Spectrum for a Thermonuclear Weapon (Normalized to 1 kt) ▉

being representative. They are merely examples.

███ The spectral characteristics, however, will vary with weapon design even for weapons with the same total neutron output per kiloton.

5-2 Exoatmospheric (Vacuum) Transport ███

███ Neutron environments are completely specified by the description of the source and the distance from the source to the point of interest if the explosion occurs in a vacuum. If an explosion occurs sufficiently high that essentially vacuum conditions prevail, it is designated an exoatmospheric explosion. Since in any case, the vacuum will be less than perfect, the distinction between exoatmospheric and endoatmospheric explosions will depend on the degree to which effects vary from those predicted for a vacuum.

███ For perfect vacuum conditions, the neutron fluence is given by

$$\varphi = \frac{N_o}{4\pi R^2} \text{ n/cm}^2$$

where N_o is the total number of neutrons emitted by the weapon and R is the distance in centimeters. Under these conditions the spectrum will remain constant, since no interactions can take place in a vacuum. However, as a result of the energy differences the flux (neutrons cm^{-2} sec^{-1}) will be a function of the distance from the source, i.e., the more energetic neutrons will arrive ahead of the less energetic ones. The energies associated with neutrons produced by nuclear explosions are sufficiently low compared

to their rest mass energy that their velocities may be determined from their kinetic energy by non-relativistic mechanics, i.e.,

$$\frac{1}{2}Mv^2 = \text{K.E.},$$

where M is the neutron mass, 1.67×10^{-24} gm, v is the velocity, cm/sec, and K.E. is the kinetic energy in ergs. Using the relationship

$$1 \text{ MeV} = 1.6 \times 10^{-6} \text{ ergs},$$

the velocity is related to the kinetic energy in MeV as follows

$$v = 1.38 \times 10^9 \ \sqrt{\text{K.E. (MeV)}} \text{ cm/sec},$$

or

$$v = 1.38 \times 10^4 \ \sqrt{\text{K.E. (MeV)}} \text{ km/sec.}$$

Thus the velocities of 14 MeV, 4 MeV, and 1 MeV neutrons are

$$v_{14} = 1.38 \times 10^4 \ \sqrt{14} = 5.16 \times 10^4 \text{ km/sec},$$

$$v_4 = 1.38 \times 10^4 \ \sqrt{4} = 2.76 \times 10^4 \text{ km/sec},$$

$$v_1 = 1.38 \times 10^4 \ \sqrt{1} = 1.38 \times 10^4 \text{ km/sec.}$$

Expressed in a different manner, the times of flight will be 19.3, 36.2, and 72.4 μ sec/km for the 14 MeV, 4 MeV, and 1 MeV neutrons, respectively. Thus, although the spectrum will remain unchanged, the neutrons will arrive at points several kilometers from the explosion over periods of tens of microseconds.

5-3 Neutron Transport Through Materials ███

███ Neutrons undergo three main types of reactions when traversing matter: elastic scatter-

ing; inelastic scattering; and capture. In the elastic scattering process, the neutron interacts with the nucleus of an atom and is scattered away from its original line of flight. If the nucleus is light (e.g., the proton that constitutes a hydrogen nucleus), the neutron may transmit a significant amount of its energy to the nucleus, and the scattered neutron will be less energetic than the incident neutron. If the nucleus is heavy, however, the energy transmitted to the nucleus will be insignificant, and the neutron will continue in a new direction with essentially the same energy as before the collision. In the inelastic scattering process, the neutron interacts with the nucleus with the subsequent emission of a gamma ray and a neutron with degraded energy. There are a variety of capture reactions, most of which result in the subsequent emission of a charged particle (generally a proton or alpha particle) and/or a gamma ray. When the reaction results solely in the emission of a gamma ray, it is generally referred to as a radiative capture reaction. As a rule, the probability for capture reactions is small compared to elastic and inelastic scattering when the neutron energy exceeds a few keV. The nuclei remaining after neutron capture are frequently radioactive. The fission process described in paragraph 1-1 is a special case of neutron-induced reactions. Neutrons that do not undergo any of the reactions described above will decay into a proton and an electron with a half life of about 12.8 minutes. The same is true of neutrons that undergo scattering, if they do not undergo some other reaction prior to decaying. The probabilities of the various reactions are such that the decay process is most important for neutrons traveling upwards from a relatively high altitude burst.

██████ The primary reactions that occur during neutron transport through air are elastic scattering, inelastic scattering, and capture by nitrogen nuclei. These latter two reactions provide a source of secondary gamma rays that can be

important in some cases, as will be discussed in subsequent paragraphs.

██████ The neutron environment produced by nuclear explosions within the atmosphere are much more complicated than those described in paragraph 5-2 for exoatmospheric cases because of the interactions that take place with the atmospheric constituents. Even for a monoenergetic source the interactions described above alter the total neutron fluence that reaches a given range, result in a spectral distribution at that point, and change the time rate and direction of arrival at the point. As a result of scattering, the neutrons may arrive at a given point from any direction. If the source consists of a spectrum such as those shown in Figures 5-1 and 5-2, the situation is even more complex. In practice, the calculation of neutron fluences, fluxes, and spectra at some point distant from an endo-atmospheric nuclear explosion, or for the interior of a system that is operating exoatmospherically, is performed by complex computer codes. It is beyond the scope of this manual to provide the means for calculating all of these quantities or even to provide a description of the methodology. The latter is contained in Volume III of the "Weapons Radiation Shielding Handbook," DASA 1892-3 (see bibliography). Selected examples of the change in fluence and spectrum will be provided in succeeding paragraphs and figures.

██████ An extensive set of tabulated results of computer calculations of neutron fluxes and doses is contained in "Time-Dependent Neutron and Secondary Gamma-Ray Transport in an Air-Over-Ground Geometry," ORNL-4289, Vol. II, (see bibliography). These data were used to obtain the spectra that would result from the source spectra shown in Figures 5-1 and 5-2 at slant ranges of 390, 1,050, and 1,500 meters. The resulting spectra are shown in Figures 5-3 and 5-4, respectively. Note that the spectra in Figures 5-3 and 5-4 show 4π (slant range)^2 x

fluence. This does not mean that the spectra will be the same in all directions. The spectra shown in Figures 5-3 and 5-4 only apply to low air bursts and to *targets located on or near the surface of the earth*. The units for the ordinates in Figures 5-3 and 5-4 were chosen to allow a convenient visual comparison with Figures 5-1 and 5-2, respectively. Inspection of Figures 5-1 through 5-4 indicates that the shape of the fission source spectrum is not changed appreciably during transit through 1,500 meters of air (the relative abundance of extremely low energy neutrons, much lower energies than shown in Figures 5-1 through 5-4, will increase, however). The shape of the thermonuclear spectrum, on the other hand, does change as the neutrons penetrate air. The peak that exists at 14 MeV at the source becomes lower relative to the total, and the valley between about 8 and 12 MeV at the source becomes filled in as the higher energy neutrons are degraded to the 8 to 12 MeV range.

███████ Figures 5-5 and 5-6 show the neutron fluence for a receiver located on or near the surface of the earth as a function of slant range for the source spectra shown in Table 5-1. The fluence is shown for each of the energy intervals in Table 5-1. The total number fluence for neutron energies above 3.3 keV is also shown for each source. Once again the user is cautioned that these fluences should not be considered representative. They are presented as illustrative examples. Changes in weapon design will change the source spectrum, and this will modify the spectrum as well as the total number fluence at some distance from the explosion. Figures 5-5 and 5-6 also illustrate the large change in the spectral characteristics of the thermonuclear spectrum when compared to the variations in the fission spectrum with slant range.

███████ The preceding paragraphs have provided estimates of neutron fluences and spectra from low air bursts for detectors on or near the surface of the ground. The presence of an air-

ground interface can increase or decrease the neutron intensities by as much as an order of magnitude compared to intensities at corresponding distances in an infinite air medium as a result of reflections and absorption by the ground. For source detector separation distances less than a mean-free path,[*] localized reflection from the ground generally tends to increase the intensity of high energy neutrons; however, initial nuclear radiation is only of interest at very low yields at such short distances since other weapon effects normally will be dominant. At longer distances, the high energy neutron intensity may be reduced by a factor of five or more compared to infinite air when both the source and the detector are at the ground surface. These effects have been included in the calculations from which the preceding figures were derived.

███████ The estimation of neutron environments around an endoatmospheric nuclear explosion for receivers away from the surface of the earth requires a knowledge of the atmospheric properties along any path that a neutron might traverse from the weapon to the point of interest. Although atmospheric properties can change from day to day and from place to place, most calculations are based on a standard atmosphere such as the one described by the National Bureau of Standards in 1962. The important atmospheric constituents that affect neutron transport are

	Fraction by Weight
Nitrogen	0.7553,
Oxygen	0.2318.

███ A mean-free path is the distance in which the radiation intensity is decreased by a factor of e, where e is the base of the natural logarithms (about 2.718). The length of a mean-free path depends on the neutron energy and on whether only the direct fluence or the total (direct plus scattered) fluence is being considered.
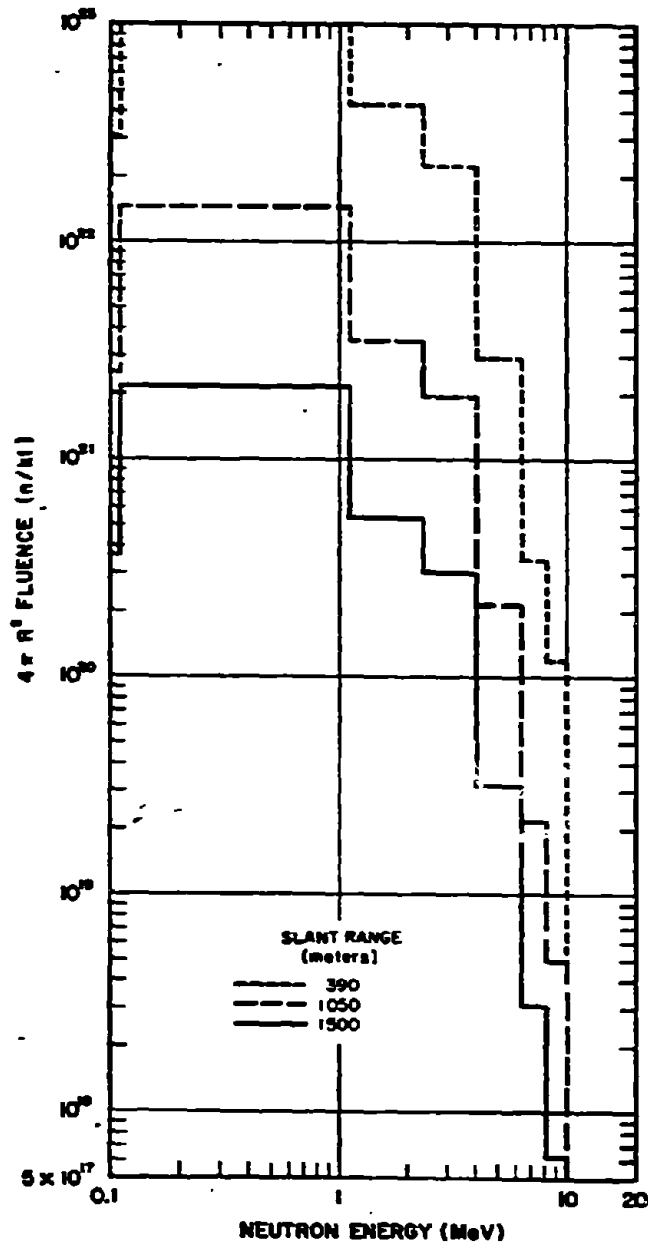
5-7

Figure 5-3. ▮▮▮▮ Spectra from the Fission Source
of Figure 5-1 with the Receiver
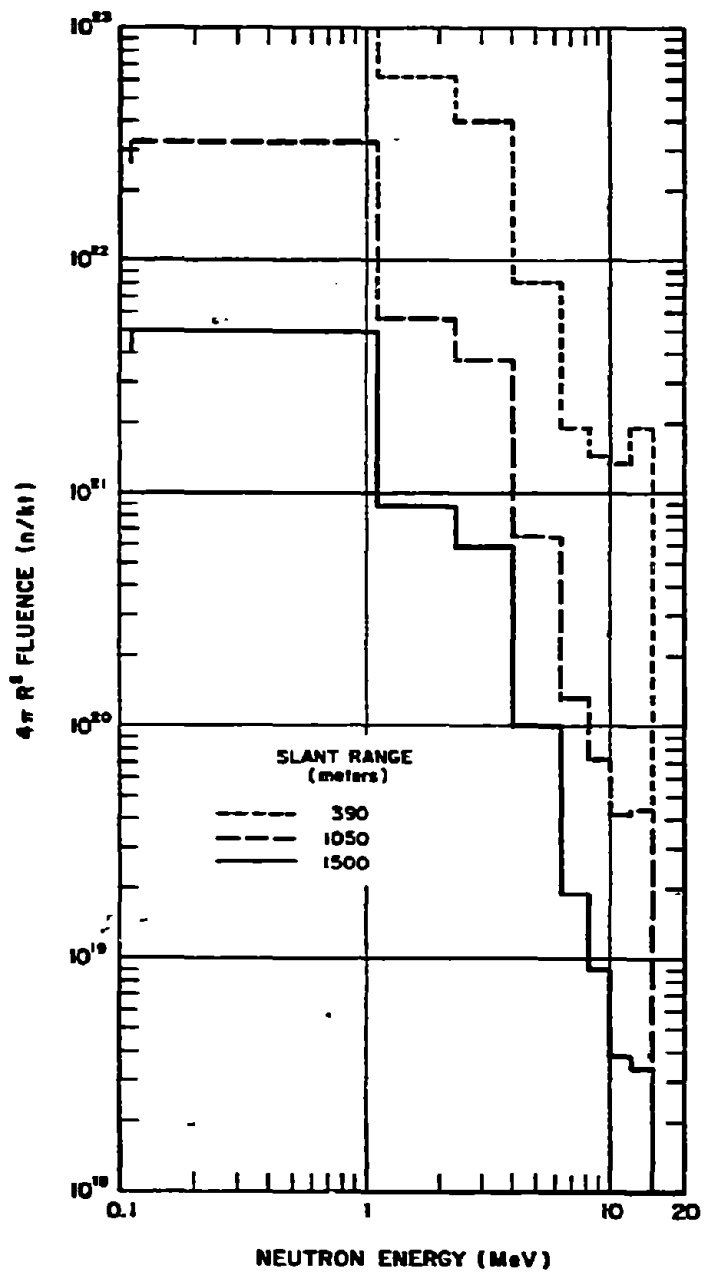On or Near the Surface of the
Earth at Various Slant Ranges ▮▮▮

Figure 5-4. ▮▮▮ Spectra from the Thermonuclear Source
of Figure 5-2 with the Receiver On or
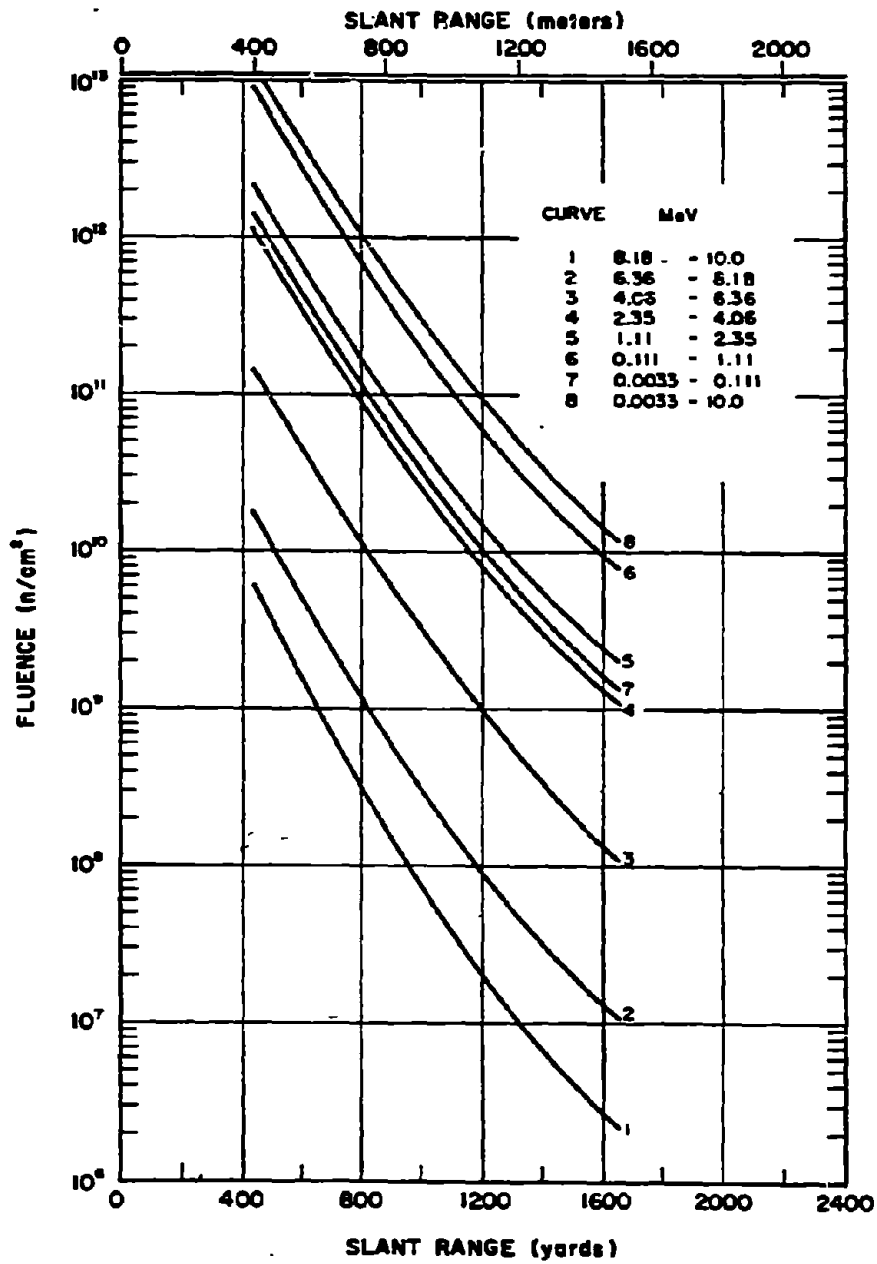Near the Surface of the Earth
at Various Slant Ranges ▮▮▮

SLANT RANGE (meters)

CURVE	MeV	
1	8.18	- 10.0
2	6.36	- 8.18
3	4.06	- 6.36
4	2.35	- 4.06
5	1.11	- 2.35
6	0.111	- 1.11
7	0.0033	- 0.111
8	0.0033	- 10.0

FLUENCE (n/cm²)

SLANT RANGE (yards)

Figure 5-5. ███ Neutron Fluence Incident on a Receiver Located On or Near the Surface of the Earth from the Fission Spectrum Shown in Table 5-1 and Figure 5-1 ███
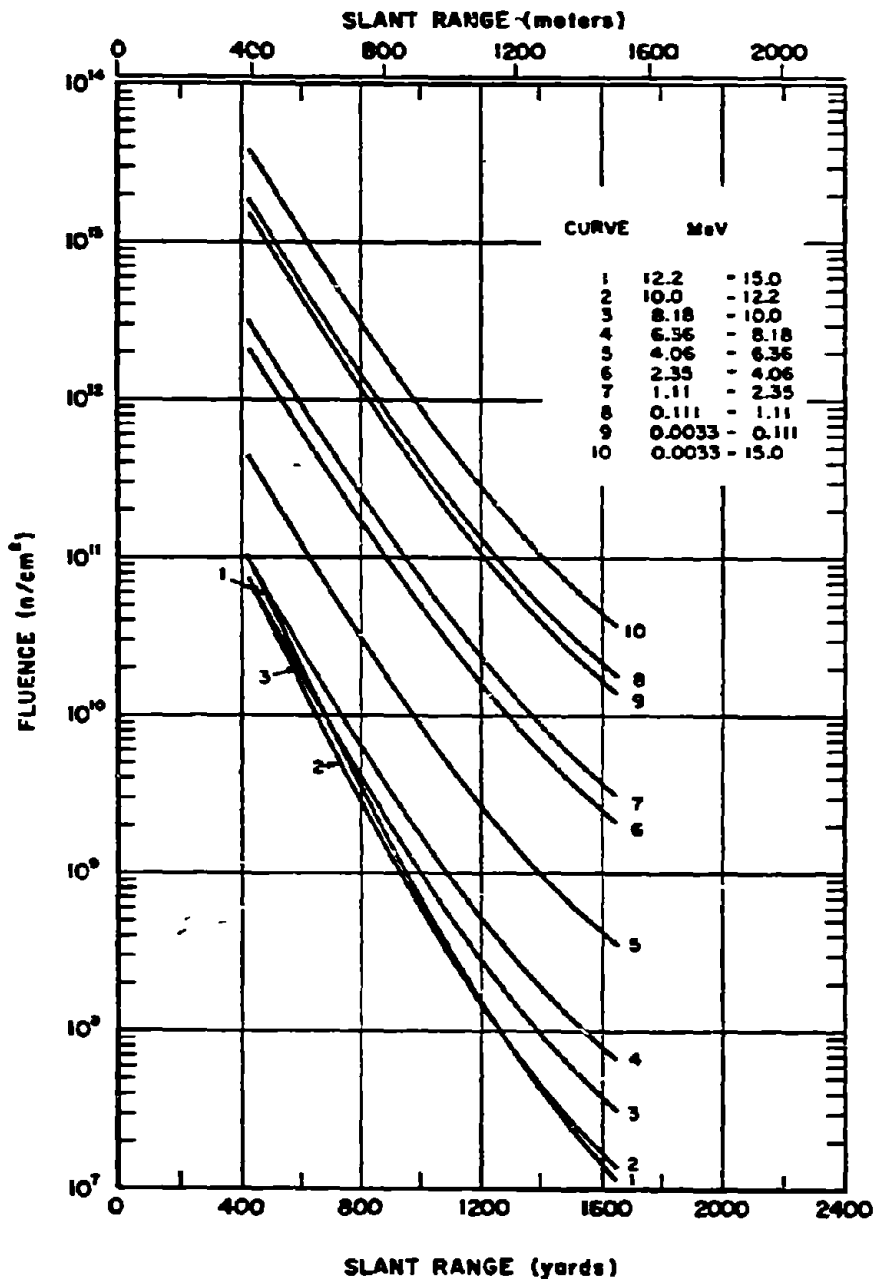
5-10

Figure 5-6. ▓ Neutron Fluence Incident on a Receiver Located On or Near the Surface of the Earth from the Thermonuclear Spectrum Shown in Table 5-1 and Figure 5-2 ▓

Other minor components of the atmosphere can be neglected without serious loss of accuracy.

The other principal feature of the standard atmosphere is its variation in density with altitude. The density, ρ, falls approximately exponentially with increasing altitude, as is shown in Table 5-2. Also shown is the quantity of air above a given altitude, h, which is given by the mass integral

$$q(h) = \int_{h}^{\infty} \rho(h')dh'.$$

Table 5-2 also shows the density normalized to the sea level density, ρ_0.

If two points are at altitudes h_1 and h_2 and are separated by a horizontal distance, d, then the slant range R is given by

$$R = \sqrt{d^2 + (h_2 - h_1)^2}$$

and the mass integral between them is given by

$$q(R) = \int_{0}^{R} \rho(h')ds' = R \frac{q(h_2) - q(h_1)}{h_2 - h_1}.$$

(U) This expression reduces to

$$q(R) = q(h_2) - q(h_1)$$

when $d = 0$ and (in the limit) to

$$q(R) = \rho(h)R$$

when $h_1 = h_2$ (the coaltitude case).*

If the air is characterized by an atomic density ρ_i for each important constituent, then

---

* The value of the mass integral as a function of altitude is shown in Figure 4-17 for various coaltitude separation distances.

Table 5-2. The Standard Atmosphere

Altitude (kft)	Air Density (g/cm³)	Mass Integral Above Altitude (g/cm²)	Density Normalized to Sea Level (ρ/ρ_0)
0	1.2250×10^{-3}	1.0331×10^{3}	1.0000×10^{0}
5	1.0556×10^{-3}	8.5967×10^{2}	8.6170×10^{-1}
10	9.0477×10^{-4}	7.1059×10^{2}	7.3859×10^{-1}
20	6.5312×10^{-4}	4.7525×10^{2}	5.3316×10^{-1}
30	4.5904×10^{-4}	3.0749×10^{2}	3.7473×10^{-1}
40	3.0267×10^{-4}	1.9305×10^{2}	2.4708×10^{-1}
50	1.8756×10^{-4}	1.1973×10^{2}	1.5311×10^{-1}
60	1.1628×10^{-4}	7.4292×10^{1}	9.4919×10^{-2}
70	7.1742×10^{-5}	4.6182×10^{1}	5.8565×10^{-2}
80	4.4174×10^{-5}	2.8855×10^{1}	3.6060×10^{-2}
90	2.7391×10^{-5}	1.8151×10^{1}	2.2360×10^{-2}

for every centimeter that a neutron traverses, there are ρ_i atoms of that type within a cross-sectional area of one cm^2 with which the neutron can interact. The probability that any reaction (elastic or inelastic scattering or neutron induced reaction) will occur is given in terms of a cross section $\sigma_{i,n}$ (so called because it has units of area), which is the probability of a given interaction (n) taking place with a given type of atom (i) under the condition that one interaction per unit area is possible. The probability of interaction per centimeter is therefore $\mu = \sum_{i,n} \rho_i \sigma_{i,n}$. Since this is also the probability that a neutron disappears from the incident beam, the beam intensity falls by a factor $e^{-\mu x}$ after having penetrated a distance x into the material. It is often convenient to express the penetration in terms of the total amount of material "seen" by a beam of neutrons, ρx, where ρ is the mass density of the material. In this case, the mass attenuation coefficient $\kappa = \mu/\rho$ is used. Thus, in the endoatmospheric case, the neutron fluence at a point depends not only on the spherical divergence described in paragraph 5-2 for the exoatmospheric case but also on exponential attenuation, so that

$$\varphi = \frac{N_0 e^{-\kappa \rho R}}{4\pi R^2} \; \text{n/cm}^2,$$

where κ is the radial distance from the source in centimeters and N_0 is the total number of neutrons emitted.

■■■ It is frequently convenient to replace the quantity ρR by the mass integral $q(R)$ described above, so that the equation for fluence becomes

$$\varphi = \frac{N_0 e^{-\kappa q(R)}}{4\pi R^2} \; \text{n/cm}^2.$$

This procedure is known as mass integral scaling. Notice that q will be different for different directions of R unless the atmosphere is essentially uniform, so that contours of constant fluence usually are not spherically symmetric about the burst point, although they usually are cylindrically symmetric about a vertical axis unless asymmetries are introduced by the weapon.

■■■ The expressions given above, however, only represent the component that reaches the point directly from the source. Scattered neutrons also reach the point from other directions. The result is that the fluence at that point is larger by a buildup factor B. The magnitude of B depends on the distance from the source, the energy spectrum of the neutrons, and the properties of the scattering material in complex ways. The flux of neutrons (neutrons/cm^2-sec) is altered as a result of the fact that scattered neutrons travel longer paths and neutrons of any given energy will arrive at the point over a finite time span even after undergoing only elastic scatterings. This alteration of the flux with distance is in addition to the alterations resulting from differences in time of flight of different energy neutrons discussed for exoatmospheric transport in paragraph 5-2, and further alterations will result from the changes in the spectral distribution during endoatmospheric transport. Moreover, the value of the mass attenuation coefficient κ varies with neutron energy so that even the direct fluence must be calculated by weighting monoenergetic calculations by the spectral distribution. For a given penetration distance, this weighting process can be replaced by using an effective κ, but the value of the effective κ will change with distance as a result of spectral changes.

■■■ In practice, the most accurate method for calculating neutron fluences uses computer codes with accurate neutron cross-section for each energy group and each scattering or interaction process. This technique is also essential for following neutrons out of the direct fluence as well as for calculating the flux. It is beyond the

scope of this manual to provide methods for calculating all of these quantities. Moreover, the vulnerability criteria of electronic components and systems to neutrons that are given in Section VII of Chapter 9 and in Section IV of Chapter 14 are given in terms of fluence (>10 keV fission). While these vulnerability criteria imply a knowledge of the spectrum, the calculation of the spectrum at the point of interest for any situation would require more information concerning source spectra than is provided herein. Therefore, the following discussion will be limited to the calculation of total number fluence for low altitude (deep) endoatmospheric bursts. It should be noted that the calculations of the curves shown in Figures 5-3 through 5-6 did make use of the results of computer calculations, and these curves are accurate representations of the spectra shown in Table 5-1 at various distances from an explosion. They are, however, limited to low air bursts and receivers on or near the surface. Likewise, the calculations of neutron dose presented in a later subsection are based on computer code transport calculations.

Low altitude (deep) endoatmospheric explosions are the next simplest case — after vacuum detonations — because the air density is sufficiently high that most of the attenuation occurs close to the burst point. Therefore, there are no large variations in density to affect critically the computation of fluences. In particular, the density of air through which the scattered neutrons reach a given point does not differ greatly from that through which the direct neutrons penetrate. Although whether or not altitudes are low (explosions are deep) depends on the energy spectrum of the weapon, if deep endoatmospheric conditions do prevail, the neutron fluence can be approximated by mass integral scaling. The total quantity of air (the mass integral) between the source and the point of interest is computed as described above, and then the appropriate buildup factors are applied

5-14

to the vacuum fluences calculated for the given energy spectrum as described in paragraph 5-2. Examples of such calculations are provided below.

No simple analytic expression gives the build-up factor, but Figure 5-7 shows the build-up in neutron fluences for various monoenergetic neutron sources. The curves in Figure 5-7 are based on Monte Carlo transport calculations in uniform air. Use of the curves in Figure 5-7 will provide reasonably accurate results up to burst altitude of about 60 kilofeet. The build-up factors in Figure 5-7 may be used with somewhat less confidence up to burst altitudes of 85 kilofeet. The effects of a non-uniform atmosphere become significant above 85 kilofeet, and computer calculations should be made for each burst altitude and spectrum of interest for burst altitudes between 85 and 200 kilofeet. It is beyond the scope of this manual to provide neutron environments for bursts in this altitude regime. For bursts above about 200 kilofeet, the vacuum calculations described in paragraph 5-2 may be used. Note that the build-up factors in Figure 5-7 are given as fractions of the vacuum fluence.

The source energy intervals used in the Monte Carlo calculations from which the curves in Figure 5-7 were derived are shown below:

Nominal Source Energy (MeV)	Source Energy Interval (MeV)
14.1	12.5 -16.0
10.0	9.0 -12.5
7.5	6.0 - 9.0
4.0	3.0 - 6.0
1.3	0.7 - 3.0
0.5	0.3 - 0.7
0.1	0.09- 0.3
0.03	0.01- 0.09

It is unfortunate that the source energy intervals used in the Monte Carlo calculations

FRACTION OF VACUUM NUMBER FLUENCE

10^1

10^0

10^{-1}

10^{-2}

10^{-3}

14.1 MeV

10 MeV

4 MeV

7.5 MeV

0.03 MeV

0.1 MeV

7.5 MeV

10 MeV

14.1 MeV

4 MeV

0.5 MeV

1.3 MeV

0   100   200   300
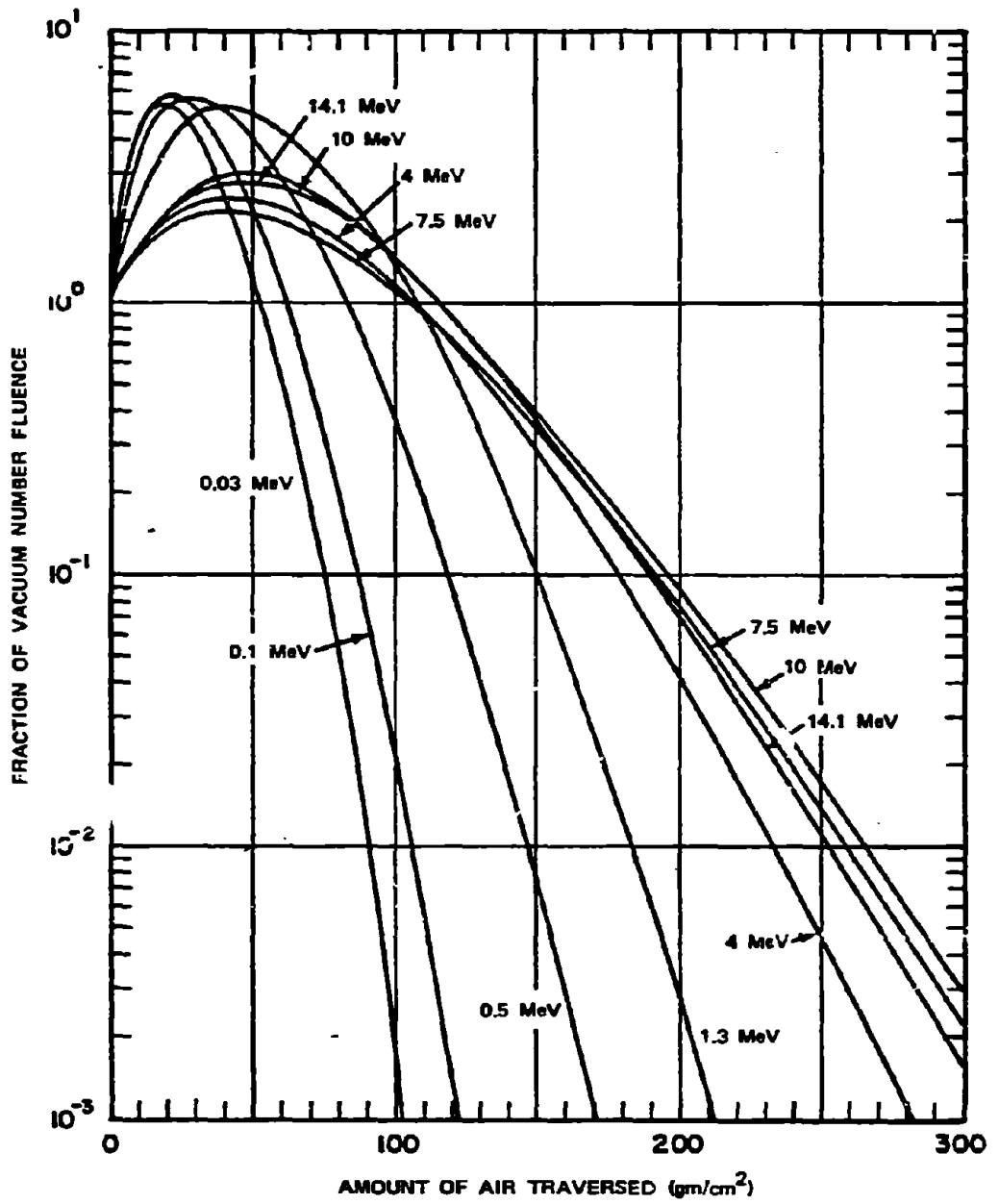
AMOUNT OF AIR TRAVERSED (gm/cm^2)

Figure 5-7. ▬ Neutron Energy Build-Up Factors for Various Monoenergetic Sources in Homogeneous Air ▬

differ from those shown in Table 5-1. However, many different source energy intervals will be found in reported weapon spectra. Most of the reported spectra will contain a uniform distribution (neutrons per MeV) within an energy band; however, some will contain an uneven distribution for the lower energies, e.g., 1/energy for energies below 0.1 MeV. In any case, it generally will be possible to divide the spectrum into energy groups that correspond roughly to those used in the preparation of Figure 5-7. Interpolation between the curves in Figure 5-7 should not be attempted; the spectral intervals should be adjusted to use the curves.

As an example of the use of Figure 5-7, consider a hypothetical weapon with the following spectrum:

Nominal Source Energy (MeV)	Neutrons per kt
14.1	1.23×10^{22}
10.0	3.00×10^{21}
7.5	3.80×10^{21}
4.0	1.36×10^{22}
1.3	4.25×10^{22}
0.5	1.72×10^{22}
0.1	2.74×10^{22}
0.03	8.24×10^{22}
Total	2.02×10^{23}

Assume that the neutron number fluence coaltitude at a distance of one mile from a 1 Mt explosion of such a weapon at a burst altitude of 60,000 feet is desired. The distance in centimeters is

$$1 \text{ (mile)} \times 1.609 \times 10^5 \text{ cm/mile}$$
$$= 1.609 \times 10^5 \text{ cm.}$$

The vacuum fluence, φ_i, for each of the monoenergetic neutron sources, N_{oi}, is

$$\varphi_i = \frac{N_{oi}}{4\pi R^2} = \frac{N_{oi}}{4\pi(1.609 \times 10^5)^2} = \frac{N_{oi}}{3.25 \times 10^{11}},$$

e.g., for the 14.1 nominal source energy, the vacuum fluence is

$$\varphi_{14.1} = \frac{(1.23 \times 10^{22} \text{ n/kt}) (10^3 \text{ kt/Mt})}{3.25 \times 10^{11}}$$

$$\varphi_{14.1} = 3.78 \times 10^{13} \text{ n/cm}^2.$$

In the same manner, the vacuum fluences for remaining source energies are determined to be

Nominal Source Energy (MeV)	Vacuum Fluence (n/cm^2)
14.1	3.78×10^{13}
10.0	9.22×10^{12}
7.5	1.17×10^{13}
4.0	4.18×10^{13}
1.3	1.31×10^{14}
0.5	5.29×10^{13}
0.1	8.42×10^{13}
0.03	2.53×10^{14}
Total	6.22×10^{14}

From Table 5-2, the ambient air density at 60 kilofeet is 1.1628×10^{-4} gm/cm^3. The mass integral at a coaltitude distance of one mile is

$$q(R) = \rho(h)R,$$

$$q(R) = (1.1628 \times 10^{-4})(1.609 \times 10^5),$$

$$q(R) = 18.7 \text{ gm/cm}^2.$$

From Figure 5-7, the build-up factors corresponding to traversal of 18.7 gm/cm^2 are

Nominal Source Energy (MeV)	Build-Up Factor (fraction of vacuum fluence)
14.1	2.0
10.0	2.0
7.5	1.75
4.0	1.9
1.3	3.5
0.5	5.0
0.1	5.6
0.03	5.2

The neutron fluences in air are obtained by multiplying the vacuum fluences by the build-up factors:

Nominal Source Energy (MeV)	Neutron Fluence in Air (n/cm²)
14.1	7.56×10^{13}
10.0	1.84×10^{13}
7.5	2.05×10^{13}
4.0	7.94×10^{13}
1.3	4.59×10^{14}
0.5	2.64×10^{14}
0.1	4.72×10^{14}
0.03	1.32×10^{15}
Total	2.71×10^{15}

Thus, 2.71×10^{15} neutrons/cm² are incident at a point coaltitude at a distance of 1 mile from a 1 Mt explosion of the hypothetical weapon described above burst at 60,000 feet. The corresponding vacuum fluence at the same distance would have been 6.22×10^{14} neutrons/cm². Thus, there is a factor of

$$\frac{2.71 \times 10^{15}}{6.22 \times 10^{14}} = 4.36$$

in the number of fluence for the explosion at 60,000 feet compared to the same distance from the same explosion in a vacuum. Note that the only meaningful fluence in air is the *total* number of fluences. Fluences shown for each nominal source energy represent number fluence *resulting* from that source energy, but any given source energy fluence would contain a spectrum of energies at the receiver. No information concerning the spectrum at the receiver can be obtained by the mass integral scaling demonstrated above.

If the point of interest is at an altitude that differs from that of the burst, but is still below 85 kilofeet, the only change in the pro-

cedure for determining the neutron fluence in air is in the determination of $q(R)$ to enter Figure 5-7. The appropriate value may be determined by the equations given previously together with the tabulated values in Table 5-2. Examples of the calculation of $q(R)$ for other than coaltitude cases are given in Problems 4-5 and 4-6, Chapter 4, which deal with mass integral scaling of X-rays. The same procedures for determining $q(R)$ apply to mass integral scaling of neutron fluences.

GAMMA RAYS

5-4 Gamma Ray Sources

As mentioned in the introductory paragraph to this section, there are several sources for the gamma rays that contribute to the initial nuclear radiation (that radiation delivered within 1 minute) from a nuclear explosion. These sources include the gamma rays that are released essentially simultaneously with the fission process, gamma rays resulting from non-fission interactions with weapon materials, gamma ray resulting from inelastic scattering of neutrons by atoms of the air (paragraph 5-3), gamma rays resulting from isomeric decays of weapon materials,* gamma rays resulting from neutron capture in nitrogen, and finally, gamma rays emitted during the decay of the fission products. Figure 5-8 provides an illustration of the time dependence of these various sources of gamma rays in terms of energy released per unit time

---

*Isotopes that have the same atomic number and the same atomic weight may differ in some property of their nuclei; these isotopes are called isomers. The nuclear property by which isomers may differ may be the type of particle emitted, the half-life or energy of the particle or the presence or absence of radioactivity. Here the interest is in those that emit gamma rays, either with or without accompanying particulate emissions. The gamma may be emitted by nuclei of weapon materials that have simply been raised to energy states above their normal state and return to their ground state by emitting one or more gamma rays.

per kt from a large yield weapon. The dotted curves in Figure 5-8 show the source as it would exist in a vacuum, i.e., the gammas resulting from inelastic scattering and neutron capture in the air would not be present under vacuum conditions. Not shown in Figure 5-8, but of potential importance for receivers near the surface of the earth in the vicinity of a low air burst are gammas that result from neutron interactions with the ground. It is convenient to divide the initial gamma radiation into two components: prompt gamma rays that result from the fission process and some neutron interactions with weapon materials, and are generally emitted within 1 to 2 shakes;* and delayed gamma radiation which originates from the sources described above subsequent to the prompt gamma ray emission and up to 1 minute after burst.

5-5 Prompt Gamma Rays ▮

▮▮▮ Prompt fission gamma rays are released essentially simultaneously with the fission process and thus their source rate behavior is determined by the rate profile of fission events in the weapon. These gamma rays escape before the detonation has appreciably deformed the weapon case or perturbed the atmosphere. The energy distribution of the fission gamma rays has been investigated using small samples of fissionable material; however, extrapolation of the small sample information to a weapon source involves considerable uncertainty because of the requirements to define the fission rate profile and to evaluate the attenuation provided by weapon materials as a function of time.

▮▮▮ Another source of very early gamma rays that contributes to the prompt pulse results from the non-fission interaction of neutrons with weapon materials.† These two sources combine to form a pulse of extremely short duration. Although the total amount of radiation given off during this period is small relative to the total, the peak rate of the pulse is extremely

high. In some cases, such as for high altitude systems, the high ionization rate produced by this pulse may be the damage mechanism extending to the greatest range from the explosion. At low altitudes, the peak rate is attenuated rapidly, as a result of gamma ray absorption and scattering out of the time region of the peak rate.

▮▮▮▮ The prompt gamma environment is very sensitive to weapon design and to weapon yield. Moreover, comparison of theory and experiment for specific weapons is poor. Most calculations and experiments agree that the prompt gamma yield ranges between 0.1 and 0.3 percent of the total yield. The prompt gamma energy output rate may be expressed as

$$\Phi_{\gamma p} = \frac{2.6 \times 10^{25} \, fW}{\tau} \text{ MeV/sec,}$$

where f is the fraction of the weapon energy emitted as prompt gamma, W is the weapon yield in kt, and τ is the emission time (2.6 x 10^{25} is the energy equivalent of 1 kt in MeV; see paragraph 1-1). Using the limits quoted above for f and τ would lead to

$$\frac{(2.6 \times 10^{25})(10^{-3})}{2 \times 10^{-8}} \leq \Phi_{\gamma p} \text{ (MeV/sec/kt)}$$

$$\leq \frac{(2.6 \times 10^{25})(3 \times 10^{-3})}{10^{-8}}$$

$$1.3 \times 10^{30} \leq \Phi_{\gamma p} \text{ (MeV/sec/kt)} \leq 7.8 \times 10^{30}.$$

▮ A shake is 10^{-8} seconds.

† ▮ Gamma rays from these interactions may continue to times on the order of 10 microseconds, but their contribution is generally small compared to other sources after one or two shakes beyond the time of peak gamma emission.
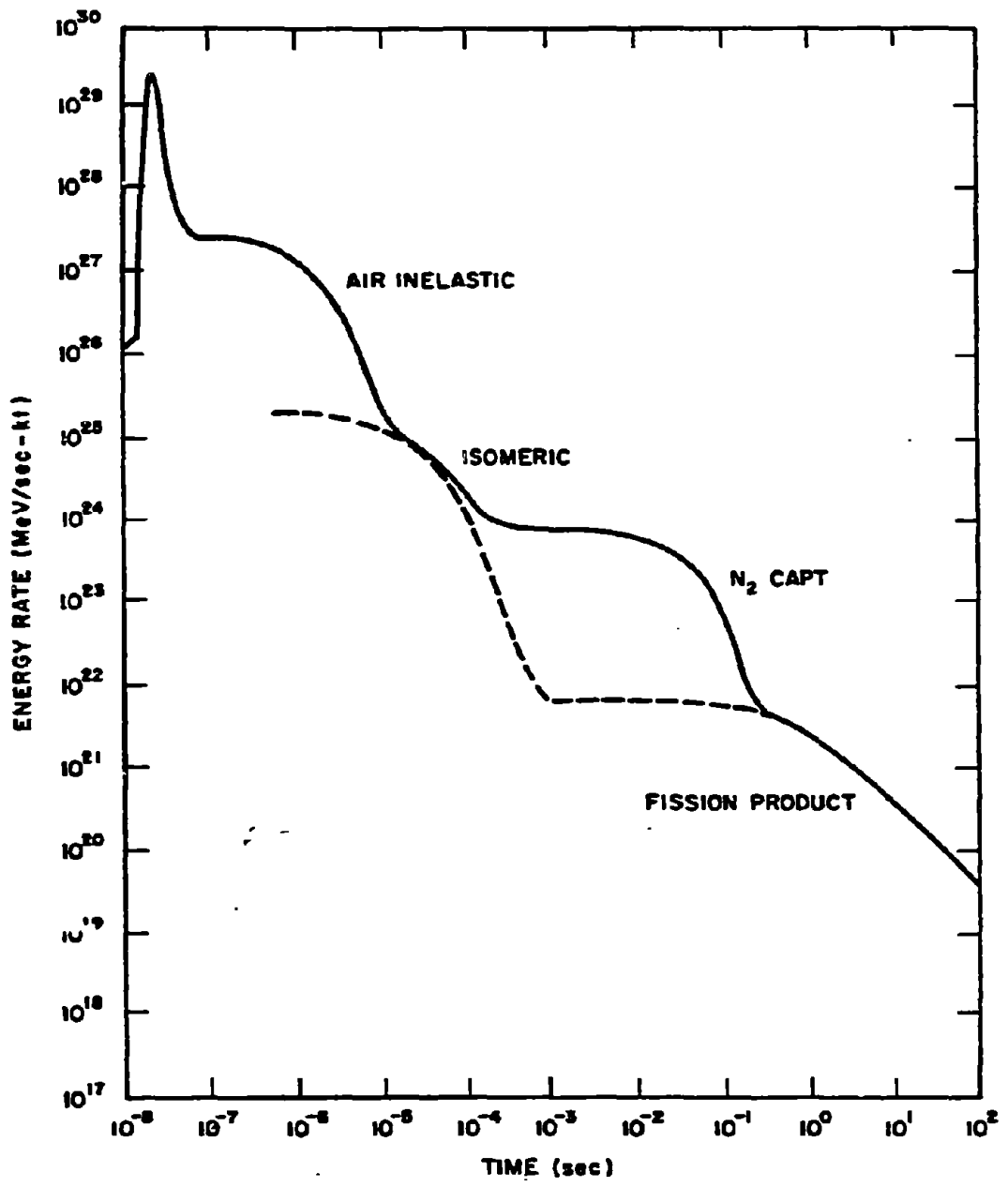
5-18

Figure 5-8. ▮▮▮▮ Calculated Time Dependence of the Gamma Ray
Output from a Large Yield Explosion,
Normalized to 1 kt ▮▮▮▮

However, results of calculations and experiments indicate that the peak gamma energy output rate is more likely to lie between 5×10^{29} MeV/sec/kt and 1×10^{31} MeV/sec/kt. As mentioned previously, the peak gamma energy output rate depends on yield and on weapon design. The yield dependence shows a rough correlation as follows

$$\Phi_{\gamma P} = (W)^{-0.29} \times 10^{31} \text{ MeV/sec/kt,}$$

at least between about 2 kt and 10 Mt. However, this does not account for the variation with weapon design, which might introduce differences on the order of plus or minus a factor of 3. Therefore, rather than use the yield dependent expression given above, it is recommended that the upper and lower limits given above be used for defensive and offensive estimates of the peak gamma energy output rate, respectively. Since no interactions take place in a vacuum, the peak prompt gamma exposure for exoatmospheric conditions should lie between

$$\Phi_{\gamma P} = \frac{10^{31} W}{4\pi R^2} \text{ MeV/cm}^2/\text{sec, and}$$

$$\Phi_{\gamma P} = \frac{5 \times 10^{29} W}{4\pi R^2} \text{ MeV/cm}^2/\text{sec,}$$

where W is the yield in kilotons, and R is the slant range in centimeters. These expressions are equivalent to

$$\Phi_{\gamma P} = \frac{8.57 \times 10^{20} W}{R_f^2} \text{ MeV/cm}^2/\text{sec, and}$$

$$\Phi_{\gamma P} = \frac{4.28 \times 10^{19} W}{R_f^2} \text{ MeV/cm}^2/\text{sec,}$$

where R_f is the slant range in kilofeet.

Gamma rays interact with matter in three ways. The first is called the Compton effect. In this type of interaction, a gamma ray (primary photon) collides with an electron, and its energy is transferred to the electron. A secondary photon, with less energy, is created and departs in a direction at an angle to the direction of motion of the primary photon. The second type of interaction of gamma rays with matter is the photoelectric effect. A gamma ray with energy somewhat greater than the binding energy of an electron in an atom, transfers all its energy to the electron, which is consequently ejected from the atom. Since the photon involved in the photoelectric effect transfers all of its energy, it ceases to exist and is said to be absorbed. The third type of interaction is pair production. When a gamma ray photon with energy in excess of 1.02 MeV passes near the nucleus of an atom, the photon may be converted into matter with the formation of a pair of electrons, equally but oppositely charged. The positive electron soon annihilates with a negative electron to form two photons, each having an energy of at least 0.51 MeV. In some cases, if the interaction takes place near the nucleus of a heavy atom, only one photon of about 1.02 MeV energy may be created. Figure 6-1, Chapter 6, illustrates the three processes qualitatively.

Any photon (e.g., an X-ray or a gamma ray) can produce ionization in a material by these processes of creating secondary electrons that deposit their kinetic energy by ionizing the medium in which they are created. The relative importance or frequency with which each process occurs depends upon the photon energy and the characteristics of the material. The Compton process is the dominant ionization mechanism for most gamma rays of interest, particularly in electronic materials such as silicon, of which many solid-state devices are fabricated.

The spectra of the prompt gamma rays are sensitive to weapon design and yield, just as

the gamma energy output rate is. It is beyond the scope of this manual to provide spectral information concerning sufficient samples of weapons spectra to be of general use (some such samples are provided in "Status of Neutron and Gamma Output from Nuclear Weapons (U)," DASA 2567 (see bibliography)). Moreover, with the wide range of prompt gamma output energy rates provided above, precise spectral data would be of little use. However, most of the prompt gamma rays lie in the energy range between 0.2 and 2 MeV, and in this energy range the Compton fractional energy loss is relatively constant. As mentioned above, the Compton process is the dominant energy transfer process for most electronic materials of interest (atomic number less than 20). These facts lead to a simplification in the relations between the incident prompt gamma energy fluence or energy flux and the energy absorbed by the material.

The unit of the absorbed energy, or dose, is the rad. One rad is the absorption of 100 ergs per gram of material being irradiated. Thus, the rad is independent of the type of radiation (e.g., gamma rays, neutrons, X-rays), but the material absorbing the radiation must be specified (e.g., rad (Si), rad (Ge), rad (tissue)). However, in view of the simplification mentioned above, in the case of *prompt gamma rays* and *materials with atomic numbers less than 20*, a simple conversion is possible, i.e.,

$$1 \text{ rad} = 2 \times 10^9 \text{ MeV/cm}^2, \text{ or}$$

$$1 \text{ rad/sec} = 2 \times 10^9 \text{ MeV/cm}^2/\text{sec}.$$

These are, of course, approximations. However, in view of the approximate nature of the prompt gamma energy flux that has been provided, and in view of the fact that effects of the prompt gamma dose rates on electronics given in Section VII of Chapter 9 and Section 4 of Chapter 14 are not provided for system design or for specific system vulnerability analyses but only as a general guide to vulnerability, the approximation is considered to be adequate.

As an example of the use of the dose conversion, consider a system with essentially no shielding for gamma rays that is operating exoatmospherically and that is 2,000 feet from a 100 kt explosion. It is desired to determine the peak gamma dose rate to a silicon transistor within the system. From the equations given previously, the maximum peak gamma energy flux incident on the system is expected to be

$$\Phi_{\gamma p} = \frac{8.57 \times 10^{20} W}{R_f^2},$$

$$\Phi_{\gamma p} = \frac{(8.57 \times 10^{20})(100)}{(2)^2}$$

$$\approx 2 \times 10^{22} \text{ MeV/cm}^2/\text{sec},$$

and the minimum energy flux is expected to be

$$\Phi_{\gamma p} = \frac{4.28 \times 10^{19} W}{R_f^2},$$

$$\Phi_{\gamma p} = \frac{(4.28 \times 10^{19})(100)}{(2)^2}$$

$$\approx 1 \times 10^{21} \text{ MeV/cm}^2/\text{sec}.$$

Thus the peak dose rate is expected to lie between

$$\dot{D}_{\gamma p} = \frac{2 \times 10^{22}}{2 \times 10^9} = 10^{13} \text{ rads (Si)/sec, and}$$

$$\dot{D}_{\gamma p} = \frac{10^{21}}{2 \times 10^9} = 5 \times 10^{11} \text{ rads (Si)/sec.}$$

In view of the lack of spectral data that has been provided, the prompt gamma ener-

gy flux for endoatmospheric can only be determined by use of an effective mass attenuation coefficient (see the discussion of neutron transport in paragraph 5-3). A reasonable effective mass attenuation coefficient for prompt gammas is about 2.8×10^{-2} cm^2/gm. Combining this with the exoatmospheric equations given previously, the direct peak prompt gamma ray energy flux may be estimated to lie between

$$\Phi_{\gamma p} = \frac{10^{31} W}{4\pi R^2} e^{-(2.8 \times 10^{-2})\rho R} \text{ MeV/cm}^2\text{/sec, and}$$

$$\Phi_{\gamma p} = \frac{5 \times 10^{29} W}{4\pi R^2} e^{-(2.8 \times 10^{-2})\rho R} \text{ MeV/cm}^2\text{/sec,}$$

where W is the yield in kt, ρ is the density in gm/cm^3, and R is the range in centimeters. As in the case for neutrons, the quantity ρR may be replaced by the mass integral $q(R)$. The mass integral may be determined from the equations given in paragraph 5-3 and the data tabulated in Table 5-2.

████ The prompt gamma dose may be bounded by multiplying the minimum and maximum dose rates by 1 and 2 shakes, respectively.

5-6 Air-Ground Secondary Gamma Rays ████

████ Potentially important sources of secondary gamma rays result from the inelastic scattering of high-energy neutrons by the nuclei of the air and ground, and the capture of thermal neutrons by the nitrogen-14 in the air and by various elements in the ground. The relative importance of the inelastic and capture gamma rays depends strongly upon the neutron spectrum of the source.

████ Most of these gamma rays are produced near the neutron source where the neutron fluence is highest. The short neutron flight time to the regions of most intense interaction, and the practically instantaneous character of the nu-

clear interaction accounts for the early ($10^{-7} < t < 10^{-5}$ sec) appearance of the secondary gamma components. The number of inelastic-scattering gamma rays relative to the total depends directly on the relative abundance of high-energy neutrons. The fraction of the total may be negligible in fission warheads or in large thermonuclear warheads. As the fusion yield fraction is increased the importance of the inelastic component will increase.

████ Any determination of the intensity of inelastic-scattering gamma rays must rely primarily upon analysis because of the difficulty in distinguishing the source of the different gamma rays measured in field tests. The first step in the analysis is that of neutron transport calculations. The local source strength of inelastic gamma rays is an energy dependent response to the local fluence of neutrons. Once the source intensity resulting from neutron interactions in air and ground is known, a gamma ray transport calculation must be performed to obtain the intensity at points of interest.

████ The energy spectrum of the gamma rays evolved in elastic scattering depends on the energy of the neutrons and the energy level structure of the nuclei with which the neutrons interact. However, the inelastic gamma rays are generally high in energy and, consequently, take on added significance when the target is behind a shield such as in a hardened military installation. Even though only a few percent of the gamma radiation incident on the shield results from inelastic scattering, it may be the source that is responsible for the maximum rate experienced by equipment inside the shielded installation since prompt gamma rays are attenuated more rapidly by shielding materials than the inelastic scattered gamma rays. Thus, where hardened installations are concerned, the inelastic gamma rays should be evaluated even in cases where they do not constitute a large fraction of the total free-field exposure. Methods for calculating the

tissue dose from secondary gamma rays are provided in the following subsection.

5-7 Fission Product Gamma Rays

Gamma rays produced by the decay of fission products following a fission detonation are an important source of radiation during the initial radiation time regime (the first minute following the explosion). The intensity of fission product gamma rays reaching a location of interest is affected by the complex source and media dynamics consisting of the formation and evolution of the fireball, the cloud expansion and rise, and the decay of the fission products with time. The fission products disperse throughout the cloud with the passage of time and the shape of the cloud may vary from spherical to toroidal as the materials forming the cloud rise through the atmosphere.

The formation of the fireball and the expansion and rise of the cloud depends upon weapon yield, weapon design, atmospheric conditions, and other parameters. The distribution of fission products in the cloud as a function of time is not well known, and, consequently, the attenuation of fission-product gamma rays within the cloud can only be approximated.

Atmospheric perturbation caused by the passage of the shock front also has a pronounced effect on the transport of fission-product gamma rays. The distribution of energy from a low altitude conventional fission weapon is such that roughly 50 percent of the energy is released in the form of blast and shock. The actual percentage depends on the weapon design and yield and on the nature of the surrounding environment (see Section I, Chapter 2). The percentage decreases for neutron enhanced weapons.

The sudden release of energy in the form of blast and shock produces an immediate increase in temperature and pressure thus produc-

ing hot, compressed gases from the weapon material. A pressure wave is initiated in the surrounding medium (paragraphs 1-4 through 1-6, 1-8, and Section I, Chapter 2). The characteristics of a shock wave is that there is a sudden increase of pressure at the front with a gradual decrease behind it. A severe change in the density of the heated air behind the shock front is associated with the pressure change. The large reduction in the air density, or optical depth, between the rising source and the receiver produces an enhancement of gamma ray intensities from hydrodynamic effects that is known as "hydrodynamic enhancement." These effects may last for several minutes and may extend to large distances from the explosion. The intensity and duration of hydrodynamic effects are yield dependent.

At early times when the shock front is located between the cloud and the receiver, the gamma ray intensity may increase because of the geometric displacement of the air. After the blast wave has passed the receiver, the gamma ray intensity is enhanced as a result of the reduced air density. This hydrodynamic enhancement becomes increasingly more important with higher weapon yields. For high yield weapons (in the megaton range), hydrodynamic enhancement can increase the fission-product gamma ray intensity by several orders of magnitude, with the result that fission product gamma rays can become the most important of all initial radiation sources.

With minimal hydrodynamic enhancement, as in the case of very low-yield weapons, the intensity of fission product gamma rays reaching a given point may be of approximately the same magnitude as that resulting from the secondary gamma ray sources. However, the average energy of the fission product gamma rays is considerably less than that of the secondary gamma rays, and the angle distribution of the fission product gamma rays is diffused by

the rise of the cloud. Each of these factors tends to reduce the penetrating power of fission product gamma rays relative to secondary gamma rays.

███ A reasonably accurate calculation of the transport of fission product gamma rays must consider such time-dependent parameters as ████ ███ ██████ decay, and hydrodynamic enhancement. The curves presented in the following subsection that show tissue dose from fission product gamma rays were constructed by the use of such a model.*

███████ INITIAL RADIATION DOSE TO PERSONNEL ██

███ The preceding paragraphs have described the complexity of the calculations of the source and environments produced by the initial nuclear radiations. Simplified, but reasonably accurate, methods have been developed to predict the dose to personnel located on or near the surface of the earth. These methods are described in the succeeding paragraphs and figures, and illustrations of their use are provided in four problems.†

███ Various units have been used to describe the radiation dose to personnel. One of the earliest, originally used to describe X-ray environments, is the roentgen, which is defined in terms of ionization produced in air. In view of the long history of the roentgen, various attempts have been made to develop units that described the response of living creatures or physical objects in terms of "roentgen equivalent" units. None of these was completely satisfactory since they depended strongly on the type and energy of the radiation, and their relationship to an exposure measured in roentgens was not always descriptive of the response of the target. Since the response of a target to radiation generally can be related to the energy absorbed, the rad has come into general use for the description of dose to any target. As previously defined in paragraph

5-5, one rad is the absorption of 100 ergs per gram of material being irradiated. Thus, the rad is independent of the type of radiation, but the material absorbing the radiation must be specified. The curves provided in this subsection provide a methodology for determining the dose in rads (tissue) for the various components of the initial nuclear radiation. The response of personnel, as a function of absorbed dose, is given in Section III of Chapter 10.

███ In view of the strong dependence of the neutron and secondary gamma ray environments on weapon design, no one representative weapon could be chosen to provide a basis for calculating dose to humans. The fission product dose is relatively independent of design specifics, but it is strongly dependent on total yield and the ratio of fission yield to total yield. Consequently, eight different weapons, for which case output data were available, were selected to perform the basic calculations from which the curves presented below were developed. It is believed that these eight weapons provide a sufficiently wide spectrum of designs that one of the eight will represent a given weapon of interest in a reasonable manner. The eight weapons are described in Table 5-3.

5-8 Initial Neutron Dose ███

███ Figures 5-9 through 5-11 provide all of the information necessary to calculate the contribution of neutrons to the initial nuclear radiation dose from each of the weapon types listed

*█ The development of this model is explained in "Improved Models for Predicting Nuclear Weapon Initial Radiation Environments (U)," DASA 2615 (see bibliography).

†██ ATR, which stands for Atmospheric Radiation Transport library, may be used to obtain exact answers to problems involving radiation transport in the atmosphere without the necessity of making specific transport calculations. ATR is documented in DNA 28031, "Models of Radiation Transport in Air – the ATR Code" (see bibliography). The Code itself may be obtained from the Radiation Shielding Information Center (RSIC), Oak Ridge, Tennessee.

Table 5-3. ███ Representative Types of Nuclear Weapons ██

Type	Description	Representative Yield Range
I	Subkiloton Fission	
II	Pure Fission Implosion	
III	Large (physically) Boosted Fission	
IV	Small (physically) Boosted Fission	
V	Enhanced Neutron Weapon	
VI	Gun-Assembly Fission Weapon	
VII	Thermonuclear Weapon	
VIII	Thermonuclear Weapon	

DNA
(k)(3)

in Table 5-3. Problem 5-1 describes the use of these figures to obtain the neutron dose.

5-9 Air-Ground Secondary Gamma Ray Dose ██

███ Figures 5-11 through 5-13 provide all of the information necessary to calculate the contribution of air-ground secondary gamma rays to the initial nuclear radiation dose from each of the weapon types listed in Table 5-3. Problem 5-2 describes the use of these figures to obtain the air-ground secondary gamma ray dose.

5-10 Fission Product Gamma Ray Dose ██

███ Figures 5-14 through 5-17 provide all of

the information necessary to calculate the contribution of fission product gamma rays to the initial nuclear radiation dose. Problem 5-3 describes the procedures for obtaining the fission product dose from these figures. Note the caution given in Problem 5-3 concerning interpolation between the hydrodynamic enhancement curves.

5-11 Total Dose ██

███ The total initial radiation dose is simply the sum of the contributions of the neutrons, the secondary gamma rays, and the fission product gamma rays. Problem 5-4 illustrates the calculation of total initial radiation dose.

Problem 5-1. Calculation of Neutron Radiation Dose

The spectrum and intensity of neutron radiation depends strongly upon the details of design of a nuclear weapon; however, it is possible to obtain neutron dose to personnel from a weapon of interest with reasonable accuracy if it is "similar" to one for which detailed calculations have been made. Eight "representative" types of weapons, listed in Table 5-3, provide the basis for such calculations within the following constraints:

● The weapon of interest must be similar to one of the representative types,

● The range of interest must lie between 400 and 5,000 yards,

● The detonation takes place in the "lower atmosphere," and

● The target is located on or near the surface of the earth.

Within the constraints listed above, Figures 5-9 through 5-11 provide the information necessary to obtain the dose to personnel located on or near the surface of the earth. If the air density is $\rho_0 = 1.225 \times 10^{-3}$ gm/cm^3, the neutron dose is

$$D_N = \frac{WF_N H_1}{R^2}$$

where

D_N is the total neutron dose (rads (tissue)),

R is the slant range (yards)

F_N is the value taken from Figure 5-9a or b or from Figure 5-10a or b for the most representative weapon type (yards^2 rads/ kt).

W is the weapon yield (kt), and

H_1 is the detonation height correction factor from Figure 5-11 (dimensionless).

If the air density differs from ρ_0, Figures 5-9 or 5-10 are entered with a scaled range R_ρ which is given by

$$R_\rho = \frac{\rho}{\rho_0} R = \bar{\rho} R,$$

where $\bar{\rho}$ is the relative air density. Values of ρ/ρ_0 are given in Table 5-2, and with smaller altitude increments in Table 2-1, Chapter 2. If the values of ρ/ρ_0 are different at the burst and the receiver, the average value should be used for $\bar{\rho}$. Note that R, not R_ρ, is still used in the denominator of the equation given above for D_N.

Example 1:

Given: A 30 kt surface burst of a weapon similar to type IV in air of average relative density $\bar{\rho} = 1.0$.

Find: The neutron dose delivered to a surface target 1,500 yards from the burst.

Solution: From Figure 5-9a, $F_N = 8.5 \times 10^6$ yards^2 rad (tissue)/kt for a type IV weapon at 1,500 yards.

Answer: The neutron dose delivered to a surface target 1,500 yards from a 30 kt surface burst of a type IV weapon is:

$$D_N = \frac{(30)(8.5 \times 10^6)(1.0)}{(1,500)^2},$$

$$D_N = 113 \text{ rads (tissue)},$$

Example 2

Given: A 500 kt burst at a   ht of 100 yards of a weapon similar to type   I in air of average relative density $\bar{\rho} = 0.9$.

Find: The neutron dose delivered to a target near the surface 2,000 yards from the burst.

Solution: The scaled range R_p = (0.9)(2,000) = 1,800 yards. From Figure 5-10a, F_N = 1.6 x 10^6 yards^2 rads (tissue)/kt for a type VII weapon at 1,800 yards. From Figure 5-11, H_1 = 2.07 for type VII at 100 yards *HOB.*

Answer: The neutron dose delivered to a target near the surface 2,000 yards from a type VII weapon at 100 yards *HOB* is:

$$D_N = \frac{(500)(1.6 \times 10^6)(2.07)}{(2,000)^2}$$

D_N = 414 rads (tissue).

Reliability. For weapons closely similar to one of the eight representative types, the predicted neutron dose is estimated to be correct within ±25 percent.

Related Material. See paragraphs 5-1 through 5-3. See also Tables 5-2 and 5-3.

Problem 5-2. Calculation of Secondary Gamma Ray Dose

████ Secondary gamma rays are those that result from neutron interactions, primarily with nitrogen in the air, as described in paragraph 5-6. Since the neutron output is strongly dependent upon details of weapon design, the secondary gamma ray output also depends upon weapon design; however, it is possible to obtain the secondary gamma ray dose to personnel from a weapon of interest if it is "similar" to one for which detailed calculations have been made. Eight "representative" types of weapons, listed in Table 5-3, provide the basis for such calculations within the following constraints:

- The weapon of interest must be similar to one of the representative types,
- The range of interest must lie between 400 and 5,000 yards,
- The detonation takes place in the "lower atmosphere," and
- The target is located on or near the surface of the earth.

████ Within the constraints listed above, Figures 5-11 through 5-13 provide the information necessary to obtain the secondary gamma dose to personnel located on or near the surface of the earth. If the air density is $\rho_0 = 1.225 \times 10^{-3}$ gm/cm^3, the secondary gamma dose is

$$D_{\gamma s} = \frac{W \, F_{\gamma s} \, H_1}{R^2}$$

where

$D_{\gamma s}$ is the secondary gamma ray dose (rads (tissue)),

R is the slant range (yards),

$F_{\gamma s}$ is the value taken from Figure 5-12a or b or from Figure 5-13a or b for the most representative weapon type (yards^2 rads/ kt),

W is the weapon yield (kt), and

H_1 is the detonation height correction factor from Figure 5-11 (dimensionless).

████ If the air density differs from ρ_0, Figures 5-12 or 5-13 are entered with a scaled range R_ρ.

$$R_\rho = \frac{\rho}{\rho_0} R = \bar{\rho} R.$$

where $\bar{\rho}$ is the relative air density. Values of ρ/ρ_0 are given in Table 5-2, and with smaller altitude increments in Table 2-1, Chapter 2. If the values of ρ/ρ_0 are different at the burst and the receiver, the average value should be used for $\bar{\rho}$. Note that R, not R_ρ, is still used in the denominator of the equation given above for $D_{\gamma s}$.

████ *Example 1* ████

Given: A 15 kt explosion at a height of 150 yards of a weapon similar to weapon type VI, in air of average relative density $\bar{\rho} = 1.0$.

Find: The secondary gamma ray dose delivered to personnel on the surface 1,500 yards from the burst.

Solution: From Figure 5-13a, $F_{\gamma s} = 3.7 \times 10^6$ yards^2 rads (tissue)/kt for a type VI weapon at 1,500 yards. From Figure 5-11, $H_1 = 2.03$ for a type VI weapon burst at 150 yards.

Answer: The secondary gamma ray dose delivered to a surface target 1,500 yards from a 15 kt burst of weapon type VI at 150 yards HOB is:

$$D_{\gamma s} = \frac{(15)(3.7 \times 10^6)(2.03)}{(1,500)^2}$$

$$D_{\gamma s} = 50 \text{ rads (tissue)}$$

████ *Example 2* ████

Given: A 0.08 kt burst at a height of 20

yards of a weapon similar to type I in average air density of $\bar{\rho} = 0.9$.

Find: The secondary gamma ray dose delivered to personnel on the surface 500 yards from the burst.

Solution: From Figure 5-12a, $F_{\gamma s} = 1.6 \times 10^8$ yards^2 rads/kt for a type I weapon at 500 yards. From Figure 5-11, $H_1 = 1.52$ for a type I weapon burst at 20 yards.

Answer: The secondary gamma ray dose delivered to a target near the surface 500 yards from a 0.08 kt burst of a type I weapon at 20 yards *HOB* is

$$D_{\gamma s} = \frac{(0.08)(1.6 \times 10^8)(1.52)}{(500)^2}$$

$$D_{\gamma s} = 78 \text{ rads (tissue)}.$$

Reliability. For weapons closely similar to one of the eight representative types, the predicted secondary gamma ray dose is estimated to be correct to within ±25 percent for slant ranges up to 1,500 yards. At longer ranges, the predicted values might be high although a precise estimate cannot be made.

Related Material. See paragraph 5-6. See also Tables 5-2 and 5-3.

Problem 5-3. Calculation of Fission Product Gamma Ray Dose

███████ Figures 5-14 through 5-17 provide the information necessary to calculate the fission product contribution to the initial nuclear radiation dose to personnel on or near the surface of the earth. Figures 5-14a through c provide the nominal dose per kt fission yield as a function of slant range for several relative air densities. The gamma dose as a function of slant range depends on cloud rise, which depends on weapon yield. The effects of cloud rise on exposure for a given yield depends on the burst height, and, to a slight extent, on the ambient air density. Analysis of the interdependence of these parameters has shown that reasonable accuracy can be retained by the use of two independent burst height adjustment factors, one associated with slant range, as shown in Figure 5-15, and the other associated with weapon yield, as shown in Figure 5-16. Figures 5-17a through e show hydrodynamic enhancement factors as a function of slant range for selected yields and several air densities. In using Figures 5-17a through e, no attempt should be made to perform a visual interpolation of the hydrodynamic enhancement factor between yields that are shown. Rather, a ▪▪▪ ▪▪ ▪▪▪ hydrodynamic enhancement factor as a function of yield should be made at the slant range and relative air density of interest, and the hydrodynamic enhancement factor should be obtained from this plot for the desired yield.

███████ The tissue dose from fission product gamma rays is obtained as follows:

$$D_{\gamma f} = W_f F_{\gamma f} H_R H_W E$$

where

$D_{\gamma f}$ is the fission product gamma ray dose at slant range R (rads (tissue)),

W_f is the fission yield (kt),

$F_{\gamma f}$ is the value taken from Figures 5-14a through c (rads (tissue)/kt),

H_R is the range dependent burst height adjustment factor from Figure 5-15 (dimensionless),

H_W is the yield dependent burst height adjustment factor from Figure 5-16 (dimensionless), and

E is the hydrodynamic enhancement factor from Figures 5-17a through e (dimensionless).

███████ Note that *fission* yield is used in the equation given above for fission product gamma ray dose; however, *total* yield is used to enter Figure 5-16 and Figures 5-17a through e.

███ *Example 1* ███

Given: A 50 kt pure fission weapon burst at a height of 100 yards in air of relative air density $\overline{\rho} = 0.8$.

Find: The fission product gamma ray dose to personnel on the ground at a slant range of 2,000 yards from the burst.

Solution: From Figure 5-14a, $F_{\gamma f} = 1.5$ rads (tissue)/kt for $\overline{\rho} = 0.8$ at 2,000 yards. From Figure 5-15, $H_R = 0.94$ for a height of burst of 100 yards and a slant range of 2,000 yards. From Figure 5-16, $H_W = 0.71$ for 50 kt total yield at a height of burst of 100 yards. From Figure 5-17d ($\overline{\rho} = 0.8$), $E = 6$ for a 50 kt total yield at 2,000 yards.

Answer:

$$D_{\gamma f} = (50)(1.5)(0.94)(0.71)(6),$$

$$D_{\gamma f} = 300 \text{ rads (tissue).}$$

███████ *Example 2* ███

Given: A 200 kt, 1:1 fission/fusion ratio

5-30

(i.e., 1/2 fission, 1/2 fusion) surface burst in air of average relative density $\bar{\rho} = 1.1$.

Find: The fission product gamma ray dose delivered to a target near the ground 1,000 yards from the burst.

Solution: The fission yield $W_f = (1/2)(200) = 100$ kt for a 1:1 fission/fusion ratio. From Figure 5-14a, $F_{\gamma f} = 17$ rads (tissue)/kt for $\bar{\rho} = 1.1$ at 1,000 yards. From Figure 5-15, $H_R = 0.94$ for a surface burst at 1,000 yards range. From Figure 5-16, $H_W = 0.63$ for a surface burst at 200 kt total yield. From Figure 5-17a, $E \simeq 24$ for 200 kt total yield at 1,000 yards (the best interpolation scheme for this figure is to make a plot on linear paper of E vs W at a constant R, and draw a smooth curve through the points).

Answer: The fission product gamma ray dose delivered to a target near the ground 1,000 yards from a 200 kt (1:1 fission/fusion) surface burst in air of average relative density 1.1 is:

$$D_{\gamma f} = (100)(17)(0.94)(0.63)(24)$$

$$D_{\gamma f} = 2.4 \times 10^4 \text{ rads (tissue)}.$$

Reliability. For submegaton yields the radiation dose predicted by equation 5.4 will be within 15 percent of the values calculated by the most sophisticated methods. The variations may approach 40 percent for megaton yields at ranges less than 1,000 yards; however, these are generally not interesting combinations. The total gamma ray dose predicted by the methods illustrated in Problems 5-2 and 5-3 when added together generally agrees with weapons test data within 50 percent and seldom disagrees by more than a factor of 2.

Related Material. See paragraph 5-7. See also Table 5-2.

Problem 5-4. Calculation of Total Initial Radiation Dose

The total initial radiation dose may be determined by calculating the neutron dose, the secondary gamma ray dose, and the fission product gamma ray dose separately, as described in Problems 5-1, 5-2, and 5-3 and summing the individual results.

Example

Given: A 10 Mt burst, 2:3 fission/fusion ratio (i.e., 2/5 fission, 3/5 fusion), of a weapon similar to type VIII at a height of 2,000 yards in air of average relative density $\bar{\rho} = 0.8$.

Find: The total radiation dose delivered to a target near the surface at a slant range of 4,000 yards from the burst.

Solution: For the neutron dose, the scaled range is $R_\rho = (0.8)(4,000) = 3,200$ yards. From Figure 5-10b, $F_N = 5 \times 10^3$ yards^2 rads (tissue)/kt for type VIII at 3,200 yards. From Figure 5-11, $H_1 = 2.16$ for type VIII over 200 yards HOB. For the secondary gamma ray dose, the same scaled range and height correction factors apply. From Figure 5-13b, $F_{\gamma s} = 5 \times 10^4$ yards^2 rads (tissue)/kt for type VIII at 3,200 yards. For the fission product gamma ray dose, the fission yield is $W_f = (2/5)(10,000) = 4,000$ kt for a 2:3 fission/fusion ratio. From Figure 5-14b, $F_{\gamma f} = 1.3 \times 10^3$ rads (tissue)/kt for $\bar{\rho} = 0.8$ at 4,000 yards. From Figure 5-15, $H_R = 0.62$ for a 2,000 yard HOB and a slant range of 4,000 yards. From Figure 5-16, $H_W = 0.24$ for a 2,000 yard HOB and a total yield of 10 Mt. From Figure 5-17d, $E = 4.1 \times 10^3$ for 10-Mt total yield at 4,000 yards.

Answer:

$$D_N = \frac{WF_N H_1}{R^2}$$

$$D_N = \frac{(10,000)(5 \times 10^3)(2.16)}{(4,000)^2}$$

$$D_N = 6.8 \text{ rads (tissue)}$$

$$D_{\gamma s} = \frac{WF_{\gamma s} H_1}{R^2}$$

$$D_{\gamma s} = \frac{(10,000)(5 \times 10^4)(2.16)}{(4,000)^2}$$

$$D_{\gamma s} = 68 \text{ rads (tissue)}$$

$$D_{\gamma f} = W_f F_{\gamma f} H_R H_W E$$

$$D_{\gamma f} = (4,000)(1.3 \times 10^{-3})(0.62)(0.24)(4.1 \times 10^3)$$

$$D_{\gamma f} = 3,170 \text{ rads (tissue)}$$

$$\text{Total Dose} = D_N + D_{\gamma s} + D_{\gamma p}$$

Total Dose = 6.8 + 68 + 3,170 = 3,245 rads (tissue).

Reliability. See problems 5-1, 5-2, and 5-3 for reliability statements for the individual components of the total dose. There are no corroborating data; however, it is estimated that the total dose prediction would fall within ±25 percent of the true value, except for megaton yield weapons at slant ranges less than 1,000 yards, where the error is likely to be ±50 percent.

Related Material. See paragraphs 5-5 through 5-7. See also Tables 5-2 and 5-3.
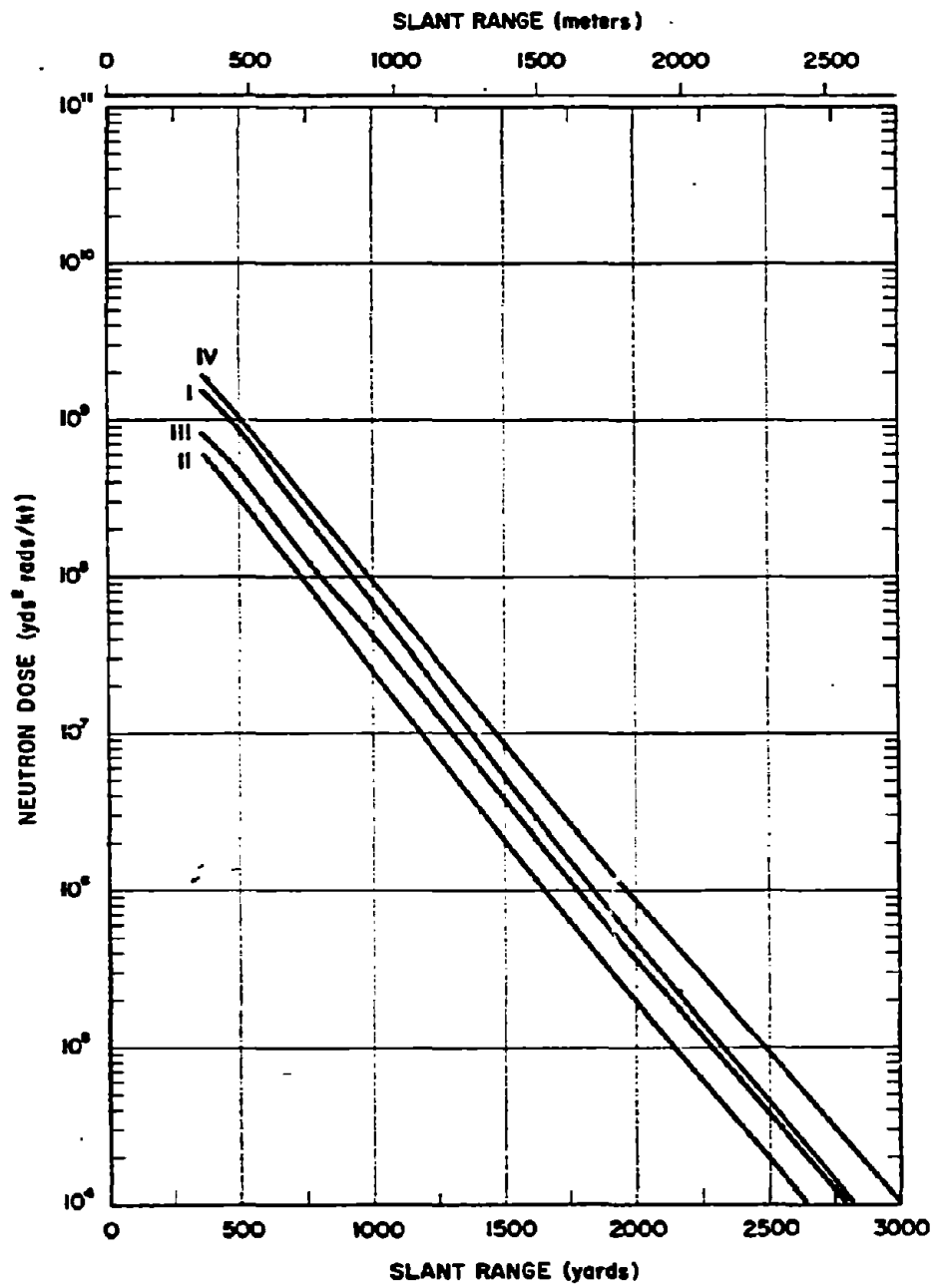
Figure 5-9a. ▓▓▓ Neutron Dose as a Function of Slant Range from a 1 kt Surface Burst, Weapon Types I through IV, Short Ranges ▓▓▓
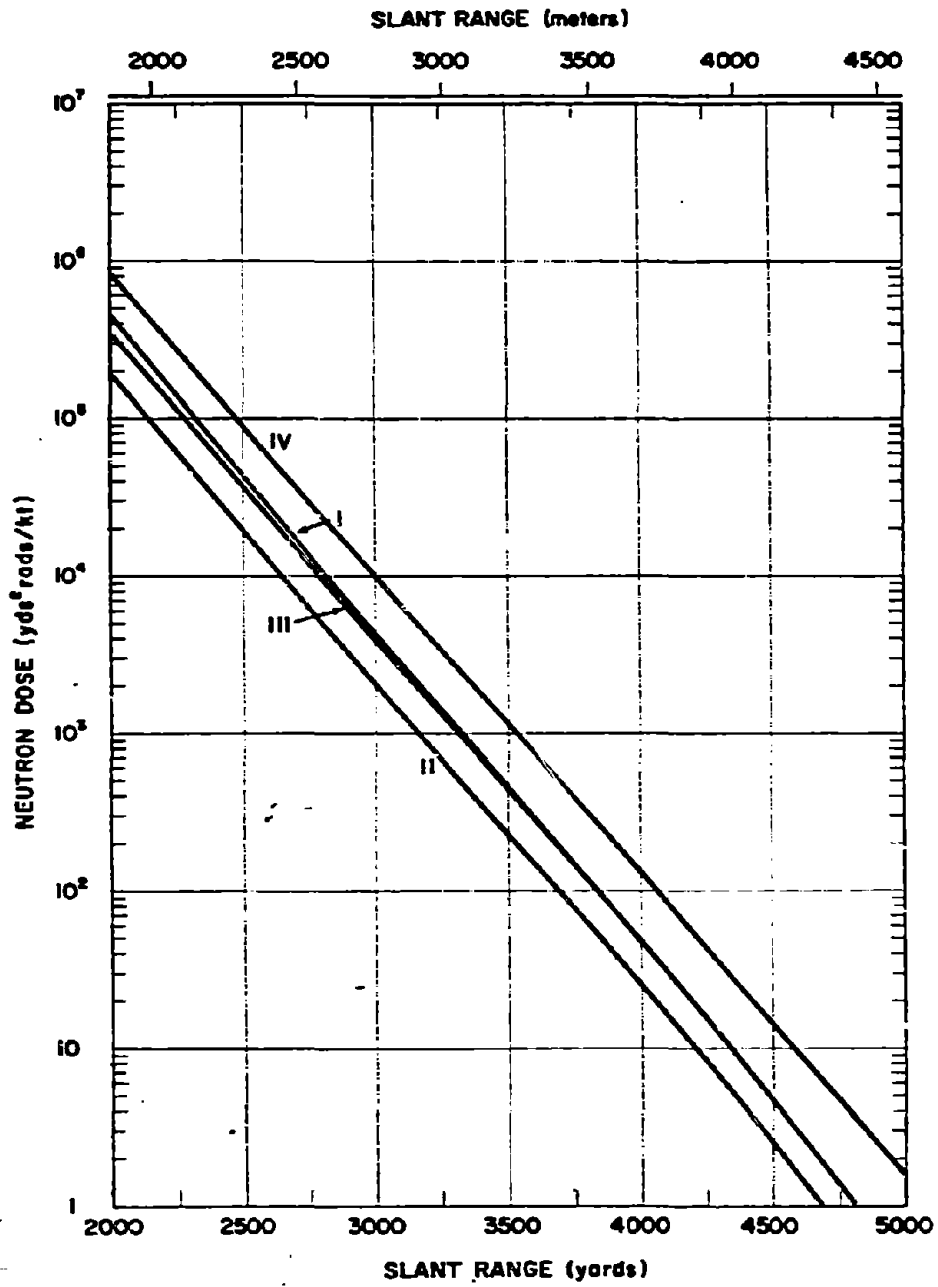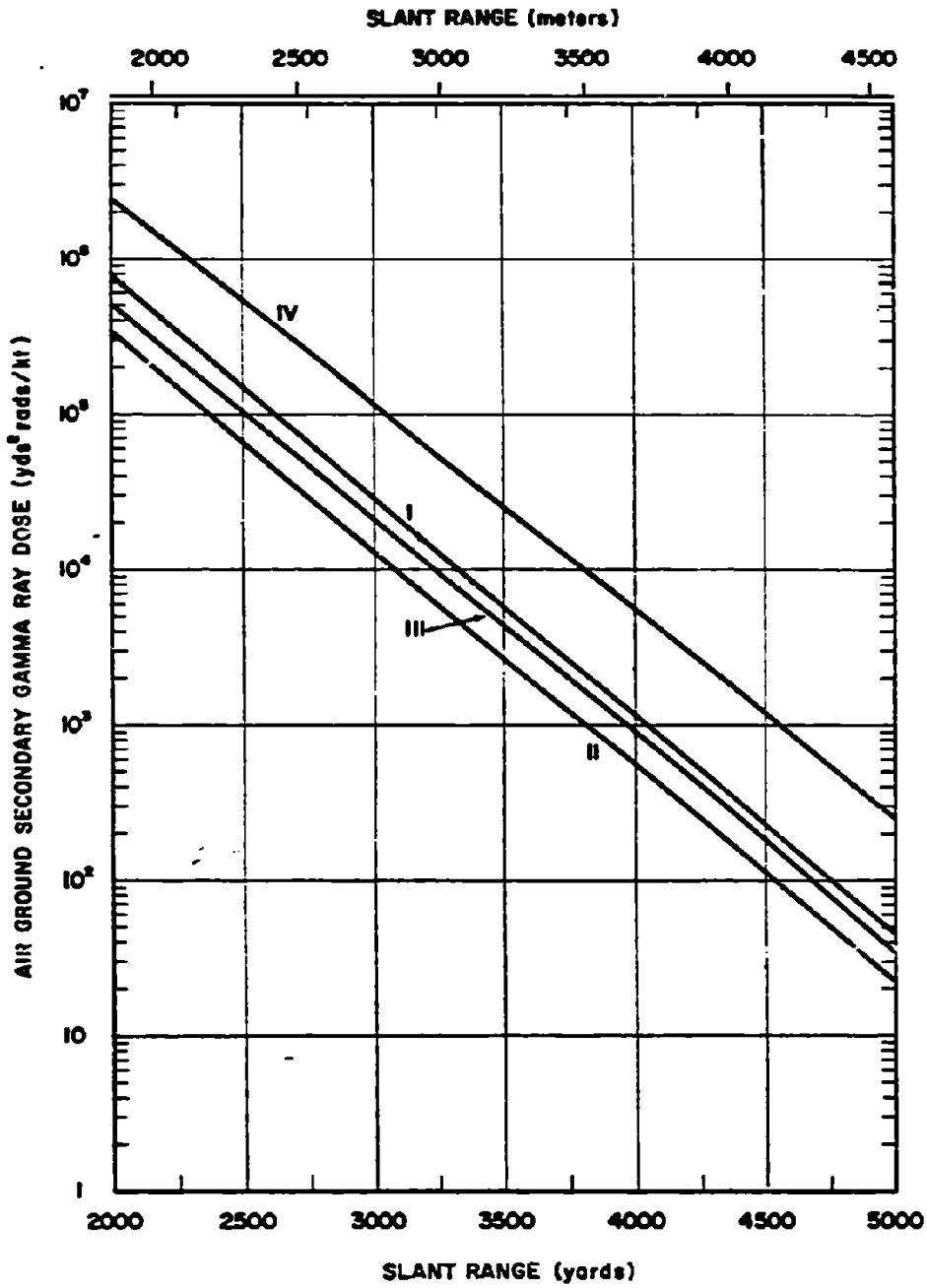
Figure 5-9b. ▆▆ Neutron Dose as a Function of Slant Range from a 1 kt Surface Burst, Weapon Types I through IV, Long Ranges ▆▆
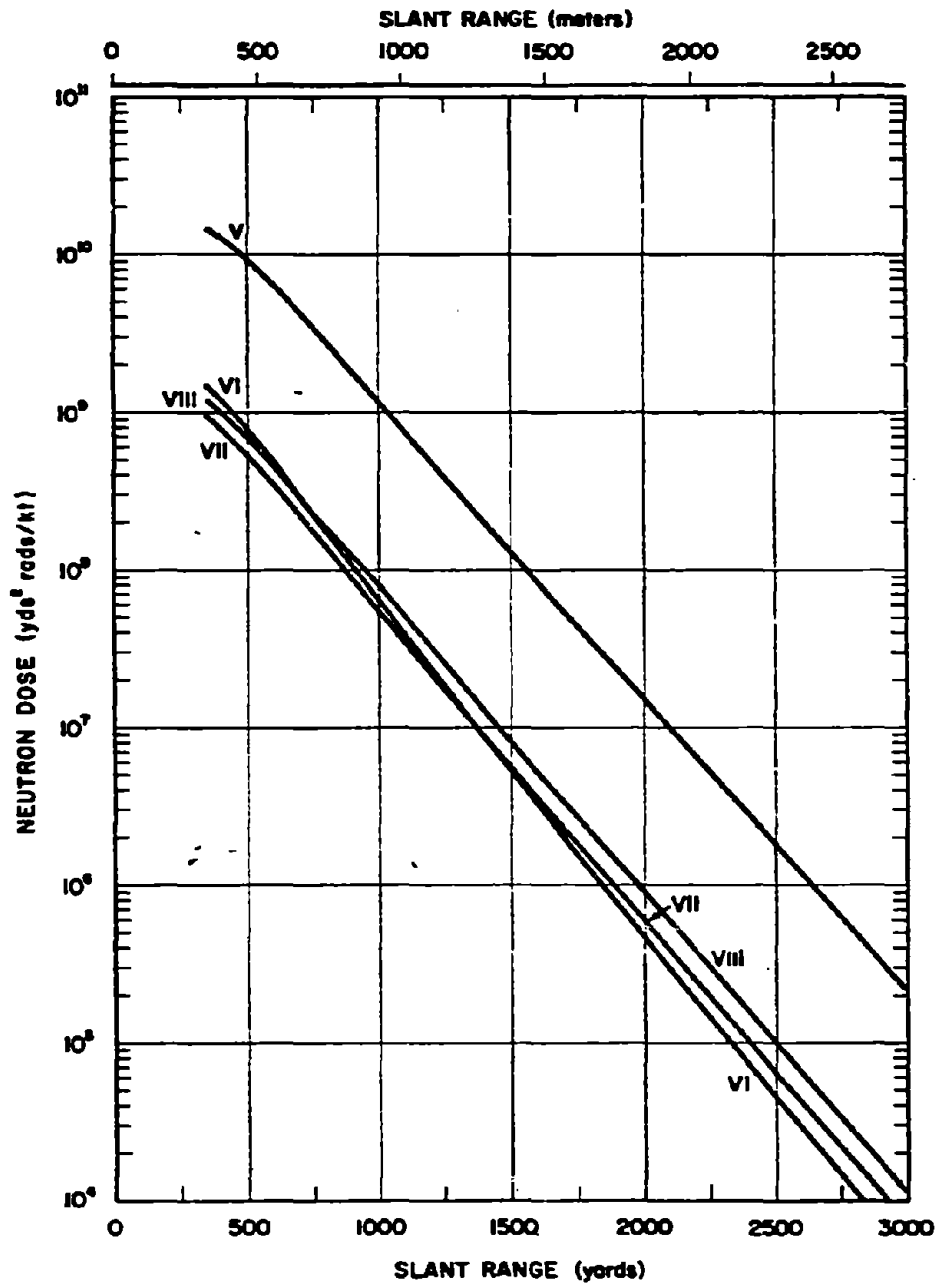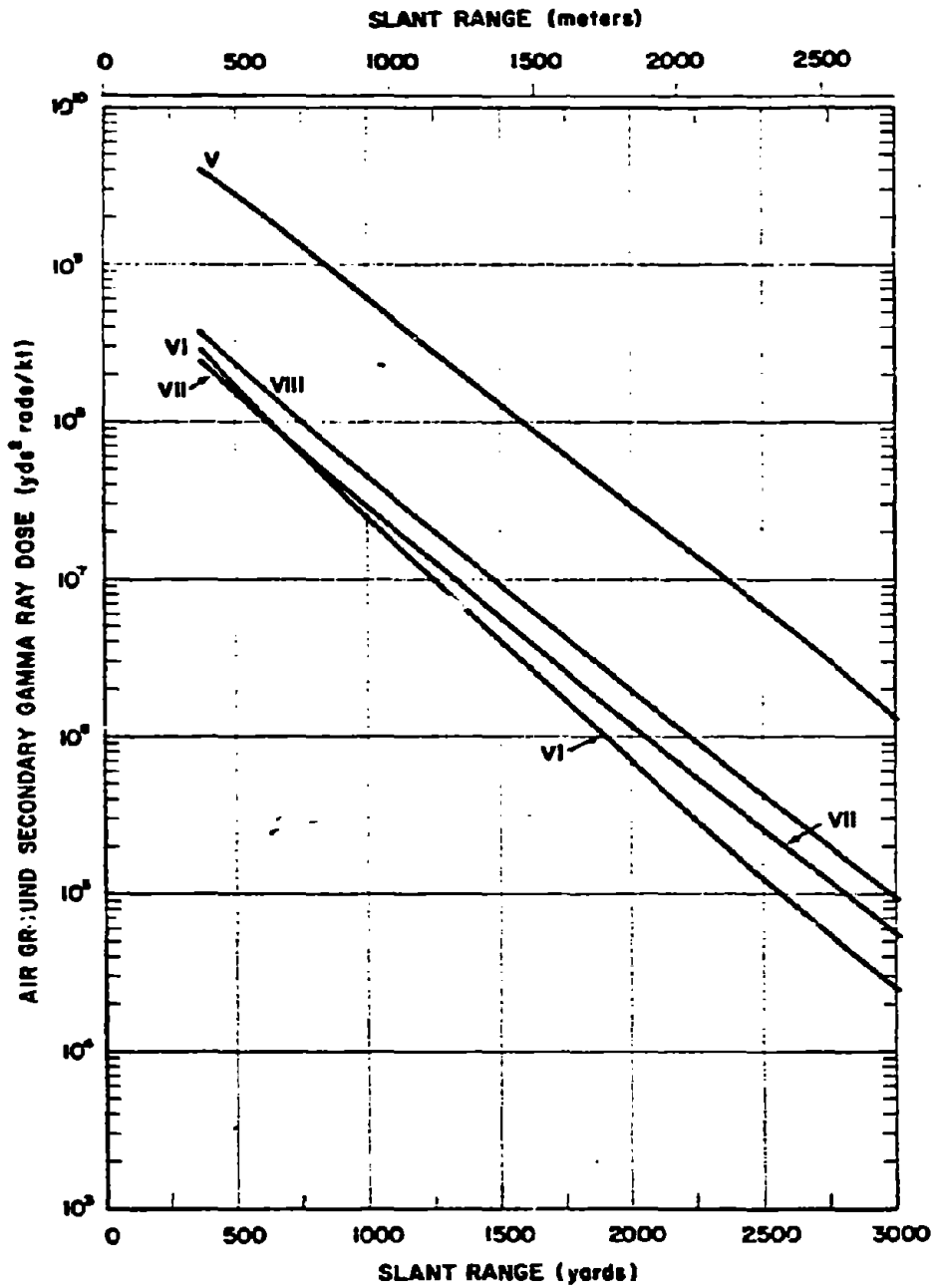
Figure 5-10a. ▮▮▮ Neutron Dose as a Function of Slant Range from a 1 kt Surface Burst, Weapon Types V through VIII, Short Ranges ▮▮▮
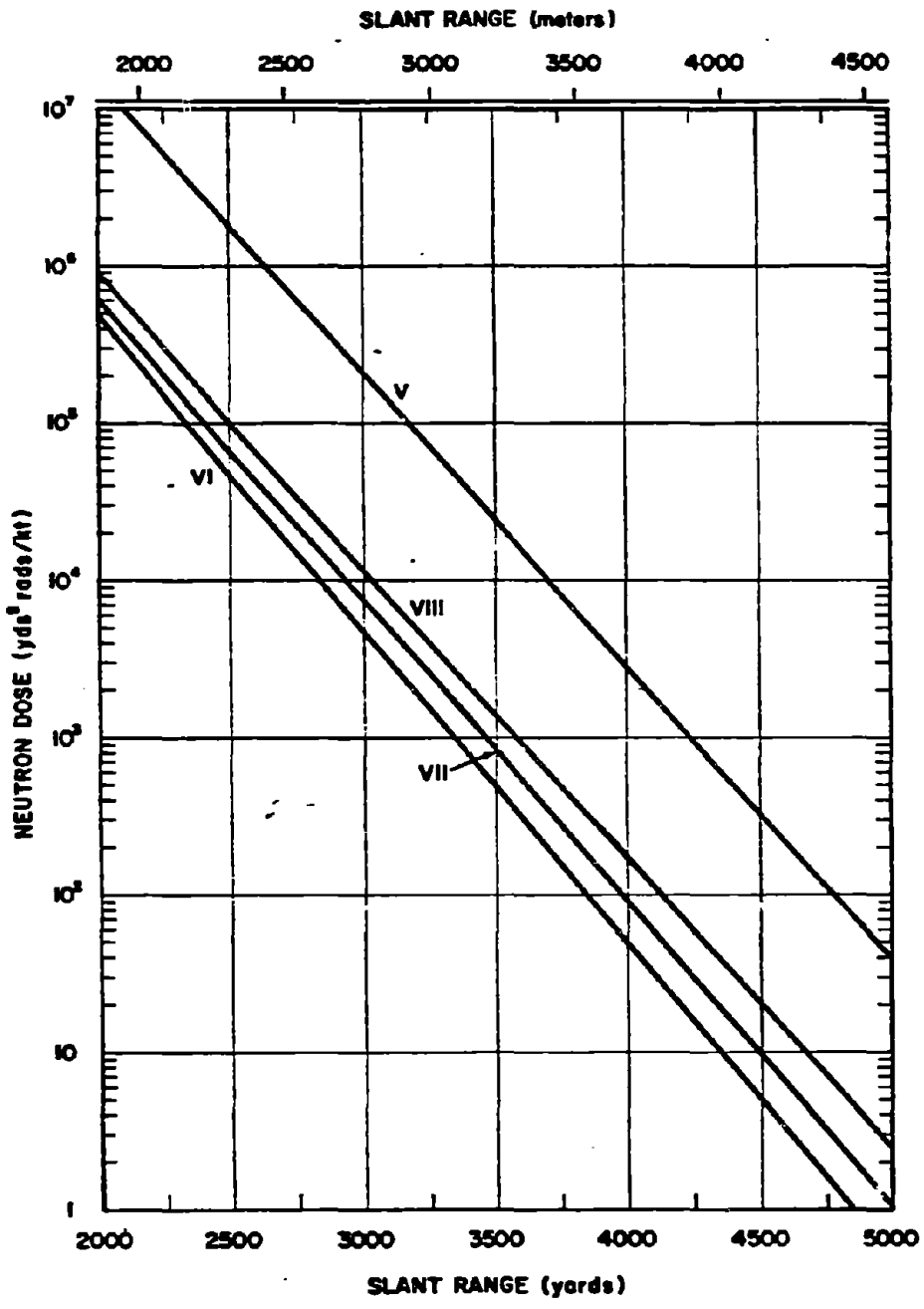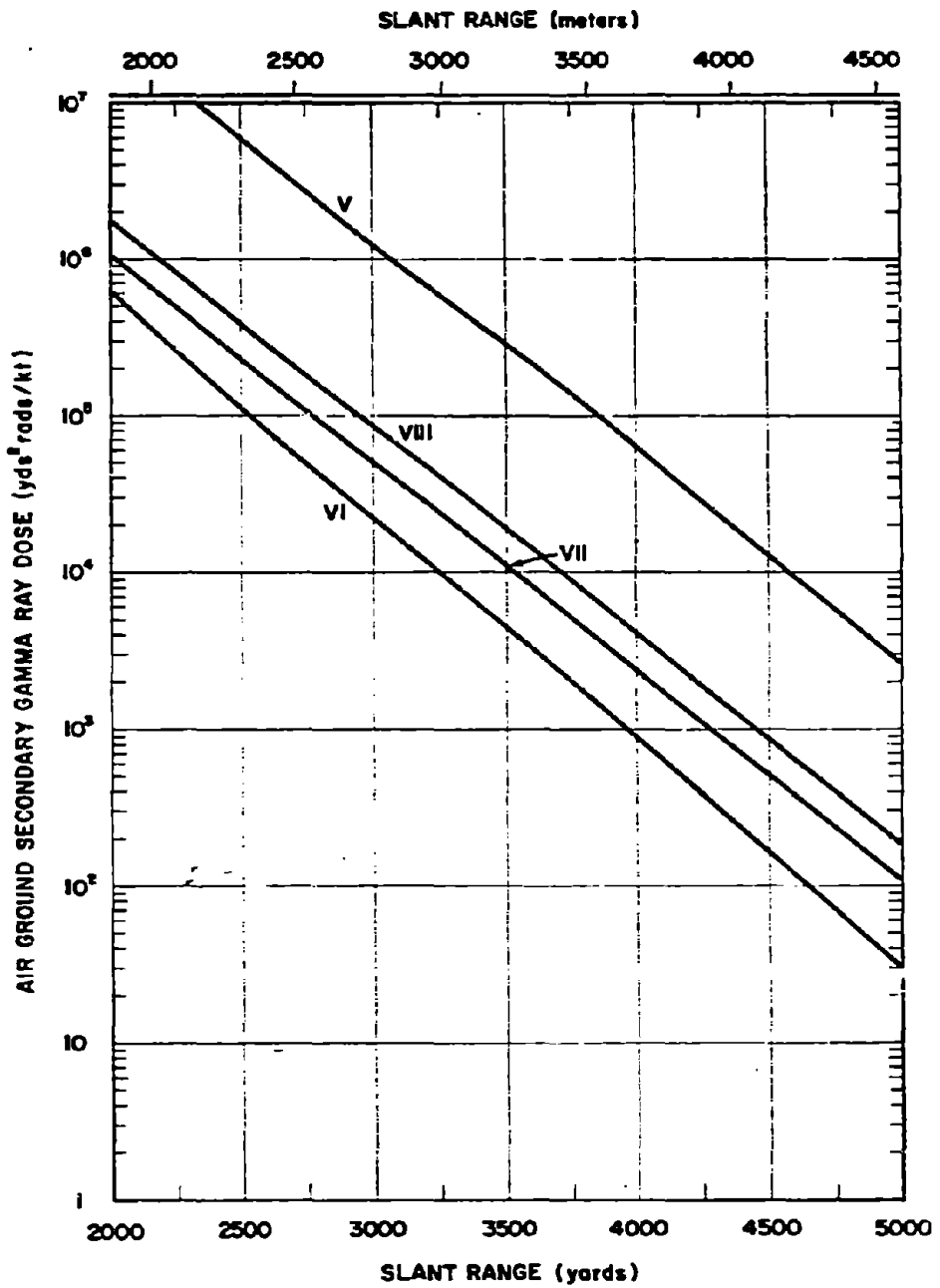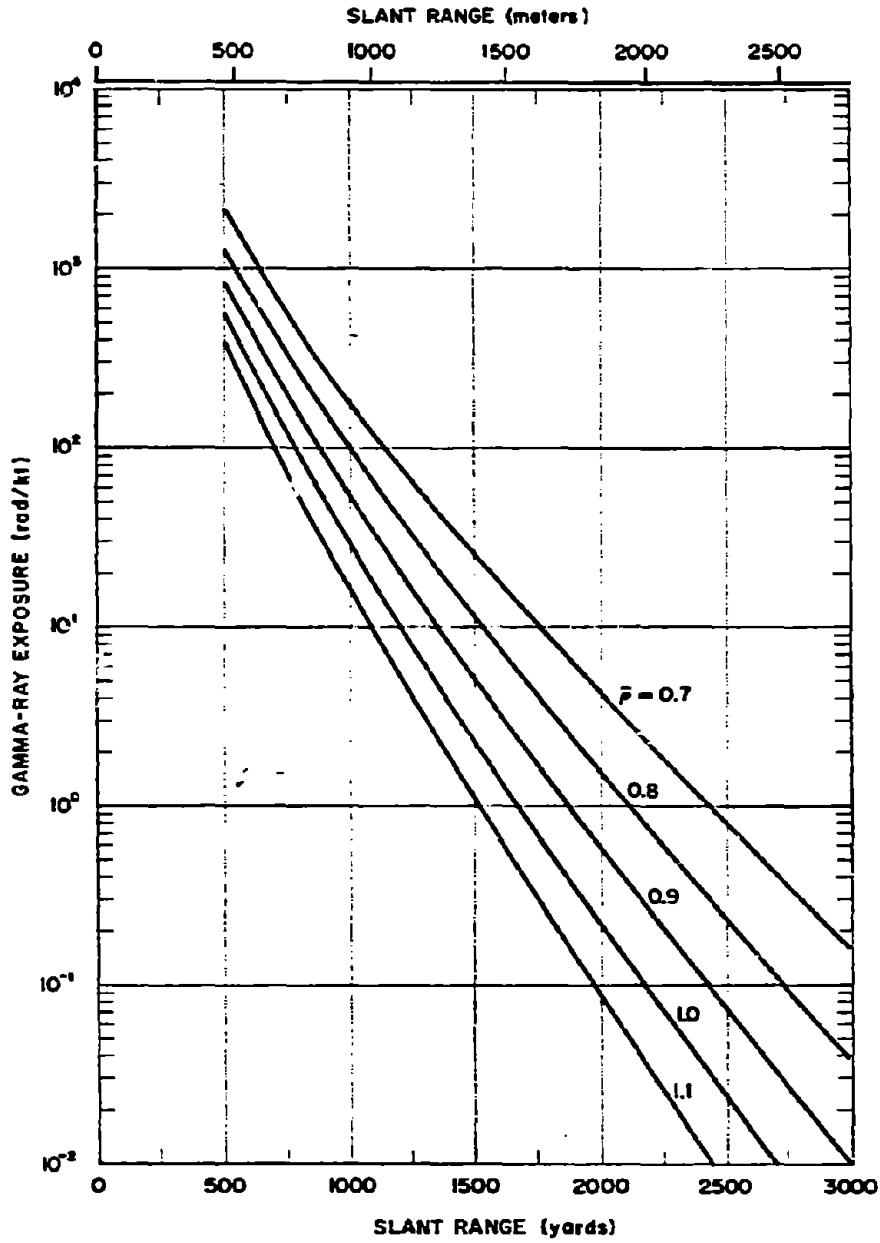
Figure 5-10b. ▓▓ Neutron Dose as a Function of Slant Range from a 1 kt
Surface Burst, Weapon Types V through VIII, Long Ranges ▓▓

HEIGHT OF BURST (meters)
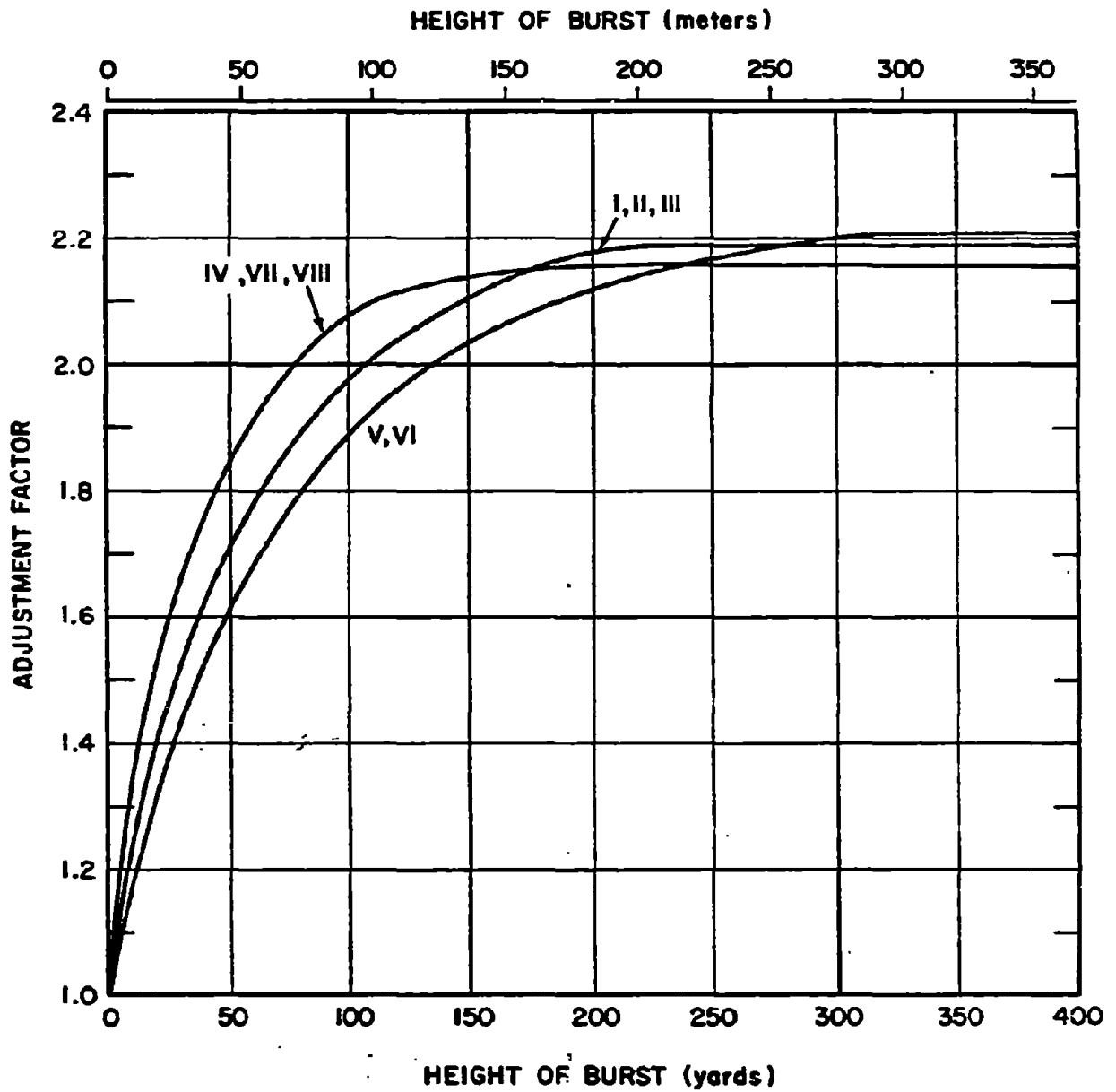
Figure 5-11. ⬛ Burst Height Adjustment Factors for Neutrons and Secondary Gamma Rays ⬛

SLANT RANGE (meters)

AIR GROUND SECONDARY GAMMA RAY DOSE (yds²rods/kt)

SLANT RANGE (yards)
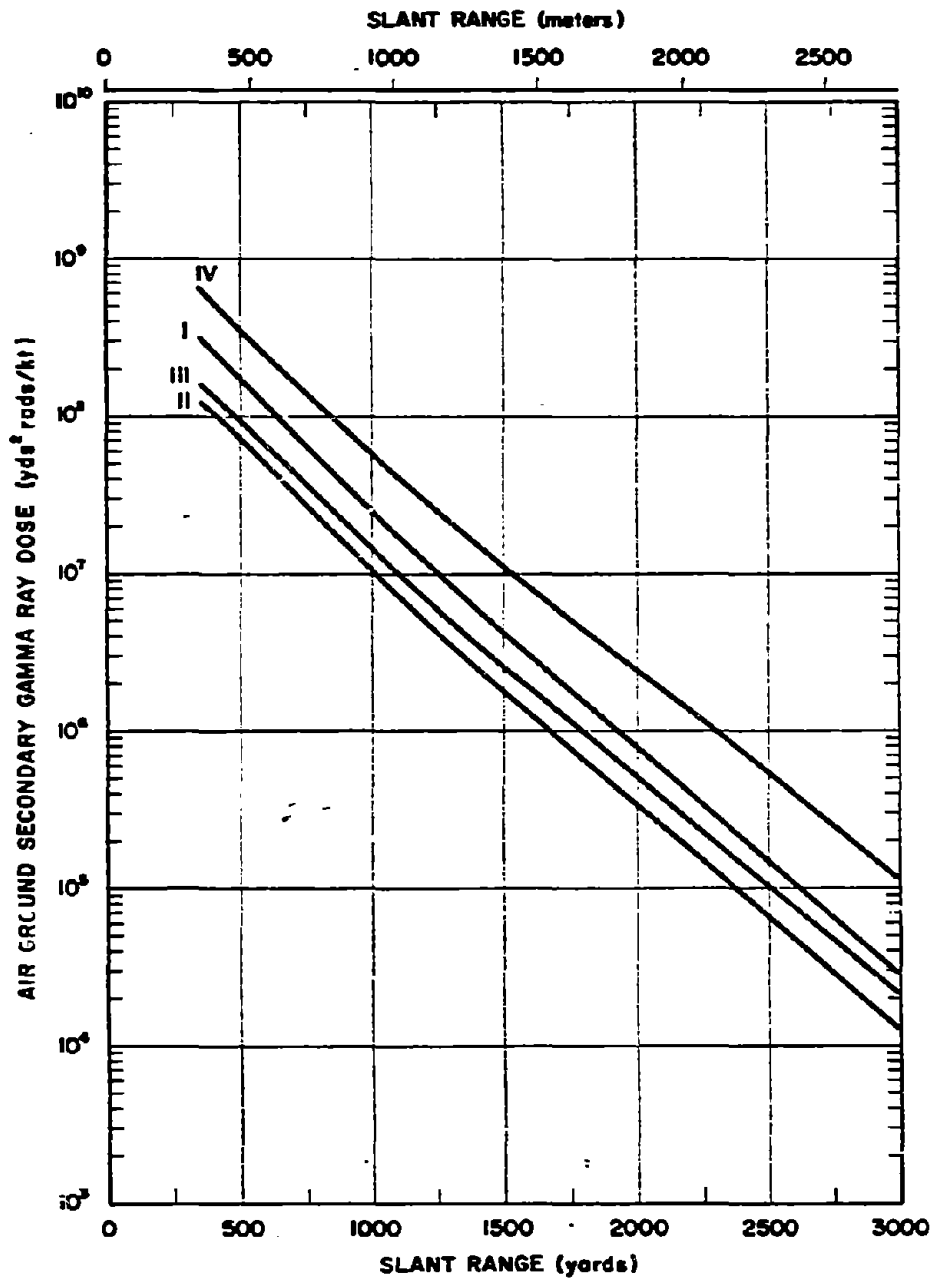
Figure 5-12a. ▮▮▮ Secondary Gamma Ray Dose as a Function of Slant Range from a 1 kt Surface Burst, Weapon Types I through IV, Short Ranges ▮▮▮

SLANT RANGE (meters)

Figure 5-12b. ▨▨ Secondary Gamma Ray Dose as a Function of Slant Range from a 1 kt Surface Burst, Weapon Types I through IV, Long Ranges ▨▨

Figure 5-13a. ▓▓▓ Secondary Gamma Ray Dose as a Function of Slant Range from a 1 kt Surface Burst, Weapon Types V through VIII, Short Ranges ▓▓▓

SLANT RANGE (meters)

AIR GROUND SECONDARY GAMMA RAY DOSE (yds²rads/kt)

SLANT RANGE (yards)

Figure 5-13b. ████ Secondary Gamma Ray Dose as a Function of Slant Range from a 1 kt Surface Burst, Weapon Types V through VIII, Long Ranges ████

5-41

Figure 5–14a. ▮▮▮ Fission Product Gamma Ray Dose as a Function of Slant Range from a 1 kt (Fission Yield) Surface Burst, Short Ranges ▮▮▮

SLANT RANGE (meters)
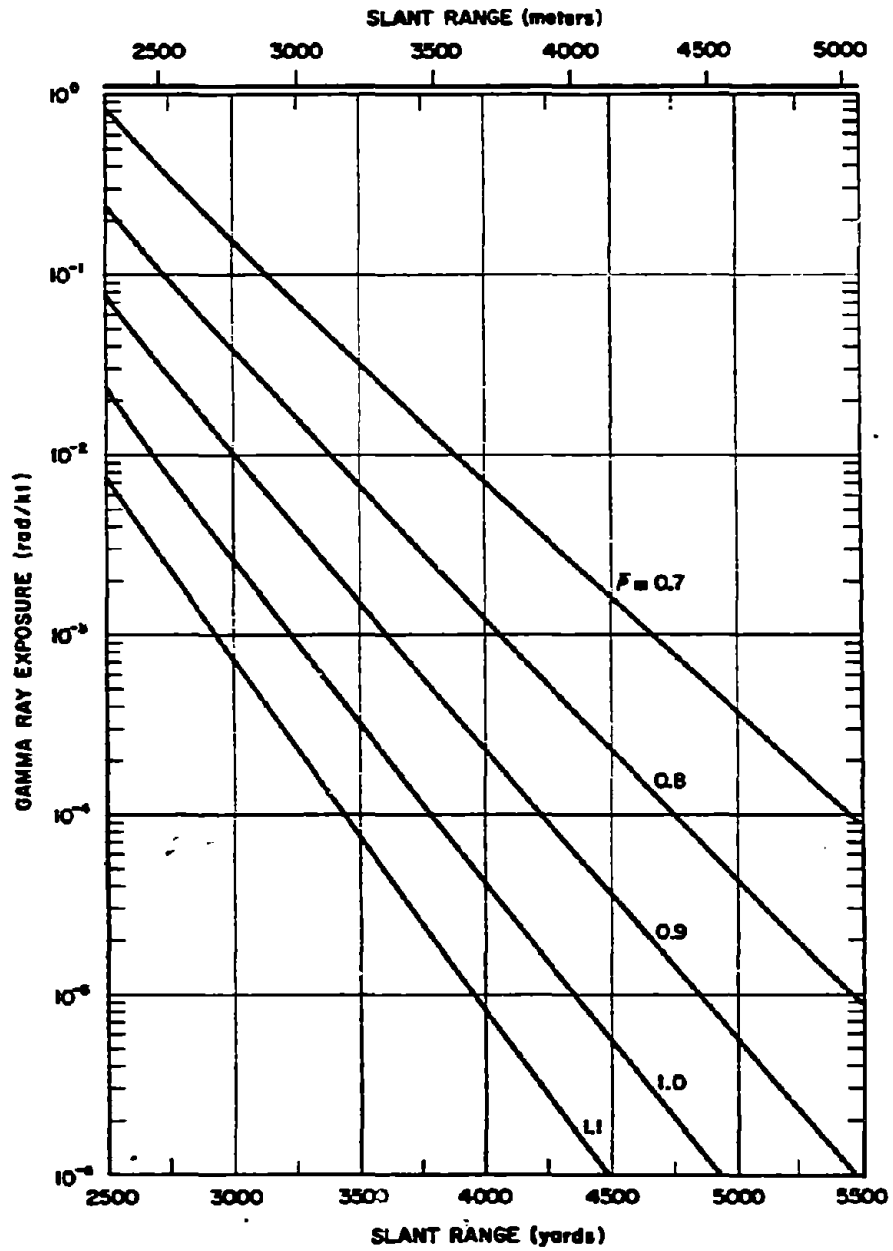
Figure 5-14b. ▮▮▮ Fission Product Gamma Ray Dose as a Function of Slant Range from a 1 kt (Fission Yield) Surface Burst, Intermediate Ranges ▮▮▮
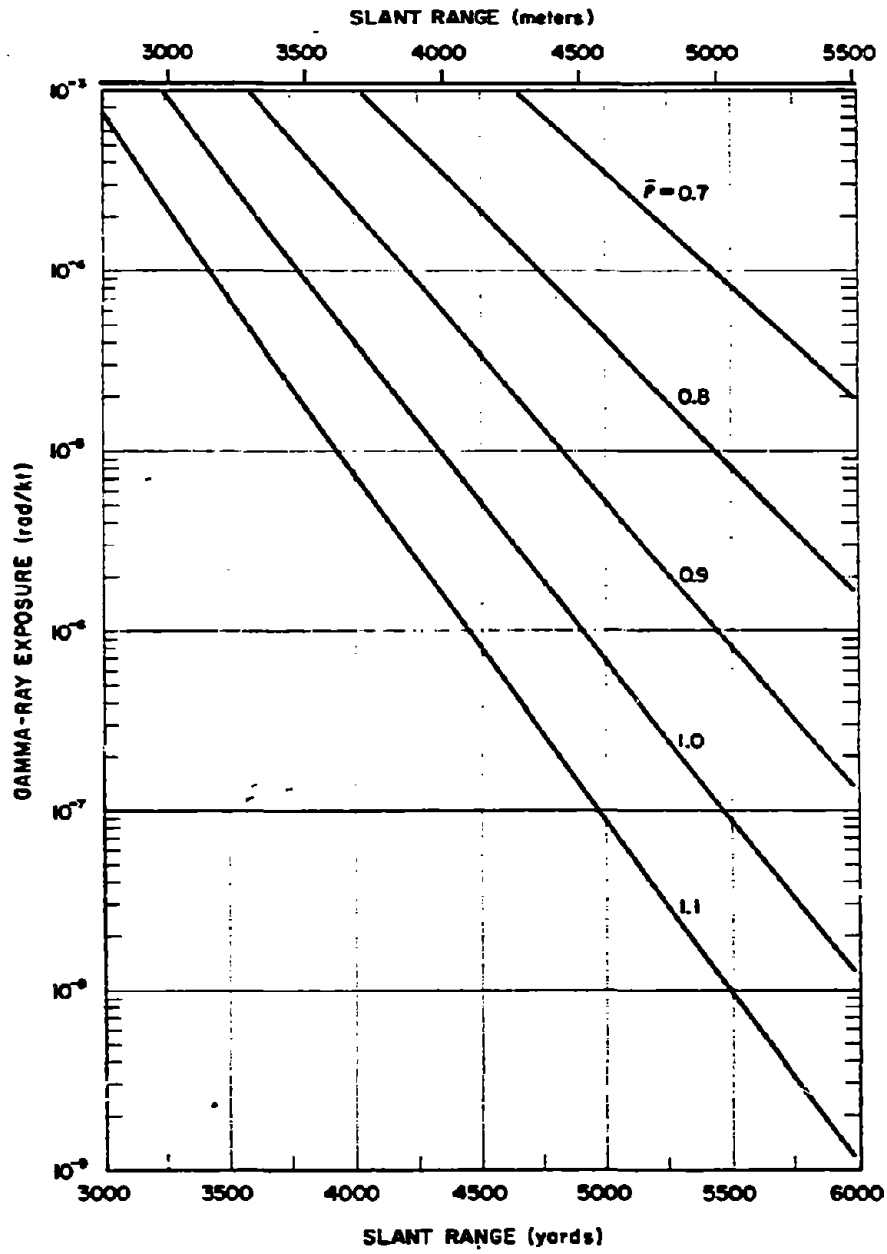
Figure 5-14c. ██████ Fission Product Gamma Ray Dose as a Function of Slant Range from a 1 kt (Fission Yield) Surface Burst, Long Ranges ██████

SLANT RANGE (meters)

ADJUSTMENT FACTOR

0

100

250

500   1000

2000   DETONATION HEIGHT (yds)

SLANT RANGE (yards)
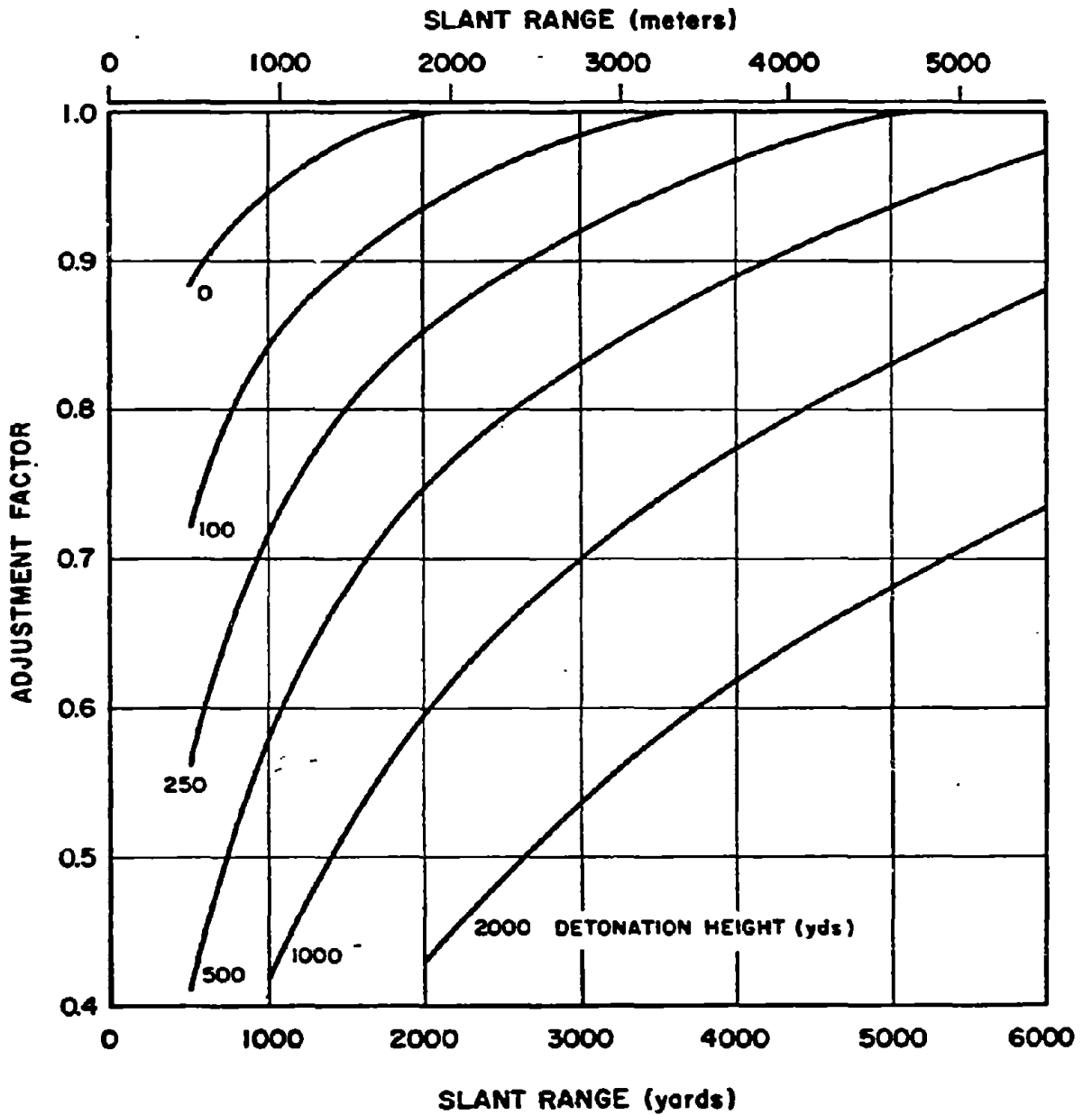
Figure 5-15. ▮ Range Dependent Burst Height Adjustment Factors
for Fission Product Gamma Rays ▮
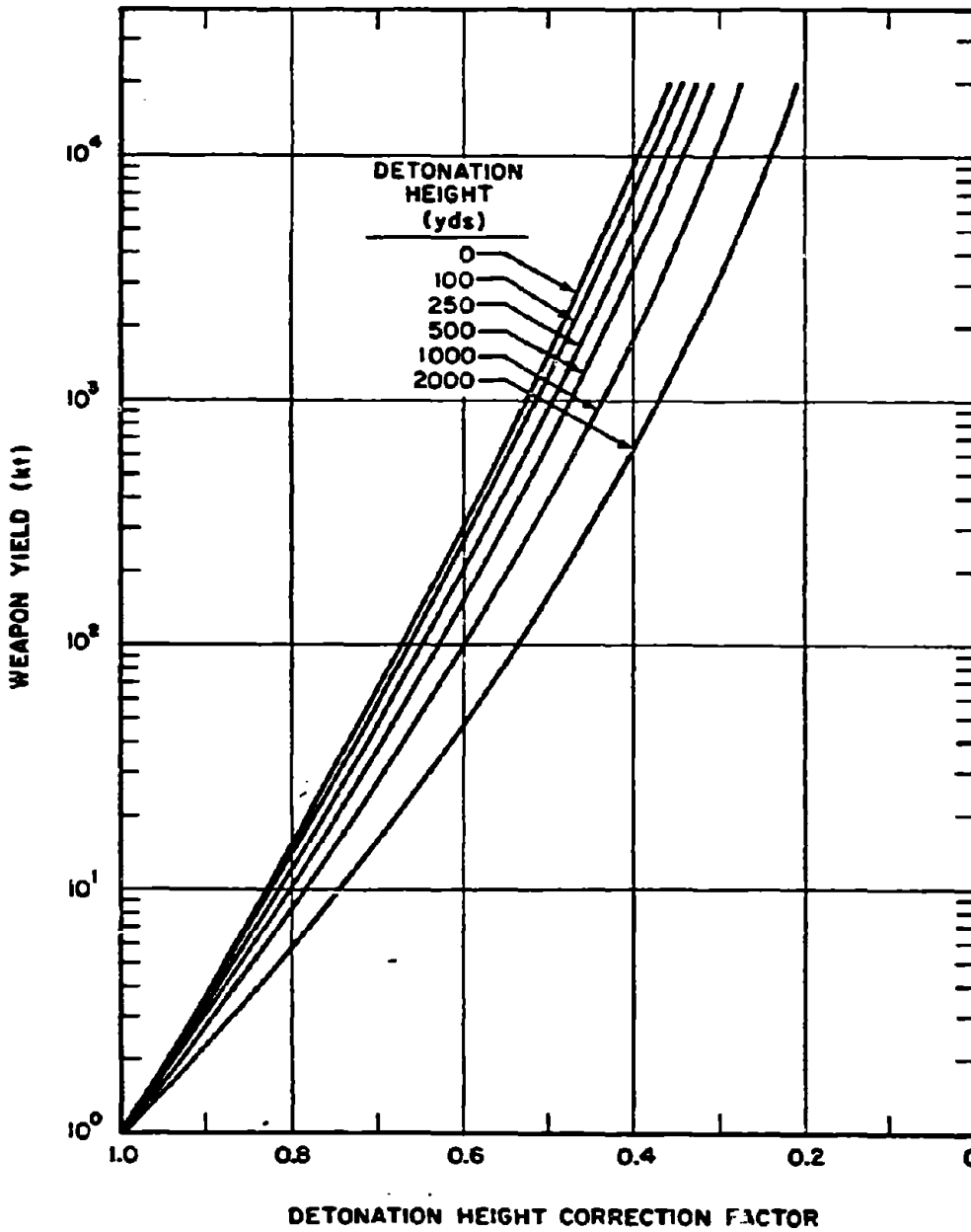
Figure 5-16. ▮▮▮ Yield Dependent Burst Height Adjustment Factors for Fission Product Gamma Rays ▮▮

SLANT RANGE (meters)

HYDRODYNAMIC ENHANCEMENT

$\rho/\rho_0 = 1.1$

20 Mt

10

x 1/10

5

1 Mt

500 Kt

100

50

10

5

1 Kt

SLANT RANGE (yards)
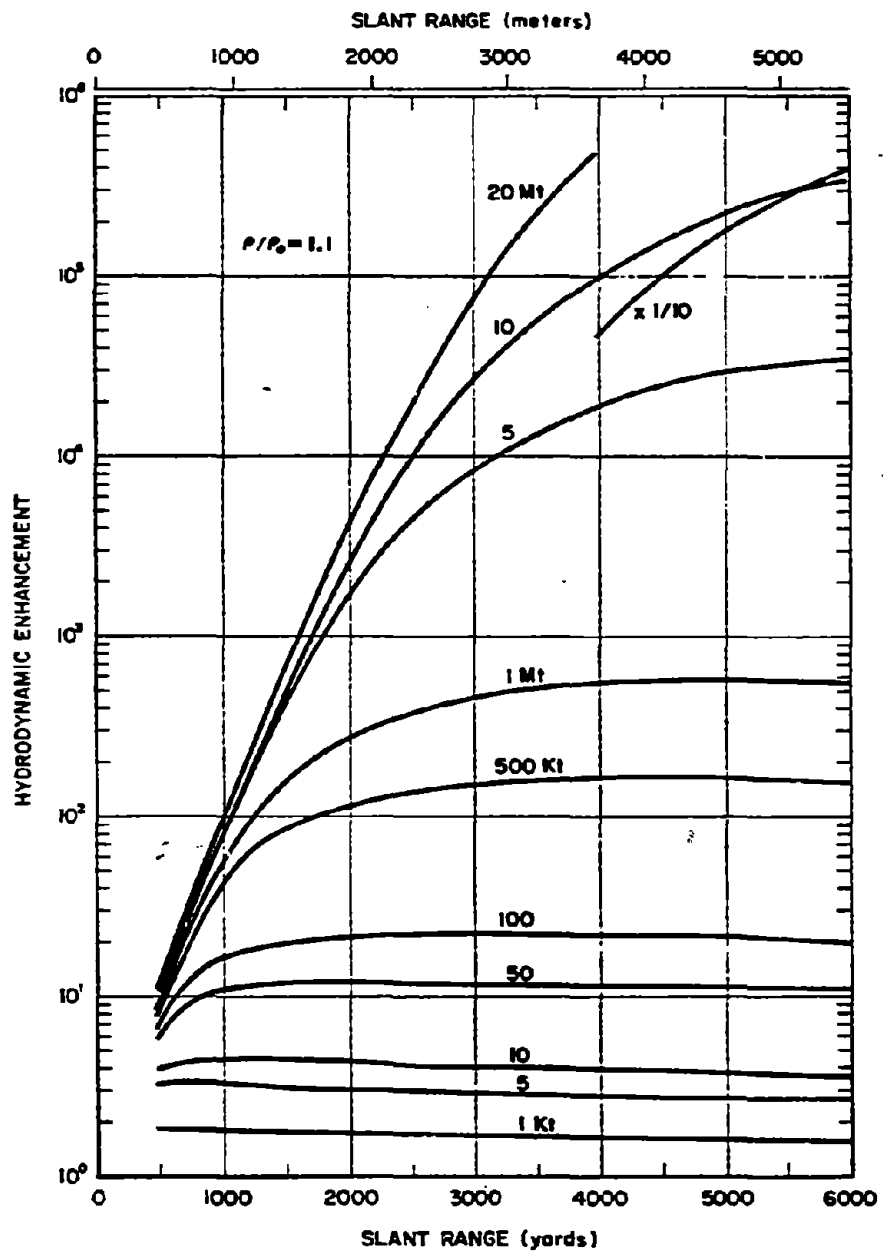
Figure 5-17a. ▮▮▮ Fission Product Gamma Ray Hydrodynamic Enhancement Factors
as a Function of Slant Range for Relative Air Density of 1.1 ▮▮▮
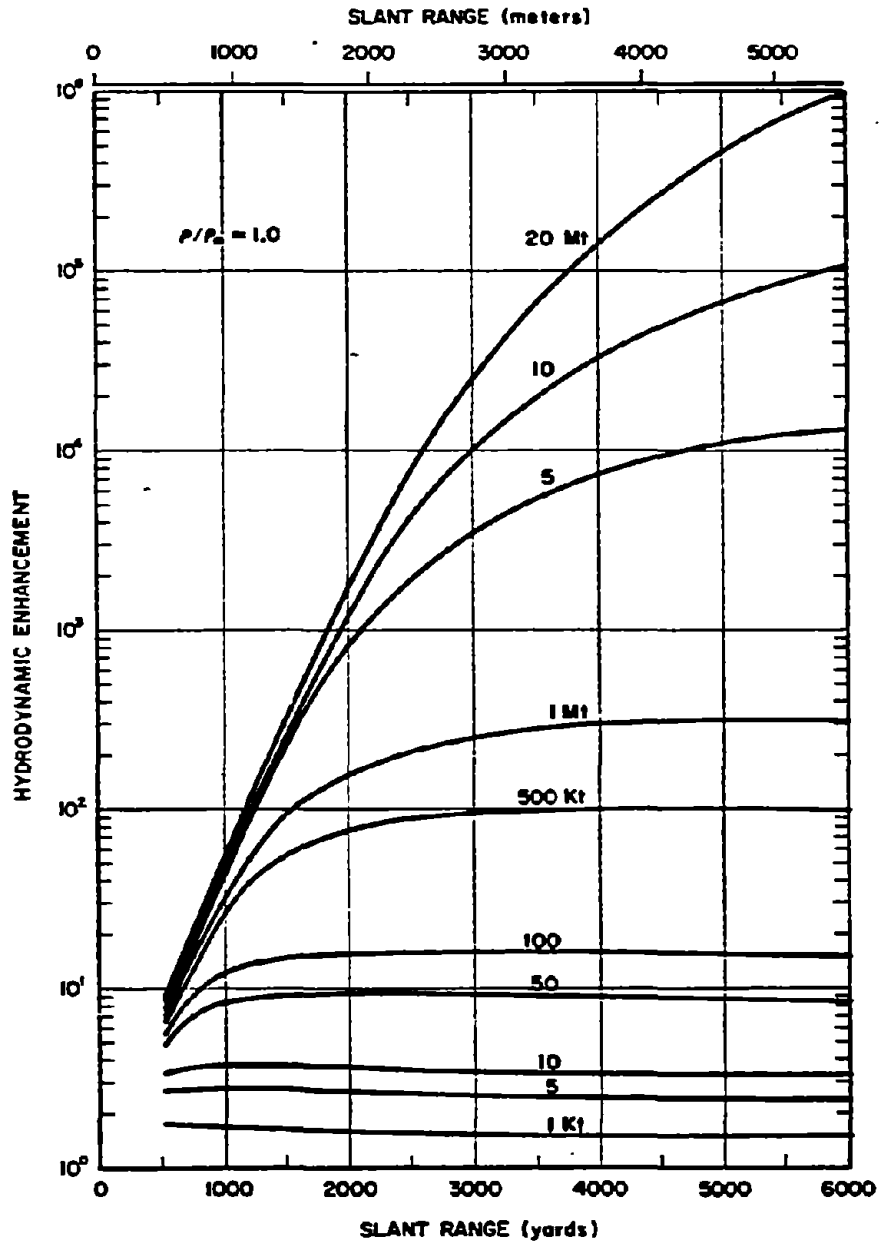
Figure 5-17b. ▮▮▮ Fission Product Gamma Ray Hydrodynamic Enhancement Factors as a Function of Slant Range for Relative Air Density of 1.0 ▮▮▮
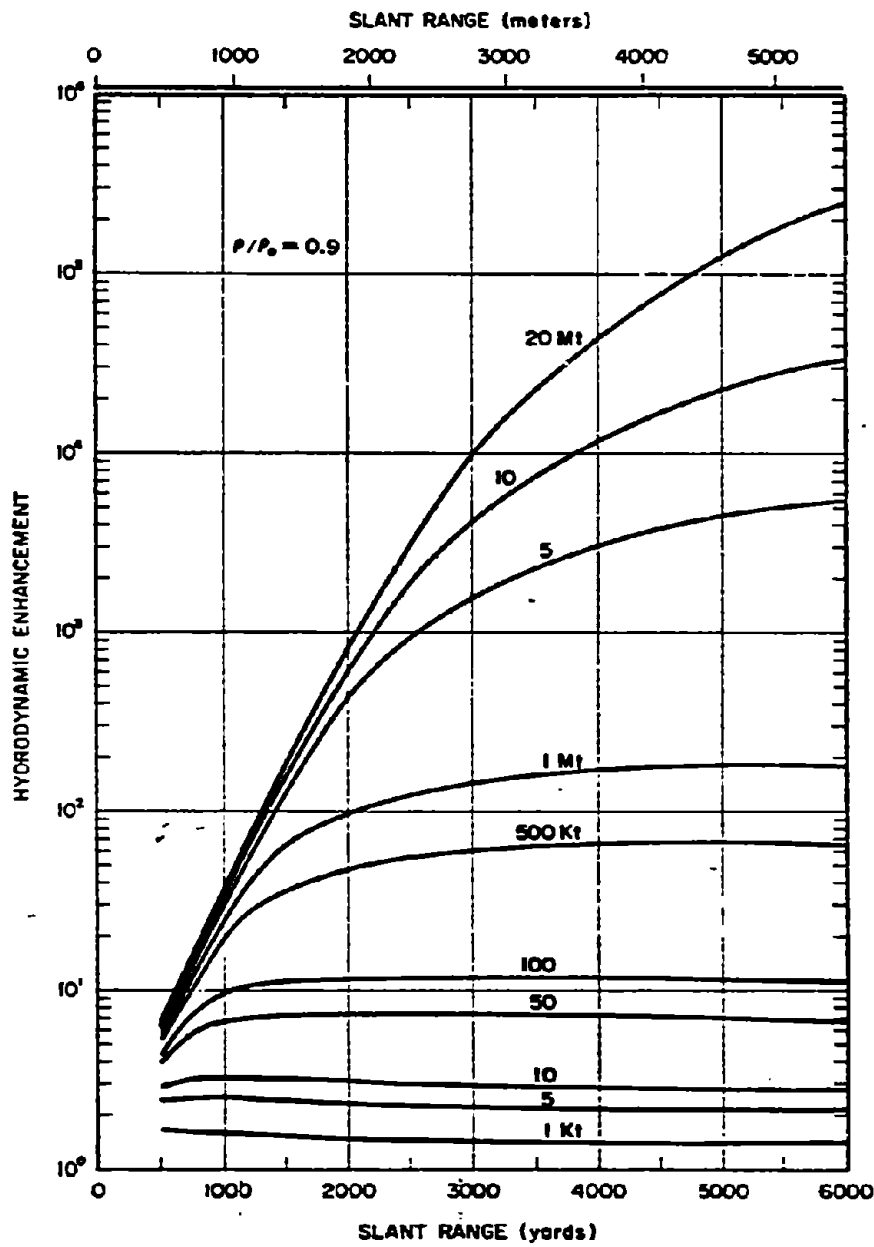
Figure 5-17c. ▮▮▮ Fission Product Gamma Ray Hydrodynamic Enhancement Factors as a Function of Slant Ranges for Relative Air Density of 0.9 ▮▮
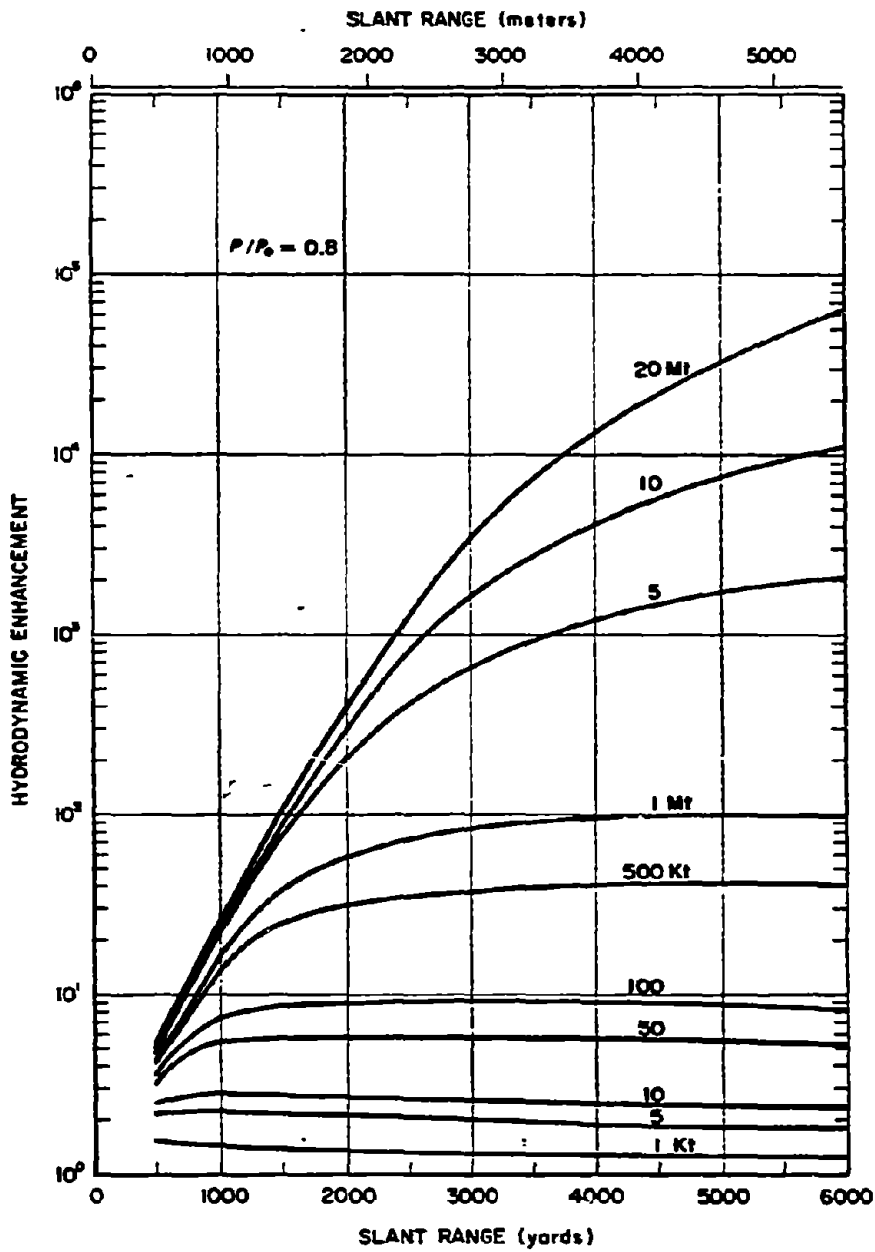
Figure 5-17d. ▇▇ Fission Product Gamma Ray Hydrodynamic Enhancement Factors as a Function of Slant Range for Relative Air Density of 0.8 ▇▇

SLANT RANGE (meters)

HYDRODYNAMIC ENHANCEMENT

$\rho/\rho_o = 0.7$

20 Mt

10

5

1 Mt

500 Kt

100

50

10

5

1 Kt

SLANT RANGE (yards)
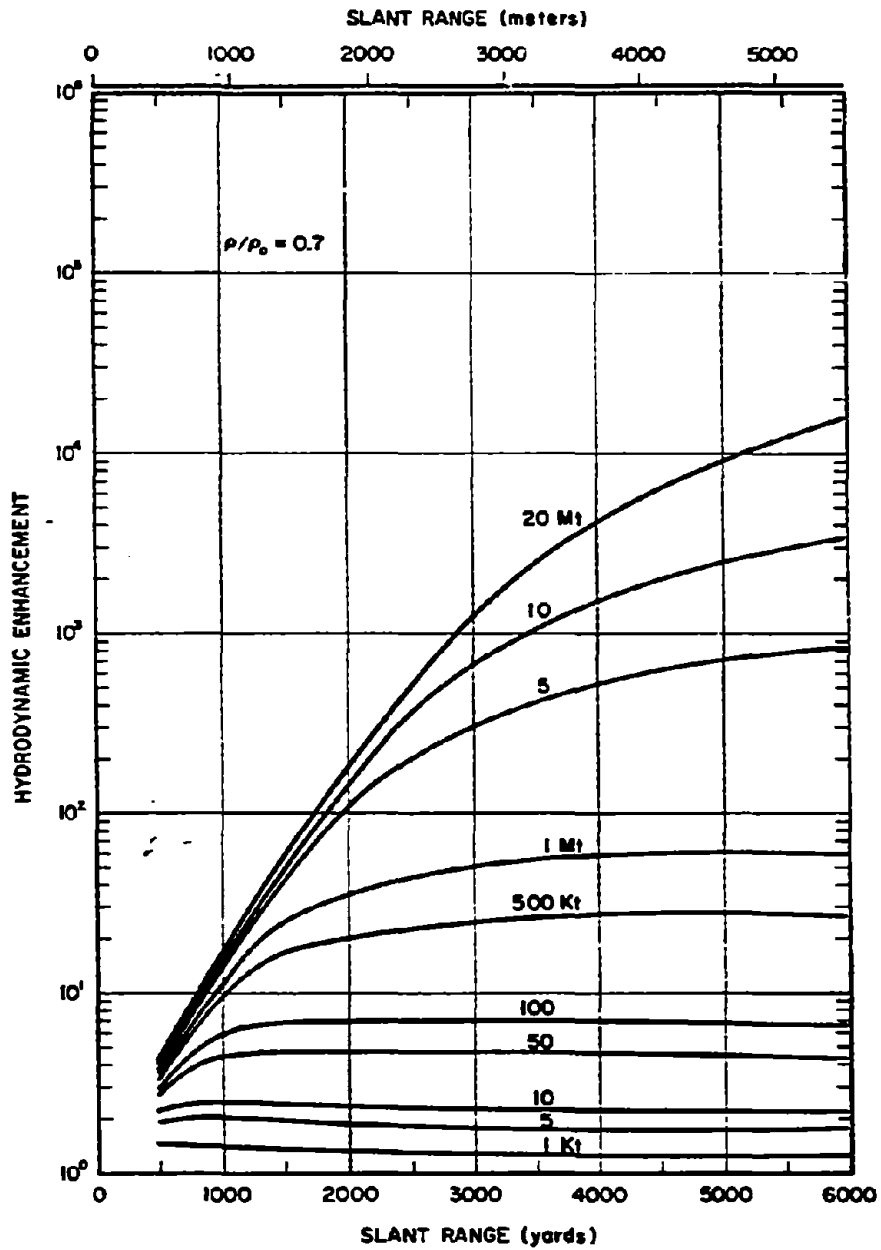
Figure 5-17e. ▇▇▇ Fission Product Gamma Ray Hydrodynamic Enhancement Factors as a Function of Slant Range for Relative Air Density of 0.7 ▇▇

SECTION II

██ NEUTRON-INDUCED ACTIVITY IN SOILS ██

██ As mentioned in paragraph 5-3, the neutrons emitted during a nuclear explosion undergo three main types of reactions when traversing matter: elastic scattering; inelastic scattering; and neutron capture. There are a variety of capture reactions, most of which result in the subsequent emission of a charged particle (generally a proton or alpha particle) and/or a gamma ray. When the reaction results solely in the emission of a gamma ray, it is generally referred to as radiative capture. As a rule, the probability for capture reactions is small compared to elastic and inelastic scattering when the neutron energy exceeds a few keV. The nuclei remaining after neutron capture are frequently radioactive, generally emitting a beta particle, a gamma ray(s), or both. The extent of the hazard to personnel that results from radioactivity induced in the soil by neutrons from a nuclear explosion is described in this section.

5-12 Height of Burst ██

██ The residual radioactive contamination (fallout) that results from fission products that are distributed subsequent to a contact surface or subsurface burst (Section III of this chapter) is much greater than the radioactive contamination that results from the neutron activity discussed in this section. Thus, the neutron-induced activity may be neglected for contact surface and subsurface bursts.* If a weapon is burst at such a height as to be in the transition zone as far as fallout is concerned, the neutron-induced activity generally can be neglected if the burst height is in the lower three-quarters of the fallout transition zone, i.e., if the burst is below about $75W^{0.35}$ feet (see Section III). If the height of burst is in the upper quarter of the transition zone (between about $75W^{0.35}$ feet

and $100W^{0.35}$ feet), the neutron-induced activity may not be negligible compared to fallout. When fallout dose rate contours determined by the methods described in Section III are much smaller than those for a surface burst, the neutron-induced activity should be obtained by the methods described below. The overall contour values may be obtained by summing the dose rate values for induced activity and fallout at a particular time; however, as will be shown in succeeding paragraphs of this chapter, the radioactivity from fallout and that from neutron-induced activity decay at different rates. Therefore, the dose rate from each source must be determined separately for each time of interest, or the total doses over some period of time must be determined separately, and then the appropriate summing may be performed.

██ For burst heights that are sufficiently high, the various forms of attenuation described in paragraph 5-3 will result in a neutron fluence at the surface of the earth that is too small to produce significant induced activity. Since the neutron-induced gamma radiation depends on soil type as well as weapon type and yield, a height of burst above which neutron-induced activity will cease to be important cannot be defined. In general, however, this effect will only be important for low air bursts (just above the height of burst at which fallout ceases to be important).

5-13 Soil Types ██

██ The type, intensity, and energy distribution of the induced activity produced by the neutrons will depend on which isotopes are produced and in what quantity. These factors depend on the number and energy distribution of the incident neutrons and the chemical composi-

---

*██ The induced activity contribution may, however, assume more importance if Plowshare type nuclear devices are adapted for military use.

tion of the soil. Induced contamination contours are independent of wind, except for some wind redistribution of the surface contaminant. The contours can be expected to be roughly circular.

■ Examination of several thousand analyses of the chemical composition of soils and the relative probabilities of neutron capture by the various elements present in the various samples has indicated that sodium, manganese, and aluminum generally will contribute most of the induced radioactivity. Small changes in the quantities of these materials can change the activity significantly. Other elements can also influence the radioactivity. Some elements have a relatively high probability for capturing neutrons (cross section), but the isotope that is formed after the capture either is not radioactive, does not emit gamma rays, or has such a long half life that the low activity does not produce a hazardous dose rate. The presence of such elements in the soil will tend to lower the hazard from neutron-induced activity.

■ As described in paragraph 5-3, scattering of neutrons from light elements may cause the neutron to transmit a significant amount of its energy to the nucleus, and the scattered neutron will be less energetic than the incident neutron. Since the probability of neutron capture generally increases as the neutron energy decreases (in particular, this is true for sodium, manganese, and aluminum), the presence of light elements in the soil will tend to cause a larger number of neutrons to be captured near the surface rather than at some depth (the peak intensity from neutron activated radionuclides generally is two to three inches below the surface). Thus, it might be expected that the presence of light elements might increase the hazard from neutron-induced activity by raising the primary gamma ray source to a level nearer the surface, where attenuation of the earth above the source would be less. A study of many soil samples indicates that the light element that is most likely to

cause such an effect is hydrogen that might be present in moisture (water) in the soil.* Thus, it might be expected that soil saturated with water might be more hazardous from neutron-induced activity than the same soil when dry. However, competing effects occur because the hydrogen absorbs neutrons to form nonradioactive deuterium. These neutrons otherwise could produce gamma ray emitters. Experiments have confirmed that moisture content does increase the hazard from neutron-induced activity; however, this effect does not appear to be of major importance in view of the uncertainties in soil composition and variations in possible weapon neutron outputs.

■ Four soils have been chosen to illustrate the extent of the hazard that may be expected from induced activity. These soils were selected to show wide variations in predicted dose rates; the activity from most other soils should fall within the range of activities presented for these soils. Table 5-4 shows the chemical composition of the selected soils. The elements listed in Table 5-4 are in the order of probable importance so far as induced activity is concerned.

■ When applying the data presented in this section to soils other than the four types shown, the activity should be estimated by using the data for the type that most closely resembles the soil in question in chemical composition. If none of the four types resembles the soil in question very closely, the following points should be kept in mind. For times less than $H + 1/2$ hour, aluminum is the most important contributor. Between $H + 1/2$ hour and $H + 5$ hours, manganese is generally the most important element. In the

---

* Hydrogen, being the lightest element, will have many more atoms per unit volume for the same percentage concentration by weight. It is also the most effective element in reducing the energy of the neutron, since its nucleus (a proton) has essentially the same mass as a neutron and energy transfer by elastic collision is very effective.

Table 5-4. ██ Chemical Composition of Illustrative Soils ██

	Percentage of Soil Type (by weight)			
Element	Type I (Liberia, Africa)	Type II (Nevada desert)	Type III (lava, clay, Hawaii)	Type IV (beach, sand, Pensacola, Florida)
Sodium	—	1.30	0.16	0.001
Manganese	0.008	0.04	2.94	—
Aluminum	7.89	6.90	18.79	0.006
Iron	3.75	2.20	10.64	0.005
Silicon	33.10	32.00	10.23	46.65
Titanium	0.39	0.27	1.26	0.004
Calcium	0.08	2.40	0.45	—
Potassium	—	2.70	0.88	—
Hydrogen	0.39	0.70	0.94	0.001
Boron	—	—	—	0.001
Nitrogen	0.065	—	0.26	—
Sulfur	0.07	0.03	0.26	—
Magnesium	0.05	0.60	0.34	—
Chromium	—	—	0.04	—
Phosphorous	0.008	0.04	0.13	—
Carbon	3.87	—	9.36	—
Oxygen	50.33	50.82	43.32	53.332

absence of manganese, the sodium content will probably govern the activity for this period. Between H +5 hours and H + 10 hours, sodium and manganese content are both important. After H + 10 hours, sodium will generally be the only large contributor. If the sodium, manganese, and aluminum contents are low, the neutron-induced activity generally will be low. Soil type IV is an example of such a soil. Using these guidelines, it may be possible to obtain better data for a given soil by using data for a different illustrative soil

at each of several times of interest. A word of caution is in order, however. While the content of sodium and aluminum will generally be relatively constant over fairly large areas, manganese generally is a trace element and the content may vary by an order of magnitude over a few hundred yards. Between H + 1/2 hour and H + 5 hours, the dose rate will vary almost directly in proportion to the magnitude of the variation in manganese content. In view of the uncertainty in the soil composition at any location under

operational conditions, and the possibility of variations in composition over short distances, the data presented herein should only be used for rough estimates and should not be used as the basis for operational planning.

5-14 Dose Rate and Dose Predictions

As described in paragraph 5-1, both the spectrum and the total number of neutrons emitted during a nuclear explosion are sensitive functions of weapon design. Thus, no "representative" weapon was used for the prediction of neutron-induced activity, and, in view of the other uncertainties discussed above, presentation of prediction techniques for several weapon designs is not warranted. Figure 5-18 shows a broad band that indicates the variation of neutron-induced gamma activity as a function of slant range from the explosion. It is believed that the activity produced by most weapons will fall within the band.* Dose rates at $H + 1$ hour after burst may be obtained by multiplying the dose rates from Figure 5-18 by the multiplying factors given in Problem 5-5.

Figure 5-19 represents the radioactive decay characteristics of the four soil types shown in Table 5-4. The decay factors taken from Figure 5-19 are multiplied by the $H + 1$ hour dose rate for a particular soil to give the dose rate for that soil at any other time.

Figures 5-20 through 5-23 are presented to facilitate the computation of total dose. Multiplying factors may be obtained from these figures, which, when applied to the $H + 1$ hour dose rate for the particular soil, will give the dose accumulated over any of several periods of time for various times of entry into the contaminated area.

---

*This band considers the representative types of nuclear weapons shown in Table 5-3 with the exception of Type V.

Problem 5-5. Calculation of Neutron-Induced Activity at 1 Hour After Explosion

Figure 5-18 shows a range of normalized neutron-induced dose rates as a function of slant range from a 1 kt explosion. To estimate the H +1 hour dose rate, enter the slant range axis with the slant range in yards and read the range of normalized dose rates. Multiply these dose rates by the appropriate factor for the soil type of interest from the following list.

Soil Type	Multiplying Factor
I	1.0
II	9.1
III	109.0
IV	0.024

Scaling. For yields other than 1 kt, multiply the dose rates obtained from Figure 5-19 by the weapon yield in kt.

Example

Given: A 50 kt explosion at a height of burst of 900 feet above soil type III.

Find: The range of H + 1 hour dose rates that might be expected: at ground zero and at a ground distance of 950 yards from ground zero.

Solution: The corresponding slant ranges are 300 yards to ground zero and 996 yards to a point at a ground distance of 950 yards from ground zero. From Figure 5-18, the normalized H + 1 hour dose rate at a slant range of 300 yards from ground zero are expected to be be-

tween 0.8 rad/hr/kt and 1.8 rads/hr/kt. The corresponding dose rates at a slant range of 996 yards are 1.6 x 10^{-2} rad/hr/kt and 5 x 10^{-2} rad/hr/kt. The multiplying factor for soil type III is 109.

Answer: The H + 1 hour dose rates at ground zero should be between

$$50 \times 109 \times 0.8 = 4,360 \text{ rads/hr,}$$

and

$$50 \times 109 \times 1.8 = 9,800 \text{ rads/hr.}$$

The H + 1 hour dose rates at a ground distance of 950 yards from ground zero should be between

$$50 \times 109 \times 1.6 \times 10^{-2} = 87 \text{ rads/hr,}$$

and

$$50 \times 109 \times 5 \times 10^{-2} = 272 \text{ rads/hr.}$$

Reliability. H + 1 hour dose rates are expected to fall within the limits of the band shown in Figure 5-19 for the specific soils shown. For other soils, even with small variations in the content of sodium and manganese, the data merely will furnish an estimate of the magnitude of the hazard.

Related Material. See paragraphs 5-1 through 5-3, and paragraphs 5-12 through 5-14.
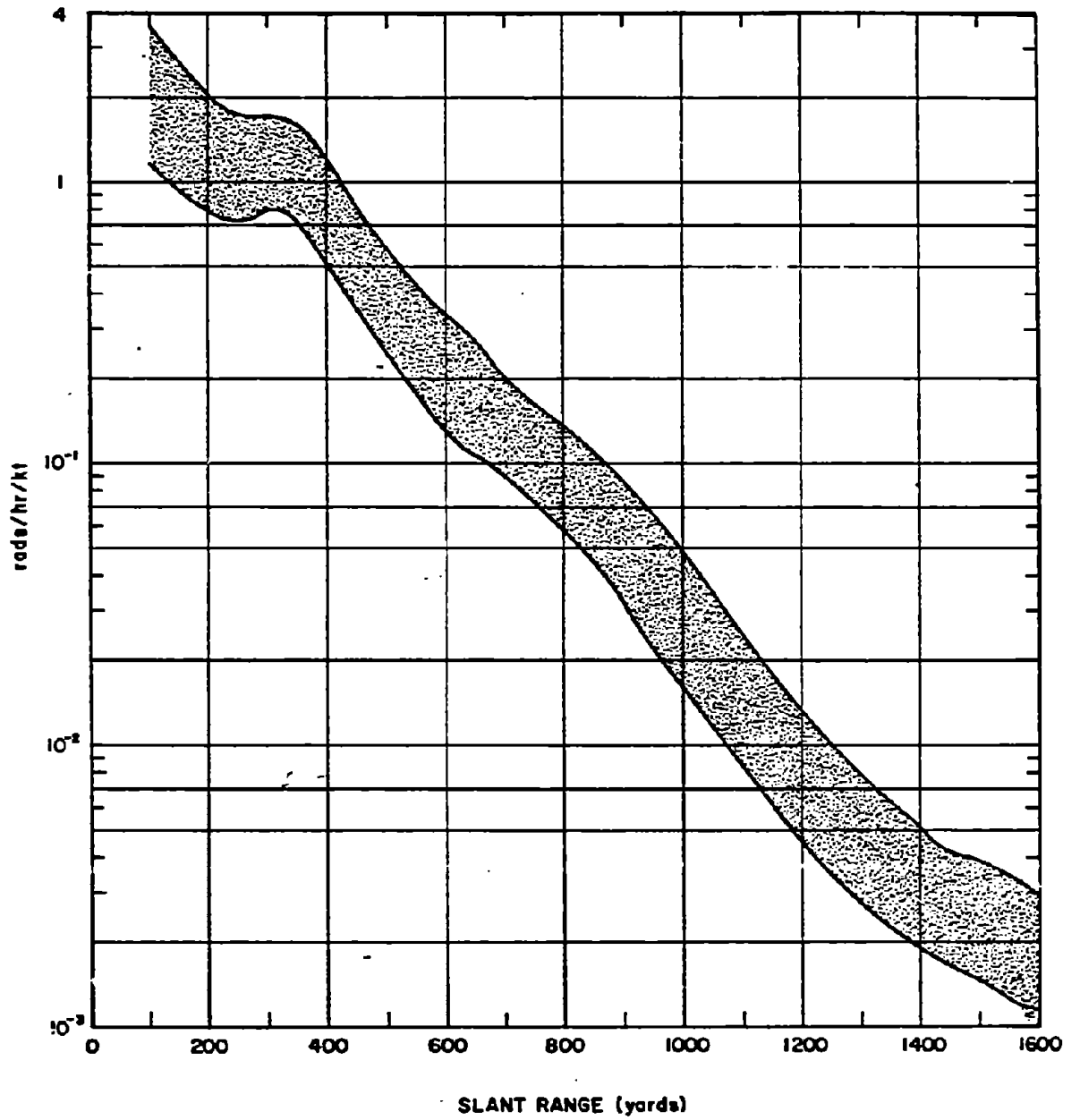
Figure 5-18. ▆ Neutron-Induced Gamma Dose Rate as a Function of Slant Range at a Reference Time of 1 Hour After Burst ▆

Problem 5-6. Calculation of Neutron-Induced Gamma Activity at Times Other than $H + 1$ Hour

The dose rate at any time after burst may be determined by multiplying the $H + 1$ hour dose rate by the decay factor appropriate to the soil of interest from Figure 5-19. The decay curves may also be used to determine the value of the dose rate at $H + 1$ hour from the dose rate at a later time. In this case, the measured dose rate is divided by the appropriate decay factor. The dose rate at any other time then may be determined from the $H + 1$ hour dose rate.

Example 1

Given: The dose rate at a given point on soil type I is 30 rads/hr at $H + 1$ hour.

Find: The dose rate at that point at $H + 1/2$ hour and at $H + 10$ hour.

Solution: From Figure 5-19, the decay factors for soil type I for 1/2 hour and 10 hours are 3 and 0.083, respectively.

Answer: The dose rate at 1/2 hour is:

$$30 \times 3 = 90 \text{ rads/hr}$$

and the dose rate at 10 hours is

$$30 \times 0.083 = 2.5 \text{ rads/hr.}$$

Example 2

Given: The measured dose rate at a point over type II soil is 375 rads/hr 3 hours after the explosion.

Find: The dose rate at the same point 50 hours after the explosion.

Solution: From Figure 5-19, the decay factors for soil type II are 0.75 and 0.06 for times of $H + 3$ and $H + 50$ hours, respectively. The $H + 1$ hour dose rate at the point is

$$\frac{375}{0.75} = 500 \text{ rads/hr.}$$

Answer: The $H + 50$ hours dose rate at the point is

$$(500)(0.06) = 30 \text{ rads/hr.}$$

Reliability. The curves of Figure 5-19 are estimated to represent the decay of the soil compositions shown in Table 5-4 to within ± 10 percent; however, small changes in the chemical composition of the soil, particularly in the content of sodium, manganese, and aluminum, may change the decay characteristics drastically. Uncertainties associated with the *prediction* of $H + 1$ hour dose rates will affect the prediction of dose rates at any other time.

Related Material. See paragraphs 5-13 and 5-14. See also Problem 5-5.
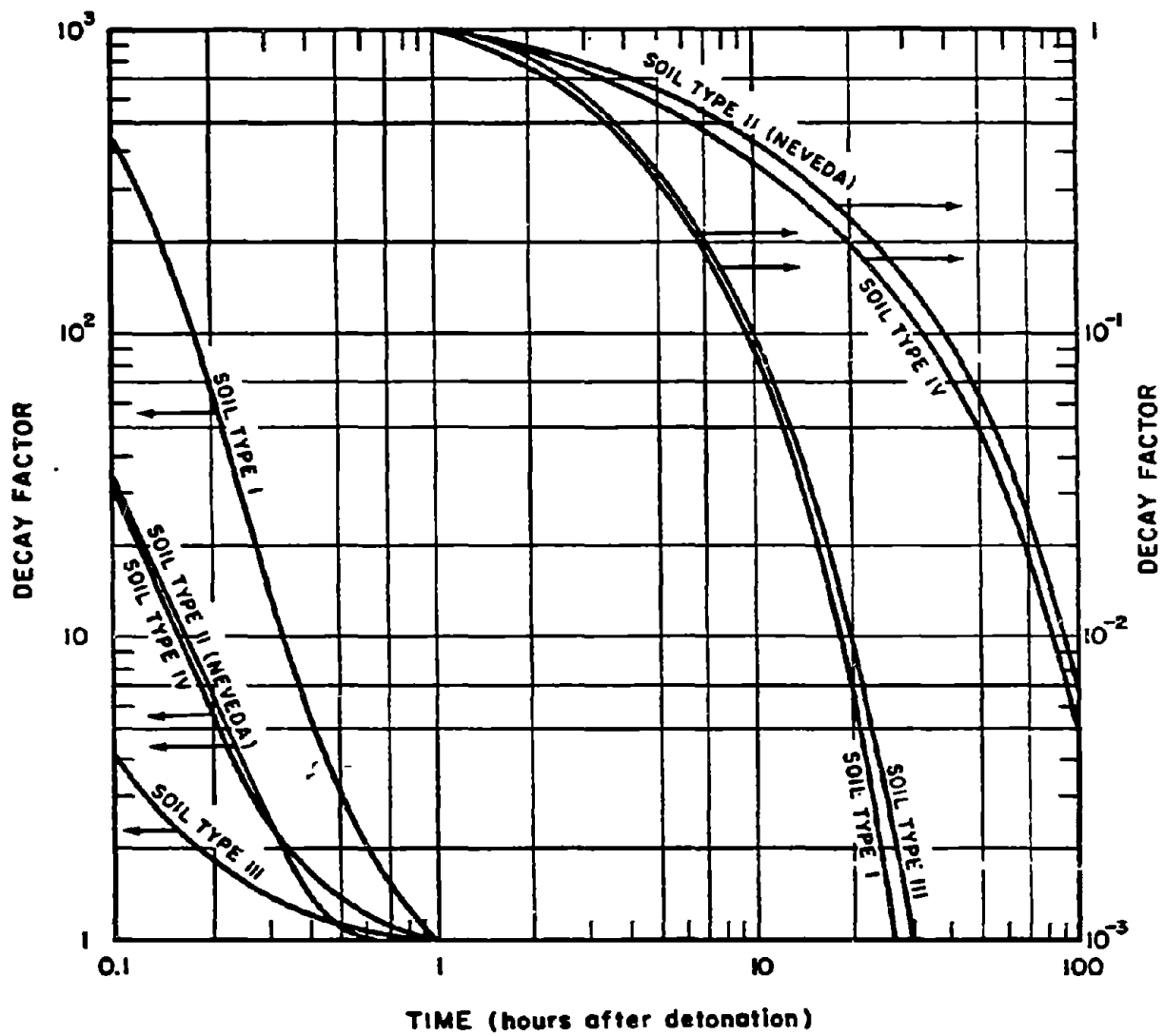
Figure 5–19. ▇▇ Decay Factors for Neutron-Induced Gamma Activity ▇▇

The graph shows DECAY FACTOR (vertical axes, ranging from 1 to 10³ on the left, and 10⁻³ to 1 on the right) versus TIME (hours after detonation) from 0.1 to 100 on the horizontal axis. Curves are labeled:

- SOIL TYPE II (NEVEDA)
- SOIL TYPE IV
- SOIL TYPE I
- SOIL TYPE II (NEVEDA)
- SOIL TYPE IV
- SOIL TYPE III
- SOIL TYPE I
- SOIL TYPE III

Problem 5-7. Calculation of Total Dose from Neutron-Induced Activity

Figures 5-20 through 5-23 provide the means to obtain the total dose received when entering an area contaminated with neutron-induced activity and remaining for a specified interval of time. The various curves represent times that an individual remains in the contaminated area. To determine the dose, obtain the multiplying factor from the vertical axis that corresponds to the time of entry on the horizontal axis and the stay time from the appropriate curve (or by interpolation between curves).

Example

Given: A dose rate of 105 rads/hr was measured on entering a contaminated area of soil type III 5 hours after an air burst nuclear explosion.

Find: The total dose that would be received by an individual who remained in that area for 1 hour.

Solution: From Figure 5-19, the decay factor for soil type III at $H + 5$ hours is 0.35. The 1 hour dose rate is therefore

$$\frac{105}{0.35} = 300 \text{ rads/hr.}$$

Figure 5-22 is the appropriate figure from which the dose multiplying factor should be obtained for soil type III. From this figure, the intersection of the line for a time of entry of 5 hours after burst with the 1 hour stay time curve gives a factor of 0.32.

Answer: If the individual remains in the area for 1 hour, the accumulated dose will be

$$(0.32)(300) = 96 \text{ rads.}$$

Reliability. Figures 5-20 through 5-23 are integrals of the curves in Figure 5-19. The same reliability statement given in Problem 5-6 applies.

Related Material. See paragraphs 5-13 and 5-14. See also Problems 5-5 and 5-6.
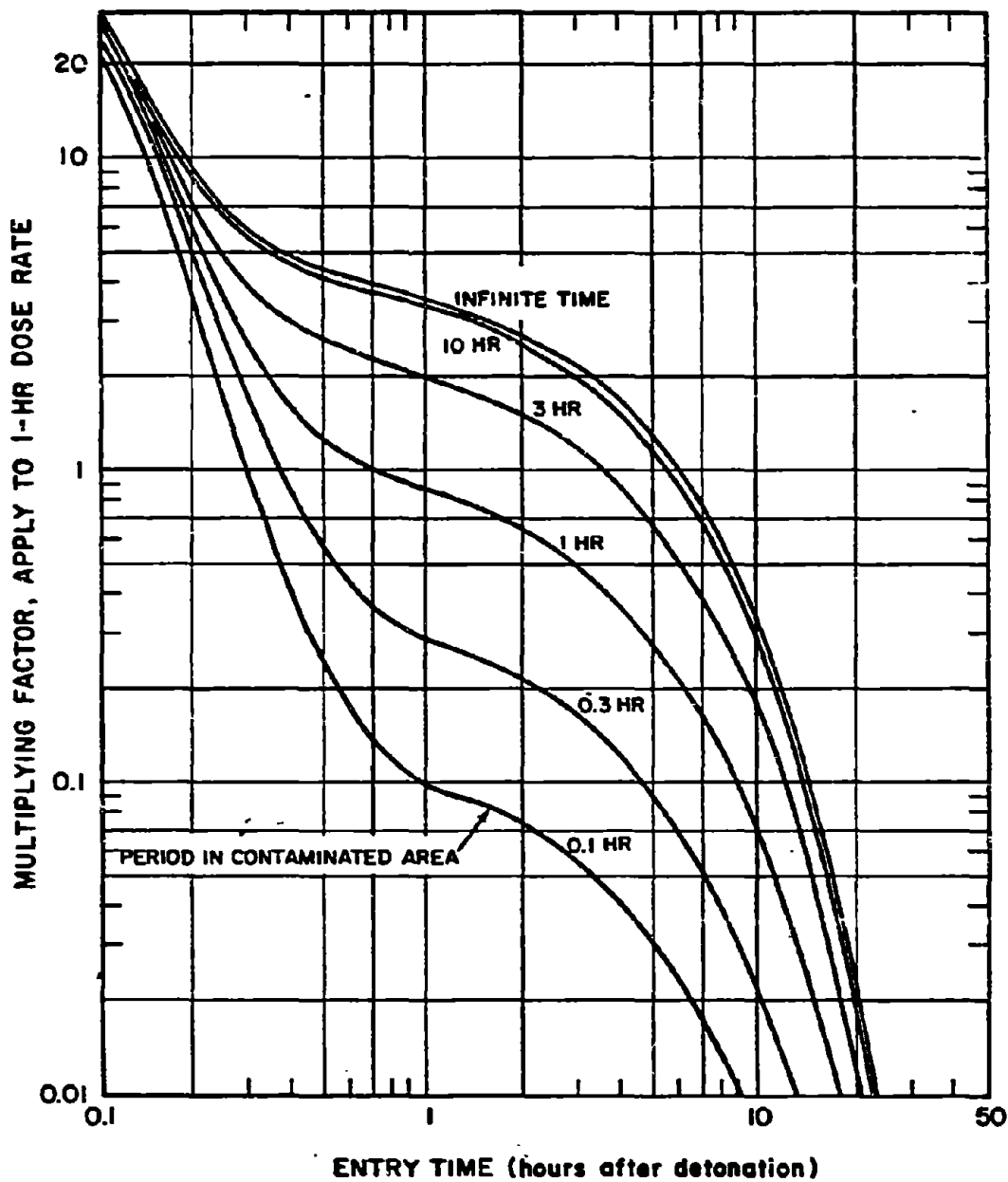
Figure 5-20. ▓ Total Radiation Dose Received in an Area Contaminated by Neutron-Induced Gamma Activity, Soil Type I ▓
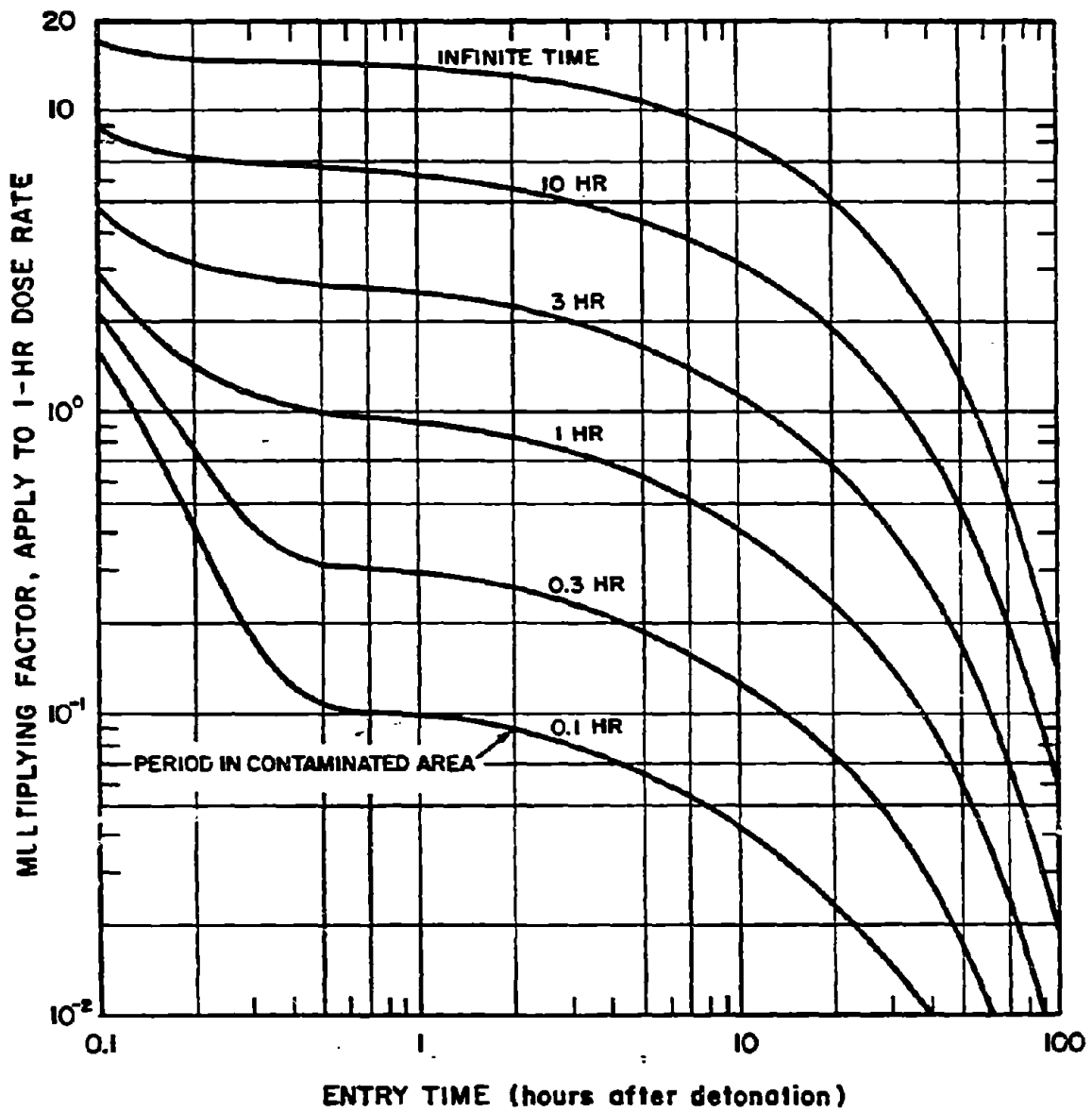
Figure 5-21. ███ Total Radiation Dose Received in an Area Contaminated by Neutron-Induced Gamma Activity, Soil Type II ████
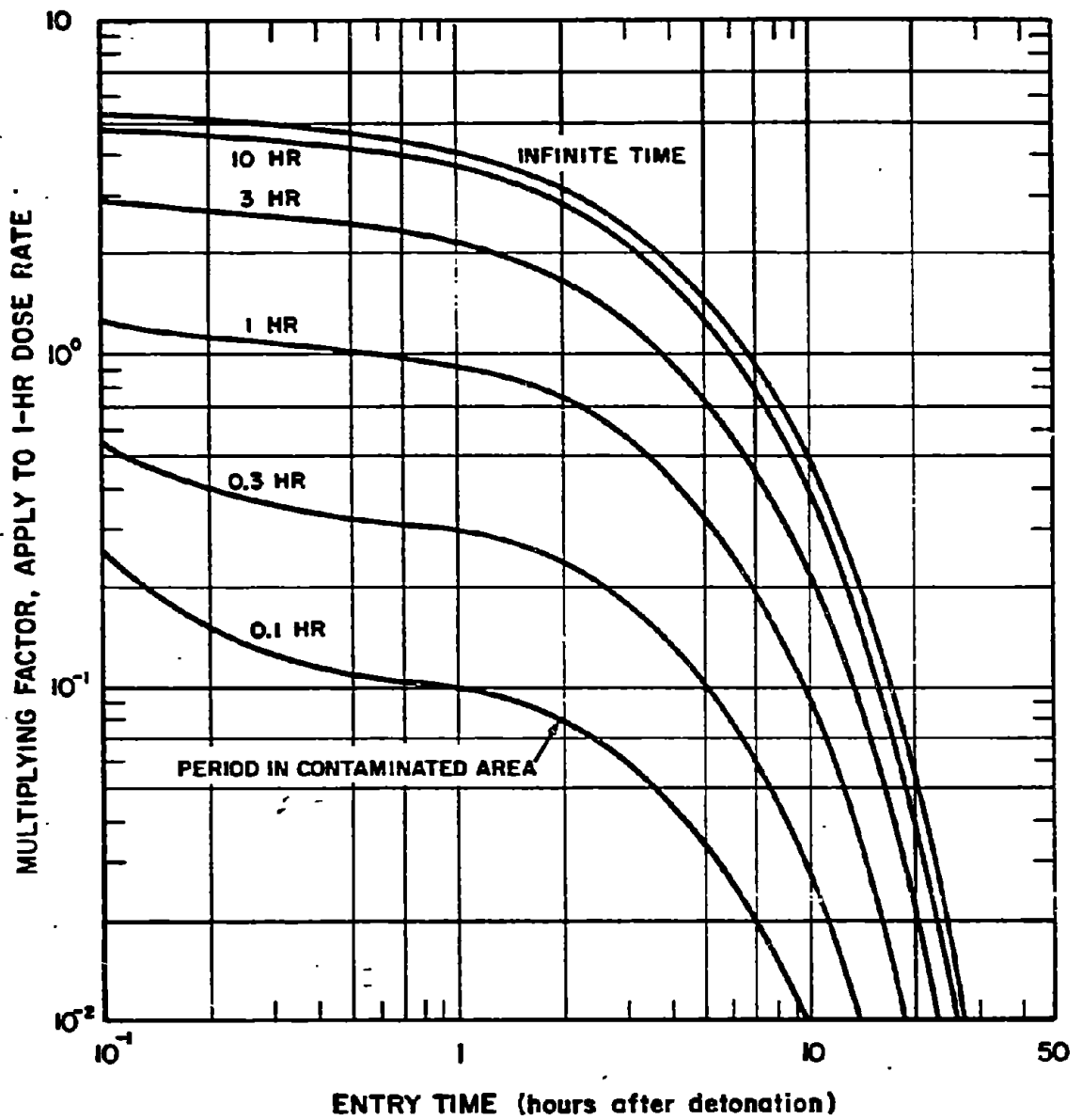
Figure 5-22. ▮ Total Radiation Dose Received in an Area Contaminated by Neutron-Induced Gamma Activity, Soil Type III ▮
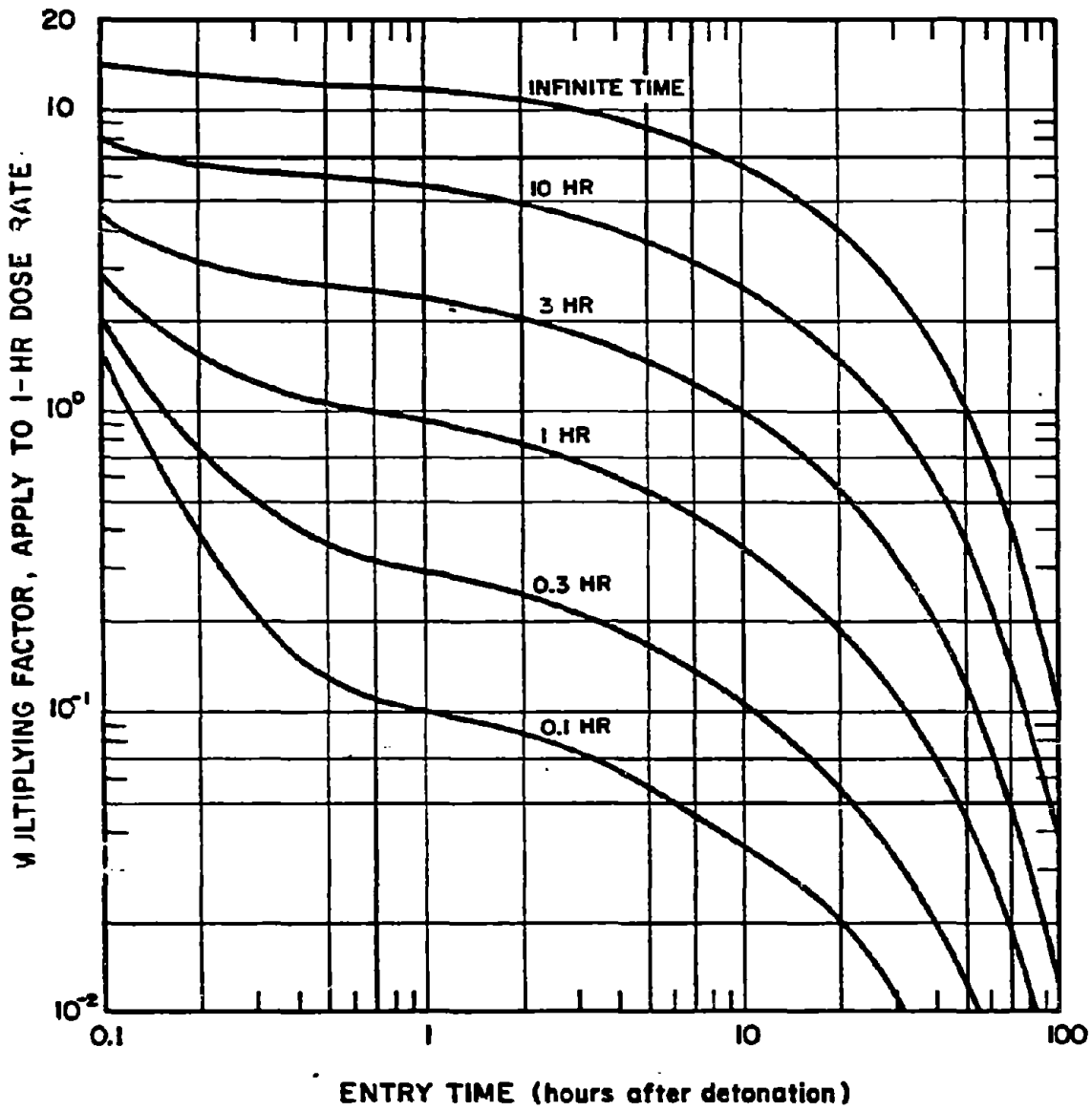
Figure 5-23. ▨ Total Radiation Dose Received in an Area Contaminated by Neutron-Induced Gamma Activity, Soil Type IV ▨

SECTION III

RESIDUAL RADIATION

Residual radiation is that radiation that is emitted later than one minute after the explosion. The sources and characteristics of this radiation vary depending on the extent to which fission and fusion reactions contribute to the energy of the weapon. Residual radiation from a fission weapon arises mainly from fission products and, to a lesser extent, from radioactive isotopes formed by neutron reactions in weapon materials and from uranium and/or plutonium that have escaped fission. Other sources of residual radiation hazard are the activity induced by neutrons that interact with various elements present in the earth, sea, air, or other substances in the explosion environment. The most important of these sources is the neutron-induced activity in soils that is discussed in Section II of this chapter. The radioactivity from a thermonuclear weapon will not contain the same quantity of fission products that are associated with a pure fission weapon of the same yield; however the large number of high energy neutrons will produce larger quantities of neutron-induced activity in weapon components and the surroundings. The total radioactivity from such a weapon will, however, generally be less than from a pure fission weapon of the same yield.

FALLOUT

The main hazard of residual radiation results from the creation of fallout particles that incorporate the radioactive weapon residues and the induced activity in the soil, water, and other materials in the vicinity of the explosion that are sucked up from the earth's surface into the rising fireball. The wind disperses these particles over large areas. Another hazard may arise from neutron-induced activity on the earth's surface in the immediate neighborhood of the burst point. Both the absolute and relative contributions of the fission product and induced radioactivity will depend on the total yield and fission yield of weapon, the height of burst, the nature of the surface at the burst point, and the time after the explosion.

Two phases of fallout may be considered: early (local) and delayed (worldwide). Early fallout reaches the ground during the first 24 hours following a nuclear explosion. It is tl early fallout from surface, subsurface, or low a.. bursts that produces radioactive contamination over large areas, with an intensity great enough to represent an immediate biological hazard. Delayed fallout, which arrives after the first day, consists of very fine, invisible particles that settle in low concentrations over a considerable part of the earth's surface. Radioactive decay during the relatively long time the delayed fallout remains suspended in the atmosphere reduces the radiation intensity from the fission products and other substances significantly. Because of these characteristics, the radiations from the delayed fallout pose no significant military effect and are not considered here.

5-15 Early Fallout

The early fallout from a nuclear weapon consists of fission products and neutron activation products in quantities that are related to the fission and total yields of the weapon, respectively. In the case of a weapon in which large quantity of the energy is derived from fusion reactions, and especially for bursts high in the transition zone between surface (fallout producing) bursts and air bursts where little soil mixes with bomb debris to form fallout, the induced activity can be more important than that from fission products (see Section II). The relative importance of these two sources of residual radiation depends upon the fission-fusion ratio, type and composition of the surface material under the detonation and the height of burst.

For detonations over land, where the particles consist mainly of soil minerals, the fission-product vapors condense onto solid and diffuse into molten soil particles and other particles that may be present. The vapors of the fission products also may condense with vapors of other substances to form mixed solid particles of small size.

The fact that different materials condense at different temperatures, and at different times after detonation, changes the composition of fallout particles, giving rise to the phenomenon known as "fractionation." The occurrence of fractionation is shown, for example, by the fact that in a land surface burst the larger particles, which fall out of the fireball early and are found near ground zero, have radioactive compositions different from the smaller particles that leave the cloud later and reach the ground some distance downwind. The phenomena that account for fractionation are not all completely understood, but models have been developed to explain the phenomena reasonably satisfactorily. An example of fractionation is the change in physical state of fission products, such as krypton and xenon, as they decay. These two example products are gaseous in their normal state and do not combine with other elements to form compounds. During their radioactive decay, however, they form rubidium and cesium, respectively. These decay products can condense onto solid particles. In early fallout, the solid particles will be depleted not only in krypton and xenon, but also in their various decay (or daughter) products. In delayed fallout, small particles that have remained in the cloud for some time will have rubidium and cesium, and their daughters, strontium and barium, condensed upon them. Hence, the delayed fallout will be relatively richer in these elements.

5-16 Air Bursts

The surface contamination effects of fallout from an air-burst weapon are militarily insignificant in most cases, because the cloud carries most of the radioactive weapon debris to high altitudes. In general, by the time this material can fall back to earth, dilution and radioactive decay decreases the activity to levels that are no longer militarily important. An exception may occur in the case of a nuclear weapon cloud that is intercepted by a rainstorm from above. This special case of fallout, called "rainout" is discussed in a subsequent subsection.

5-17 Land Surface Bursts

The activity available from a nuclear explosion at a reference time of 1 hour after burst corresponds roughly to 450 megacuries per kiloton of fission yield.*

Roughly half of the available activity is deposited as early fallout during the first 24 hours following a surface burst. This deposited radioactivity can extend several hundred miles from the burst point, depending on the yield and the prevailing winds. The winds of the upper atmosphere (the stratosphere) slowly deposit the remainder of the activity, or the delayed fallout, over the earth's surface, mainly in the hemisphere of detonation. The land surface burst is used as the standard for the development of deposition patterns and idealized contours that are discussed below. Adjustments to correct these idealized contours for bursts in the transition zone (heights of burst between an air burst and a surface burst) and for underground bursts are described in paragraphs 5-22 and 5-23.

---

* This value approximates the activity per kiloton in disintegrations per second at one hour. Actual values may range from about 430 to about 460 megacuries, depending on the fissile material and the neutron spectrum that causes the fission. The user may encounter other values in various sources, e.g., 550 gamma-megacuries per kiloton at 1 hour after explosion. This latter is a fictitious, but useful, relationship that relates the fission product gamma source to an equivalent monoenergetic source with an energy equal to the average photon energy of the fission products at 1 hour after the explosion.

5-18 Deposition Patterns

In a complete calm, the fallout contamination would form a roughly circular pattern around the point of detonation. Wind leads to an elongated area, the exact nature of which depends upon the speed and direction of the wind from the surface up to the altitude of the top of the stabilized cloud. If the direction of the wind does not vary excessively from the surface up to the top of the cloud, the ground fallout contours may be characterized by a semi-circular pattern upwind from ground zero and an elliptical pattern downwind. The upwind pattern is formed by the rapid settling of the heavier particulate matter in the stem and ejecta from the crater, whereas the downwind elliptical pattern is formed by fallout of smaller and lighter particles from the cloud.

Complicated wind patterns (wind shear) as well as variations of the wind pattern in time and space may cause extreme departures from a simple elliptical pattern. Also, the measured dose-rate contours have frequently been observed to occur in patterns that are best described as a series of islands of relatively high activity surrounded by areas of lower activity. The most common pattern of this type has been one in which the higher dose rate contours appear around two major areas and one or more smaller areas. One of the larger areas is in the immediate vicinity of ground zero; the other is in the general downwind direction from ground zero. The locations of the smaller areas of high activity have not demonstrated patterns that can be described simply in terms of the wind structure. The dose rates observed within these high activity areas have been of comparable magnitude when extrapolated back to some early time after detonation, such as $H + 1$ hour. Because of the earlier arrival of the contaminant, however, the activities actually observed near ground zero have been higher than in the areas away from ground zero. A quantitative treatment of such

complicated deposition patterns is possible only through use of a complex computational model. The simplified method for obtaining deposition patterns presented below will not predict these islands of relatively high activity.

The area covered and the degree of localization of the contamination also depend to some extent on the character of the soil at the burst point. For example, a surface detonation over dry soil with small particle sizes probably would result in a larger area enclosed by low dose rate contours and a smaller area enclosed by high dose rate contours than for the average case. A similar detonation over water covered, finely divided soil such as clay probably would result in relatively high dose rate contours over larger areas close to the detonation, with a corresponding reduction in the areas of the lower dose rate contours farther out.

5-19 Idealized Contours

In any simplified discussion of the areas affected by residual contamination from fallout, it is convenient to set up a system of contamination dose rate contours which, although simplified and idealized, fit actual contours measured in the field as closely as possible. Figure 5-24 illustrates such a contour system. The idealized contour shown consists of a nearly semicircular upwind portion and a roughly elliptical continuation of the contour in the downwind direction. The radioactivity in the vicinity of ground zero is deposited soon after the detonation, largely from heavy particulate matter, ejecta from the crater, and soil made radioactive by neutron-capture reactions. The parameters that define the contour extent in this region are the upwind distance and ground zero width. The parameters that determine the shape of the downwind contours are the downwind distance, maximum width, and distance to the maximum width. To define the downward axis, it is assumed that the downwind direction and extent are determined by a single wind of constant velocity, the so-
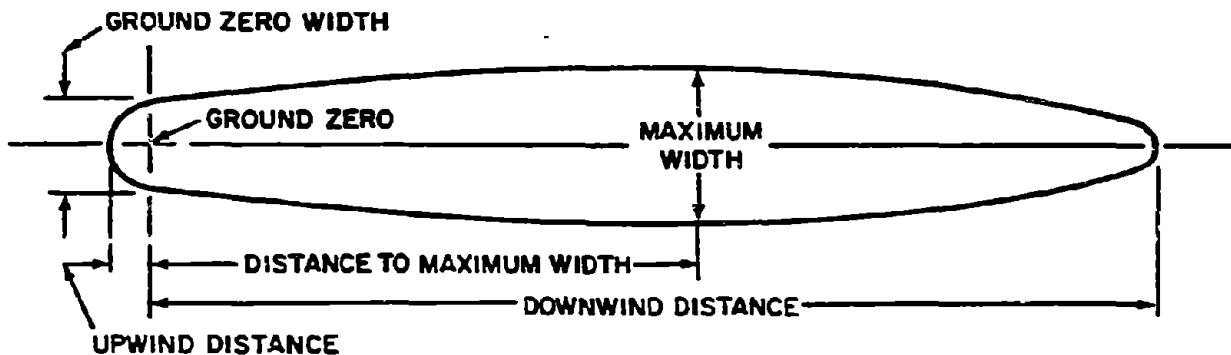
Figure 5-24. (U) Idealized Early Fallout Dose Rate Contour (U)

calied effective wind, as described in paragraph 5-20. Usually wide discrepancy from the idealized pattern will result if there are large directional shears in the winds from the surface up to the altitudes of the stabilized cloud. Such shears can distort the idealized pattern seriously, so that, in practice, radical departures from the idealized patterns can be expected. Figure 5-25 compares the idealized dose rate contour pattern to the observed pattern normalized to 1 hour after shot SMALL BOY, a low yield shot in Nevada during which the wind shear was not .... T.. .... winds had an effective velocity of about 8 knots and an effective shear of about 30 degrees (effective velocity and effective shear are defined in paragraph 5-20). The idealized pattern is shown for an effective velocity of 10 knots and an effective shear of 15 degrees, for the reasons explained in paragraph 5-20. The downwind distance is expected to increase and the crosswind distance to decrease both with an increase in velocity and with a decrease in shear. These tendencies are noticeable in Figure 5-25; however, for this case of low yield and minimal shear, the idealized contours represent a reasonable approximation of the observed contours.

Figure 5-26 shows a hodograph of a typical summer wind structure over Fort Worth, Texas. This is an example of a severely sheared wind structure. The average wind speed to altitudes of the stabilized cloud from a 2 Mt burst is about 10 knots, but, as a result of directional changes, the effective velocity is only 2.5 knots. The direction of this effective wind is 43.5 degrees east of north.

Figure 5-27 shows a comparison of the idealized dose rate contours for a 2 Mt explosion on the surface and the contours computed by the "Defense Land Fallout Interpretive Code (DELFIC)" (see bibliography) for the wind hodograph shown in Figure 5-26 assuming that the winds stayed constant in time and distance. While this comparison is not a comparison with actual data, it is a comparison with the results of a complex computer code that was developed independent of empirical data and which has demonstrated a very good agreement with available data. The general direction as well as the areas of the two patterns are quite divergent. This comparison is intended to illustrate the lack of confidence that can be placed in the idealized contours for prediction of a fallout pattern for a particular explosion, even if meteorological data

5-68

8 KNOTS EFFECTIVE VELOCITY
30° EFFECTIVE SHEAR

1 r/hr

10

100

1000

10 r/hr

100

10 KNOTS EFFECTIVE VELOCITY
15° EFFECTIVE SHEAR

1000
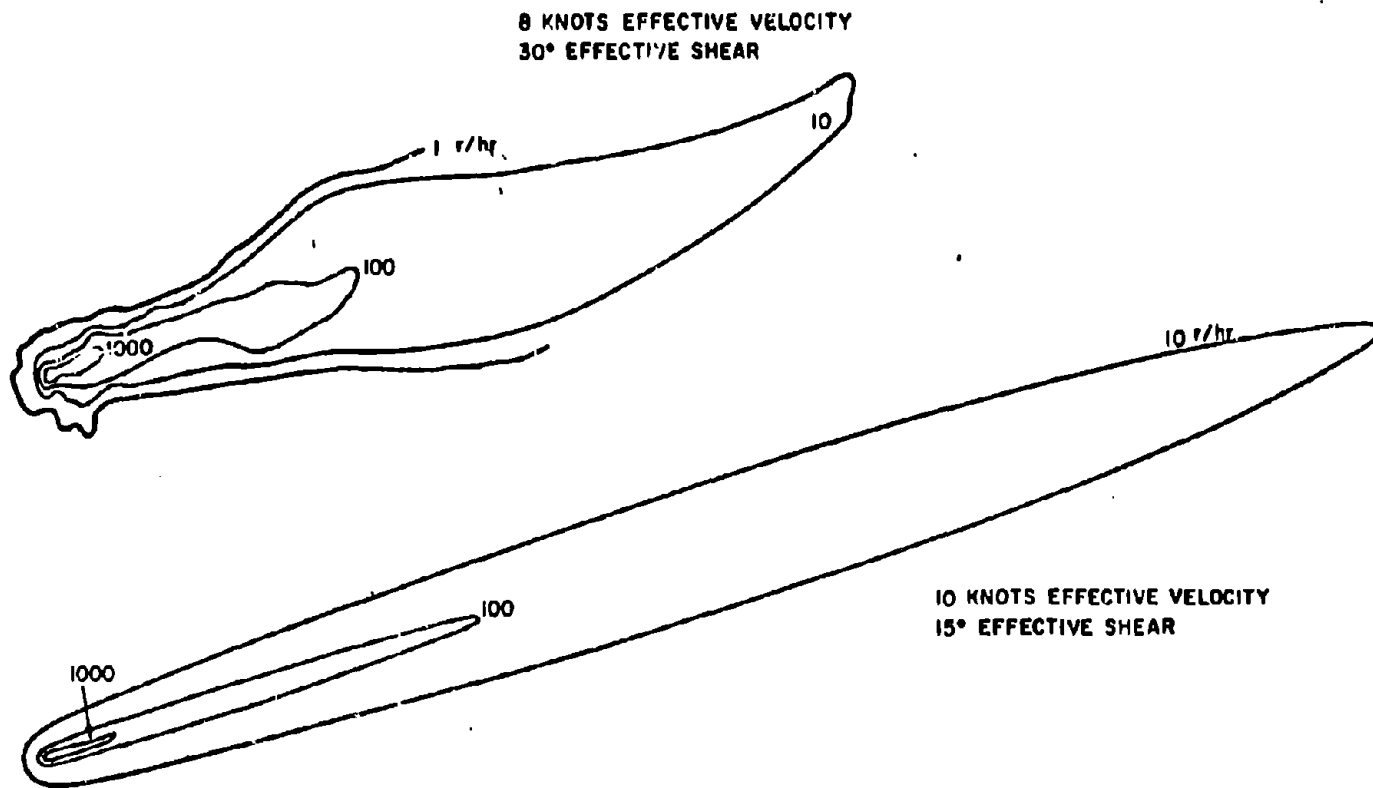
Figure 5-25. ▉ Comparison of Idealized Dose Rate Contours with Observed
Contours from a Low Yield Explosion ▉

20
KNOTS

N

5,000

10,000

20,000

15,000

0
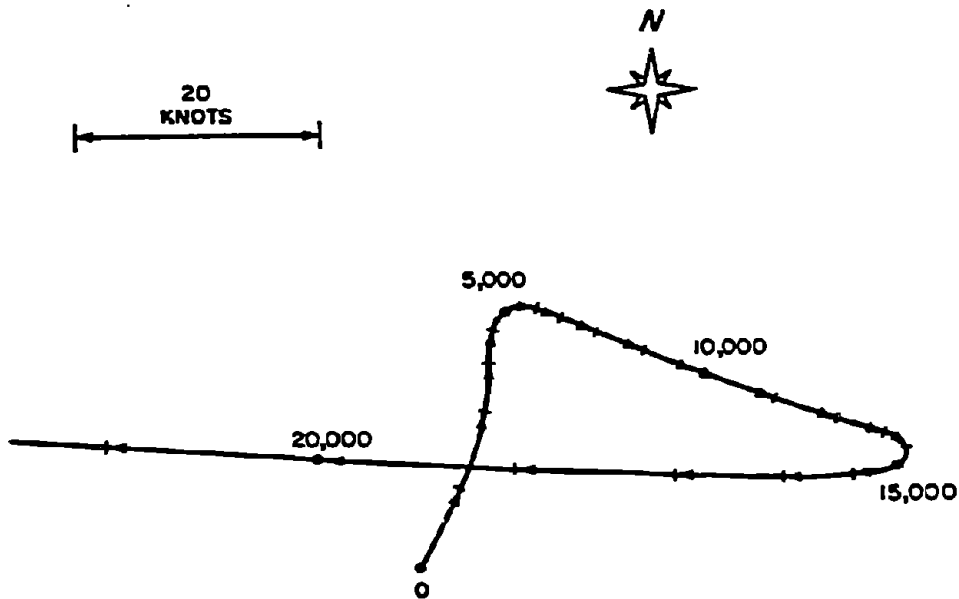
NOTE: NUMBERS ARE METERS OF ALTITUDE.

Figure 5-26. Hodograph of a Typical Summer Wind Structure Over Fort Worth, Texas

at the burst point are known. The contours for the idealized curves were extrapolated to a speed of 2.5 knots even though extrapolation below 10 knots is not recommended. On the other hand, for small yields, or for the case of many weapons, the total dose predicted by the idealized contours over large areas probably would provide a reasonable basis upon which to base casualty predictions.

5-20 Dose Rate Contour Dimensions

Figures 5-28 through 5-37 may be used to draw idealized dose rate contours for land surface explosions with yields between 0.01 kt and 30 Mt. Separate sets of curves are provided for downwind distance, maximum width, and

downwind distance to maximum width for effective wind speeds of 10, 20, and 40 knots. Since actual winds are seldom unidirectional and since the radioactive particles that cover the area around zero include many that were not carried to high altitudes, the ground zero width is presented independent of wind velocity in Figure 5-37. The upwind distance is estimated to be one-half the ground zero contour widths, i.e., they may be represented by a semi-circle, centered at ground zero, with a radius equal to one-half the ground zero width. The dose rate values obtained from the curves correspond to the values existing at a reference time of 1 hour after burst, 3 feet above a hypothetical smooth, infinite plane; therefore, they must be reduced to account for ground roughness. A reduction
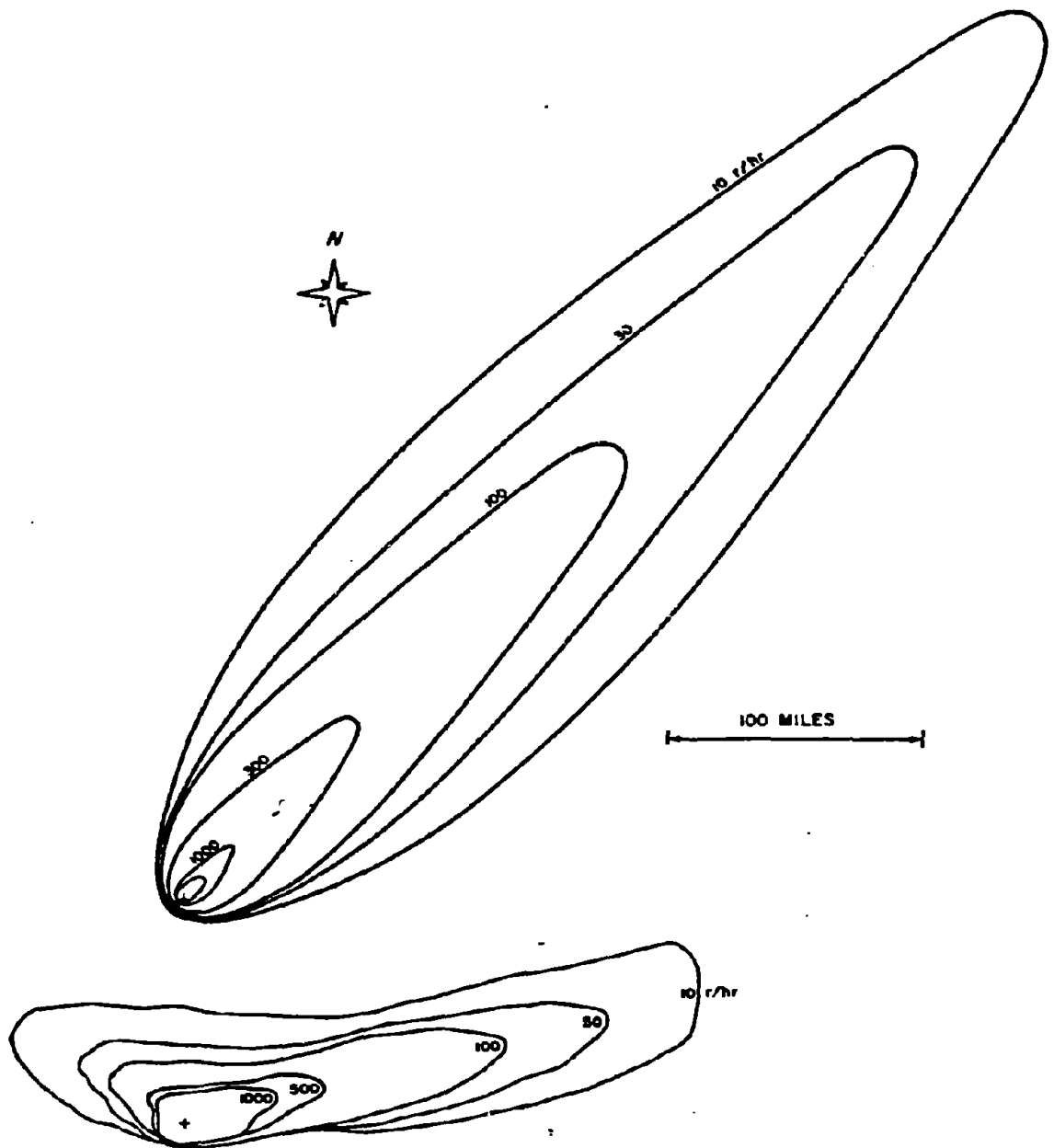
Figure 5-27. ██ Comparison of Idealized Dose Rate Contours with Those Calculated
by a Complex Computer Code for a 2 Mt Explosion and the Winds of Figure 5-25 ██

factor of 0.7 is appropriate for reasonably level terrain. A factor of 0.5 to 0.6 would be more appropriate for rough and hilly terrain. If additional shielding exists (e.g., foxholes, buildings, tanks), additional shielding factors should be obtained from Section VI, Chapter 9.

To obtain the effective wind for use with Figures 5-28 through 5-36, a wind hodograph similar to that shown in Figure 5-26 should be prepared. The vector averages of the winds from ground zero to the base of the stabilized cloud and to the top of the stabilized cloud should then be obtained. The average of-these two average vectors is the effective wind for use with Figures 5-28 through 5-36. The heights of the bottom and top of the stabilized cloud are shown as a function of yield in Figures 5-38 and 5-39, respectively. For wind speeds between the values of 10, 20, and 40 knots that are shown in Figures 5-28 through 5-36, contour values may be obtained by linear interpolation. Extrapolation to values below 10 knots or above 40 knots is not recommended.

As used herein the term "effective shear" refers to the angle between the average vectors to the bottom and top of the stabilized cloud. In the absence of a sufficient quantity of test data with which empirical curves for determining the idealized contours could be generated by use of the Defense Land Fallout Interpretive Code (DELFIC) (see bibliography). An effective shear of 15 degrees was used in the computer calculations from which the curves of Figures 5-28 through 5-36 were derived. In general, increased wind velocity tends to lengthen and narrow the pattern, while increased directional shear tends to shorten and widen the pattern. An effective velocity and an effective directional shear do not define a unique wind structure, i.e., different wind structures could have the same effective velocity and directional shear. It is not recommended that any attempt be made to change the

contour values for effective directional shears different from 15 degrees; however, the user should be aware that differences from this value are more likely to result in idealized contours that are farther from reality than if the shear is nearly equal to 15 degrees.

5-21 Decay of Early Fallout

Fission products are composed of a complex mixture of over 200 different forms (isotopes) of 36 elements. Most of these isotopes are radioactive, decaying by the emission of beta particles, frequently accompanied by gamma radiation. About 2 ounces of fission products are formed for each kiloton (or 125 lb/Mt) of fission energy yield. The total radioactivity of the fission products initially is extremely large but it falls off rapidly as the result of radioactive decay.

At 1 minute after a nuclear explosion, when the residual nuclear radiation is postulated to begin, the gamma ray activity of the 2 ounces of fission products from a 1 kt fission yield explosion is comparable with that of about 30,000 tons of radium. For explosions in the megaton-energy range the amount of radioactivity produced is enormous. Although there is a decrease from the 1 minute value by a factor of over 6,000 by the end of a day, the radiation intensity still will be large.

Early fallout consists mainly, but not entirely, of fission products. The following rule indicates how the dose rate of the actual mixture decreases with time: for every seven-fold increase in time after the explosion, the dose rate decreases by a factor of 10. For example, if the radiation dose rate at 1 hour after the explosion is taken as a reference point, then at 7 hours after the explosion the dose rate will have decreased to 1/10; at 7 x 7 = 49 hours (or roughly 2 days) it will be 1/100; and at 7 x 49 = 343 hr (or roughly 2 weeks) the dose rate will be 1/1,000 of that at 1 hour after the burst.

5-72

Another aspect of the rule is that at the end of 1 week (7 days), the radiation dose rate will be 1/10 of the value after 1 day. This rule is accurate to within about 25 percent up to 2 weeks or so, and is applicable to within a factor of 2 up to roughly 6 months after the nuclear detonation. After 6 months, the dose rate decreases at a much more rapid rate than predicted by this rule.

██ Information concerning the decrease of dose rate in the early fallout can be obtained from the continuous curve in Figure 5-40, in which the ratio of the approximate exposure dose rate at any time after the explosion to a convenient reference value, called the 1 hour reference dose rate, is plotted as a function of time in hours.

██ Table 5-5 gives the results of Figure 5-40 in more convenient, although somewhat less complete, form. The dose rate, in any suitable units, is taken as 1,000 at 1 hour after a nuclear explosion; the expected dose rate in the same units at a number of subsequent times, for the same quantity of early fallout, is then as shown in the table. If the actual dose rate at 1 hour (or any other time) after the explosion is known, the value at any specified time, up to 1,000 hours, can be obtained by simple proportion.

██ It should be noted that Figure 5-40 and Table 5-5 are used for calculations of dose *rates*. To determine the total radiation dose received it is necessary to multiply the average dose rate by the exposure time. Since the dose rate is decreasing steadily during the exposure, however, appropriate allowance for this must be made. The results of the calculations based on Figure 5-40 are expressed by the curve in Figure 5-41, which gives the total dose received from early fallout, between 1 hour and any other specified time after the explosion, in terms of the 1 hour reference dose rate.

██ The continuous curve in Figure 5-40, which represents the decrease in dose rate due to

Table 5-5. ██ Relative Theoretical Dose Rates from Early Fallout at Various Times After a Nuclear Explosion ██

Time (hr)	Relative Dose Rate	Time (hr)	Relative Dose Rate
1	1,000	36	14.0
1-1/2	615	48	9.6
2	435	72	5.9
3	268	100	4.0
5	145	200	1.7
6	116	400	0.75
10	63	600	0.46
15	40	800	0.33
24	22	1,000	0.25

gamma radiation from radioactive fallout, sums up the contributions of the more than 200 isotopes in the fission products and in the activity induced by neutrons in the weapons materials for various times after fission. The effects of fractionation, resulting from the partial loss of gaseous krypton and xenon (and their daughter elements), and from other circumstances, have also been taken into account (see paragraph 5-15). The dose rates calculated in this manner vary with the nature of the weapon, but the values plotted in Figure 5-40 are reasonable averages when the fallout activity arises mainly from fission products. The decrease in the dose rate with time cannot be represented by a simple equation that is valid at all times, but it can be approximated to within 25 percent by the straight dashed lines labeled $r^{-1.2}$ for times between 30 minutes to about 5000 hours (about 200 days) after the explosion. After 200 days, the fallout decays more rapidly than indicated by the $r^{-1.2}$ (broken) line, so the continuous

curve should be used to estimate dose rates from fallout at these times.

(U) While the approximation is applicable, the decay of fallout activity at a given location may be represented by the simple expression

$$\dot{D}_t = \dot{D}_1 \ r^{-1.2},$$

where $\dot{D}_t$ is the gamma radiation dose rate at time t after the explosion, and $\dot{D}_1$ is the 1 hour dose rate, which is also the reference dose rate that is used in Figures 5-28 through 5-37. The actual value of $\dot{D}_1$ will depend on the time units, that is, minutes, hours, days, and so on. In this chapter, time is generally expressed in hours, so that the unit time for the reference dose rate $\dot{D}_1$ is 1 hour.

The curves in Figure 5-40 and the equation given above apply so long as there is no change in the quantity of fallout during the time interval under consideration. Therefore, it cannot be used while the fallout is still descending, but only after it is essentially complete, at the particular location. If during the time t, any fallout material is removed, for example, by weathering or by washing away, or if any additional material is brought to the given point by wind or by another nuclear explosion, neither the curves nor the equation will predict the decay of the fallout activity correctly.

Measurements made on actual fallout from weapons tests indicate that, although the $r^{-1.2}$ decay represents a reasonable average, exponents in the range of -0.2 to -2, rather than -1.2, are sometimes needed to represent the rate of decay. In fact, different exponents are sometimes needed for different times after the explosion. These anomalies, which apparently arise from the particular circumstances of the explosion, are very difficult to predict, except in cases where a large quantity of neutron-induced activity is known to have been produced, either in the ground or in weapon components or both.

Furthermore, fallout from two or more explosions occurring at different times will change the observed decay rate completely. For measurements made over a long period of time after the burst, weathering will tend to alter the dose rates unpredictably. In an actual situation following a nuclear detonation, estimates based on either the $r^{-1.2}$ decay rule or even on the continuous curves in Figures 5-40 and 5-41 must be used with caution and should be verified by actual measurements as frequently as possible.

In principal, either Figures 5-40 and 5-41, or the $r^{-1.2}$ decay equation could be used to estimate the total dose received from fallout in a contaminated area, provided that all of the fallout arrives in a short time. Actually, the contaminated particles may descend for several hours, and without knowing the rate at which the fission products reach the ground, useful calculations cannot be made. However, after the fallout has ceased to arrive, either the figures or the equation will provide rough estimates of radiation doses up to about 200 days after the explosion, provided one measurement of the dose rate is available. After 200 days, the solid curve of Figure 5-40 together with Figure 5-41 should be used. However, at such long times after the explosion, it is not likely that the standard decay pattern will persist. It is advisable to make frequent measurements and to derive an appropriate decay scheme.

Table 5-6 shows the percentage of the infinity (residual radiation) dose that would be received from a given quantity of early fallout, computed from 1 hour to various times after a nuclear explosion. The infinity dose is that which would be received as a result of continued exposure to a certain quantity of early fallout for many years. These data can be used to determine the proportion of the infinity dose received during any specified period following the complete deposition of the early fallout from a nuclear explosion. If the decay followed the

Table 5-6. ███ **Percentage of the Infinite Residence Dose Received from 1 Hour to Various Times After Explosion** ███

Time (hr)	Percent of Infinite Dose	Time (hr)	Percent of Infinite Dose
2	15	72	68
4	28	200	78
6	33	500	85
12	44	1,000	89
24	53	2,000	93
48	63	5,000	98

$t^{-1.2}$ decay law given above beyond 200 days, the infinite residence dose, starting at 1 hour, would be equal to 5 times the $H + 1$ hour dose rate, and this convenient rule of thumb has been used frequently. However, in view of the more rapid decay of the actual fission product mix after about 5,000 hours (see Figure 5-40), a better rule of thumb is that the infinite residence dose is equal to 4 times the $H + 1$ hour dose rate.

███ Figure 5-42 provides a convenient means for determining the total dose received during various times of occupancy of a contaminated area as a function of time of entry. For purposes of prediction, the time of entry may be taken to be the time of arrival of the fallout. Within the accuracy of Figures 5-28 through 5-37, this time may be taken to be equal to the distance from ground zero divided by the effective wind speed, i.e., the buildup of activity during the finite arrival time is neglected.

5-22 Bursts in the Transition Zone ███

███ The deposition patterns and decay rate of the contamination from weapons that are

burst very close to the surface will be similar to those for a weapon of the same yield burst on the surface. However, as the height of burst increases, the activity deposited locally as fallout decreases, and the residual contamination resulting from the neutron-induced activity becomes more important. The exact scaling of the fallout dose rate contour values with height of burst is uncertain. Residual contamination from tests at heights of burst immediately above or below $100W^{0.35}$ feet has been small enough to permit approach to ground zero within the first 24 to 48 hours after detonation without exceeding reasonable peacetime dosages. In these tests the mass of the tower, special shielding, and other test equipment contributed to considerable part of the fallout actually experienced, and neutron-induced activity in the soil added further to the total contamination. Thus, for heights of burst of $100W^{0.35}$ feet or greater, contamination from fallout will probably not be sufficiently extensive to affect military operations materially. Figure 5-43 shows this relation plotted as minimum height of burst versus weapon yield. It must not be assumed that even low to intermediate yields will never present a residual radiation problem when burst above $100W^{0.35}$ feet. The neutron-induced gamma activity can be intense in a relatively small area around ground zero. A better idea of the contamination pattern, dose rate contour values, and decay rate of the residual radiation from the above types of explosions generally will be obtained by basing the predictions on the induced activity as described in Section II of this chapter. In view of the uncertainty involved and the lack of experimental data for high yields burst over land at heights of burst near $100W^{0.35}$ feet, a more conservative estimate of $180W^{0.4}$ feet may be desirable for use under some circumstances as the height at which fallout becomes negligible.

███ A rough estimate of the dose rate contour values for bursts in the transition zone may

be obtained by applying an adjustment factor from Figure 5-44 to the dose rate contour values obtained from Figures 5-28 through 5-37. For bursts in the upper quarter of the fallout transition zone, neutron-induced activity must also be considered. For bursts in the lower three-quarters of the transition zone the neutron-induced gamma activity generally can be neglected compared to the fallout activity.

5-23 Underground Bursts ▇▇▇

▇▇▇▇ A large amount of residual contamination is deposited in the immediate vicinity of the burst point after an underground detonation, because most of the radioactive material falls from the column and cloud to the surface rapidly. A very shallow underground burst conforms closely to the contamination mechanisms and patterns described in paragraphs 5-19 and 5-20 for land surface bursts. As depth of burst increases, a greater percentage of the total available contaminant is deposited as local fallout, until for the case of no surface venting, all of the contamination is contained in the volume of ruptured earth surrounding the point of detonation.

▇▇▇▇ Figure 5-45 shows a depth multiplication factor as a function of scaled depth of burst for yields between 1 kt and 1 Mt. These factors

are applied to the linear dimensions of the dose rate contours for a land surface burst of the same yield, which must be obtained from Figures 5-28 through 5-37. This treatment yields dose rate contours for underground bursts that have shapes similar to the comparable surface burst dose rate contours. Although there is some reason to believe that this is not a valid representation, this treatment does yield a fair representation of the total activity deposited in early fallout patterns. Variations in soil type and other factors introduce additional uncertainties, which are reflected by the broad band in Figure 5-45.

5-24 Beta Radiation ▇▇▇

▇▇▇▇ The hazard from the gamma rays of the residual radiation generally will exceed that from beta particles, except in those cases where intimate contact with beta emitting particles occurs. Such contact may result when an individual lies prone in a contaminated area, or when particles fall directly on the scalp. Burns that range from being superficial to severe may result from such exposures (see paragraph 10-27, Chapter 10). The severity of the burn will depend both on the intensity of the radiation source in contact with the body and on the promptness with which the particles are washed from the skin, i.e., the length of exposure.

Problem 5-8. Calculation of Fallout Gamma Radiation
Dose Rate Contours for Surface Bursts

Figures 5-28 through 5-37 show idealized dose rate contour parameters for residual fallout radiation from surface bursts of weapons with yields between 0.01 kt and 30 Mt. The dose rates are given in terms of exposure rate in roentgens per hour as calculated by the DELFIC computer code for a receiver 3 feet above an infinite plane surface. Within the accuracy of the data, 1 roentgen may be taken to be equal to 1 rad. The actual exposure will be about 0.7 times that shown for the plane surface if the terrain is smooth, and 0.5 to 0.6 times the values for the plane surface if the terrain is rough or hilly. The basic data are presented for weapons from which all the yield results from fission; but, as described below, the data can also be used to obtain fallout contours for weapons for which the fission yield is only a fraction of the total yield, and for which essentially all of the contamination produced (90 percent or more) results from fission products. The dose rate values are given for a reference time of $H + 1$ hour. The more distant parts of the larger contours do not exist at $H + 1$ hour, because the fallout that eventually reaches some of these more distant areas is still airborne at that time. The dose rate contours do exist at later times when fallout is complete, but with dose rate contour values reduced according to the appropriate decay factor from Figure 5-40. Visual interpolation may be used for dose rate contour values between those for which curves are given. Extrapolation to dose rate contour values higher or lower than those shown in the families of curves cannot be done accurately and should not be attempted.

An approximate estimate of the area within particular dose rate contour may be calculated by assuming that the roughly elliptical contour obtained by plotting the parameters

given in Figures 5-28 through 5-37 is an ellipse. The formula for this area is: Area = $\pi ab/4$ where a is downwind distance plus upwind distance, and b is maximum crosswind distance. It mus be realized that the dose rate contours ar ¬ot true ellipses, and that this formula is oni, an approximation.

The decay factors from Figure 5-4 should be used to obtain dose rate values fc times other than $H + 1$ hour. To obtain contoi values for effective winds other than those gi\. in the curves, that is, 10, 20, and 40 knots, linear interpolation may be used. Thus, the downward distance for a 30 knot effective wind speed would be midway between the 20 knot and 40 knot downwind distances.

Contour shapes and sizes are a function of the total yield of the weapon, whereas the dose rate contour values are determined by the fission yield. Thus, if only a fraction of the total yield of the weapon results from fission, and this fraction is known, Figures 5-28 through 5-37 may be used to estimate fallout contours resulting from the detonation of such a weapon. The dose rate for the dimension of interest as read from the figures opposite the total yield must be multiplied by the ratio of fission yield to total yield to obtain the true dose rate value for that dimension. Similarly, to obtain contour dimensions for a particular dose rate, the value of the desired dose rate must be divided by the ratio of fission to total yield, and the dimension of the resultant dose rate read from the figure opposite the total yield.

Example

Given: A hypothetical weapon with a total yield of 600 kt, of which 200 kt results from fission, is detonated on a land surface with 10 knot effective wind conditions.

Find: The contour parameters for a dose rate of 50 rads/hr at $H + 1$ hour reference time over rough, hilly terrain.

Solution: The 50 rads/hr contour for a fission yield to total yield ratio of 200/600 = 1/3 corresponds to the contour of 50 ÷ 1/3 = 150 rads/hr for a weapon for 600 kt fission yield. The dose rate above contaminated rough and hilly terrain is about one-half that above an ideal smooth plane. Thus the desired contour parameters can be obtained by entering Figures 5-28, 5-31, 5-34, and 5-37 with a yield of 600 kt and reading the parameter values corresponding to an $H + 1$ hour dose rate of 2 x 150 = 300 rads/hr (the factor 2 corrects for the rough, hilly

terrain).

Answer: The $H + 1$ hour dose rate parameter values are shown below.

Reliability. The degree to which wind and other meteorological conditions affect these contour parameters cannot be overemphasized. The contours presented in these curves have been idealized in order to make it possible to present average, representative values for planning purposes. Due to these limitations, a meaningful percentage reliability figure cannot be assigned to the idealized fallout pattern.

Related Material. See paragraphs 5-17 through 5-20.

Parameter	Source Figure	Parameter Value for a 10 Knot Effective Wind (miles)
Downwind Distance	5-28	80.0
Maximum Width	5-31	9.0
Distance to Maximum Width	5-34	25.0
Ground Zero Width	5-37	4.4
Upwind Distance	5-37*	2.2

*Upwind distance equals one-half the ground zero width.

Figure 5-28. ▓▓▓ Downwind Distance as a Function of Yield, 10 Knot Effective Wind ▓▓▓
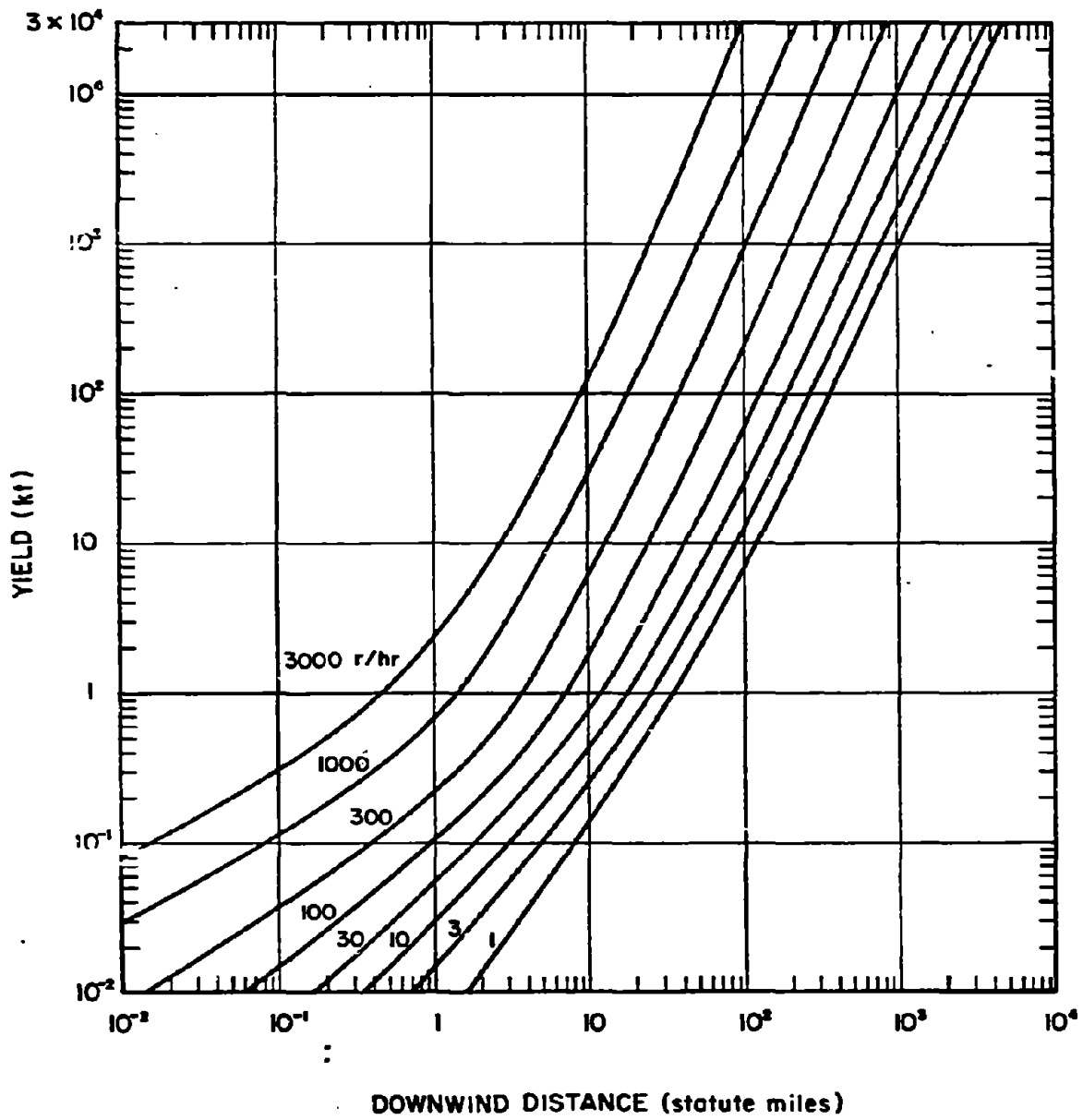
Figure 5-29. ███ Downwind Distance as a Function of Yield, 20 Knot Effective Wind ███
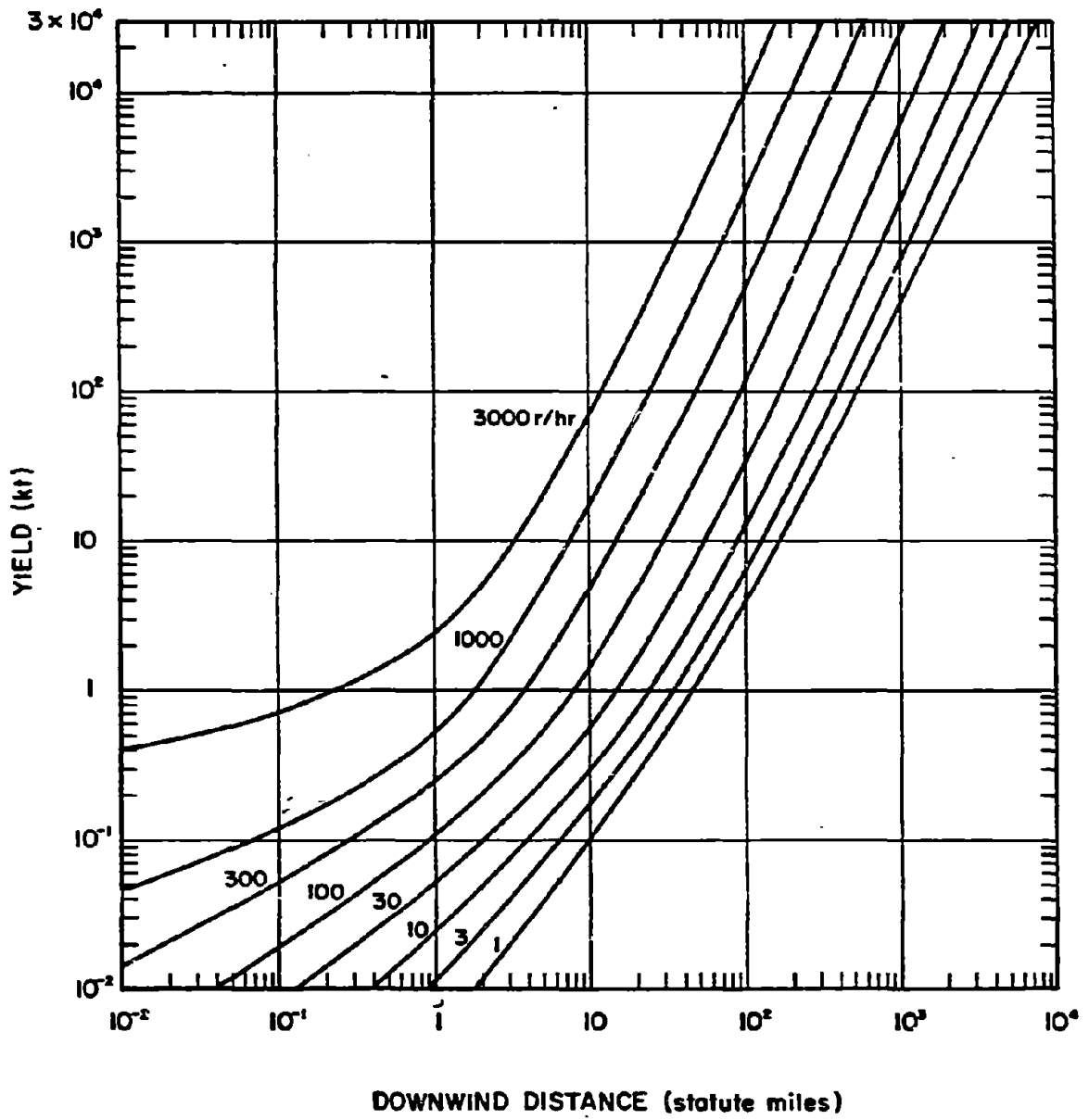
Figure 5-30. ███ Downwind Distance as a Function of Yield, 40 Knot Effective Wind ███

YIELD (kt) — vertical axis: 10^{-2}, 10^{-1}, 1, 10, 10^2, 10^3, 10^4, 3×10^4

Curve labels: 3000 r/hr, 1000, 300, 100, 30, 10, 3, 1

MAXIMUM WIDTH (statute miles) — horizontal axis: 10^{-2}, 10^{-1}, 1, 10, 10^2, 10^3
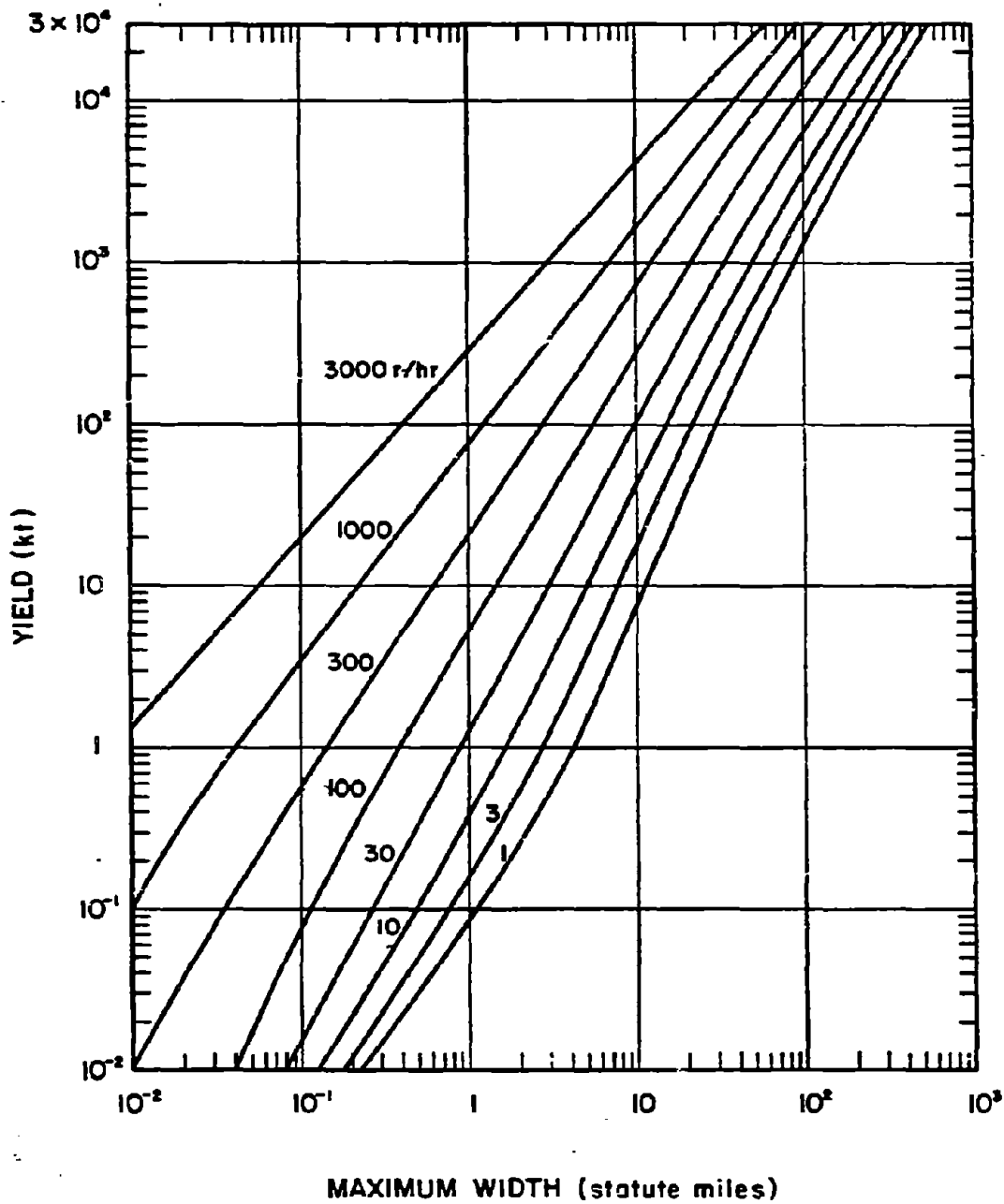
Figure 5-31. ▮▮▮ Maximum Width as a Function of Yield, 10 Knot Effective Wind ▮▮▮

YIELD (kt)

MAXIMUM WIDTH (statute miles)
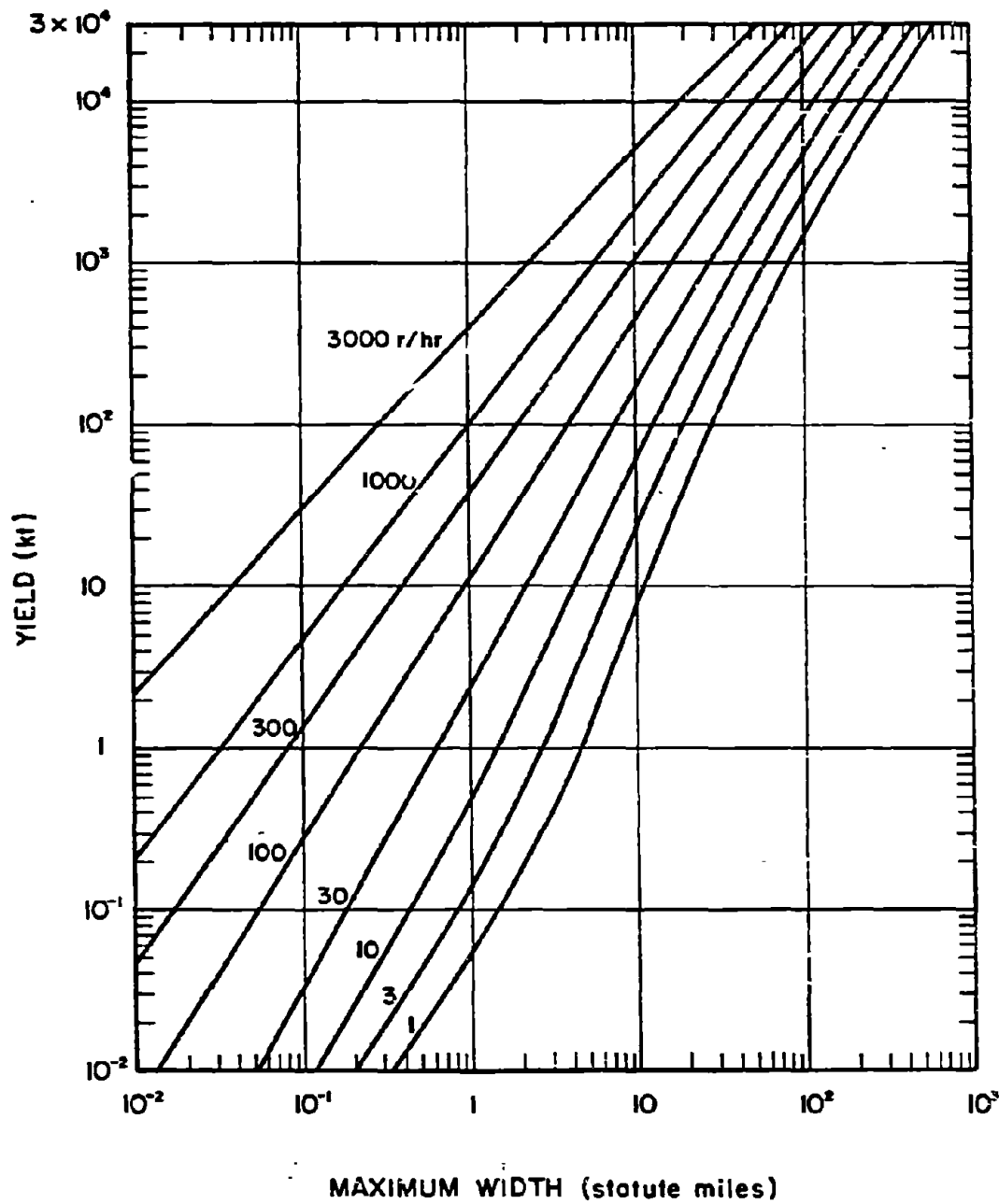
Figure 5-32. ▨ Maximum Width as a Function of Yield, 20 Knot Effective Wind ▨

MAXIMUM WIDTH (statute miles)
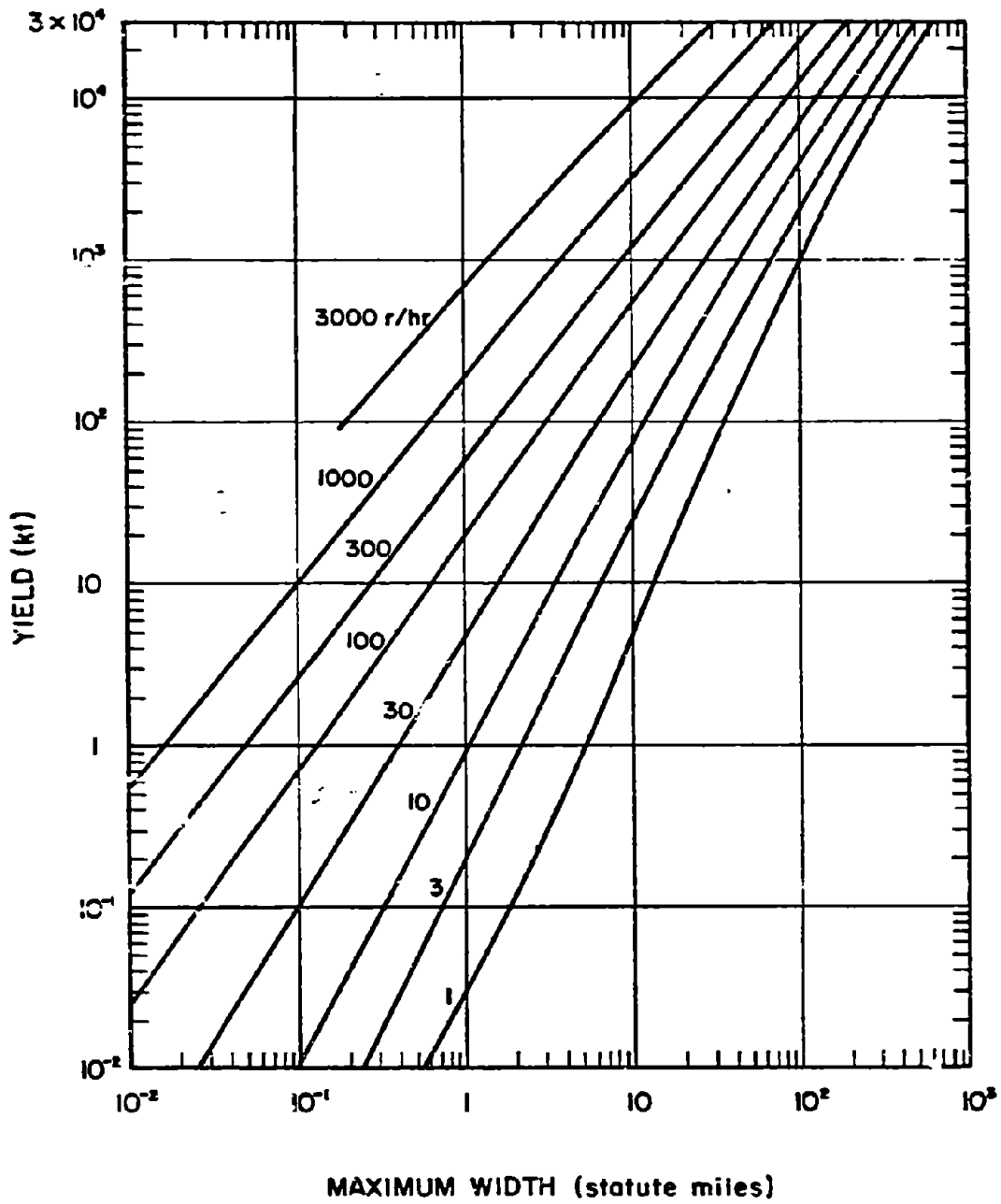
Figure 5-33. ▮▮▮ Maximum Width as a Function of Yield,
40 Knot Effective Wind ▮▮▮

DISTANCE TO MAXIMUM WIDTH (statute miles)
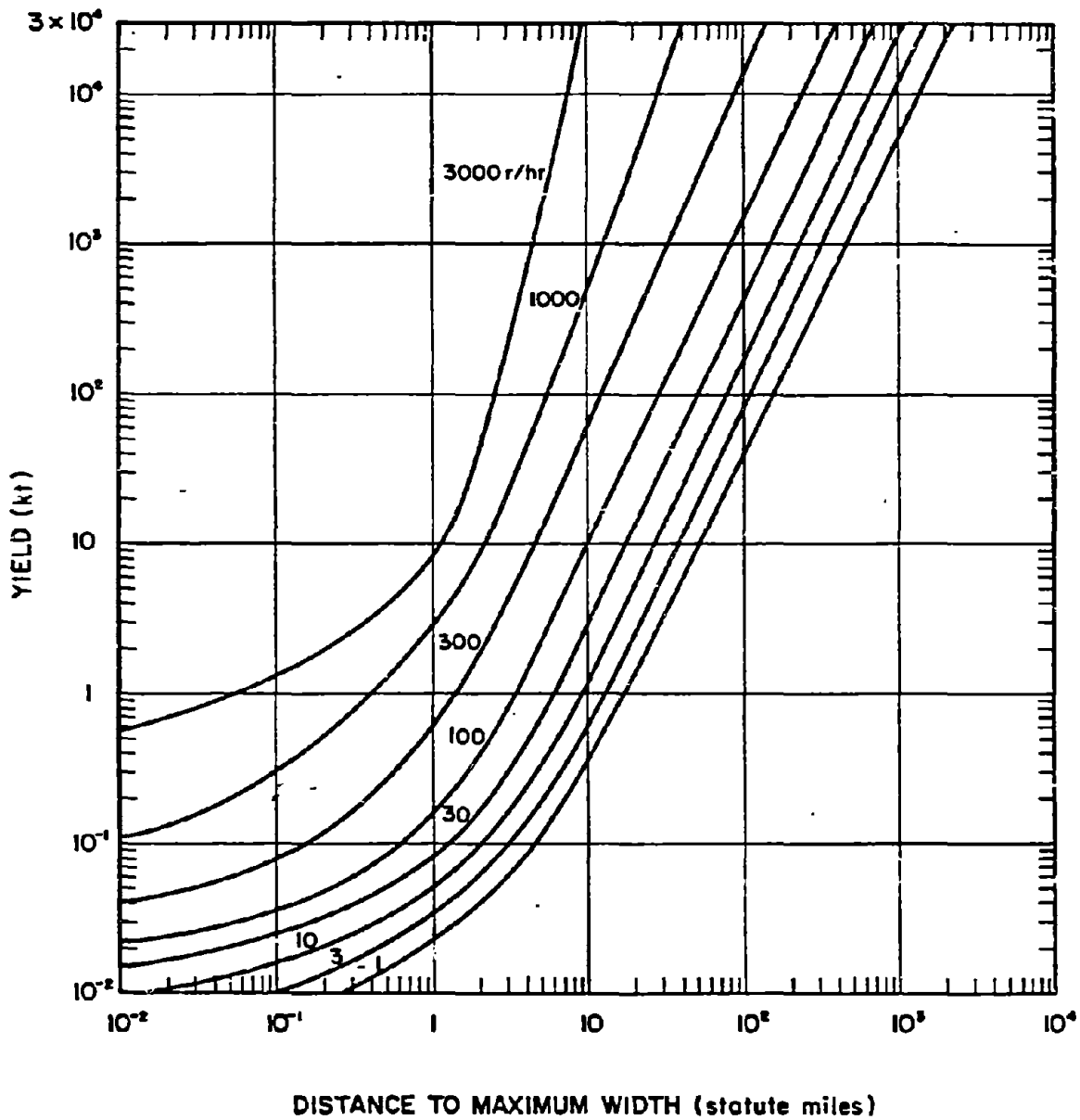
Figure 5-34. Distance to Maximum Width as a Function of Yield, 10 Knot Effective Wind
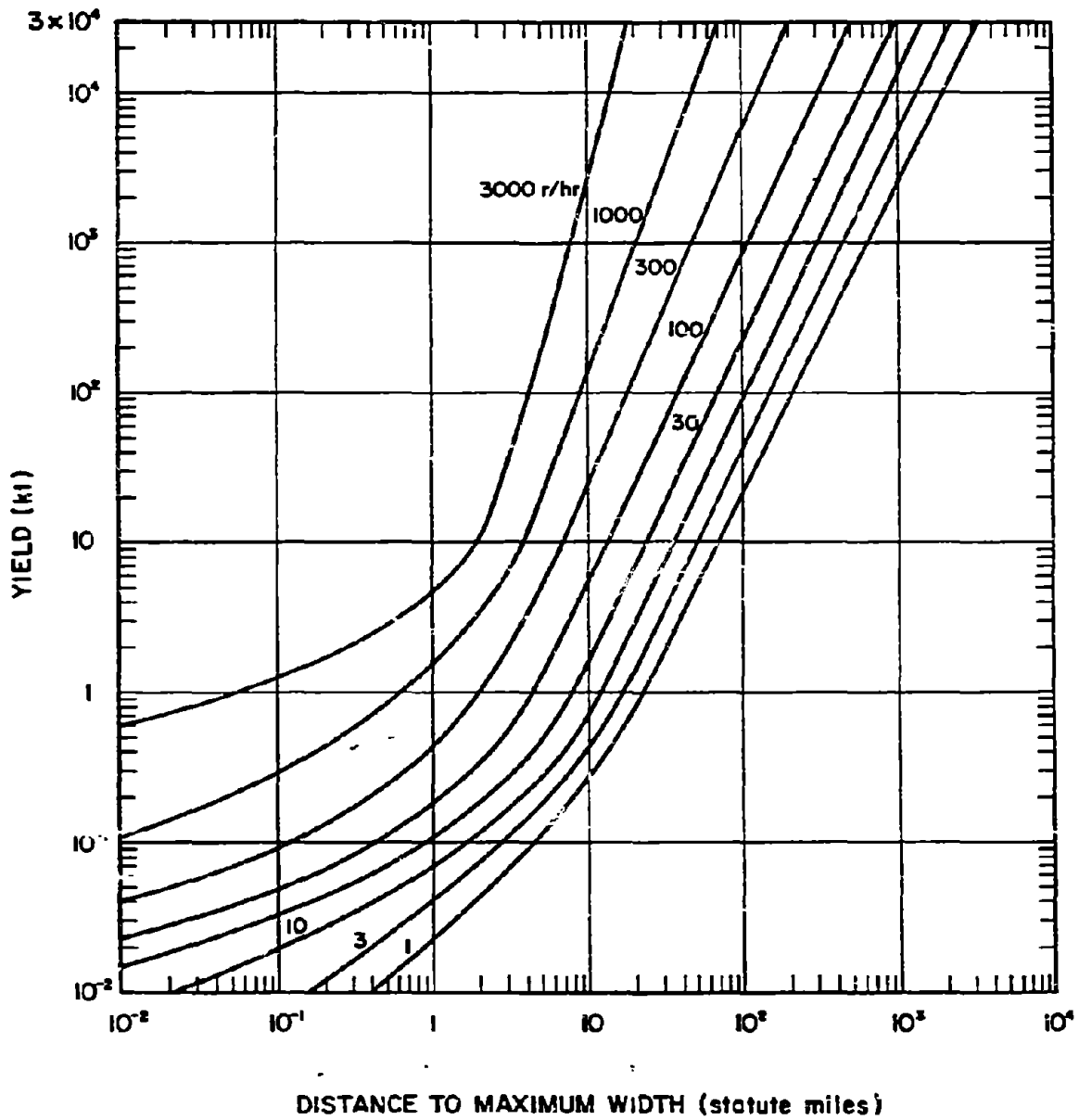
Figure 5-35. ▮▮▮ Distance to Maximum Width as a Function of Yield, 20 Knot Effective Wind ▮▮▮

DISTANCE TO MAXIMUM WIDTH (statute miles)
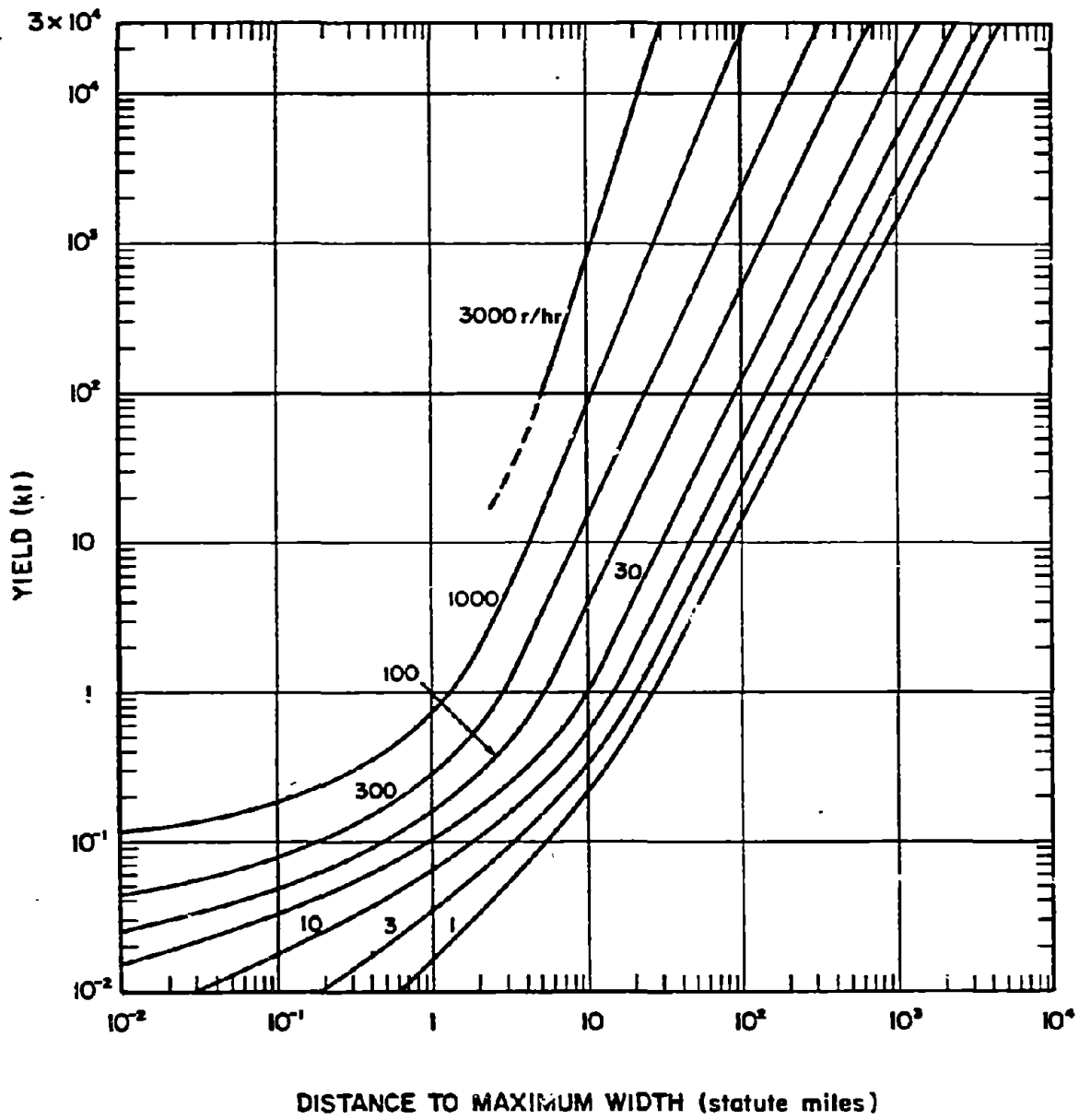
Figure 5-36. ▮ Distance to Maximum Width as a Function of Yield, 40 Knot Effective Wind ▮
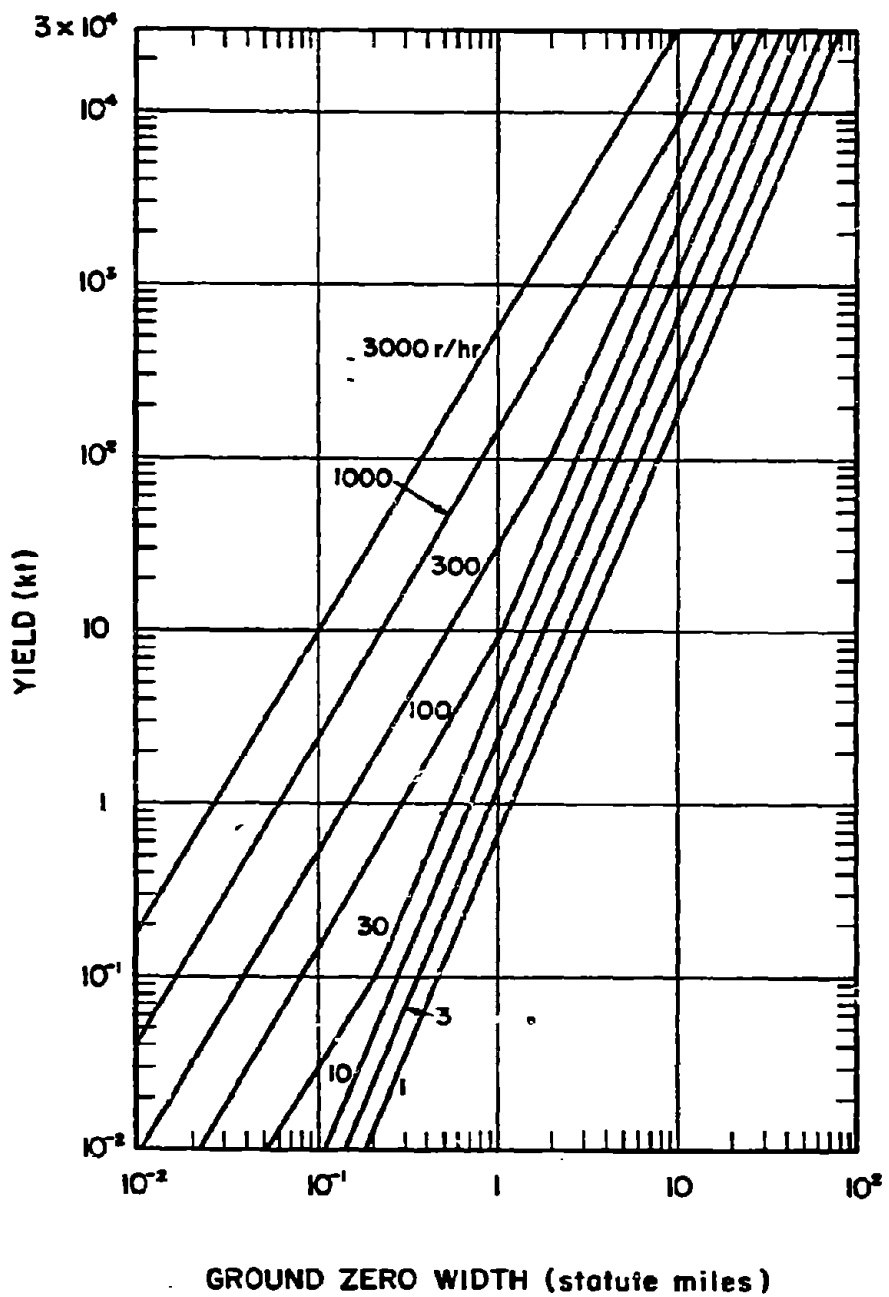
GROUND ZERO WIDTH (stotute miles)

Figure 5-37. ▮▮▮ Ground Zero Width as a
Function of Yield ▮▮▮

5-88
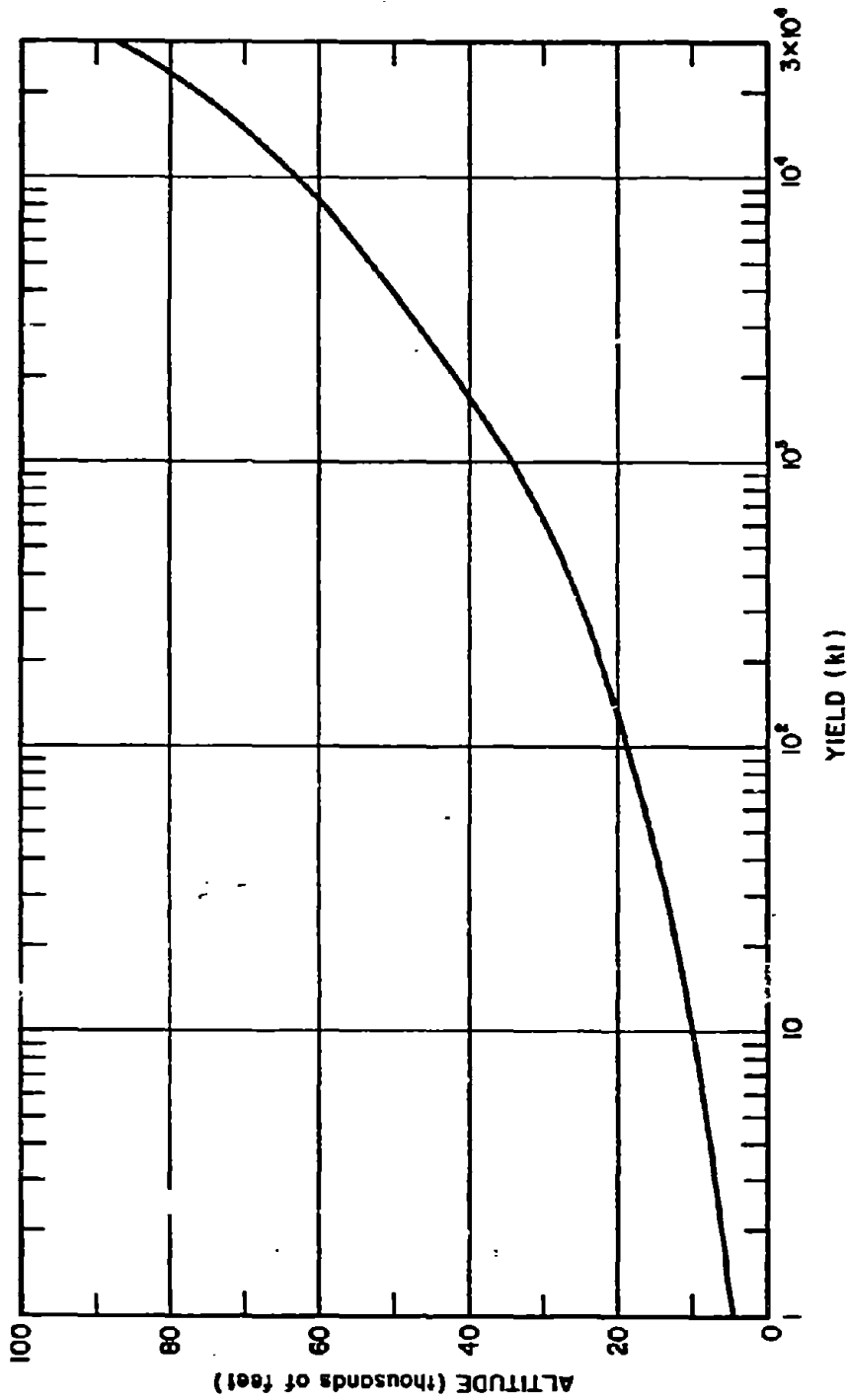
Figure 5-38. ████ Height of the Stabilized Cloud Bottom
as a Function of Yield ████
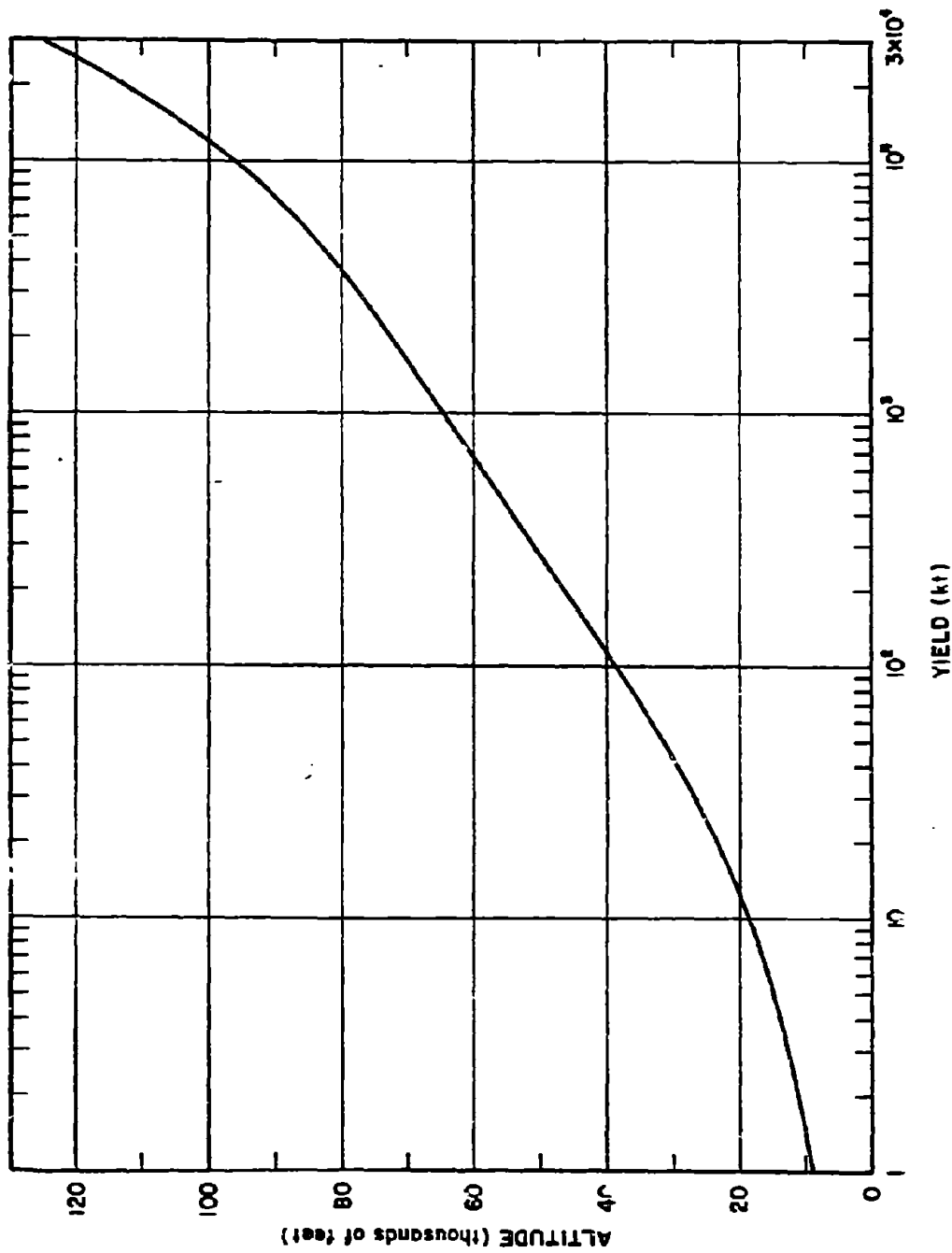
Figure 5-39. ▨ Height of the Stabilized Cloud Top as a Function of Yield

Problem 5-9. Calculation of Fission Product Decay

Figure 5-40 provides fission product decay factors as a function of time after burst. The dose rate at any time can be obtained by multiplying the $H + 1$ hour dose rate by the appropriate decay factor from Figure 5-40. The decay curve also may be used to determine the value of the $H + 1$ hour dose rate from the dose rate measured at a later time. In this case the measured dose rate is divided by the appropriate decay factor.

Example 1

Given: The dose rate at a given point at 1 hour after a nuclear explosion is 500 rads/hr.

Find: The dose rate at that point 12 hours after the explosion.

Solution: From Figure 5-40, the decay factor at 12 hours is 0.05.

Answer: The dose rate at 12 hours is

$$500 \times 0.05 = 25 \text{ rads/hr.}$$

Example 2

Given: The dose rate at a given point 10 hours after detonation is 72 rads/hr.

Find: The dose rate at the same point 1 hour after the detonation.

Solution: From Figure 5-40, the decay factor at 10 hours is 0.06.

Answer: The dose rate at 1 hour is

$$\frac{72}{0.06} = 1,200 \text{ rads/hr.}$$

Related Material. See paragraph 5-21. See also Figure 5-42.
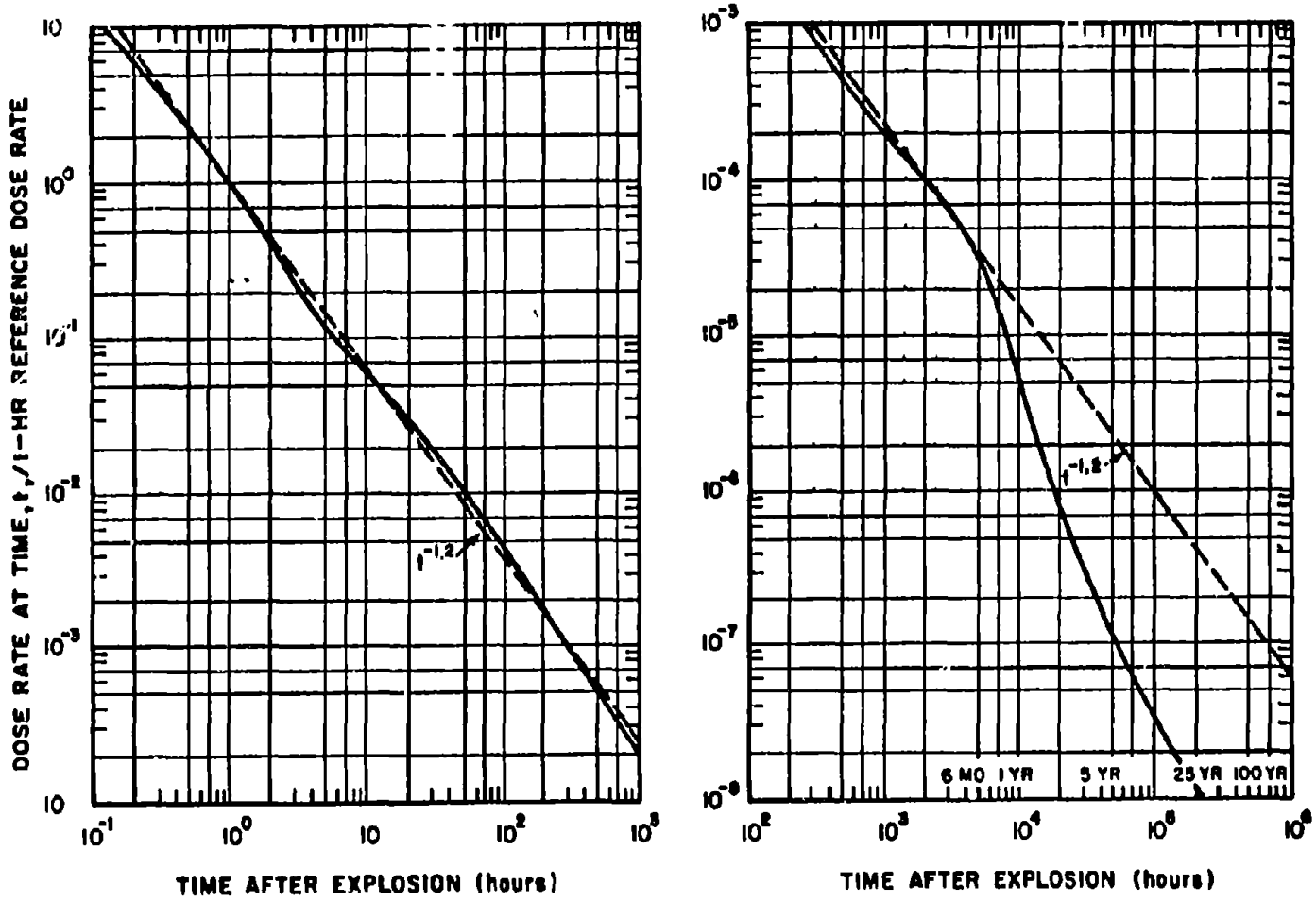
Figure 5-40. ■ Fission Product Decay Factors Normalized
to Unity at 1 Hour After Detonation ■

Problem 5-10. Calculation of Gamma Radiation
Dose as a Function of Time

Figure 5-41 shows the integrated gamma dose received in a fallout-contaminated area as a function of time after $H + 1$ hour (~0.042 day). This curve was generated by integrating the solid curve of Figure 5-40. If the true dose rate at some time between $H + 1$ hour and $H + 1,000$ days is known, Figure 5-41 can be used to estimate the dose accumulated during any time interval in this time range, *provided* the fallout decays as shown in Figure 5-40.

Example

Given: A dose rate of 20 rads/hr is measured in a fallout contaminated area 4 hours after the explosion (fallout had ceased to arrive at this time).

Find: The dose received by personnel who enter the area at $H + 4.8$ hours and remain for 2.5 hours before leaving the area.

Solution:

$$H + 4.8 \text{ hr} = H + 0.2 \text{ day}$$

$$(H + 4.8 + 2.5) \text{ hr} = H + 7.3 \text{ hr}$$

$$= H + 0.304 \text{ day}$$

From Figure 5-41, the normalized dose that would be received between $H + 1$ hour and $H + 0.304$ day is 1.55. Similarly, the normalized dose received between $H + 1$ hour and $H + 0.2$

day is 1.3. Therefore, the *normalized* dose received by these personnel between $H + 0.2$ and $H + 0.304$ day would be:

$$1.55 - 1.3 = 0.25$$

To convert this to actual dose received, use is made of the $H + 4$ hour dose rate (20 rads/hr). From Figure 5-40, the normalized dose rate at $H + 4$ hour is found to be 0.18. The $H + 1$ hour dose rate is

$$\frac{20}{0.18} = 111 \text{ rads/hr.}$$

Answer: The dose that the personnel can expect to receive is found by multiplying the $H + 1$ hour dose rate by the normalized dose obtained from Figure 5-41:

$$111 \times 0.25 \approx 28 \text{ rads.}$$

NOTE: The dose calculated above is only the dose received during the stay at the particular spot in question. Additional dose would be accumulated during entry and exit. The amount of the additional dose would depend on the means of transportation and the size of the contaminated area.

Related Material. See paragraph 5-21. See also Figure 5-42.
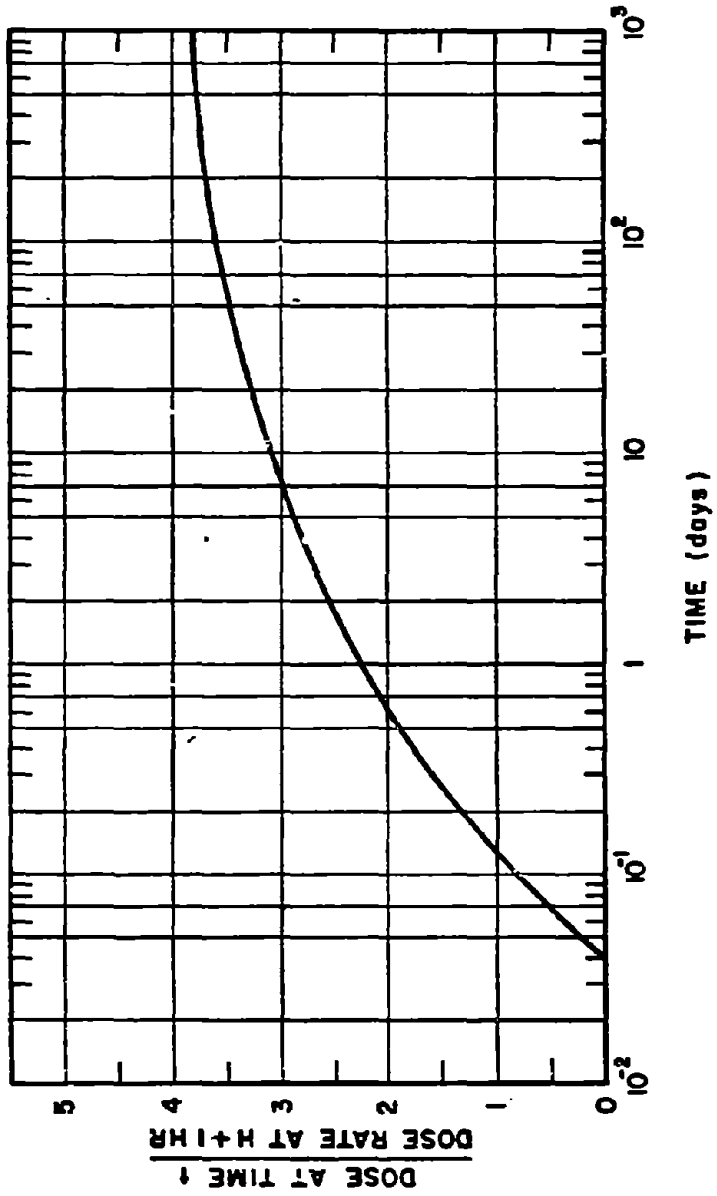
Figure 5-41.   Normalized Dose Accumulated In a Fallout Contaminated Area from H + 1 Hour to H + 1,000 Days

Problem 5-11. Calculation of Total Gamma Radiation
Dose Received in a Contaminated Area

Figure 5-42 gives the total dose received if a contaminated area is entered at a specified time and occupied for a specified interval of time. The vertical axis gives the accumulated dose for each unit (rads/hr) of dose rate at one hour after the detonation. The various curves represent time of stay in the contaminated area. To determine the accumulated dose, a factor is taken from the vertical axis corresponding to the time of entry and the time of stay. The product of this factor and the dose rate at one hour is the accumulated dose.

Example

Given: The dose rate in a given area at 1 hour after a nuclear explosion is 500 rads/hr.

Find: The total dose received by a man who enters the area 2 hours after the explosion and remains 4 hours.

Solution: From Figure 5-42, the intersection of the line for a time of entry of 2 hours after burst with the 4 hour curve gives a factor of 0.8.

Answer: The accumulated dose is:

$$500 \times 0.8 = 400 \text{ rads.}$$

Related Material. See paragraphs 5-21. See also Figures 5-40 and 5-41.

ENTRY TIME (days after detonation)
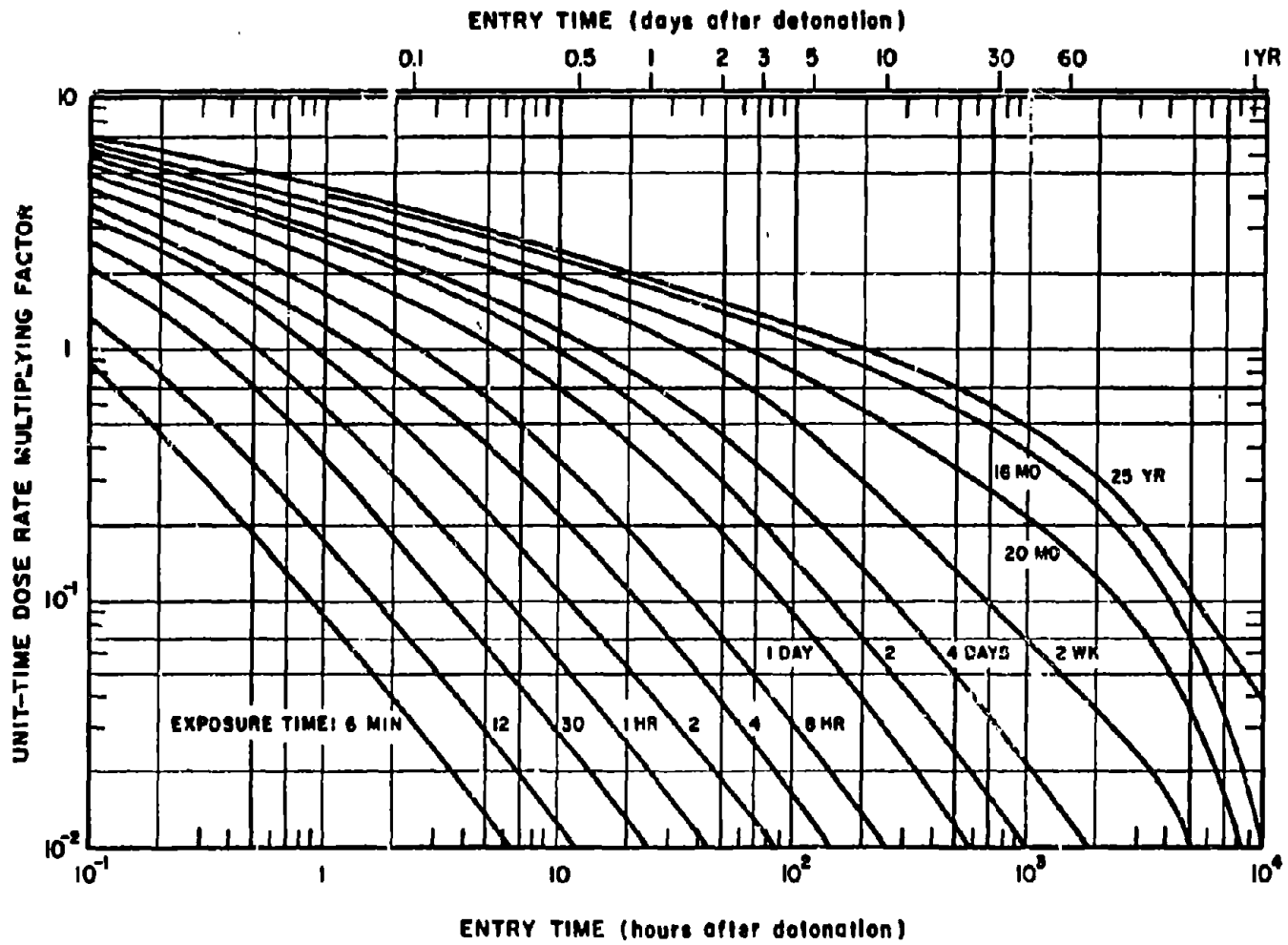
Figure 5-42. ███ Total Radiation Dose from Early Fallout as a Function
of Entry Time and Stay Time, Normalized
to Unit Time Reference Dose Rate ███

Problem 5-12. Calculation of Fallout Gamma Radiation Dose Rate
Contours for Bursts in the Transition Zone

Figure 5-43 may be used to determine whether or not a burst is in the transition zone, i.e., below a height of burst of $100W^{0.35}$ feet. Burst heights below the curve in Figure 5-43 are in the transition zone. Burst heights above the curve are air bursts. In some situations, it may be desirable to consider bursts below $180W^{0.4}$ feet to be in the transition zone for conservative estimates. The means for doing this are discussed below. When a burst occurs in the transition zone, an approximation of the resulting fallout contamination patterns may be obtained by multiplying the dose rate contour values for a contact surface burst weapon of the same yield by an adjustment factor from Figure 5-44. The curves of Figure 5-44 were constructed under the assumption that the ratio of the dose rate values from a burst in the transition zone to the dose rate values for the same contour from a surface burst are proportional to the ratio of the volume of a segment of a sphere intercepted by the ground surface to the volume of the hemisphere, where the radius of the sphere is $100W^{0.35}$ feet, i.e.,

$$\text{Adjustment Factor} = \frac{\left(100 - \frac{h}{W^{0.35}}\right)^2 \left(200 + \frac{h}{W^{0.35}}\right)}{2 \times 10^6},$$

where h is the actual height of burst in feet, and W is the total weapon yield in kilotons.

In view of the lack of data from bursts in the transition zone over a land surface, a more conservative estimate may be desired. In this case, the height of burst for the upper limit of the transition zone is taken to be $180W^{0.4}$ feet. The adjustment factor to be applied to dose rate values for the same contours from a surface burst of the same yield can be calculated from:

$$\text{Adjustment Factor} = \frac{\left(180 - \frac{h}{W^{0.4}}\right)^2 \left(360 + \frac{h}{W^{0.4}}\right)}{1.17 \times 10^7}.$$

Example

Given: A hypothetical weapon with a total yield of 600 kt, of which 200 kt results from fission, is burst 560 feet over a land surface with 10 knot effective wind conditions.

Find: The contour parameters for a dose rate of 15 rads/hr at $H + 1$ hour reference time over smooth terrain.

Solution: From Figure 5-43, a 600 kt weapon burst below about 940 feet would be in the transition zone. A height of burst of 560 feet is less than three quarters of the limiting altitude of the transition, so fallout is the only residual radiation to be considered. The 15 rads/hr contour for a fission yield to total yield ratio of $200/600 = 1/3$ corresponds to the contour for $15 \div 1/3 = 45$ rads/hr for a weapon of 600 kt fission yield. The dose rate over reasonably level terrain is about 70 percent of that over an ideal smooth plane. Thus, the ideal smooth plane contour parameters for this weapon burst on the surface would correspond to

$$\frac{45}{0.7} = 64 \text{ rads/hr.}$$

From Figure 5-44 (or from the normal adjustment factor equation given above) the height of burst adjustment factor for a 600 kt weapon burst at 560 feet is 0.21. Therefore, the desired contour parameters can be obtained by entering Figures 5-28, 5-31, 5-34, and 5-37 with a yield of 600 kt and reading the parameter values corresponding to an $H + 1$ hour dose rate of

$$\frac{64}{0.21} = 300 \text{ rads/hr.}$$

5-97

Answer: The $H + 1$ hour dose rate parameter values are shown below:

Parameter	Source Figure	Parameter Value for a 10 Knot Effective Wind (miles)
Downwind Distance	5-28	80.0
Maximum Width	5-31	9.0
Distance to Maximum Width	5-34	25.0
Ground Zero Width	5-37	4.4
Upwind Distance	5-37*	2.2

*Upwind distance equals one-half the ground zero width.

NOTE: These are the same dose rate contour parameters that were obtained in Problem 5-8 for the 50 rad/hr contour from an identical weapon burst on the surface of rough, hilly terrain.

Reliability. There is little data to support the height of burst correction factors. Additionally, the degree to which wind and other meteorological conditions affect these contour parameters cannot be overemphasized. The contours presented in these curves have been idealized in order to make it possible to present average, representative values for planning purposes. Due to these limitations, a meaningful percentage reliability figure cannot be assigned to the idealized fallout pattern.

Related Material. See paragraphs 5-17 through 5-22.

MINIMUM HEIGHT OF BURST (meters)

YIELD (kt)

MINIMUM HEIGHT OF BURST (feet)

Figure 5-43. Minimum Height of Burst for No Fallout as a Function of Yield

Figure 5-44. Height of Burst Adjustment Factors for Various Yields

Figure 5-45 presents depth multiplication factors for the surface burst contour parameters in Figures 5-28 through 5-37. If the weapon yield and depth of burst in land are known, a multiplication factor can be determined from this curve, or a range of values can be determined for deep bursts. The idealized contour parameters of a surface burst of the same yield are multiplied by this factor to obtain idealized contour parameters for the underground burst.

Figures 5-28 through 5-37 must be used to obtain surface burst parameters. These curves present idealized contour parameters for various effective wind speeds and for yields from 0.01 kt to 30 Mt. These parameters are for a *reference* time of one hour after detonation on an infinite smooth plane. Since these surface burst parameters must be used to determine contours for underground bursts, all conditions that apply to Figures 5-28 through 5-37 also apply to the resulting underground burst contours. For example, to obtain dose rate values for times other than $H + 1$ hour, adjustment procedures are the same for underground bursts as those for surface bursts as discussed in the explanatory text for those figures.

Figure 5-45 shows the depth multiplication factor as a function of depth of burst for a 1 kt explosion. Factors may be obtained for

other yields by the scaling procedures.

Scaling. For yields other than 1 kt, scale as follows:

$$db_1 = \frac{db}{W^{1/3}},$$

where db_1 is the depth of burst for 1 kt and "" is the depth of burst for a yield of W kt. On the equivalent depth of burst for 1 kt has been determined, the depth multiplication factor may be read from Figure 5-45. This factor is applied to dose rate contour values obtained from Figures 5-28 through 5-37 for a yield of W kt.

Example:

Given: A 20 kt explosion at a depth of 135 feet under 20 knot effective wind conditions.

Find: The idealized dose rate contour parameters for a dose rate of 100 rads/hr at 1 hour after the explosion.

Solution: The equivalent depth of burst for a 1 kt explosion is

$$db_1 = \frac{db}{W^{1/3}} = \frac{135}{(20)^{1/3}} = 50 \text{ ft.}$$

From Figure 5-45, the depth multiplication factor corresponding to this depth of burst for a 1 kt explosion is 1.2.

Answer: The $H + 1$ hour dose rate parameters for a 20 kt explosion at a depth of 135 feet are shown below:

Parameter	Source Figure	Surface Burst Value (statute miles)	Depth Multiplication Factor	Underground Burst Value (statute miles)
Downwind Distance	5-29	35.0	1.2	42.0
Maximum Width	5-32	1.4	1.2	1.7
Distance to Maximum Width	5-35	18.0	1.2	21.6
Ground Zero Width	5-37	1.4	1.2	1.7
Upwind Distance	5-37	0.7	1.2	0.8

Reliability. The limitations present in Figures 5-28 through 5-37 and the treatment of surface bursts apply to this treatment of underground bursts. Also, more stringent restrictions must be placed on the use of this treatment of underground bursts. In the absence of sufficient data, the results of a complex computer code were used to generate the idealized dose rate parameter contour values for surface bursts. The results of an equivalent code are not available for underground bursts. Thus, the dependence of the size and shape of a particular contour on depth of burst cannot be predicted in detail,

even under the restrictions of the idealized model presented here. Variations in soil type also are expected to affect the fallout pattern of underground bursts to a greater degree than surface bursts, but there are little data to substantiate this belief. Some of the uncertainties are reflected by the shaded region in Figure 5-45. Although the predictions cannot be considered reliable, this treatment should give a rough picture of the general behavior of the fallout pattern.

Related Material. See paragraphs 5-18 through 5-21 and paragraph 5-23. See also Problem 5-8 and Figures 5-28 through 5-37.
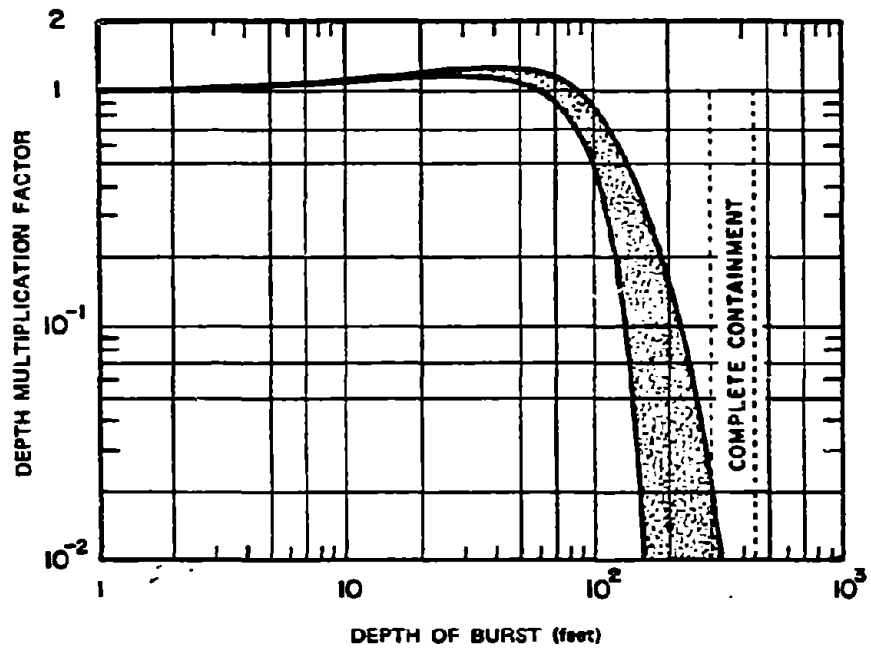
Figure 5-45. ███ Depth Multiplication Factor for Linear
Dimensions of the Fallout Pattern from a 1 kt
Explosion as a Function of Depth of Burst ███

RESIDUAL RADIATION FROM WATER SURFACE AND UNDERWATER BURSTS ▮

▮ The distinction between initial and residual radiation from underwater bursts is much less distinct than it is for air bursts or land surface or subsurface bursts. The radiation accompanying the base surge expands sufficiently rapidly as to become merged with what is normally considered initial radiation. In the case of water surface bursts, the distinction between initial and residual radiation is somewhat more clear cut, but in most cases the residual radiation will not be of great significance.

5-25 Water Surface Bursts ▮

▮ A base surge (paragraph 2-75, Chapter 2) is not expected to form as a result of a water surface burst, consequently a separation between initial and residual nuclear radiation can be made as in the case of a land surface explosion. An approximation of the initial nuclear radiation dose may be obtained from Figures 5-9 through 5-17 in Section I of this chapter. It must be emphasized, however, that the dose so obtained will be an approximation. The curves of Figures 5-9 through 5-17 are based on extensive computer calculations for a receiver on or near a *land* surface. These calculations included the effect of the ground-air interface, and a number of comparisons with measured data have substantiated the validity of the calculations. A limited number of comparisons of the same computer calculations have also indicated good agreement with initial gamma ray dose measurements made near a water surface after high yield explosions; however, these were not true water surface explosions, and no comparisons with neutron dose are available. Thus, in the absence of data and in the absence of comprehensive computer calculations, the curves of Figures 5-9 through 5-17 provide the best available data for

simplified calculations of initial nuclear radiation dose from water surface bursts.

▮ For yields of more than a few kilotons, the cloud from a sea water surface burst is similar to that from a land surface or low air burst of the same yield. The cloud height and horizontal extent are determined primarily by the yield and by atmospheric conditions. For megaton yields, the maximum cloud height may be somewhat greater than that for a land surface burst, as a result of the release of latent heat from condensation of vaporized sea water. For very low yields, it is possible that the maximum cloud height may be less than for a land or low air burst, as a result of interference from the disturbed water. It is also possible, under certain atmospheric conditions, that the sea salt raised and dispersed in the atmosphere by low yield explosions may have a cloud-seeding effect. In this event, the water burst could produce a larger, higher cloud than a land burst, and the dispersion of salt would trigger a rainout of radioactivity.

▮ The possible cloud seeding described above is only one example of the extreme sensitivity of fallout from water surface bursts to atmospheric conditions, especially relative humidity. This sensitivity results from the hygroscopic (water-absorbing) nature of the fallout particles. These particles consist mainly of sea salt and water. When dry, they are generally much smaller and lighter than fallout particles from land surface bursts. Because water burst particles are smaller than those from land bursts, water bursts produce less close-in fallout than land bursts. In particular, water bursts, unlike land bursts, generally will not produce a region of intense fallout (several thousand r/hr) near surface zero. The one possible exception is a water burst in an extremely humid atmosphere.

▮ Water surface bursts are even less likely to produce regular cigar-shaped fallout patterns than land surface bursts. The effect of atmo-

spheric humidity introduces further irregularities in fallout patterns. Also, because water surface burst particles take longer to fall than particles from land surface bursts, wind and weather conditions are more likely to change during the time of fallout transport and deposition. It is often difficult to define a downwind direction in the fallout pattern. The apparent downwind direction may vary with yield and with time after burst at which the pattern is observed or calculated.

In almost all cases, the region of maximum deposit intensity is not around surface zero but considerably downwind. Thus, for a 10 Mt burst, the calculated region of a normalized dose rate of at least 300 r/hr at 1 hour extends from about 125 to 300 miles from surface zero. The dose rate would, of course, be much lower at the time of arrival and would vary throughout the area as a result of varying arrival times.

As material in the cloud rises, it cools by entraining ambient air, and by expanding with increasing altitude. Fallout particles form by condensation of vapor and grow by coagulation; that is, by collision and adhesion of smaller particles to form larger particles. The vapor condensation may be considered a 3-stage process.

In the first stage, calcium and magnesium from the sea water and iron, and other metals from the weapon condense as oxides. In the second stage sodium chloride, which is about 90 percent of dried sea salt, condenses on the nuclei provided by the stage 1 particles. In the third stage, water vapor condenses to liquid water or to ice, on the stage 2 particles.

The median diameter of the stage 1 particles is about 1 micron contrasted to a few hundred microns for a land surface burst. The size is expected to increase slightly with yield, because the particles are formed by diffusion onto nuclei while the fireball is cooling by thermal radiation. The larger the fireball, the slower the cooling rate. The slower the cooling

rate, the more time is available for diffusive growth.

During and after the three condensation stages, coagulation causes particle growth. Particles of sub-micron size coagulate as a result of Brownian motion. Somewhat larger particles coagulate due to turbulent accelerations in the cloud. Turbulent coagulation only appears to be of importance in clouds from megaton bursts. Even larger particles grow by gravitational coagulation; that is, as they fall through the cloud they overtake and capture smaller particles. Gravitational coagulation is particularly important for low-yield bursts in humid atmospheres. The process is similar to one of the mechanisms for growth of ordinary raindrops. The largest particles formed, i.e., those from low yield bursts in a humid atmosphere, may have actual diameters of 2,000 microns. Particles of this size fall out of the cloud rapidly. Thus, there is a practical limit on the growth of particles in the cloud.

Moisture effects play a dominant part in water surface burst fallout. In general, the more humid the atmosphere, the more radioactivity is deposited as close-in fallout. Most of the moisture contained in the clouds of low yield bursts comes from entrained air. Consequently, the higher the humidity, the greater the cloud moisture content. In turn, the salt particles absorb more water, and, as they get larger, gravitational coagulation proceeds faster.

Moisture not only has a direct effect on particle formation, but also has an indirect effect on cloud height. The top of the cloud from a 20 kt water surface burst in a very humid tropical atmosphere may reach the tropopause at about 55,000 feet. In a less humid atmosphere, the cloud from a burst of the same yield may rise less than half as high (see Figure 5-39). Salt particles absorb moisture from humid air; the moisture evaporates when the particles are exposed to relatively dry air. Consequently the

size, falling rate, and time and place of deposit of water surface burst fallout particles vary with the atmospheric humidity the particles encounter during their trajectories. As the particles fall, they usually shrink by evaporation and may become completely dry, with a diameter of at most 100 to 200 microns. They then fall very slowly, and move large horizontal distances as a result of the forces exerted by the wind. Finally, the particles reach the more humid air near sea level, begin to grow by absorbing moisture, and fall faster. Thus, although particles from a megaton burst may leave the cloud with a water content almost entirely derived from sea water, this water may evaporate completely during fall, and the water content of the particles that reach the surface is entirely atmospheric moisture. An exception to this situation could occur for a burst in an arctic atmosphere. The cold air retards evaporation, even if humidity is low, and some of the original sea water could remain on the particles.

Maximum fallout intensity, as well as the area covered by fallout from a water surface burst increases with weapon yield. For yields between 1 kt and 100 kt, the normalized $H + 1$ hour exposure rates are expected to be negligible. The highest normalized intensities from a 100 kt explosion are expected to be more than 30 roentgens per hour (r/hr), but less than 100 r/hr. The highest intensities from a 1 Mt burst are expected to be over 100 r/hr but less than 300 r/hr. Finally, a 10 Mt burst is expected to produce intensities over 300 r/hr, but less than 1,000 r/hr. Since all of these exposure intensities are normalized to $H + 1$ hour, and the fallout will arrive at significantly longer times after burst for the larger yields (depending upon the wind), the radioactivity will have decayed to much smaller levels prior to the time of arrival and fallout generally is not expected to be a governing effect from water surface bursts.

5-26   Underwater Bursts

An underwater burst creates a highly energetic bubble, whose history determines the major above-surface effects. For very shallow explosions, the bubble expands through the water surface with a high internal pressure, and develops a hollow column through which the bubble blows out into the atmosphere in the form of a cloud at the column top. For a somewhat greater depth, the bubble expands through the water surface at lower internal pressure and a column again forms, but no blowout occurs. Transition from columnar formations to plume-like eruptions, hemispherical in shape, takes place as the depth increases. The migration of the underwater bubble through the surface near its minimal phase at or shortly after its maximum-expansion phase creates the plumes. For deep explosions, the bubble may experience several oscillations as it migrates upwards. If the explosion is very deep, the bubble will degenerate and break up before reaching the surface. It is possible that an explosion may take place at such a great depth that little, if any, disturbance will be noted on the surface.

The ejected water, whether a column or a plume, will fall back to the surface rapidly. This massive subsidence creates a radially expanding aerosol cloud, or base surge, at the water surface. The base surge expands as a ring or disk until it dissipates energy received from the subsidiary plumes or columns. After expanding, it drifts with the surface winds. Some evidence suggests the base surge has the same initial bulk density as that of the plumes or columns from which it is formed, being several times the density of air. As it travels downwind, it will react to the existing atmospheric conditions; e.g., evaporating or developing into low-cloud formations. These physical phenomena are described in more detail in Section IV, Chapter 2.

Three sources of radioactivity are the

major contributors to the radiation above the surface subsequent to an underwater explosion: initial, above surface nuclear radiation; base surge; and residual radioactivity deposited in the mixed layer of the ocean. These sources are very time dependent, and they are affected by atmospheric and oceanic variables.

███ Even for a shallow underwater explosion the neutron and secondary gamma portions of the initial nuclear radiation are essentially negligible. The initial above-surface source includes the fission product activity contained in the visible column and crown, or plume. This source contains radioactivity ejected into the atmosphere as a result of underwater hydrodynamic phenomena. The scaled depth of burst is a major factor in determining the extent to which this initial radiation contributes to the total above surface exposure. The rapid development and spread of the base surge (paragraph 2-75, Chapter 2) causes the initial and residual radioactivity from an underwater burst to merge into one more or less continuous source.

███ The base surge develops as a result of both underwater flow phenomena and the collapse of the water masses associated with the initial source. This radially expanding surge grows to large dimensions as a dense, fog-like aerosol carrying with it a substantial fraction of suspended fission products. This source is either annular or disk-shaped in geometry and extends from the ocean surface to a height of several thousand feet. The base surge is influenced strongly by the wind, moving as an entity at the existing wind speed and direction. Initially it is highly radioactive; however, as it expands and dilutes, the concentration of the fission products decreases. This dispersion, coupled with rapid radioactivity decay, results in comparatively low exposure rates by the first half-hour after burst.

███ The residual radioactivity in the surface layer of the ocean is the third, and final, major source of radiation. This radioactive pool is moved by the local currents, which depend on the existing oceanographic conditions. The pool is initially a disk which upon expansion approximates an annulus, although at times significantly later than a half-hour, it reverts to an irregular disk shape. Eventual mixing down to the top of the thermocline and the action of horizontal turbulent diffusion result in rapid dilution of the pool, reducing its hazard as time progresses.

███ The gamma radiation hazard created by the initial source, base surge, and pool resulting from an underwater nuclear explosion varies significantly with weapon yield and burst depth, proximity of the ocean bottom to the point of detonation, wind velocity and current velocity. Consequently, a description of the radiation fields (exposure rate and total exposure) associated with an underwater burst is complex, and no simplified prediction system suitable for general application has been developed.

███ A prediction system, DAEDALUS, has been developed to compute the radiological effects of underwater nuclear bursts. In this system, all above-surface sources, as well as the radioactive pool, are approximated by cylinders homogeneously contaminated with mixed fission products. The dimensions, water concentrations, and fission product contents of these cylindrical sources are estimated from empirical and theoretical considerations. Having defined the radioactive sources, DAEDALUS calculates, for each time of interest, exposure rates from these sources at specified detector locations. At each location the exposure rates are summed over time and the total exposure is thus cumulated. In the absence of a simple prediction system suitable for inclusion in this manual, examples of the results of DAEDALUS calculations are presented to provide an appreciation of the potential magnitude of the problems associated with radioactivity from underwater nuclear bursts.

Table 5-7. ■ Examples Selected for Base Surge and Pool Exposure Rates ■

Yield (kt)	Explosion Depth (ft)	Depth of Water (ft)	Base Surge Figure Number	Pool Figure Number
10	65	5,000	5-46	5-52
10	65	65	5-47	5-53
10	150	5,000	5-48	5-54
10	500	5,000	5-49	5-55
10	1,000	5,000	5-50	5-56
10	1,500	5,000	5-51	5-57

■■■ A yield of 10 kt was selected to illustrate the effects of depth of burst and water depth on the time dependence of the gamma ray exposure rates from the base surge and the pool. Table 5-7 shows combinations of depth of burst and water depth that were selected. Table 5-7 also indicates the corresponding figures that show exposure rates as a function of time and radial distance from the source for the base surge and the pool respectively. A no-wind environment was chosen for these examples, and, in the case of the pools, a no-current environment was assumed.

■■ Figures 5-58 through 5-75 show the accumulated exposures for two scaled depths ($d_b \approx 30W^{1/3}$ and $d_b \approx 280W^{1/4}$), corresponding to very shallow and deep explosions, respectively (Figure 2-105, Chapter 2). The doses are shown for 1, 10, and 100 kt explosions at each scaled depth. Two minute, 10 minute, and 30 minute exposures are shown for each yield at each scaled depth. In all cases it was assumed that the depth of the water was 5,000 feet, the effective wind was 15 knots, and a no-current condition existed. Table 5-8 identifies the figure for each combination of yield, burst depth, and exposure time.

Table 5-8. ■ Examples Selected for Total Exposure ■

Yield (kt)	Explosion Depth (ft)	Exposure Time 2 Minutes	10 Minutes	30 Minutes
1	30	Fig. 5-58	Fig. 5-59	Fig. 5-60
10	65	Fig. 5-61	Fig. 5-62	Fig. 5-63
100	140	Fig. 5-64	Fig. 5-65	Fig. 5-66
1	280	Fig. 5-67	Fig. 5-68	Fig. 5-69
10	500	Fig. 5-70	Fig. 5-71	Fig. 5-72
100	890	Fig. 5-73	Fig. 5-74	Fig. 5-75

RADIAL DISTANCE FROM SOURCE AXIS (yards)
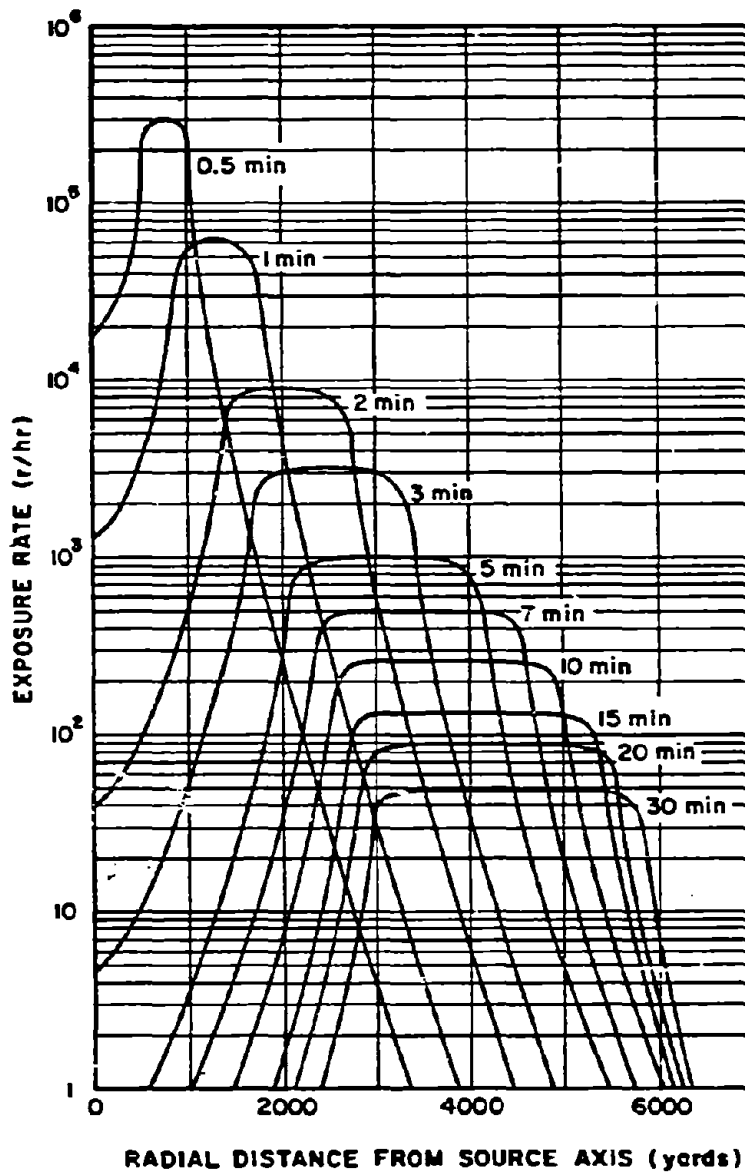
Figure 5-46. ▮▮▮ Base Surge Radiation Exposure Rate 15 Feet
Above the Water Surface from a 10 kt Explosion
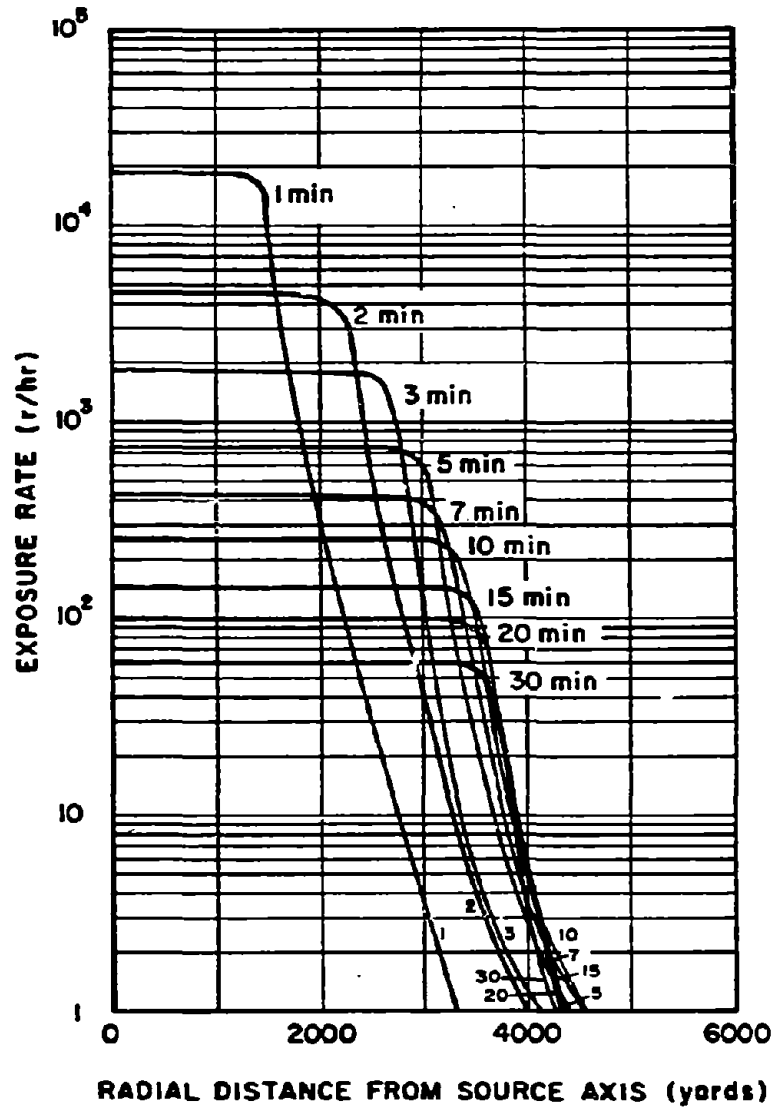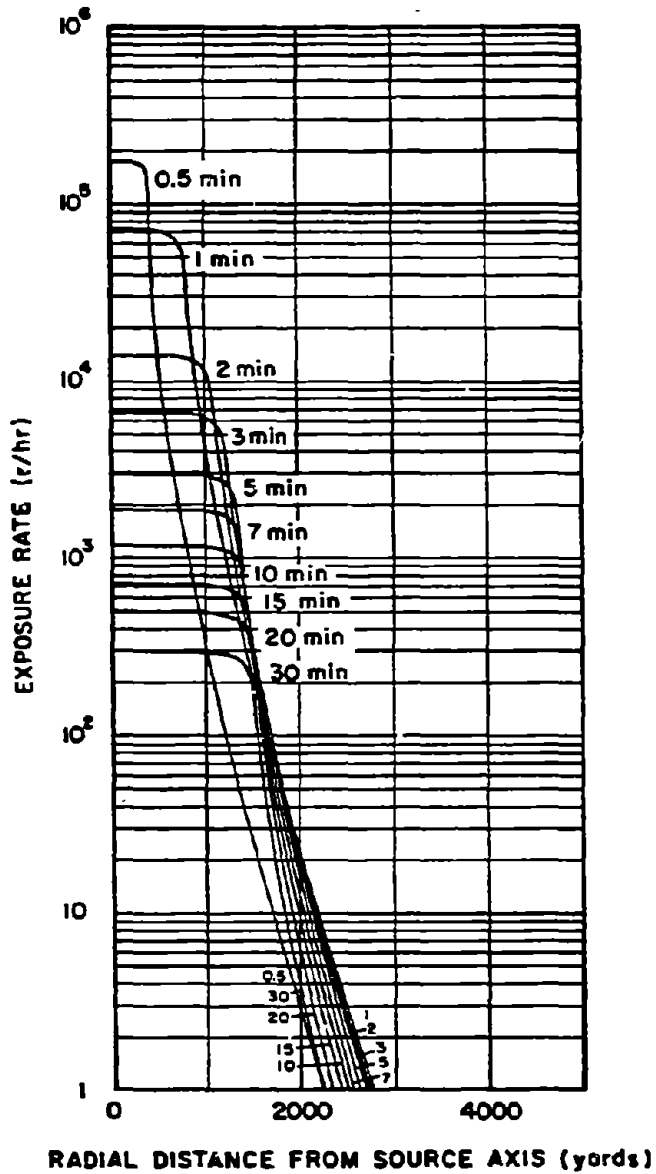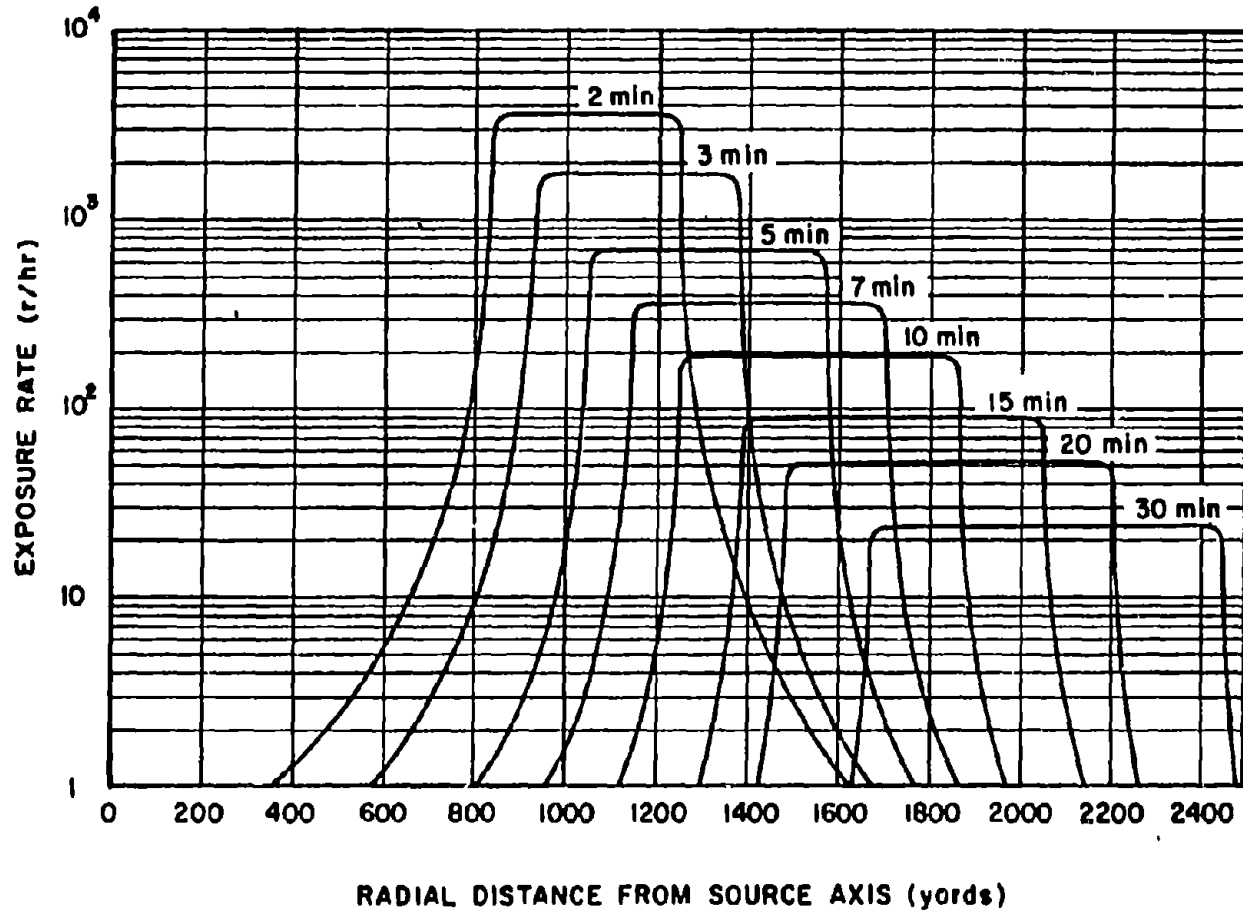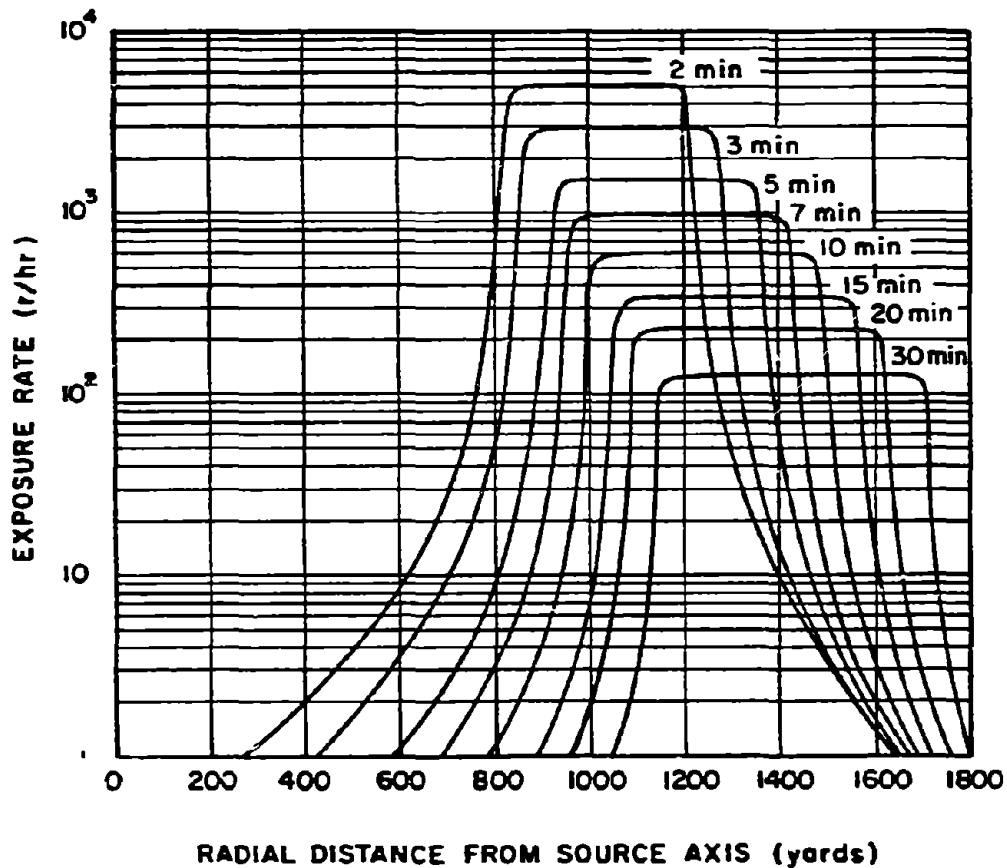at a Depth of 65 Feet in 5,000 Feet
of Water, No-Wind Environment ▮▮▮
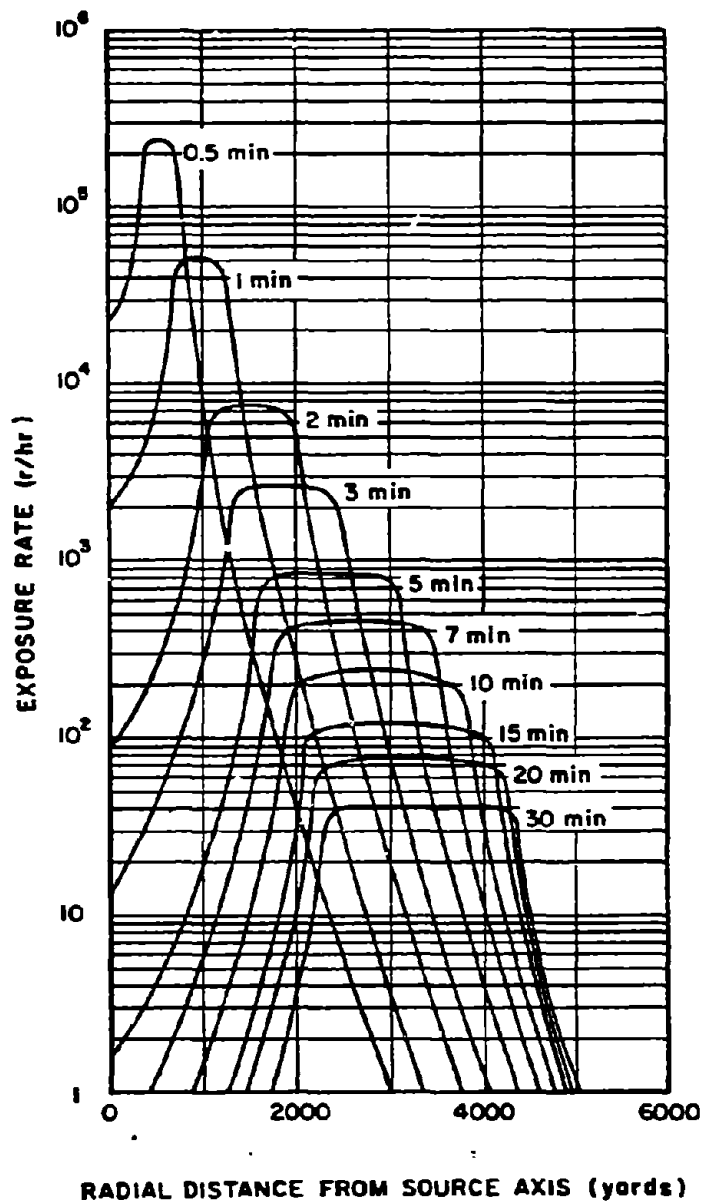
Figure 5-47. ▇▇▇ Base Surge Radiation Exposure Rate 15 Feet
Above the Water Surface from a 10 kt Explosion
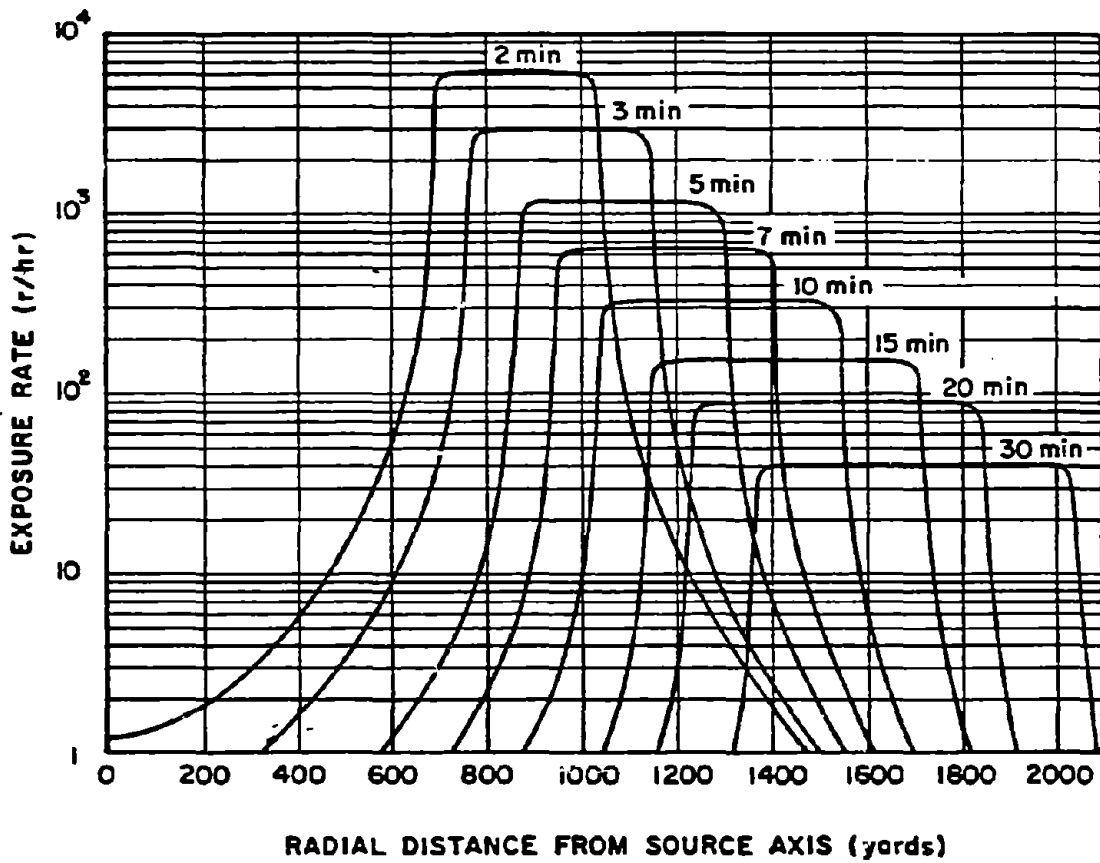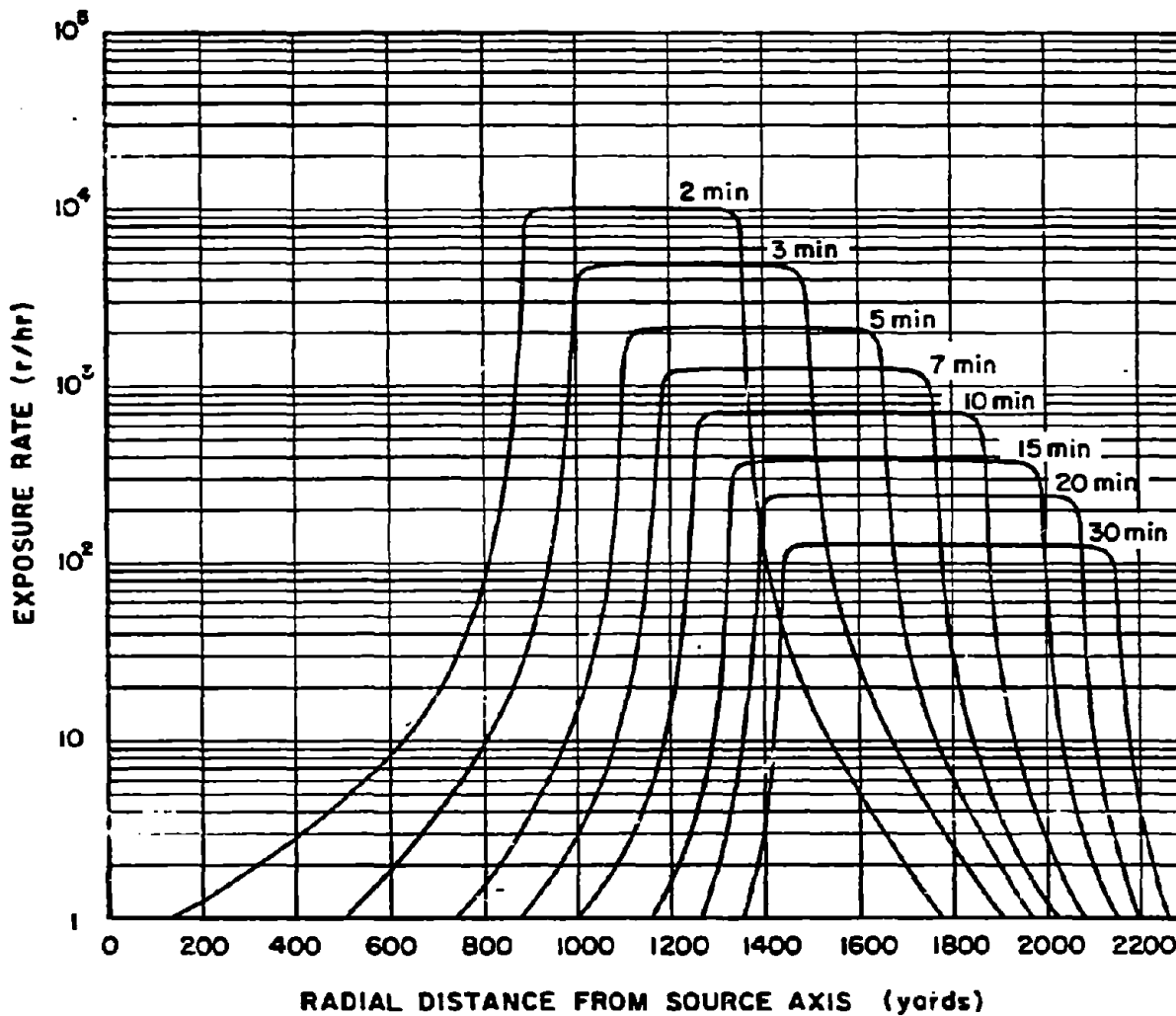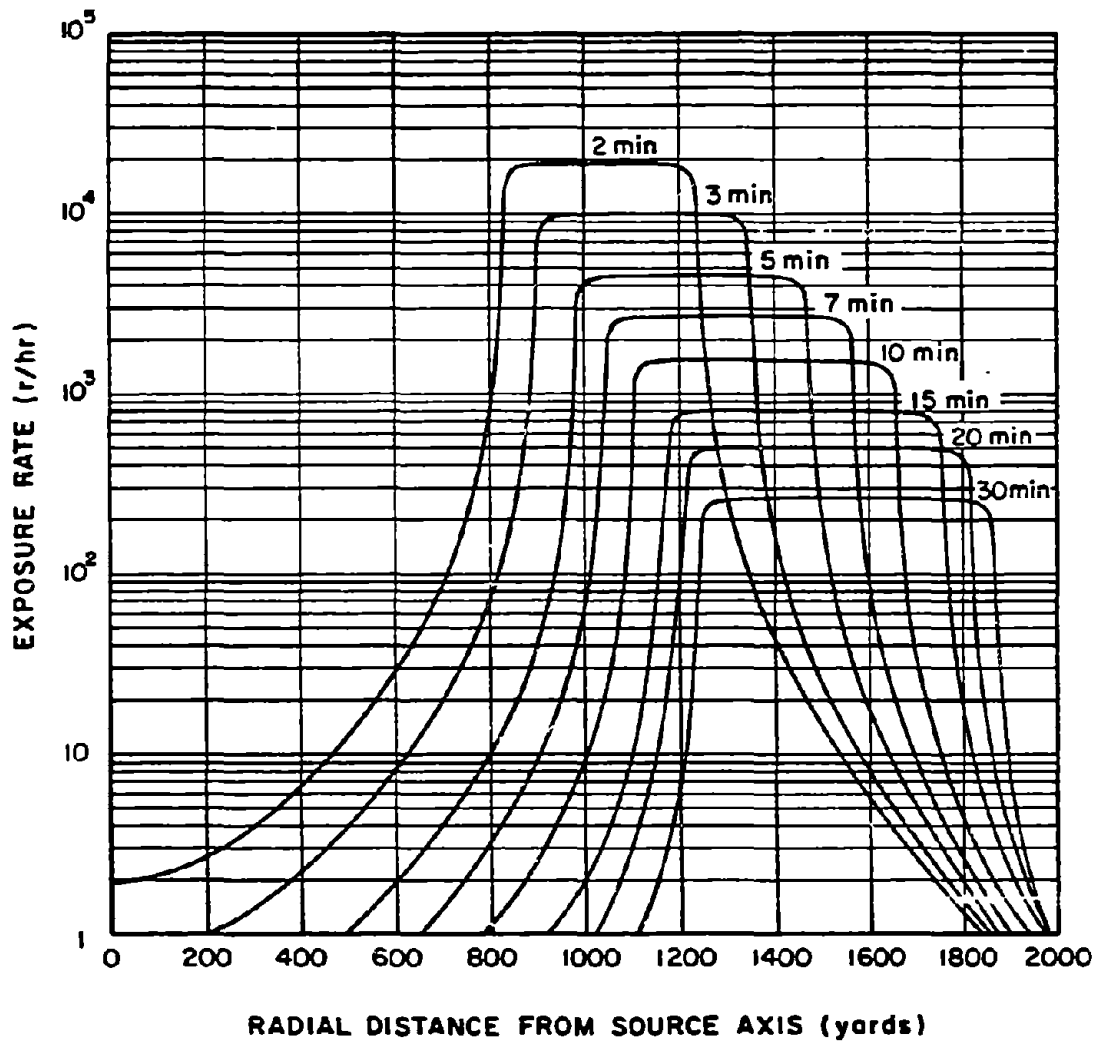on the Bottom in 65 Feet of Water,
No-Wind Environment ▇▇
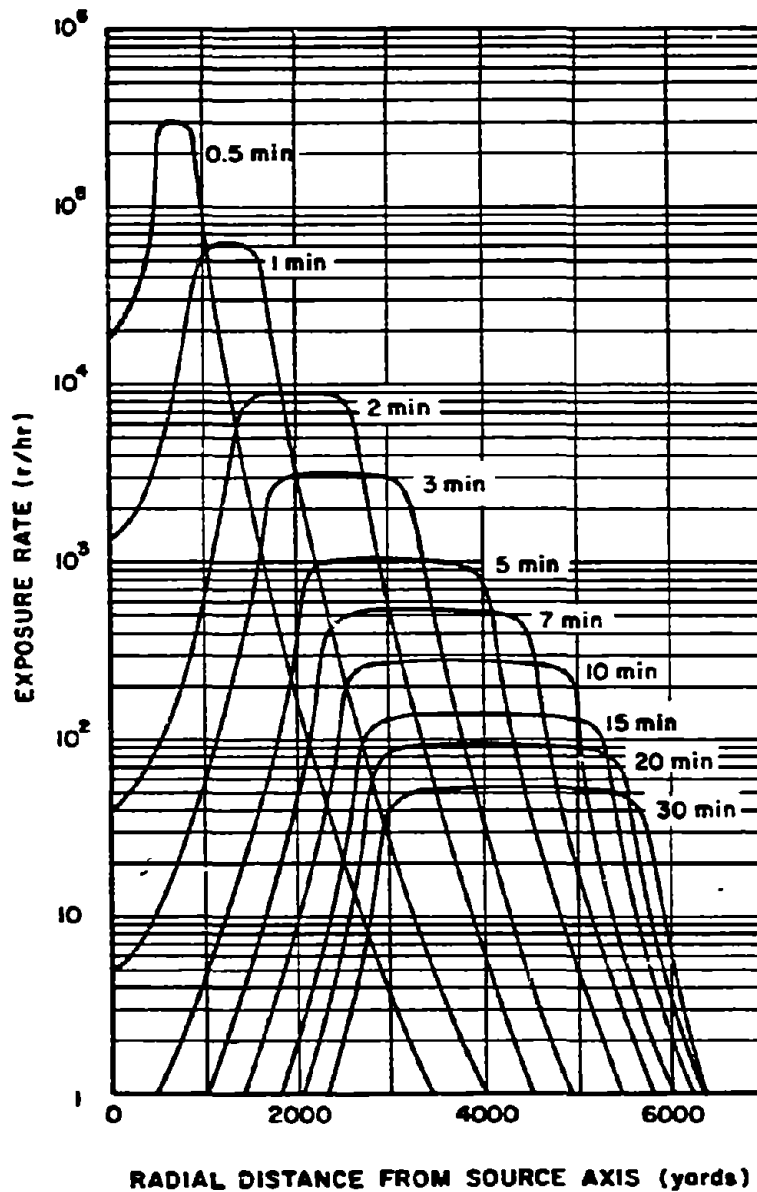
Figure 5-48. ▮▮▮ Base Surge Radiation Exposure Rate 15 Feet Above the Water Surface from a 10 kt Explosion at a Depth of 150 Feet in 5,000 Feet of Water, No-Wind Environment ▮

EXPOSURE RATE, (r/hr)

RADIAL DISTANCE FROM SOURCE AXIS (yards)
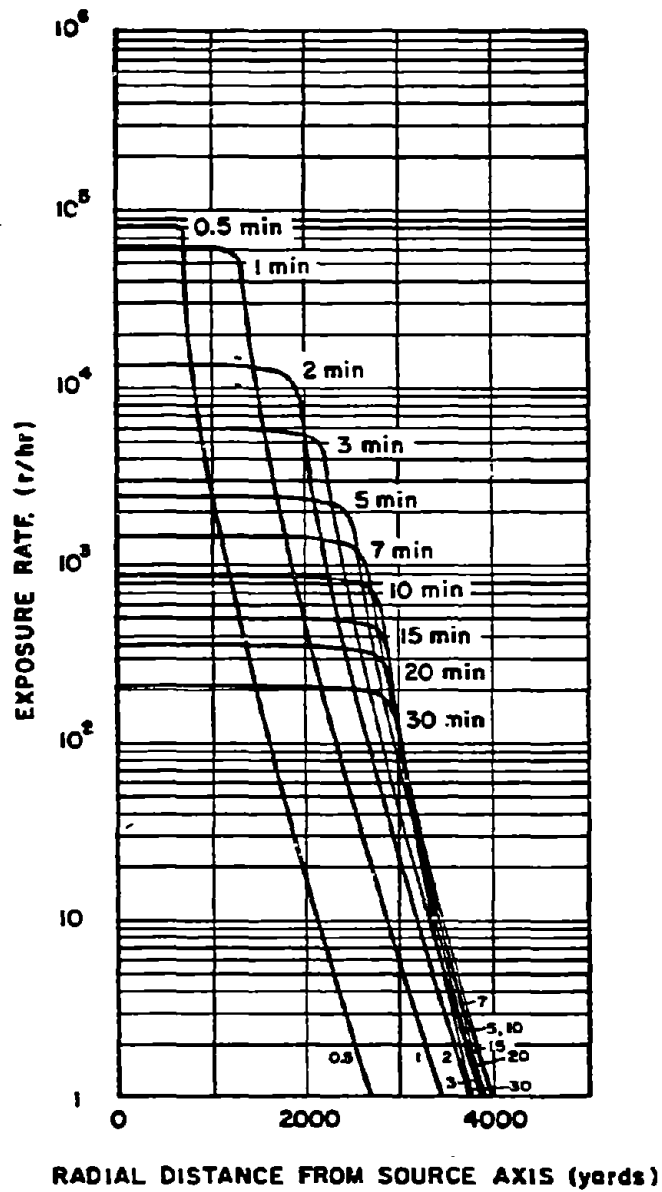
Figure 5-49. ▮▮▮ Base Surge Radiation Exposure Rate 15 Feet
Above the Water Surface from a 10 kt Explosion
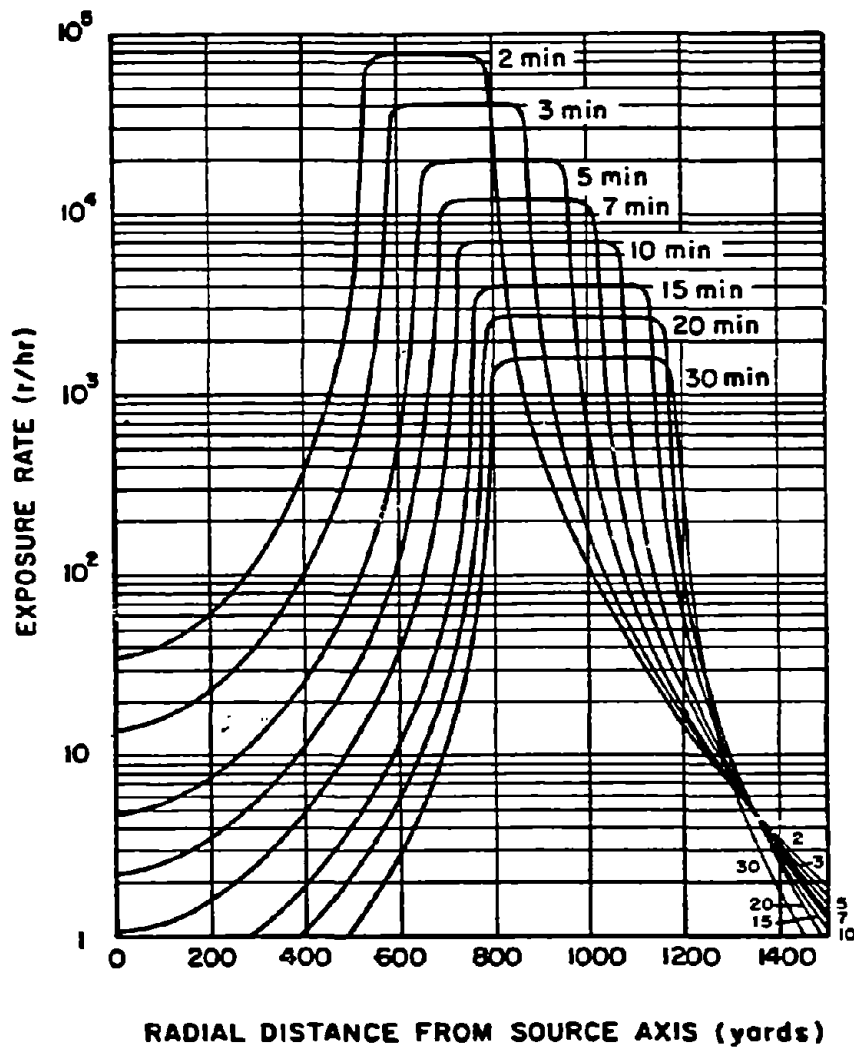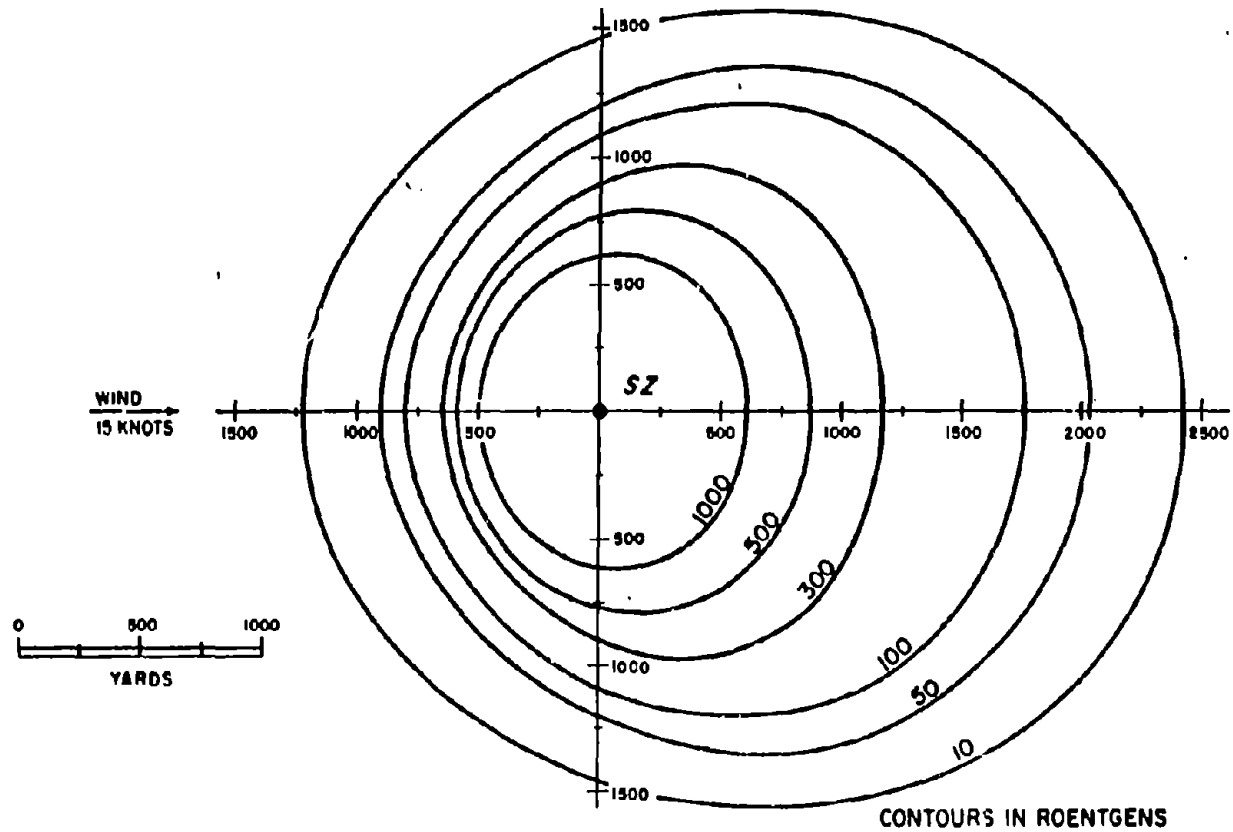at a Depth of 500 Feet in 5,000 Feet
of Water, No-Wind Environment ▮▮▮

EXPOSURE RATE (r/hr)

1 min
2 min
3 min
5 min
7 min
10 min
15 min
20 min
30 min

RADIAL DISTANCE FROM SOURCE AXIS (yards)

Figure 5-50.　█████　Base Surge Radiation Exposure Rate 15 Feet
Above the Water Surface from a 10 kt Explosion
at a Depth of 1,000 Feet in 5,000 Feet
of Water, No-Wind Environment

5-113

Figure 5-51. ▓▓▓ Base Surge Radiation Exposure Rate 15 Feet
Above the Water Surface from a 10 kt Explosion
at a Depth of 1,500 Feet in 5,000 Feet
of Water, No-Wind Environment ▓▓

Figure 5-52. ▮ Pool Radiation Exposure Rate 15 Feet Above the Water Surface
from a 10 kt Explosion at a Depth of 65 Feet In 5,000 Feet
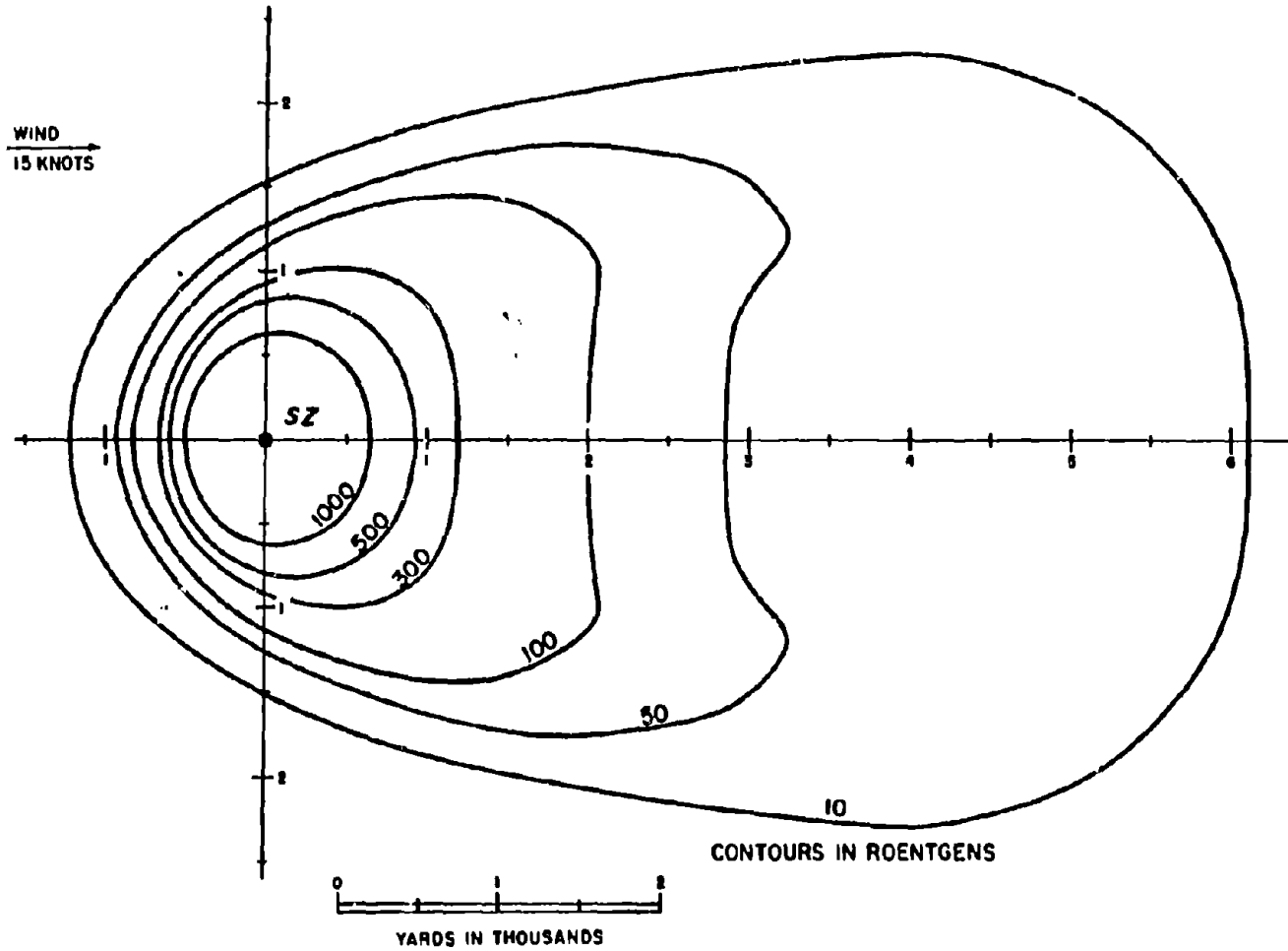of Water, No-Current Environment ▮

RADIAL DISTANCE FROM SOURCE AXIS (yards)

Figure 5-53. ▆▆ Pool Radiation Exposure Rate 15 Feet
Above the Water Surface from a 10 kt Explosion
on the Bottom in 65 Feet of Water,
No-Current Environment ▆▆

EXPOSURE RATE (r/hr) *(vertical axis)*

Curves labeled: 2 min, 3 min, 5 min, 7 min, 10 min, 15 min, 20 min, 30 min

RADIAL DISTANCE FROM SOURCE AXIS (yards)

Figure 5-54. ■ Pool Radiation Exposure Rate 15 Feet Above the Water Surface from a 10 kt Explosion at a Depth of 150 Feet in 5,000 Feet of Water, No-Current Environment ■

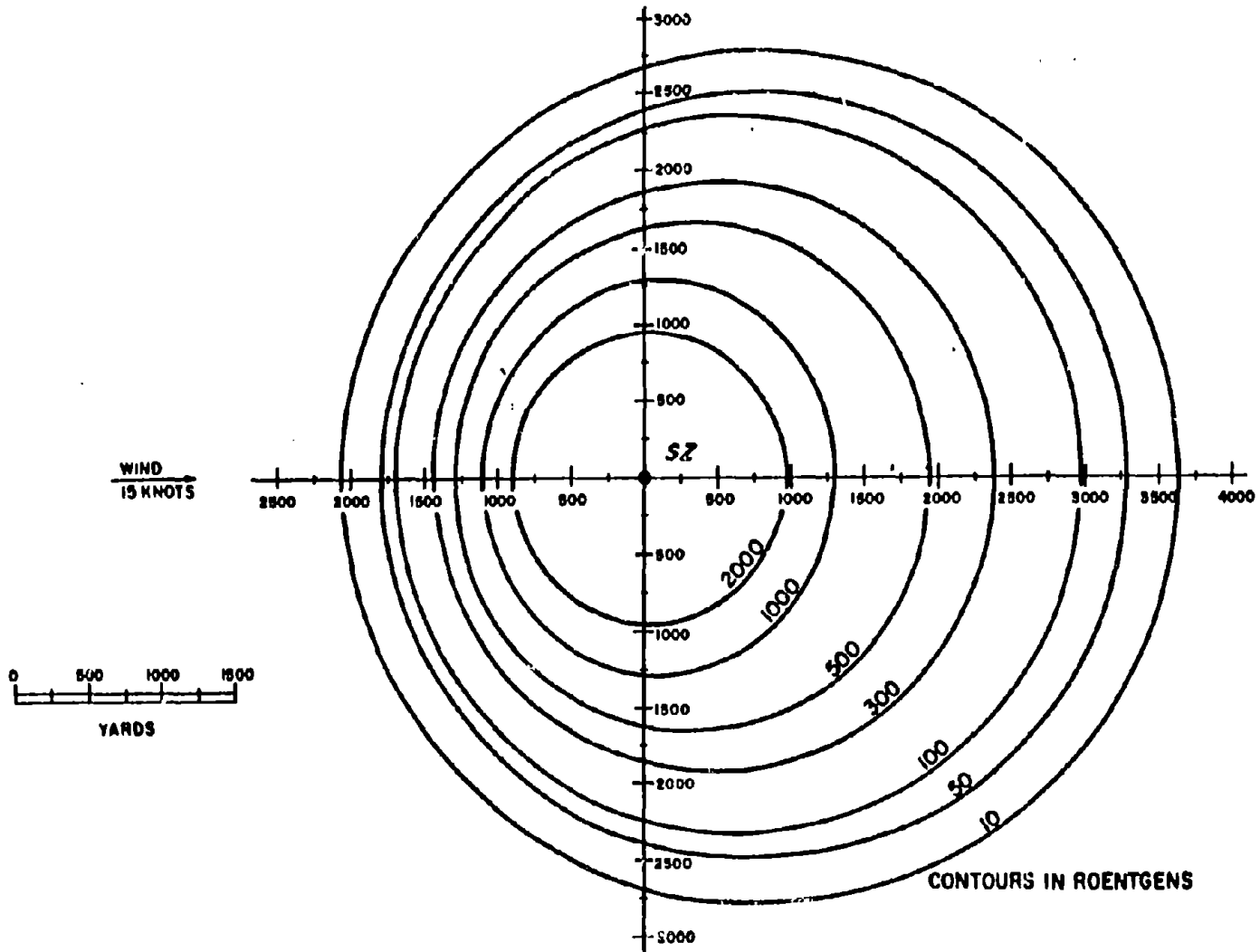Figure 5-55. ▇▇▇ Pool Radiation Exposure Rate 15 Feet Above the
Water Surface from a 10 kt Explosion at a Depth
of 500 Feet in 5,000 Feet of Water,
No-Current Environment ▇

EXPOSURE RATE (r/hr) — vertical axis labels: 10^5, 10^4, 10^3, 10^2, 10, 1

Curve labels: 2 min, 3 min, 5 min, 7 min, 10 min, 15 min, 20 min, 30 min

RADIAL DISTANCE FROM SOURCE AXIS (yards) — horizontal axis: 0, 200, 400, 600, 800, 1000, 1200, 1400, 1600, 1800, 2000

Figure 5-56. ▨ Pool Radiation Exposure Rate 15 Feet Above the
Water Surface from a 10 kt Explosion at a Depth
of: 1,000 Feet in 5,000 Feet of Water,
No-Current Environment ◼

RADIAL DISTANCE FROM SOURCE AXIS (yards)

Figure 5-57. ████ Pool Radiation Exposure Rate 15 Feet
Above the Water Surface from a 10 kt Explosion
at a Depth of 1,500 Feet in 5,000 Feet
of Water, No-Current Environment ████

Figure 5-58. ▮ Two-Minute Total Exposure 15 Feet Above the Water Surface from a 1 kt Explosion at a Depth of 30 Feet In 5,000 Feet of Water, 15 Knot Wind, No-Current Environment ▮
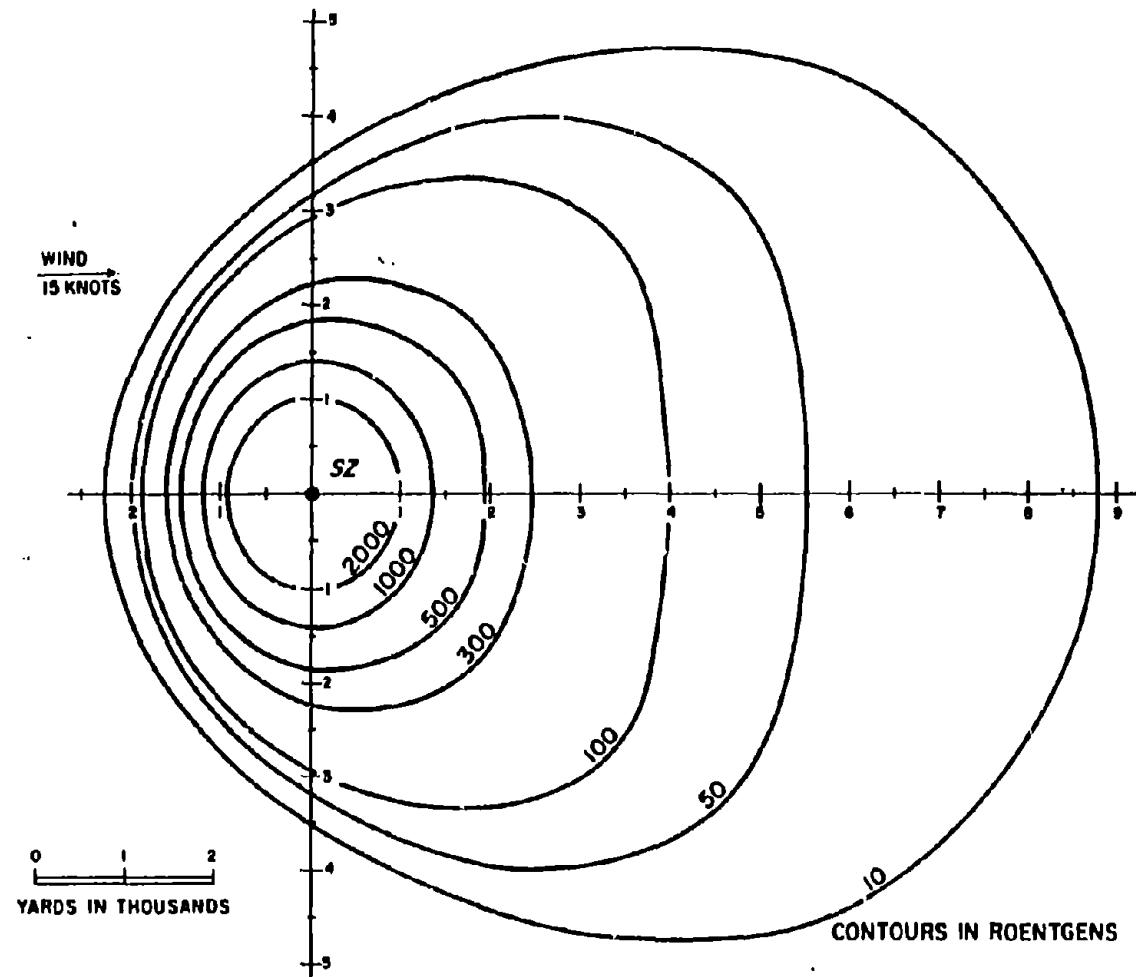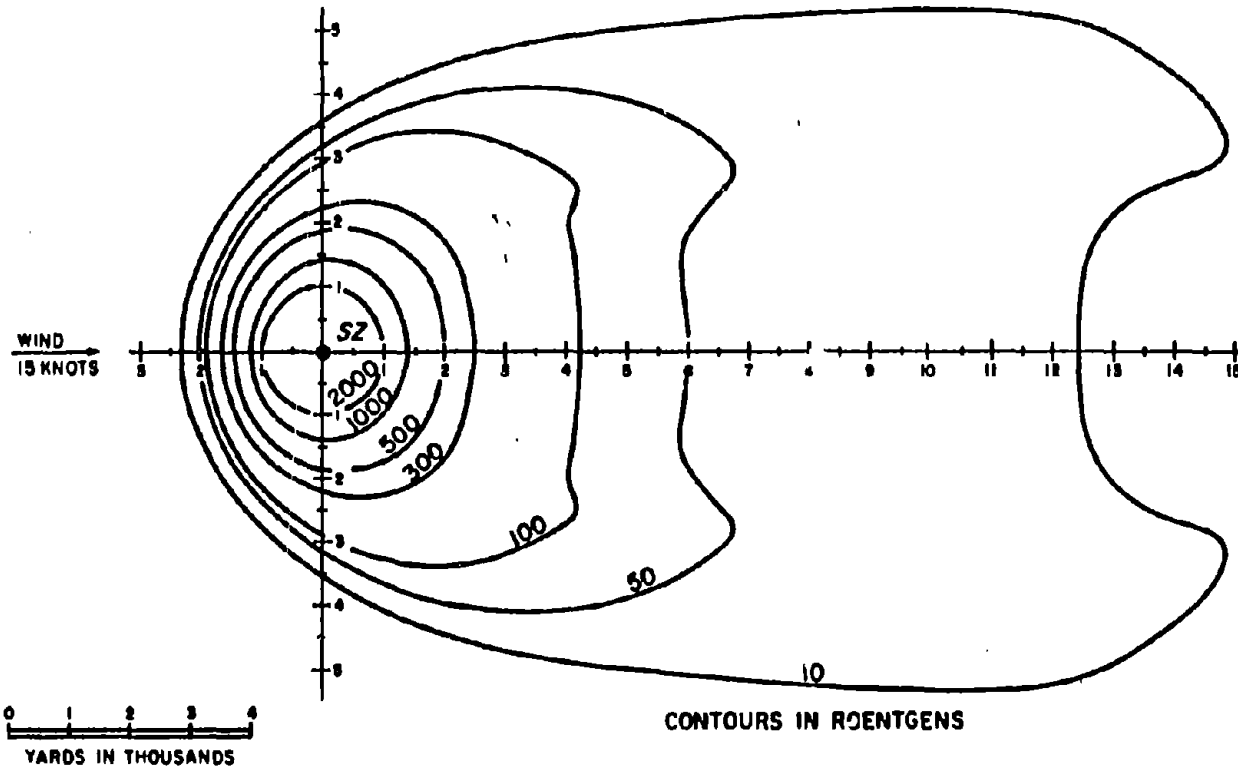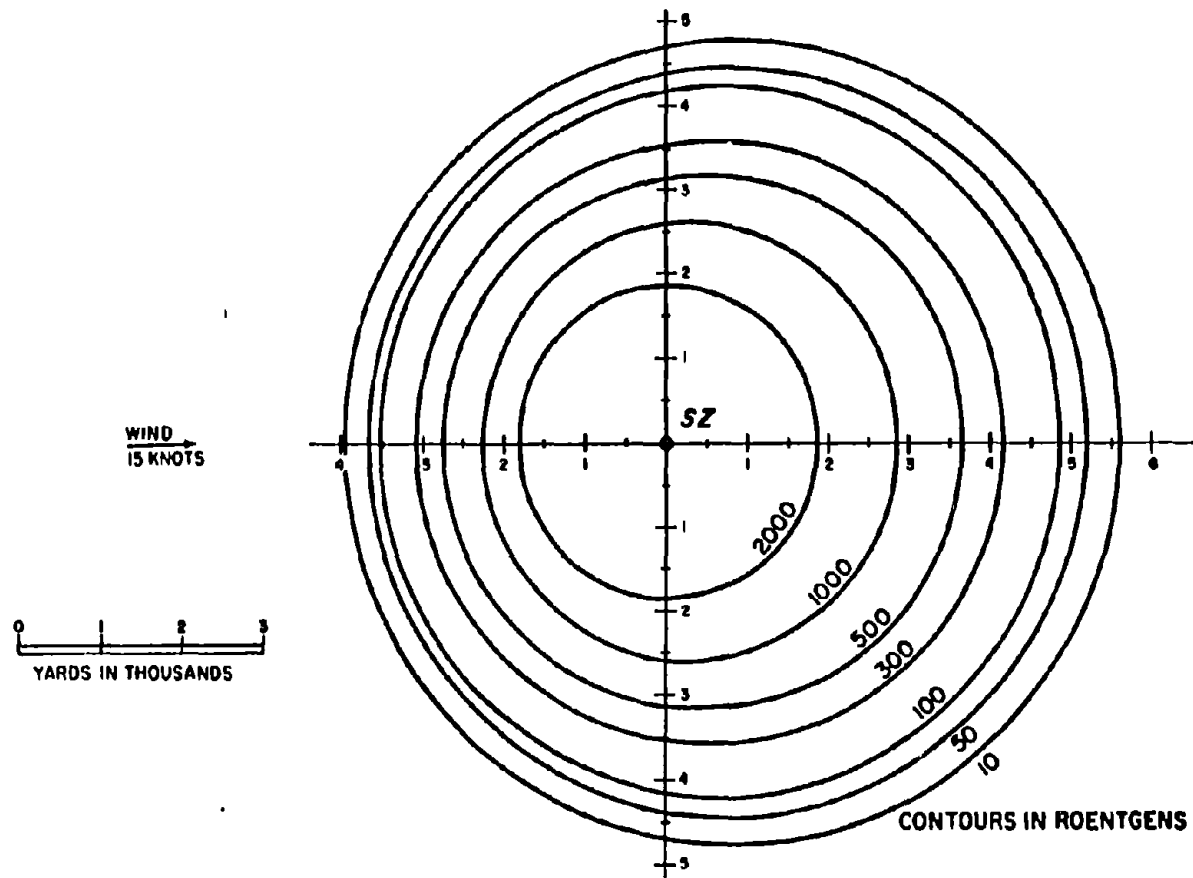
Figure 5-59. ▮ Ten-Minute Total Exposure 15 Feet Above the Water Surface
from a 1 kt Explosion at a Depth of 30 Feet In 5,000 Feet of Water,
15 Knot Wind, No-Current Environment ▮
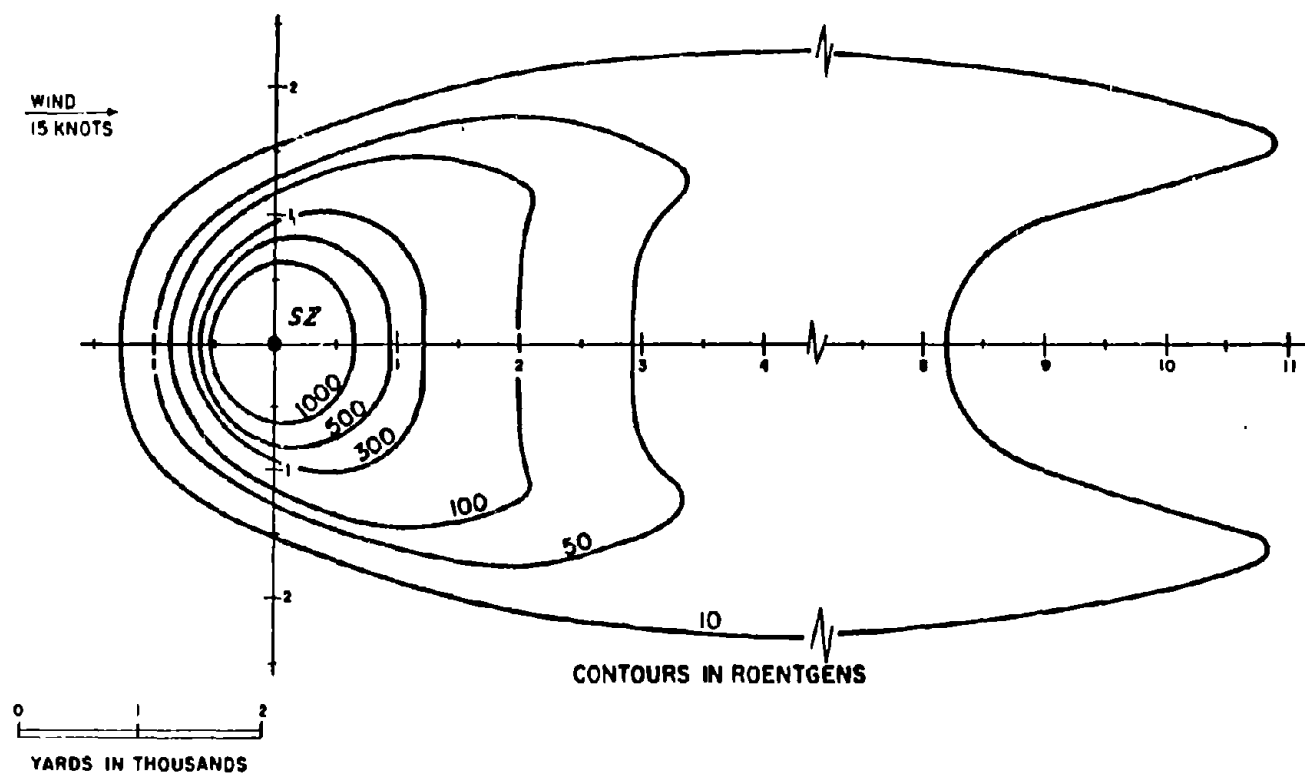
Figure 5-60. Thirty-Minute Total Exposure 15 Feet Above the Water Surface from a 1 kt Explosion at a Depth of 30 Feet in 5,000 Feet of Water, 15 Knot Wind, No-Current Environment
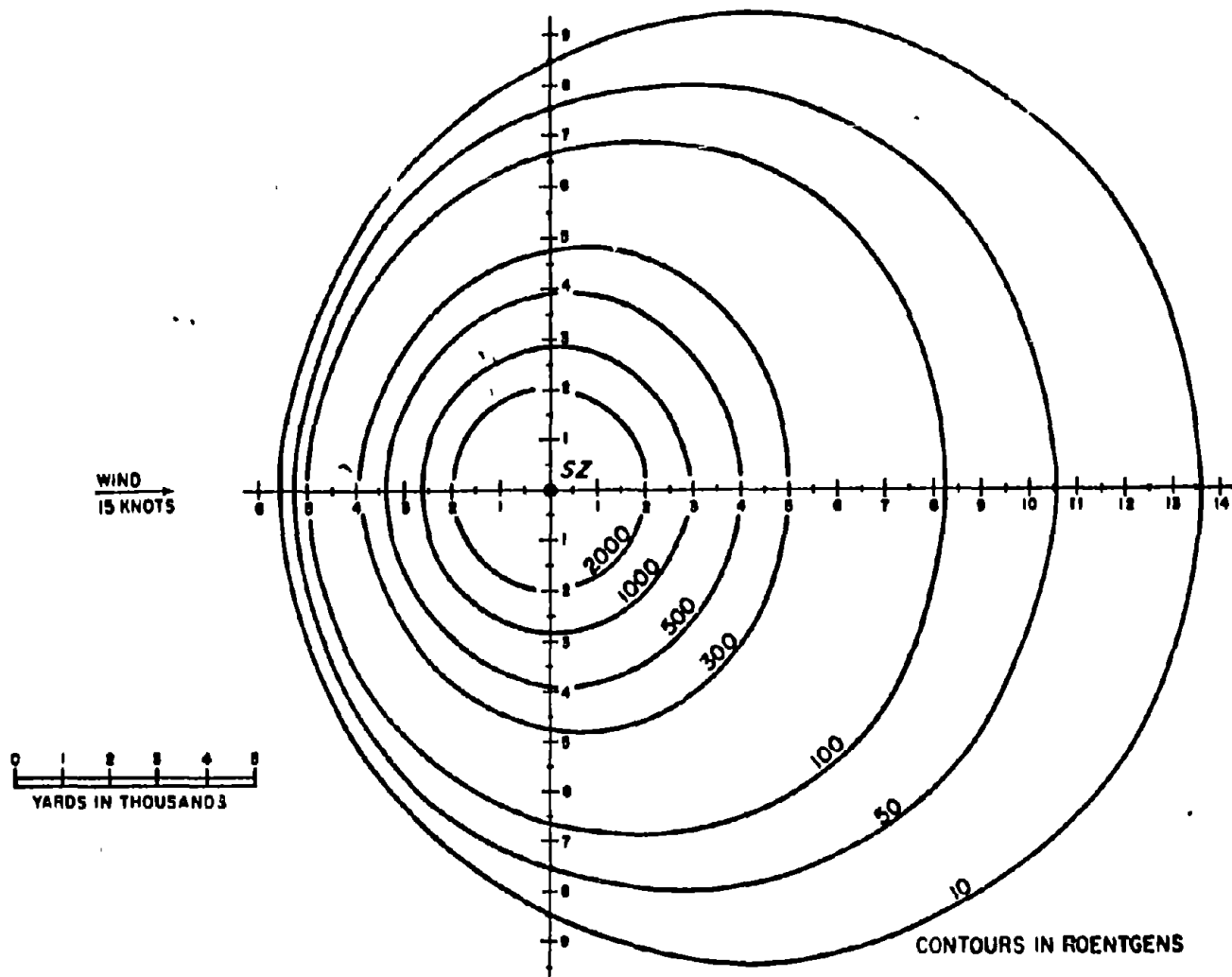
Figure 5-61. ▮▮▮ Two-Minute Total Exposure 15 Feet Above the Water Surface
from a 10 kt Explosion at a Depth of 65 Feet in 5,000 Feet of Water,
15 Knot Wind, No-Current Environment ▮▮▮

WIND
15 KNOTS

SZ

2000
1000
500
300
100
50
10

0   1   2
YARDS IN THOUSANDS

CONTOURS IN ROENTGENS

Figure 5-62. ▰ Ten-Minute Total Exposure 15 Feet Above the Water Surface
from a 10 kt Explosion at a Depth of 65 Feet In 5,000 Feet of Water,
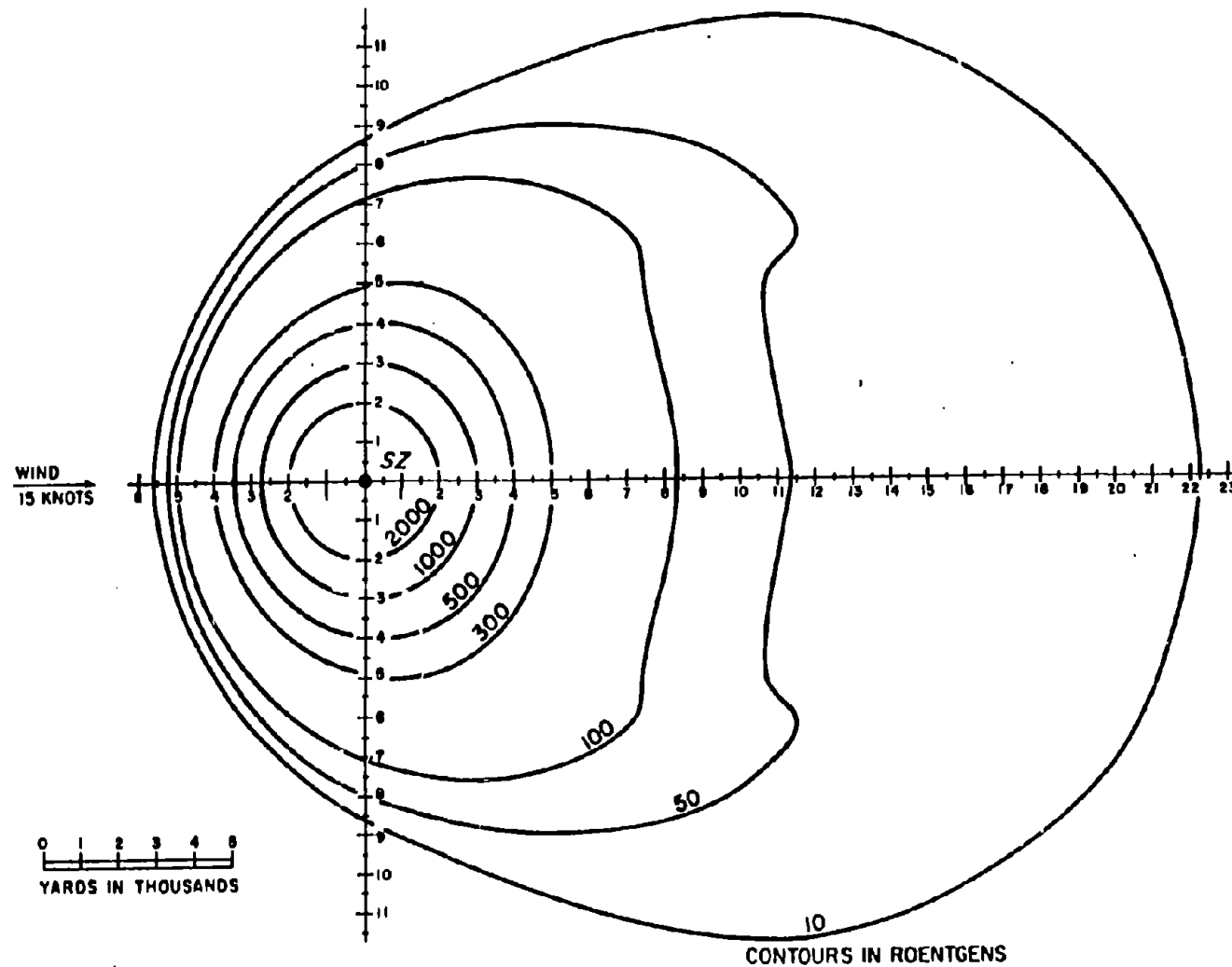15 Knot Wind, No-Current Environment ▰

WIND
15 KNOTS

SZ

2000
1000
500
300
100
50
10

CONTOURS IN ROENTGENS

0 1 2 3 4
YARDS IN THOUSANDS

Figure 5-63. Thirty-Minute Total Exposure 15 Feet Above the Water Surface
from a 10 kt Explosion at a Depth of 65 Feet in 5,000 Feet of Water,
15 Knot Wind, No-Current Environment

WIND
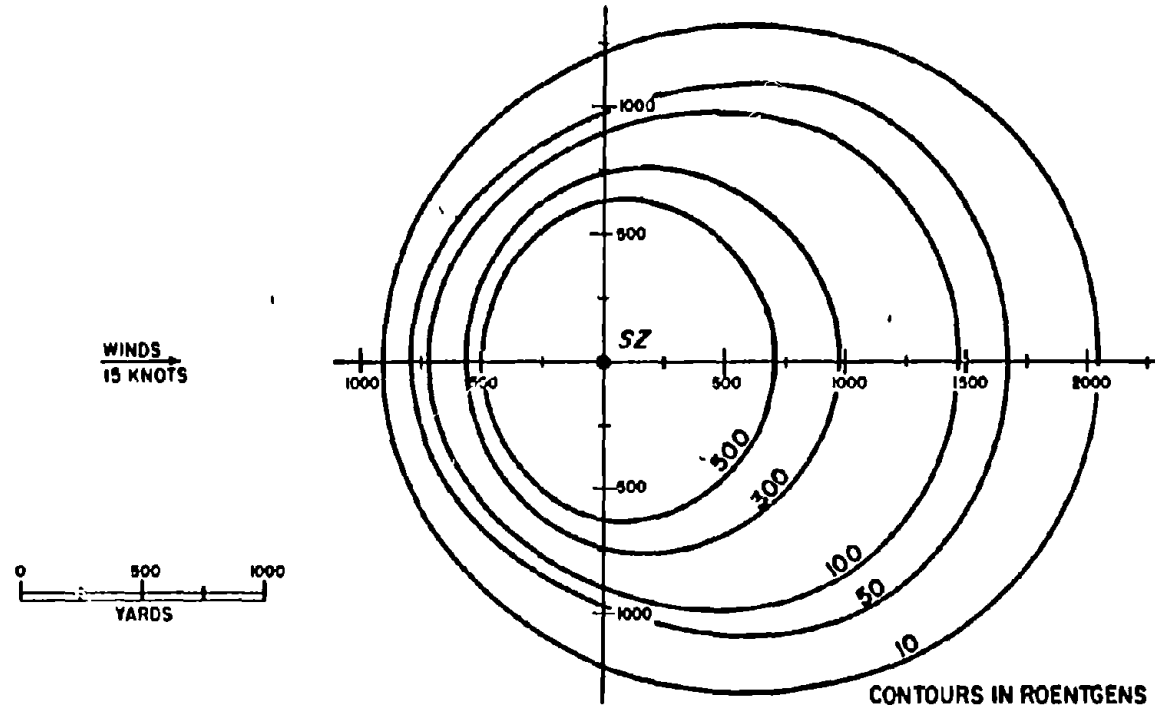15 KNOTS

0   1   2   3
YARDS IN THOUSANDS

SZ

2000
1000
500
300
100
50
10

CONTOURS IN ROENTGENS

Figure 5-64.   Two-Minute Total Exposure 15 Feet Above the Water Surface
from a 100 kt Explosion at a Depth of 140 Feet In 5,000 Feet of Water,
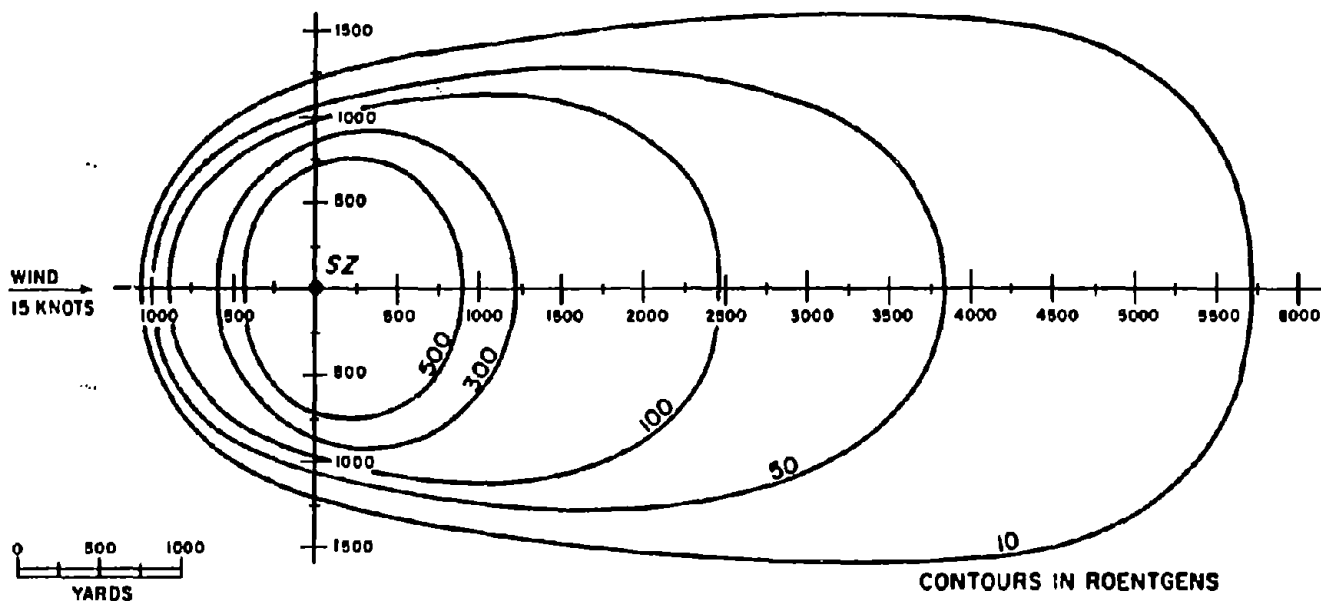15 Knot Wind, No-Current Environment

WIND
15 KNOTS

0 1 2 3 4 5
YARDS IN THOUSANDS

SZ

2000
1000
500
300
100
50
10

CONTOURS IN ROENTGENS

Figure 5-65. ▮▮▮ Ten-Minute Total Exposure 15 Feet Above the Water Surface
from a 100 kt Explosion at a Depth of 140 Feet in 5,000 Feet of Water,
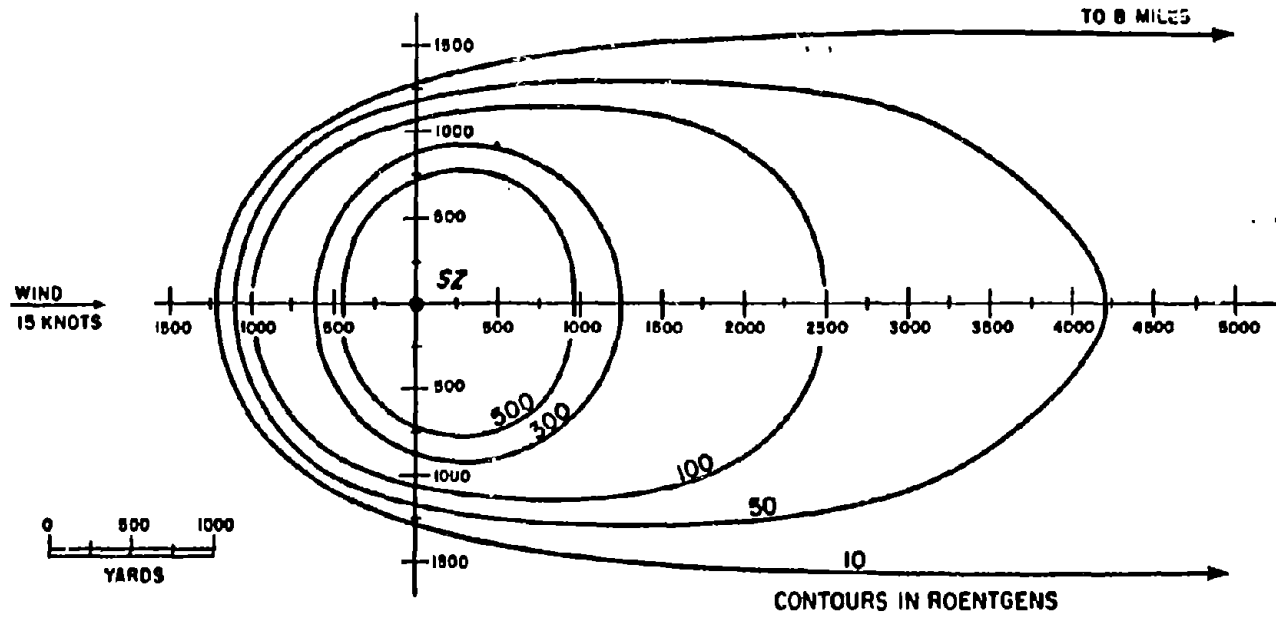15 Knot Wind, No-Current Environment ▮▮▮

Figure 5-66. ■ Thirty-Minute Total Exposure 15 Feet Above the Water Surface
from a 100 kt Explosion at a Depth of 140 Feet in 5,000 Feet of Water,
15 Knot Wind, No-Current Environment ■

WINDS
15 KNOTS

0   500   1000
YARDS

SZ

1000

500

500

1000

1000   500   500   1000   1500   2000

500

300

100

50

10

CONTOURS IN ROENTGENS

Figure 5-67.   Two-Minute Total Exposure 15 Feet Above the Water Surface
from a 1 kt Explosion at a Depth of 280 Feet In 5,000 Feet of Water,
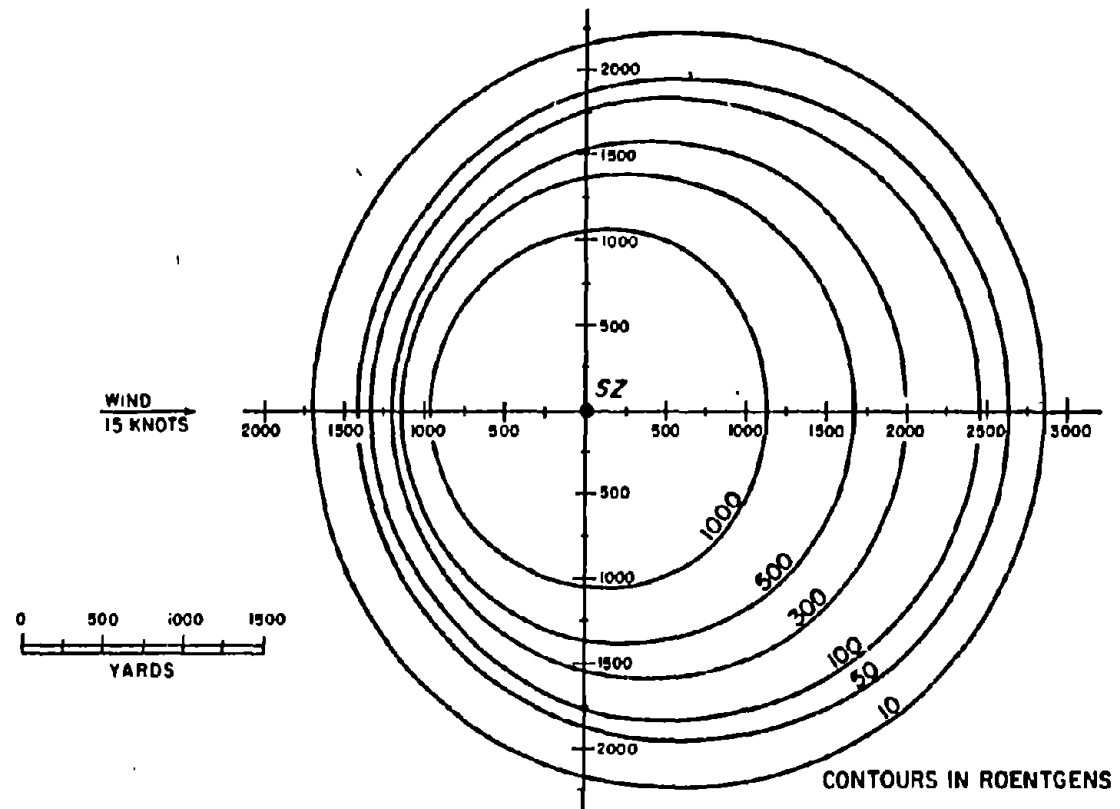15 Knot Wind, No-Current Environment

WIND 15 KNOTS

YARDS

CONTOURS IN ROENTGENS

Figure 5-69. ▆ Ten-Minute Total Exposure 15 Feet Above the Water Surface from a 1 kt Explosion at a Depth of 280 Feet in 5,000 Feet of Water, 15 Knot Wind, No-Current Environment ▆
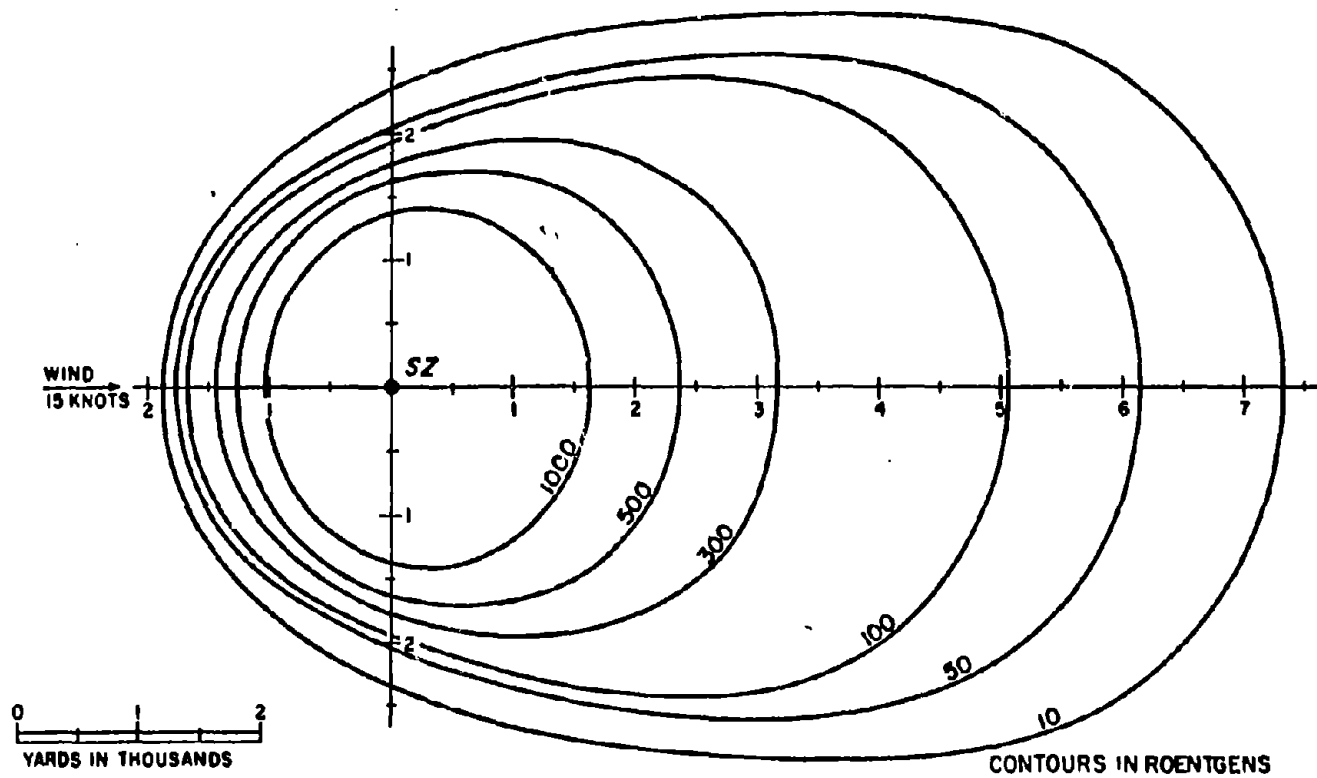
Figure 6-69. ▨ Thirty-Minute Total Exposure 16 Feet Above the Water Surface
from a 1 kt Explosion at a Depth of 280 Feet in 6,000 Feet of Water,
16 Knot Wind, No-Current Environment ▨

Figure 5-70. ▮▮ Two-Minute Total Exposure 15 Feet Above the Water Surface from 10 kt Explosion at a Depth of 500 Feet In 6,000 Feet of Water, 15 Knot Wind, No-Current Environment ▮▮

Figure 5-71. ▓▓ Ten-Minute Total Exposure 15 Feet Above the Water Surface
from a 10 kt Explosion at a Depth of 500 Feet in 5,000 Feet of Water,
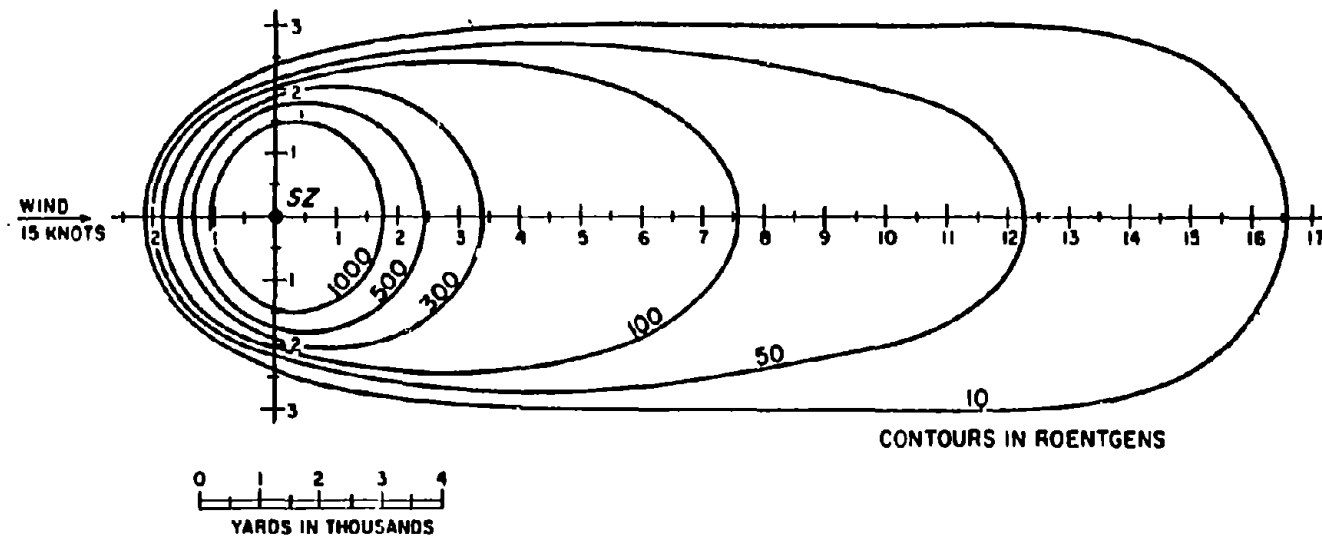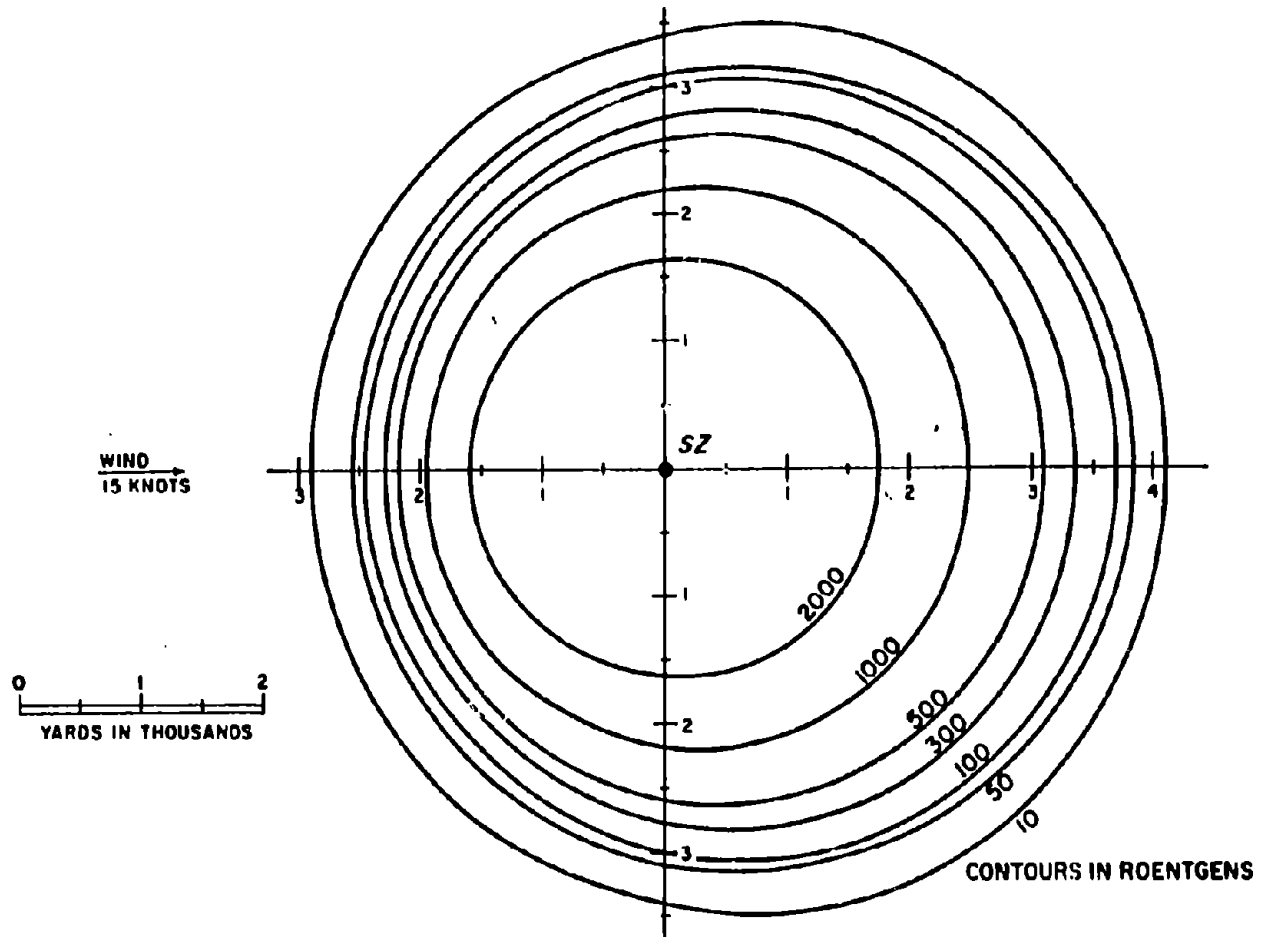15 Knot Wind, No-Current Environment ▓▓

WIND
15 KNOTS

SZ

1000
500
300
100
50
10

CONTOURS IN ROENTGENS

0   1   2   3   4
YARDS IN THOUSANDS

Figure 5-72. ███ Thirty-Minute Total Exposure 15 Feet Above the Water Surface
from a 10 kt Explosion at a Depth of 500 Feet in 5,000 Feet of Water,
15 Knot Wind, No-Current Environment ███

Figure 5·73. Two-Minute Total Exposure 15 Feet Above the Water Surface from a 100 kt Explosion at a Depth of 890 Feet in 5,000 Feet of Water, 15 Knot Wind, No-Current Environment
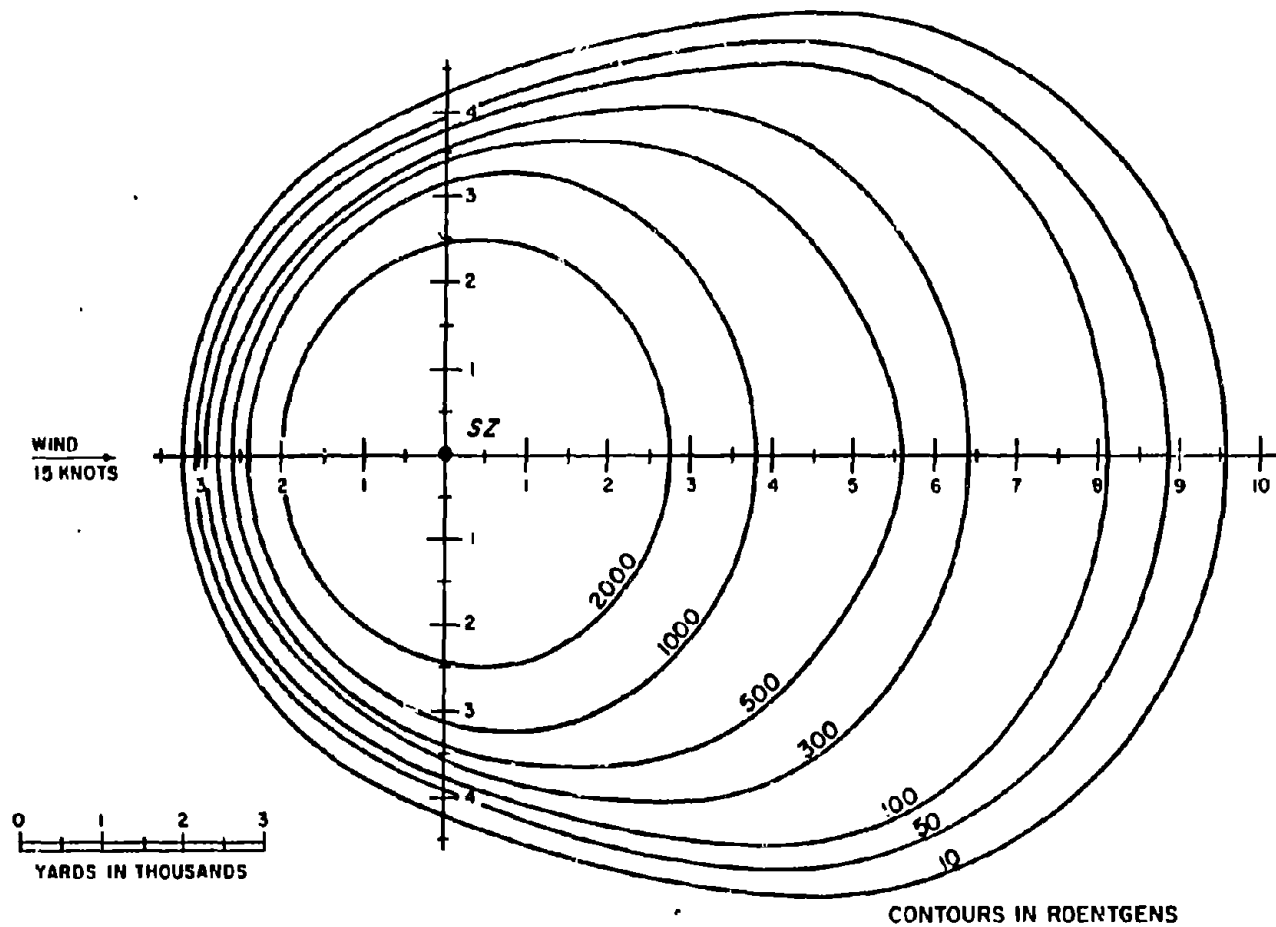
Figure 5-74. ▮▮ Ten-Minute Total Exposure 15 Feet Above the Water Surface
from a 100 kt Explosion at a Depth of 890 Feet In 5,000 Feet of Water,
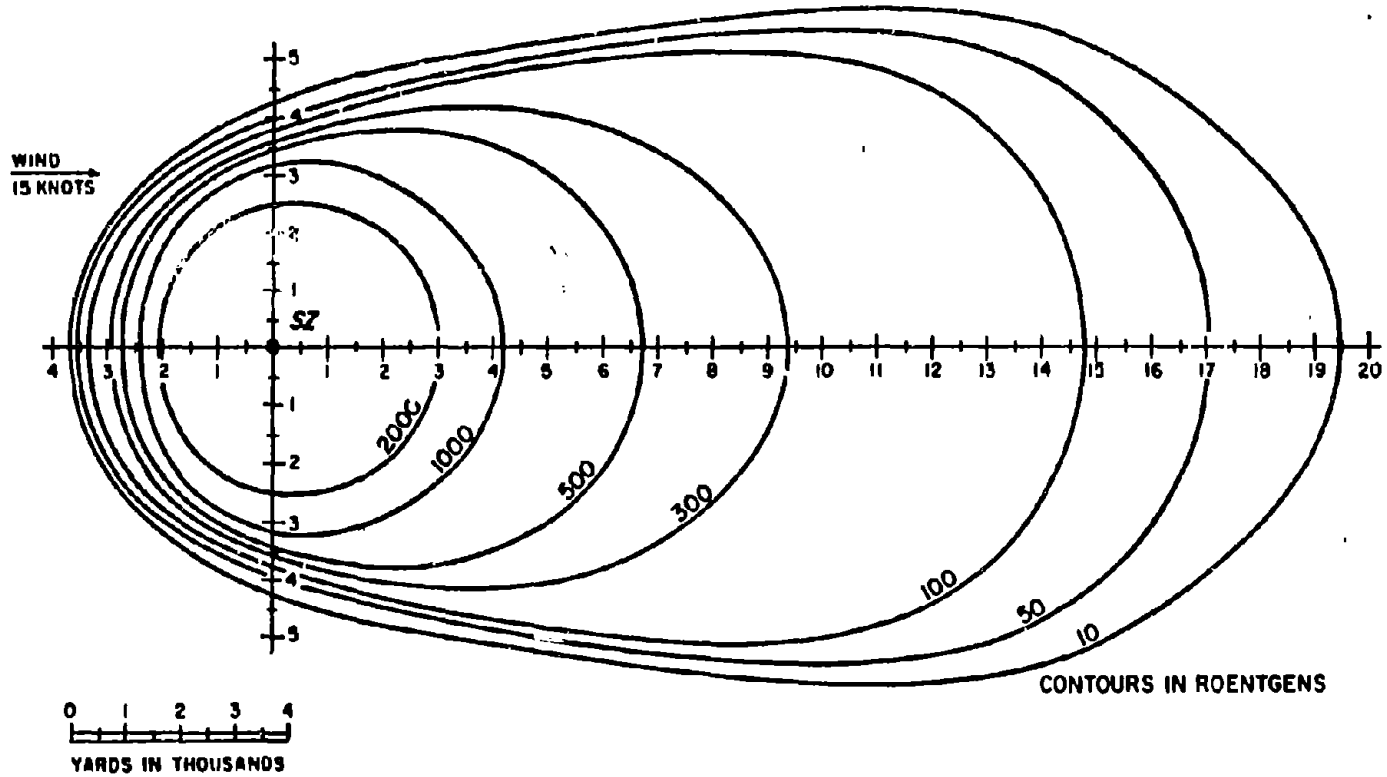15 Knot Wind, No-Current Environment ▮▮

Figure 5-75. ▬ Thirty-Minute Total Exposure 15 Feet Above the Water Surface
from a 100 kt Explosion at a Depth of 890 Feet in 5,000 Feet of Water,
15 Knot Wind, No-Current Environment ▬

DOSE RECEIVED WHILE FLYING THROUGH A NUCLEAR CLOUD

The radioactive nuclear cloud represents a potential hazard to crews of aircraft that fly through the cloud. The dose that a crew might receive will depend upon many variables including the time after burst (which determines the intensity of the radiation as well as the size of the cloud), the portion of the cloud traversed, and the length of transit time through the cloud.

After stabilization, the particles that make up the radioactive cloud will travel with the winds as they fall, and, since the wind speed and direction are both likely to vary with altitude and time, the size and shape of the cloud can only be described by complex computer codes that can accept temporal and spatial variations in weather data. No simple idealized shape can describe the cloud adequately. Even during the time of cloud rise, the winds will act on the

particles, and the cloud probably will not stabilize directly above ground zero; however, the shape can be approximated roughly by a right circular cylinder, with a stem of smaller diameter below it, at the time of stabilization. Figures 5-76 through 5-78 show the cloud diameter, the height of the cloud bottom, and the height of the cloud top, respectively, as functions of time after burst for various yields. These figures allow approximation of the cloud dimensions during the first few minutes after an explosion.

Even if the cloud geometry were known, no satisfactory model exists from which simple scaling procedures could be developed to predict the dose received while flying through the cloud. Figure 5-79 shows estimates of the transit dose as a function of transit time for several entry times. These estimates were extrapolated from a limited amount of test data. The relative hazard for flight through the stem is even less certain, but it is believed to be less than that from flight through the center of the cloud.

Problem 5-14. Calculation of Dose Received While Flying Through a Nuclear Cloud

▓▓▓ The curves in Figure 5-79 show the total dose received while passing through nuclear clouds at various times after burst. Figures 5-76 through 5-78 provide the dimensions of the cloud as a function of time after burst.

▓▓▓ *Example* **▓▓▓**

Given: An aircraft flying at 235 knots at an altitude of 23,000 feet passes through a nuclear cloud from a 50 kt weapon 5 minutes after the explosion.

Find: The probable maximum exposure of the crew, assuming that the shielding of the aircraft structure is negligible.

Solution: From Figure 5-77, the height of the cloud bottom will be about 16,000 feet 5 minutes after a 50 kt explosion, and from Figure 5-78, the corresponding height of the cloud top is 30,000 feet. Thus, the aircraft is flying at an altitude corresponding to the vertical center of the cloud. The maximum dose (corresponding to maximum transit time) will occur if the aircraft flies through the horizontal center of the cloud, i.e., if the aircraft traverses the entire diameter. From Figure 5-76, the diameter of a cloud from a 50 kt explosion will be 2.7 miles at 5 minutes after the burst. The aircraft speed is

$$235 \times 1.15 = 270 \text{ mph.}$$

The transit time is

$$\frac{2.7}{270} = 0.01 \text{ hr}$$

$$= 0.6 \text{ min.}$$

Answer: From Figure 5-79, with an entry time of 5 minutes and a transit time of 0.6 minutes, the expected dose is 37 rads. The maximum dose might be twice this value (see Reliability below), or

$$2 \times 37 = 74 \text{ rads.}$$

▓▓▓ *Reliability.* The doses obtained from Figure 5-79 are estimated to be accurate within a factor of 2 for flight paths that pass near the cloud center. If the path is near the cloud boundary, the predicted dose probably will be higher than the actual dose, although the magnitude of the error is unknown. Additional uncertainties of unknown magnitude are introduced by the prediction of the cloud size, but these uncertainties are not believed to be large for times of entry soon after burst and for short transit times.

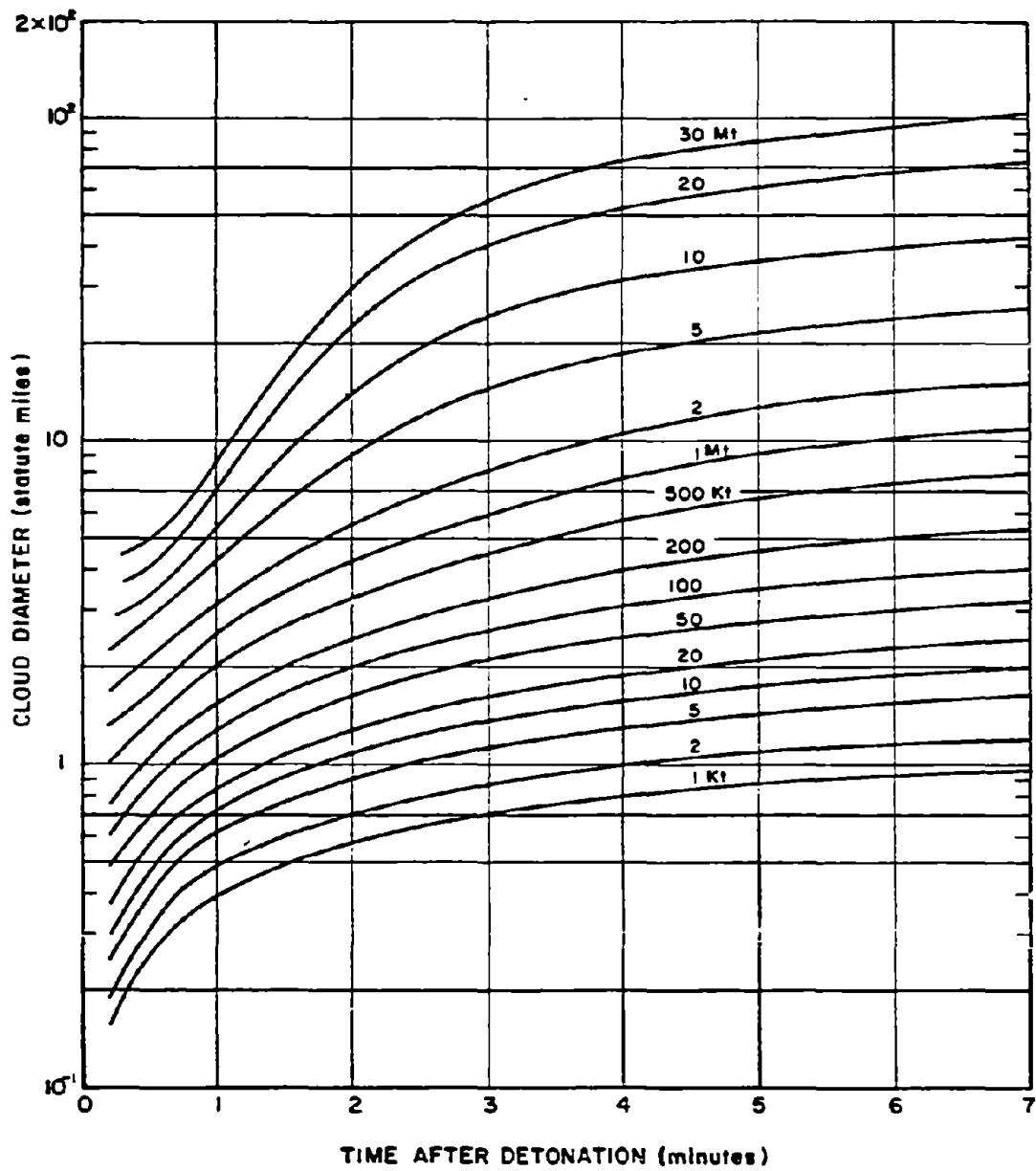**▓▓▓** *Related Material:* See paragraphs 5-15 through 5-19.

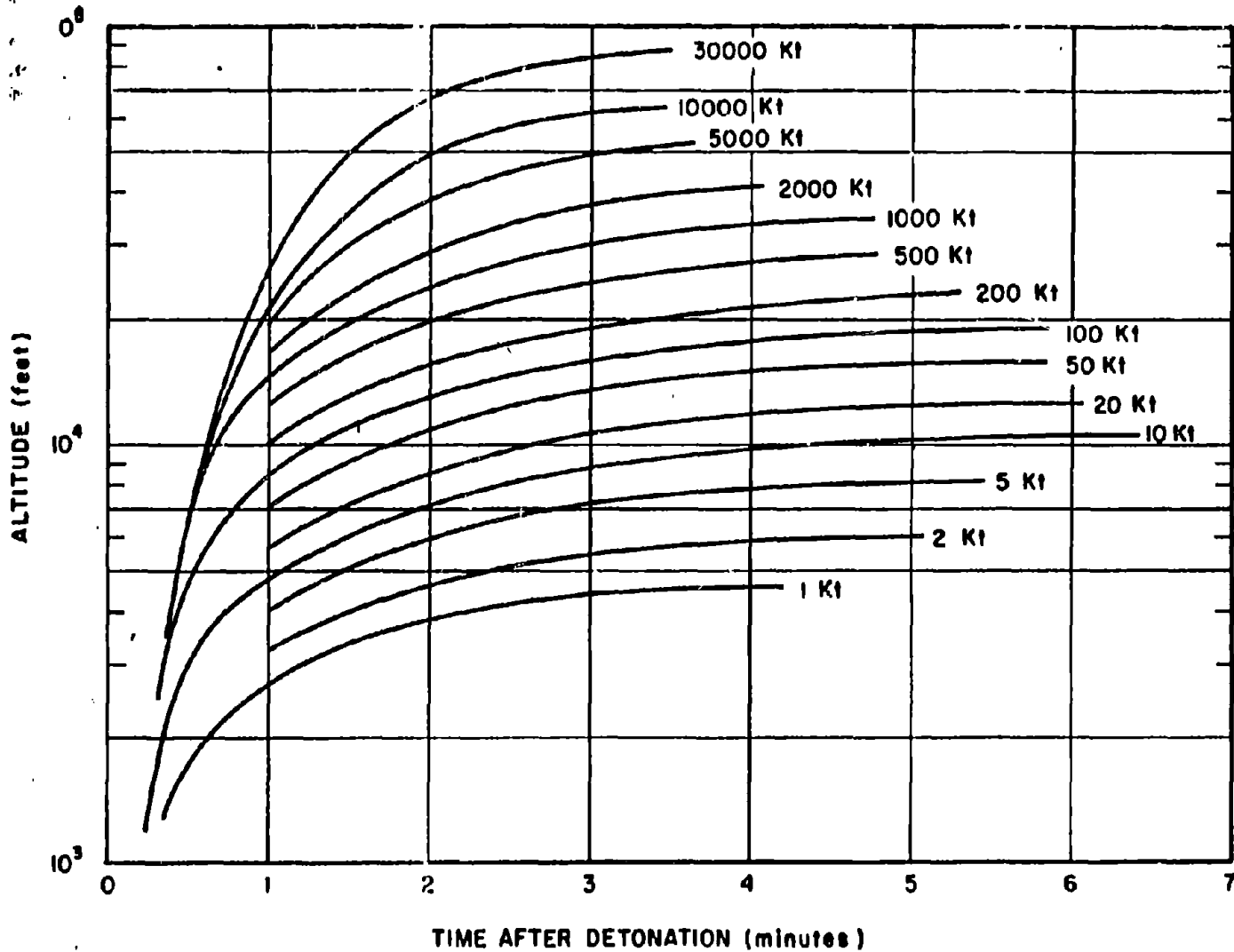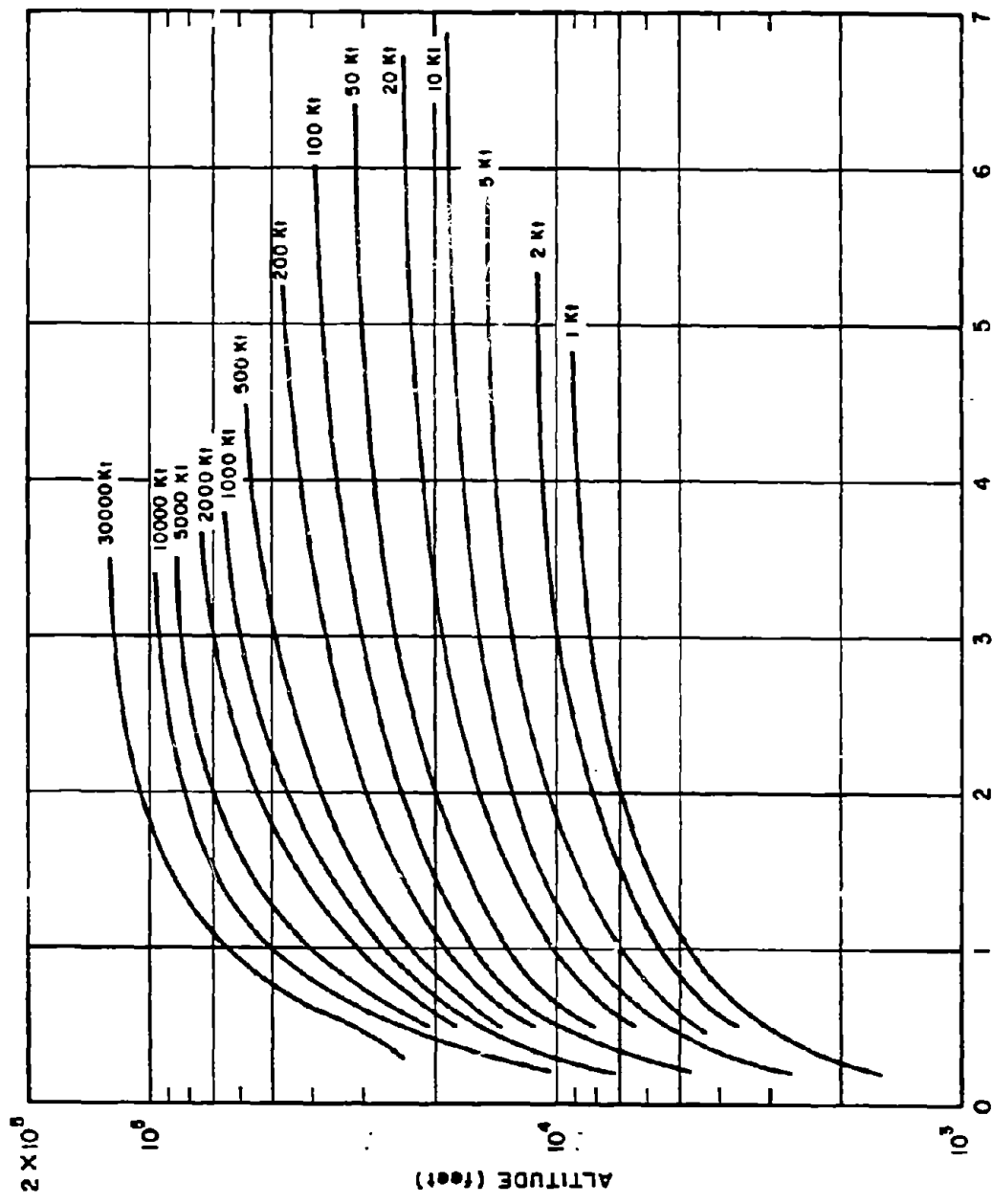Figure 5-76. ▮ Cloud Diameter as a Function of Time After Burst for Various Weapon Yields ▮

Figure 5-77. Height of Cloud Bottom as a Function of Time
for Various Weapon Yields

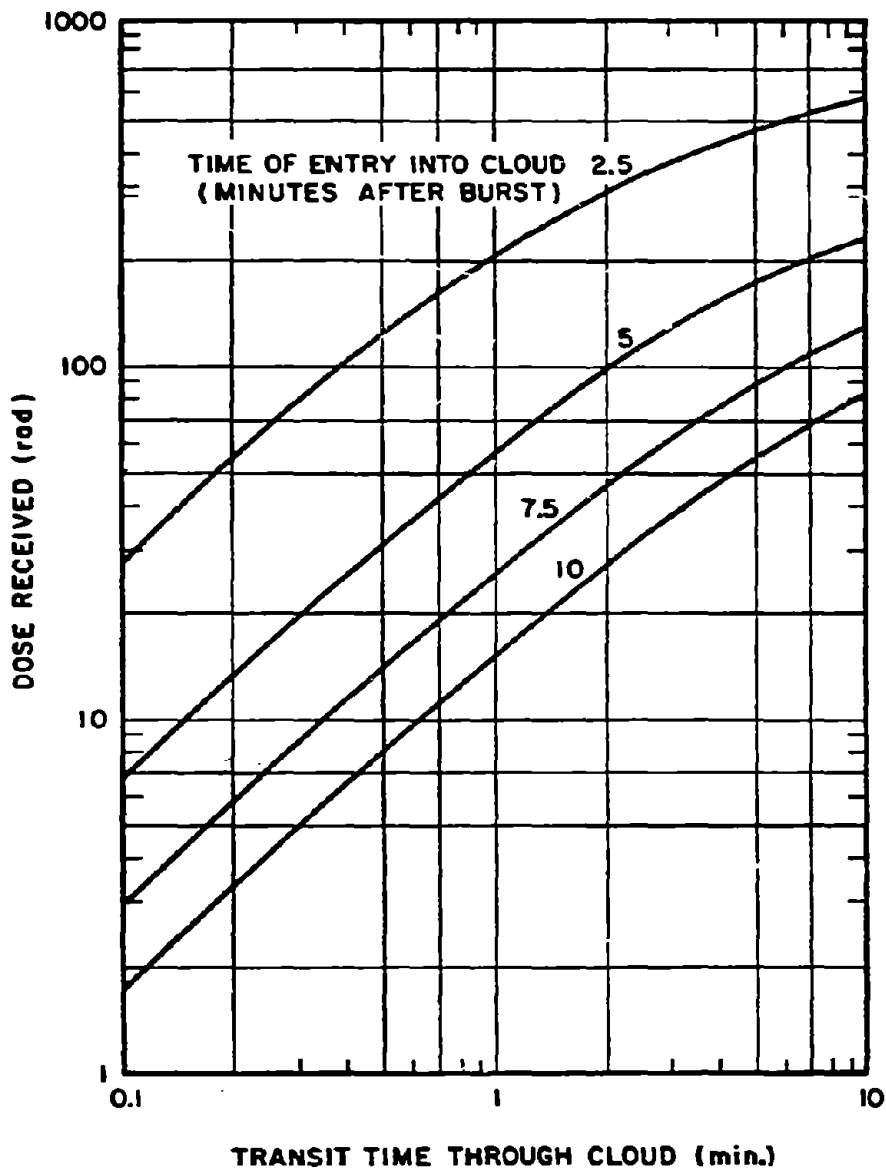Figure 5·78. Height of Cloud Top as a Function of Time for Various Weapon Yields

Figure 5-79. ████ Dose Received While Flying Through a
Nuclear Cloud as a Function of Transit
Time Through the Cloud ████

PRECIPITATION EFFECTS

As mentioned in paragraph 5-16, the surface contamination from an air burst weapon will be militarily insignificant in most cases. The radioactive particles remaining from the weapon debris are extremely small, having diameters that range roughly between 0.01 and 20 micrometers. The weapon cloud carries these particles to high altitudes, with the exact altitude being dependent on the weapon yield and atmospheric conditions. These particles are too small to fall, but they can diffuse downward and can be deposited by atmospheric turbulence processes. In the absence of precipitation, the deposition process takes place over sufficiently long periods of time that the cloud will have spread over a large volume as a result of diffusion and the action of winds at different levels, thereby reducing the particle concentration. Over this same period of time the radioactive decay decreases the activity levels. The net result is that dry deposition of particles from air burst weapons will not be militarily significant although there may be some long-term effects, e.g., thyroid exposures from radioactive iodine. If precipitation occurs in or above the nuclear cloud, however, there is a possibility that contamination that could be considered militarily significant may be deposited on the ground as a result of scavenging of the radioactive particles by the rain or snow. Precipitation also can affect the fallout from a surface or subsurface burst, but contamination is expected from these bursts with or without precipitation. The primary effect of precipitation on the contamination resulting from surface or subsurface bursts would be to change the location and shape of the militarily significant fallout contours. If precipitation scavenges and deposits that portion of the radioactive debris from surface or subsurface bursts that would have been delayed fallout rather than early fallout (see Section III,

"RESIDUAL RADIATION," "FALLOUT"), the resulting contamination on the ground is not expected to be militarily significant.

5-27 Precipitation Scavenging

Precipitation scavenging may be divided into two types: scavenging when the nuclear cloud is within the rain cloud, usually called rainout or snowout; and scavenging when the nuclear cloud is below the rain (snow) cloud, usually called washout. Rainout is generally considered to be a much more efficient form of scavenging than washout, but there are many factors that affect precipitation scavenging and the ground contamination resulting therefrom. These factors are discussed in the succeeding paragraph.

5-28 Factors Affecting the Prediction of Ground Contamination from Precipitation Effects

The prediction of the contamination patterns that may result from precipitation scavenging of air burst nuclear weapons is complicated by many factors. Some of the important factors are discussed below.

- *The burst occurs during precipitation.* If the burst occurs during heavy precipitation, or if heavy precipitation begins at the burst location during stabilization time, the pattern will be roughly circular around ground zero, and will be roughly the size of the nuclear cloud (if the rain cloud extends to distances beyond the nuclear cloud radius).

- *The weapon yield.* The cloud from low yield weapons will be completely contained beneath the rain layers; as the yield is increased, the percentage of the nuclear cloud beneath the rain layer decreases; at a sufficiently high

yield, the entire stabilized cloud will be above the rain layers. Specific yields will, of course, depend upon the height of the rain layer.

- *The size and shape of the nuclear cloud.* If no precipitation occurs during or very soon after burst, the nuclear cloud will reach its stabilized altitude. The size and shape of the radioactive cloud will depend upon the meteorological conditions after the stabilization time (the stabilization altitudes of both the top and bottom of the cloud will depend on the atmosphere within which the explosion occurs, and the position of the stabilized cloud will depend upon the winds that act on it during its rise, but these effects are generally small compared to the changes in cloud shape and size after stabilization). In the absence of precipitation or velocity shear in the wind, the dominant physical phenomena responsible for reducing the activity concentration in a nuclear cloud is diffusion produced by turbulent eddies in the atmosphere. Reasonable estimates of the diffusion in a horizontal plane exist. Less is known about vertical diffusion; however, unless the vertical diffusion causes the particles to enter a zone where the wind speed or direction changes, it will not affect the horizontal concentration. Changes in wind speed and direction can have a significant effect on the size and shape of the nuclear cloud. Since the particles from an air burst are so small that they will not actually "fall," they will be acted on by winds within a specific altitude layer. Frequently, several such layers will exist within the thickness of the cloud at stabilization, each having a different speed and/or direction. Changes in both speed and direction of the wind are likely to occur as a function of time and space. Since most of the particles within any one altitude layer will remain in that layer for long periods of time, differences in wind velocity (speed and direction) between layers, as well as changes within a layer, generally will tend to decrease the horizontal concentration as viewed from above (exceptions may occur, of course, e.g., changes in direction may cause two layer that have separated to overlap after some time). The net result of all of the factors acting on the nuclear cloud from a low altitude air burst is that it generally will tend to increase in size horizontally without drastic changes in the vertical dimension for relatively long periods of time, unless precipitation scavenging occurs. This increase in horizontal dimensions will decrease the concentration of radioactive particles available for scavenging.

- *Radioactive decay.* While the nuclear cloud is drifting, the radioactive isotopes decay continuously. Thus, the longer the time between the explosion and the time that the nuclear cloud encounters precipitation, the smaller the total intensity of radiation that will be available (see Problem 5-9 and Figure 5-40). This, together with the general decrease in horizontal concentration described above, reduces the potential hazard with increasing time.

- *The rain cloud size, and the type and during of the precipitation.* If the rain cloud is smaller than the nuclear cloud, only that portion of the nuclear cloud that is in or below the rain cloud will be available for scavenging (any part of the nuclear cloud that is above the rain cloud is not available, as discussed under the effects of yield above). If the rain cloud is larger than the nuclear cloud in horizontal dimensions, any portion of the nuclear cloud that is in or below the rain cloud will be available for scavenging. The length of time during which the nuclear cloud is available for scavenging will depend on the relative directions and speed of travel of the nuclear and

rain clouds. The efficiency of the scavenging process will depend on the debris characteristics, scavenging mechanisms, and the type of rain. Heavy precipitation generally is considered to be more efficient in the scavenging process than light rainfall. Finally, strong updrafts and downdrafts of wind are frequently found around and within a rain cloud. These vertical air motions could prevent the intersection of the nuclear cloud and the rain cloud, but under some circumstances the air motions could enchance the mixing of the two clouds.

- *The effects of precipitation on the contamination once it reaches the ground.* After radioactive particles are brought to the ground by precipitation, they may or may not stay in place. There is a possibility that water run-off will create hot spots in some areas while decreasing the activity in other areas. Some of the radioactive particles may be leached into the ground and, as a result of the attenuation by the ground between the particle and the ground-air surface, the dose rate above the ground will be reduced.

There are no data concerning precipitation effects where the resulting contamination was militarily significant. Also, no computer model has been developed that can include all of the factors described above either on a deterministic or a statistical basis. The results of theoretical studies, field simulations, and laboratory experiments have, however, provided some general conclusions concerning the importance of precipitation effects. First, contamination resulting from precipitation scavenging is *not* considered to be a major problem from the standpoint of effects on military operations. Second, weapons may be separated into three groups according to their relative importance with regard to precipitation effects: 1. weapons in the yield range from 1 to 10 kt are most likely to have an effect on military operations, if any such effect occurs; 2. weapons with yields greater than 10 kt and less than about 60 kt may have some effect on military operations, with the probability of such an effect decreasing with increasing yield; 3. weapons with yields greater than 60 kt or less than 1 kt are not expected to have any effect on military operations. The potential hazard may be reduced by making use of available shelter.

BIBLIOGRAPHY

Baum, S., P. W. Wong, and P. J. Dolan, *NUCROM: A Model of Rainout from Nuclear Clouds*, DNA 3389F, Stanford Research Institute, Menlo Park, California, August 1974

Biggers, W. A., and K. C. Kohr, *Neutron Outputs from Selected LASL Nuclear Devices*, LA 3688, Los Alamos Scientific Laboratory, Los Alamos, New Mexico, April 1967

Beyster, J. R., et al., *Status of Neutron and Gamma Output from Nuclear Weapons*, SAI 70-205, DASA 2567, Science Applications Incorporated, La Jolla, California, May 1971

Bunney, L. R., and D. Sam, *Gamma-Ray Spectra of Fractionated Fission Products*, NOLTR 71-103, Naval Ordnance Laboratory, White Oak, Silver Spring, Maryland, 18 June 1971

Canu, J. F., and P. J. Dolan, *Prediction of Neutron Induced Activity in Soils*, Technical Analysis Report AFSWP 518, Headquarters, Armed Forces Special Weapons Project, Washington, D.C., 4 June 1957

Crawford, T. V., and K. R. Peterson, *BANEBERRY — Discussion of Diffusion Calculations Including Potential Exposure to Child's Thyroid from I-131 Via the Forage-Cow-Milk Pathway*, COPK 71-20, Lawrence Radiation Laboratory, Livermore, California, 3 March 1971

Crawford, T. V., *Precipitation Scavenging and 2BPUFF*, UOPKA 71-14, Lawrence Livermore Laboratory, Livermore, California, 6 December 1971

Crocker, G. R., *Fission Product Decay Chains: Schematics with Branching Fractions, Half-Lives, and Literature References*, USNRDL-TR-67-111, U.S. Naval Radiological Defense Laboratory, San Francisco, California, 24 June 1967

Crocker, G. R., and T. Turner, *Calculated Activities, Exposure Rates, and Gamma Spectra for Unfractionated Fission Products*, USNRDL-TR-1009, U.S. Naval Radiological Defense Laboratory, San Francisco, California, 28 December 1965

Crocker, G. R., and M. A. Connors, *Gamma-Emission Data for the Calculation of Exposure Rates from Nuclear Debris, Volume I, Fission Products*, USNRDL-TR-876, U.S. Naval Radiological Defense Laboratory, San Francisco, California, 10 June 1965

Crocker, G. R., J. D. O'Connor, and E. C. Freiling, *Physical and Radiochemical Properties of Fallout Particles*, NRDL-TR-899, Naval Radiological Defense Laboratory, San Francisco, California, 15 June 1965

Department of Defense Land Fallout Prediction System, DASA 1800-I through 1800-VII, Defense Atomic Support Agency, Washington, D.C.; U.S. Army Nuclear Defense Laboratory, Edgewood Arsenal, Maryland; U.S. Naval Radiological Defense Laboratory, San Francisco, California; Technical Operations Research, Burlington, Massachusetts; 1966

Dolan, P. J., *Gamma Spectra of Uranium-235 Fission Products at Various Times After Fission*, AFSWP 524, Headquarters, Armed Forces Special Weapons Project, Washington, D.C., March 1959 ▮

Dolan, P. J., *Gamma Spectra of Uranium-238 Fission Products at Various Times After Fission*, DASA 526, Headquarters, Defense Atomic Support Agency, Washington, D.C., May 1959 ▮

Dolan, P. J., *Theoretical Dose Rate Decay Curves for Contamination Resulting from Land Surface Burst Nuclear Weapons* ▮ DASA 528, Defense Atomic Support Agency, Washington, D.C., 6 August 1959 ▮

Englemann, R. J., and W. G. N. Slinn, *Precipitation Scavenging (1970)*, AEC Symposium Series, U.S. Atomic Energy Commission, Washington, D.C., 22 December 1970 ▮

Englemann, R. J., *Priorities in Scavenging Research*, AEC Symposium Series U.S. Atomic Energy Commission, Washington, D.C., 22 December 1970 ▮

French, R. L., *A First-Last Collision Model of the Air/Ground Interface Effects on Fast-Neutron Distributions, Nucl. Sci. Engr., 19*, 151-157, 1964 ▮

Freiling, E. C., and N. E. Ballou, *Nature of Nuclear Debris in Sea Water, Nature 195*, No. 4848, pp. 1283-1287, 29 September 1962 ▮

Fritzsche, A. E., N. E. Lorimier, and Z. G. Burson, *Measured Low-Altitude Neutron and Gamma Dose Distributions Due to a 14-MeV Neutron Source, EGG 1183-1449. E. G., and G., Inc., 1969* ▮

Fritzsche, A. E., N. E. Lorimier, and Z. G. Burson, *Measured High-Altitude Neutron and Gamma Dose Distributions Due to a 14-MeV Neutron Source*, EGG 1183-1438. E. G., and G., Inc., 1969 ▮

Harris, R. J., Jr., et al., *Models of Radiation in Air — The ATR Code*, DNA 2803I, SAI-71-557.LV, Science Applications Incorporated, La Jolla, California, May 1972 ▮

Huebsch, I. O., *Fallout Predictions for Water-Surface Nuclear Bursts*, USNRDL-TR-67-147, U.S. Naval Radiological Defense Laboratory, San Francisco, California, 28 November 1967 ▮

Heubsch, I. O., *Development of a Water-Surface-Burst Fallout Model: The Formation, Dispersion and Deposition of Fallout Particles*, USNRDL Technical Report, U.S. Naval Radiological Defense Laboratory, San Francisco, California ▮

Keith, J. R., and F. H. Shelton, *Neutron Transport in Non-Uniform Air by Monte Carlo Calculation, Volume I*, DASA 2236-1 KN-774-69-1, Kaman Nuclear, Colorado Springs, Colorado, 15 January 1969 ▮

Keith, J. R., and F. H. Shelton, *Neutron Transport in Non-Uniform Air by Monte Carlo Calculation* ███ Volume II, KN-774-69-1, DASA 2236-II, Kaman Nuclear, Colorado Springs, Colorado, 15 January 196█ ████████████████

Knox, J. G., and A. L. Williams, *Rainout Studies at Lawrence Livermore Laboratory*, UCRL 51530, Lawrence Livermore Laboratory, University of California/Livermore, Livermore, California, 11 February 1974 ████████████

Krey, P. W., et al., *Soil Activation by Neutrons* ███ Project 2.1, WT-1410, U.S. Army Chemical Warfare Laboratories, Army Chemical Center, Maryland, 16 May 1960 ████████████████

Lee, H., P. W. Wong, and S. L. Brown, SEER II: *A New Damage Assessment Fallout Model*, DNA 3008F, Stanford Research Institute, Menlo Park, California, May 1972 ████████████

Marshall, J. D., and M. B. Wells, *The Effects of Cut-Off Energy on Monte Carlo Calculated Gamma-Ray Dose Rates in Air*, RRA-M67, Radiation Research Associates, Fort Worth, Texas, 1966 ████████████

Mooney, L. G., and R. L. French, *Improved Models for Predicting Nuclear Weapon Initial Radiation Environments* ███. RRA-T93, DASA 2615, Radiation Research Associates, Fort Worth, Texas, 31 December 196█ ████████████████

Norment, H. G., and E. J. Tichovolsky, *A New Fallout Transport Code for the DELFIC System: The Diffusive Transport Module*, DASA 2669, Arcon Corporation, Wakefield, Massachusetts, 1 March 1971 ████████████

Norment, H. G., *A Precipitation Scavenging Model for Studies of Tactical Nuclear Operations, Volume I — Theory and Preliminary Results, Volume II — The DELFIC-PSM Code*, DNA 3661F-1, -2, Mt. Auburn Research Associates, Inc., Newton, Massachusetts, 18 June 1975, ████████████

Read, P. A., *Neutron Induced Activity on a Beach: A Method for Calculating the Dose Rate*, USNRDL-TR-67-133, U.S. Naval Radiological Defense Laboratory, San Francisco, California, 27 October 1967 ████████████

Ritchie, R. H., and V. E. Anderson, *Some Monte Carlo Results on the Penetration of Neutrons from Weapons in an Air-Over-Ground Geometry* ███ ORNL-3116, Oak Ridge National Laboratory, Oak Ridge, Tennessee, 26 July 1962 ████████████████

Schuert, E. A., *Distribution of the Radioactive Debris and Associated Nuclear Radiation from Underwater Nuclear Explosions* ███ USNRDL-TR-67-28, DASA 1240, Part 1, Chapter 11, U.S. Naval Radiological Defense Laboratory, San Francisco, California, 15 December 1966 ████████████

Selph, W. E., and M. B. Wells, *Weapons Radiation Shielding Handbook. Chapter 6, Methods for Predicting Radiation. Fields Produced by Nuclear Weapons* ███, DASA-1892-4, Oak Ridge National Laboratory. Oak Ridge, Tennessee, December 1969 ██████

Shelton, F. H., *Nuclear Weapons as Neutron Sources, The Neutron Environments They Produce, and Some Neutron Effects on Aerospace Systems* ██ DASA-2383-1, Volume I, Neutron Sources. KN 774-69-6. Kaman Nuclear. Colorado Springs, Colorado, October 1969 ████████

Shelton, F. H., and J. R. Keith, *Nuclear Weapons as Neutron Sources. The Neutron Environments They Produce, and Some Neutron Effects on Aerospace Systems* ██ *Volume II. Neutron Environments and Some Effects.* DASA 2383-2, KN 774-69-6, October 1969 ████████

Slade, D. H. (Ed.), *Meteorology and Atomic Energy − 1968,* USAEC Report TID-24190. Environmental Science Services Administration, Washington, D.C., July 1968 █████

Smith, R. J., R. F. Benck, and E. E. Lissak, *Initial Gamma Data from Nuclear Weapon Tests. 1948 Through 1962* ██ NDL-TR-53, U.S. Army Nuclear Defense Laboratory, Edgewood Arsenal, Maryland, July 1965 ████████

Snay. H. G., *The Hydrodynamic Background of the Radiological Effects of Underwater Nuclear Explosions* ██ Proceedings of the Tripartite Symposium on the Technical Status of Radiological Defense in the Fleets, U.S. Naval Radiological Defense Laboratory, San Francisco. California, 16-20 May 1960, Vol. II, USNRDL Reviews and Lectures. No. 103 █████

Stensland, G. J., *Further Numerical Model Studies of the Washout of Hygroscopic Particles in the Atmosphere.* UCRL-51614, Lawrence Radiation Laboratory. University of California/Livermore, Livermore, California, 2 July 1974 ██████

Straker. E. A., *Time-Dependent Neutron and Secondary Gamma-Ray Transport in an Air-Over-Ground Geometry, Volume II. Tabulated Data,* ORNL 4289. Vol. II. Oak Ridge National Laboratory, Oak Ridge, Tennessee, September 1968 ██████

Williams, A. L., *Rain Scavenging of Radioactive Particles.* UCRL-517765, Lawrence Radiation Laboratory, University of California/Livermore, Livermore, California, 28 February 1975 █████

Wong, P. W., and H. Lee, *Utilization of the SEER Fallout Model in a Damage Assessment Computer Program (DACOMP).* DNA 3608F. Stanford Research Institute, Menlo Park, California, 27 February 1975 ██████

Young, F. H., et al., *The Radiological Effects from Underwater Nuclear Explosions* ██ USNRDL-TR-68-1, U.S. Naval Radiological Defense Laboratory, San Francisco, California, 17 October 1967 ██████

(This page intentionally left blank)

5-152 Change 1